Assay development for cardiac troponin T and lactate dehydrogenase as markers for disease detection

Wei Li Guo

Ph.D. **2012**

Assay development for cardiac troponinT and lactate dehydrogenase as markers for disease detection

A thesis submitted for the degree of

Doctorate of Philosophy

by

Wei Li Guo B.Sc. (Hons).

Based on research carried out at

School of Biotechnology

and

Biomedical Diagnostics Institute,

Dublin City University,

Dublin 9,

Ireland.

March 2012

Under the supervision of Professor Richard O'Kennedy

Declaration

I hereby certify that this material, which I now submit for assessment on the programme of study leading to the award of Doctorate of Philosophy, is entirely my own work, that I have exercised reasonable care to ensure that the work is original, and does not to the best of my knowledge breach any law of copyright, and has not been taken from the work of others save and to the extent that such work has been cited and acknowledged within the text of my work.

Signed: _____ ID No.: _____

Date: _____

Academic outputs

Publications

1) Guo, W.L., Leonard, P., and O'Kennedy, R. (2010). Simple method of 'on-plate' growth for improved antibody screening. Journal of Immunological Methods, 359:61-64

2) Guo, W.L., Leonard, P., and O'Kennedy, R. (2012). New 'on-plate' growth for improved ELISA-based antibody screening. Journal of Visualized Experiments. (Submitted)

3) Gilmartin. N., Guo, W.L., Viguier, C., Welbeck, K., Arora. S. and O'Kennedy. R. (2012). Lactation stage and storage conditions, in addition to quarter health, affect the concentration of indicators of mastitis. Journal of Dairy Research. (In Press).

4) Guo, W.L., Leonard, P., and O'Kennedy, R. (2012). Generation of high-affinity cardiac Troponin T antibody fragments using phage display and chain-shuffling techniques. Biochemical and Biophysical Research Communications (In preparation).

5) Guo, W. L., Leonard, P., Fitzgerald, V., and O'Kennedy, R. (2012). High throughput '2-over-2' kinetic analysis of cardiac Troponin T antibody fragments using the Biacore 4000. Analytical Biochemistry (In preparation)

Posters

1) Guo, W. L., Leonard, P., Fitzgerald, V., and O'Kennedy, R. (2010). Selecting cardiac troponin T-tailored scFv and Fab fragments in high throughput using the BIAcore 4000. School of Biotechnology Research Day, Dublin City University, Dublin, Ireland.

2) Guo, W. L., Leonard, P., Fitzgerald, V., and O'Kennedy, R. (2010). Rapid mining for recombinant cardiac troponin T antibodies using BIAcore 4000. BITeomics Life sciences' 2nd Annual International Congress of Antibodies, Beijing, China.

Conferences

1) Leonard, P., Fitzgerald, V., Guo, W.L., Conroy, P., Hearty, S. and O'Kennedy, R. (2010). High throughput screening of antibody fragments using Biacore 4000, Developments in Protein Interaction Analysis (DiPIA), Barcelona, Spain.

2) Leonard, P., Fitzgerald, V., Guo, W.L. and O'Kennedy, R. (2010). Deciphering antibody binding characteristics using the Biacore 4000, GE Healthcare International Webinar, International Webinar broadcast from DCU.

3) Leonard, P., Fitzgerald, V., Guo, W.L. and O'Kennedy, R. (2010). Deciphering antibody binding characteristics using the Biacore 4000, Biacore, Micro Cal, In Cell User meeting, London.

Table of contents

Abstract

Human cardiovascular diseases (CVDs) are leading causes of human death globally and cause huge social and economic impacts. Similarly, bovine mastitis is the most economically important disease of dairy cattle world-wide. The pathogenesis of both diseases involves an inflammatory process. Biomarkers are measurable substances, which may be used to detect the presence of specific diseases. Cardiac troponin T (cTnT) is recommended as a potential biomarker for cardiovascular disease (CVD) detection due to its high specificity and sensitivity. In addition, elevation in L-lactate dehydrogenase (LDH) levels in mastitic milk suggests that it may have potential as a biomarker for the detection of sub-clinical mastitis.

Classical CVD biomarkers, including cardiac myoglobin and creatine kinase-MB, have been extensively studied but are lacking in specificity and early–stage sensitivity. Troponin T was recommended as a potential 'gold standard' for CVD detection, and, therefore, a key aim of this project was to generate recombinant antibody fragments against cTnT and, ultimately, to develop a sensitive immunoassay for early-stage CVD diagnosis. Recombinant antibody fragments, including scFvs and Fabs, have excellent antigen recognition specificity but have additional benefits compared to standard antibodies. Current immunoassays for cTnT detection use monoclonal antibodies and the generation and application of recombinant antibodies and a novel assay platform may introduce significant improvements in cTnT assay development.

A recombinant avian anti-cTnT scFv antibody was generated and the antigen binding capacity of the antibody was improved using chain-shuffling. The chain-shuffled antibody, with sub-nanomolar affinity, was subsequently incorporated into an ELISA inhibition assay for the detection of cTnT.

Bovine mastitis is an inflammation of the mammary gland caused by invasion of pathogens. Its early detection is of paramount importance in controlling bovine health. Current diagnostic tests for mastitis have drawbacks such as high costs, lack of suitability for 'on-site' testing as well as poor specificity and sensitivity. Lactate dehydrogenase (LDH) was evaluated as a potential biomarker for the detection of sub-

clinical mastitis in this research, LDH levels in milk samples were determined using a reliable and reproducible fluorescence-based assay, and the potential of LDH as a marker of subclinical mastitis was determined. It was found that LDH levels had a good correlation with somatic cell count, the gold standard mastitis marker. Moreover, it was shown that a number of factors including lactation stage and storage conditions affected LDH levels in milk samples. These factors must be taken into account when using LDH as biomarker for sub-clinical mastitis detection.

List of Tables

List of Figures

Abbreviations

Ab	**Antibody**
Abs	**Absorbance**
ACC	**American College of Cardiology**
ACS	**acute coronary syndromes**
ADP	**adenosine diphosphate**
AHA	**American Heart Association**
AMI	**acute myocardial infarction**
ATP	**adenosine triphosphate**
ATPase	**Adenosine triphosphatase**
BM	**bone marrow**
BSA	**bovine serum albumin**
CAD	**Coronary artery disease**
cDNA	**complementary deoxyribonucleic acid**
CDR	**Complementarity determining region**
Cfu	**colony forming units**
C_H	**constant region, heavy chain of antibody**
Cκ	**constant region, kappa light chain of antibody**
CK	**creatine kinase**
CK-MB	**creatine kinase-MB**
CM	**carboxy-methylated**
CMT	**California Mastitis Test**
cTnC	**cardiac tropnin C**
cTnI	**cardiac troponin I**
cTnT	**cardiac troponin T**
CV	**coefficient of variation**
CVD	**cardiovascular disease**

dH_2O	**distilled water**
DNA	**deoxyribonucleic acid**
dNTP	**deoxyribonucleotide triphosphate**
DTT	**Dithiothreitol**
EC	**endothelial cell**
ECG	**electrocardiogram**
E. coli	***Escherichia coli***
ED	**Emergency Department of hospital**
EDC	**1-ethyl-3-[3-dimethylaminopropyl] carbodiimide hydrochloride**
EDTA	**ethylenediaminetetra acetic acid**
ELISA	**enzyme-linked immunosorbent assay**
ESC	**European Society of Cardiology**
EU	**European Union**
Fab	**antigen binding fragment**
FCA	**Freund's complete adjuvant**
FICA	**Freund's incomplete adjuvant**
Fd	**heavy chain of antibody**
FN	**false negatives**
fsTnT	**fast skeletal troponin T**
FP	**false positives**
FU	**fluorescence unit**
HA	**Haemagglutinin**
HBS	**hepes buffered saline**
His	**Histidine**
HRP	**horseradish peroxidase**
Hs-cTnT	**high sensitivity cardiac troponin T**
IFN-γ	**interferon γ**
Ig	**immunoglobin**
IgG	**immunoglobulin G (antibody molecule)**

IMAC	**immobilised metal affinity chromatography**
IMS	**industrial methylated spirits**
IPTG	**isopropyl-β-D-1-thiogalactopyranoside**
K_D	**dissociation constant (M)**
LDH	**lactate dehydrogenase**
LDL	**low density lipoprotein**
LOD	**limit of detection**
mAb	**monoclonal antibody**
MI	**myocardial infarction**
Mops	**3-morpholinopropane-1-sulfonic acid**
Myo	**myoglobin**
NAGase	**N-acetyl-β-D-glucosaminidase**
N/A	**not applicable**
NaAc	**sodium acetate**
Ni	**Nickel**
NAD^+	**nicotinamide adenine dinucleotide**
NHS	**N-hydroxysuccinimide**
OD	**optical density**
pAb	**polyclonal antibody**
PAGE	**polyacrylamide gel electrophoresis**
PBS	**phosphate buffered saline**
PBST	**phosphate buffered saline with 0.05% (v/v) Tween 20**
PCR	**polymerase chain reaction**
PEG	**polyethylene glycol**
Pfu	**phage forming units**
PMNs	**polymorphonuclear neutrophils**
POC	**point-of-care**
recHcTnT	**recombinant human cardiac troponin T**
RNA	**ribonucleic acid**

Rpm	**revolutions per minute**
RT	**reverse transcriptase**
RU	**response unit**
SB	**super broth**
SCC	**somatic cell count**
scFv	**single chain fragment variable (of antibody fragment)**
ssTnT	**slow skeletal troponin T**
sTnC	**skeletal troponin C**
sTnI	**skeletal troponin I**
sTnT	**skeletal troponin T**
SDS	**sodium dodecyl sulfate**
SDS-PAGE	**sodium dodecyl sulfate polyacrylamide gel electrophoresis**
SOC	**super optimal catabolite**
SOE	**splice by overlap extension**
SPR	**surface plasmon resonance**
ssTnT	**slow skeletal troponin T**
TB	**Terrific Broth**
TES	**N-tris (hydroxymethyl)-methyl-2-aminoethanesulfonic acid**
TMB	**tetramethylbenzidine dihydrochloride**
Tm	**Tropomyosin**
Tn	**Troponin**
TN	**true negatives**
TnC	**troponin C**
TNF α	**tumour necrosis factor α**
TnI	**troponin I**
TnT	**troponin T**
TYE	**tryptone-yeast extract**
TP	**true positives**
V_H	**variable region, heavy chain of antibody**

V_K	**variable region, kappa light chain of antibody**
V_L	**variable region, light chain of antibody**
V_λ	**variable region, lambda light chain of antibody**
WHO	**World Health Organisation**

Units

µg	**Microgram**
µL	**Microlitre**
µM	**Micromolar**
bp	**Basepair**
cm	**Centimetre**
Da	**Dalton**
FU	**Fluorescence Units**
g	**Centrifugal acceleration**
h	**Hour**
k_a	**Association rate constant**
k_d	**Dissociation rate constant**
kDa	**Kilodaltons**
K_A	**Equilibrium association rate constant**
Kb	**Kilobasepair**
K_D	**Equilibrium dissociation rate constant**
L	**Litre**
M	**Molar**
mg	**Milligram**
mL	**Millilitre**
min	**Minute**
mM	**Millimolar**
ng	**Nanogram**
nM	**Nanomolar**
^oC	**Degree Celsius**
pfu	**Plaque-forming unit**
rpm	**Revolutions per minute**
RU	**Response units**
s	**Second**
U	**Enzymatic Units**
v/v	**Volume per unit volume**
w/v	**Weight per unit volume**

µg	**Microgram**

Chapter 1
Introduction

1 Introduction

1.1 Cardiovascular diseases

1.1.1 Background to cardiovascular diseases

Cardiovascular diseases (CVDs) refer to a range of disorders and conditions that affect heart and blood vessels. Types of CVDs include atherosclerosis, angina, cerebrovascular accident (stroke), myocardial infarction (heart attack), coronary artery disease, heart valve disease, arrhythmia, aortic aneurysm, heart failure, hypertension, orthostatic hypotension, shock, endocarditis, ischemic myocardial necrosis, peripheral vascular disease and congenital heart disease (Table 1.1).

CVDs kill more people each year than any others types of diseases. More than 17.5 million people worldwide die from CVDs every year as reported by the Health Europe in 2010. It is estimated that approximately 23.6 million people will die annually from CVDs by 2030. Due to the high death rate, CVDs have consequently become a threat to social and economic stability. Huge expenditure on clinical care and treatment for CVDs has lead to significant reductions of resources available for general medical care. In addition, CVDs affect both the elderly and the working-age population. Consequently, the productive years of working-age patients are reduced due to CVDs.

Table 1.1. List of cardiovascular diseases and their characteristics

Types of cardiovascular diseases and their characteristics
Atherosclerosis
• **Major form of heart diseases** • **Hardening, thickening or furring of the walls of the arteries** • **Caused by fatty deposits on the inner lining of arteries, calcification of the wall of the arteries, or thickening of the muscular wall of the arteries from chronic hypertension**
Angina
• **Most common form of coronary heart disease** • **Heaviness or tightness of the chest caused when there is a decreased blood oxygen supply to an area of the heart muscle** • **The lack of blood supply is due to a narrowing of the coronary arteries as a result of atherosclerosis**
Coronary artery disease (CAD)
• **Begins when plaques are deposited within a coronary artery. The plaques in the coronary arteries can cause a tiny clot to form which can obstruct the flow of blood to the heart muscle** • **Leads to chest pain (angina pectoris) and heart attack (acute myocardial infarction) from the sudden total blockage of a coronary artery or sudden death, due to a fatal disturbance of heart rhythm**

Ischemic myocardial necrosis
• **Death of myocardial cells and tissue** • **Caused by the interruption of the blood supply through the coronary arteries**
High blood pressure/ hypertension
• **Elevation of systemic blood pressure in the arteries** • **Risk factor for stroke, myocardial infarction, heart failure and arterial aneurysm**
Orthostatic hypertension
• **Sudden decrease in blood pressure when one stretches or stands up** • **Arteries and veins that are able to constrict or squeeze** • **May be caused by atherosclerosis**
Heart attack / Acute myocardial infarction (AMI)
• **Interruption of blood supply to a part of the heart** • **Causing the death of heart cells** • **Caused by blockage of a coronary artery following the rupture of a vulnerable atherosclerotic plaque, which is an unstable collection of lipids (fatty acids) and white blood cells (especially macrophages) in the wall of an artery**

Cerebrovascular accident/stroke
• **Damage to the brain because of impaired blood supply** • **Causes a sudden malfunction of the brain**
Arrhythmia/ dysrhythmia
• **Refers to an irregular heartbeat; it may occur with slow, normal and rapid heart rate.** • **Caused by changes in heart muscle, injury from a heart attack or at the healing process after heart surgery** • **Can also occur in healthy hearts**
Heart valve disease
• **Occurs when the heart's valves are narrowed or do not have enough of a supply of blood** • **Caused by valvular stenosis and valvular insufficience** • **Leads to heart failure or aortic stenosis**
Heart failure (often called congestive heart failure)
• **Refers to weak pumping power of the heart** • **Caused by coronary artery disease, heart attack or cardiomyopathy** • **Symptoms including shortness of breath, leg swelling and exercise intolerance**

Cardiomyopathy
• **Damage to the heart muscle from causes other than artery or blood flow problems** • **Causes include infections, alcohol or drug abuse**
Cardiogenic shock
• **Occurs when the heart is damaged and unable to supply sufficient blood to the body** • **May be caused by heart attack or congestive heart failure**
Rheumatic heart disease
• **One of the most serious forms of heart disease of childhood and adolescence** • **Causes damage to the entire heart and its membranes** • **Usually followed attacks of rheumatic fever**
Myocarditis
• **Refers to the inflammation or degeneration of heart muscle** • **May appear as the primary disease in adults or as a degenerative disease of old age** • **May be related to dilation (enlargement due to weakness of the heart muscle) or hypertrophy (overgrowth of the muscle tissue)**

Endocarditis
• **Caused by growth of bacteria on the heart valves leading to heart infection** • **The infection may be introduced during brief periods when bacteria are present in the bloodstream, such as after dental work, colonoscopy, or other similar procedures**
Peripheral vascular disease
• **Refers to the narrowing and hardening of the arteries that supply the legs and feet** • **The narrowing of the blood vessels can lead to decreased blood flow which can injure nerves and other tissues** • **May be caused by atheriosclerosis**
Congenital heart disease
• **Refers to malformations of the heart or heart blood vessels which are present since birth** • **The most frequent form of major birth defects in newborns affecting close to 1% of newborn babies**
Aortic aneurysm
• **Describes a localized, blood-filled balloon-like bulge in the wall of a blood vessel** • **Occurs in the main artery carrying blood from the left ventricle of the heart** • **The increased size of an aneurysm may lead to a significant risk of rupture, resulting in severe hemorrhage, other complications or death**

- **Can be hereditary or caused by disease**

(Based on references: Phillips *et al.,* 2000; Davies, 2005; Gaziano, 2005; Jokni and Curzen, 2010; Butcher *et al.,* 2011; Daidoji *et al.,* 2011)

In most developed countries, CVDs account for the largest share of mortality and morbidity (WHO, 2005; Vasan, 2006). In the EU, Nearly half of all deaths (42%) are caused by CVDs each year. In Ireland, CVD is the leading killer disease which accounts for 36% of all deaths. The UK has one of the highest rates of death from CVDs. In the US, more than one third of American adults have one or more types of CVD. In developing countries, CVDs are increasing in epidemic proportions (Reddy, 2002). They already account for almost 10% of the developing world's burden of disease and are likely to become the leading cause of death. In 2001, CVDs accounted for approximately 31% of all death in Latin American and the Caribbean, and it is estimated the figure will increase to 38% by 2020 (Murray and Lopes, 1996). In Middle East and North Africa, CVDs are the leading cause of death which account for 25 to 45% of total death (Jamison *et al.,* 2006). The China Multicenter Collaborative Study of Cardiovascular Epidemiology indicated that cardiovascular disease was the major cause of death for both men and women, with stroke accounting for over 40% of deaths (Liu, 2007). According to the statistic at the 7th China Heart Congress in 2011, it was estimated that 230 million people in China suffer from CVDs, and six people die from CVDs per minute. In India, CVDs caused a loss of 9.2 million productive years of life in 2000.

CVDs also have a huge impact on the global economy. In 2003, the EU spent €169 billion on CVDs and it is estimated that annual losses due to CVDs in the EU is €192 billion (Allender *et al.,* 2008). The American Heart Association estimated that $503.2 billion were spent on direct or indirect costs associated with CVDs in 2010. Direct costs refer to direct medical costs, such as ambulance transportation, diagnostic tests, medication and surgery; while indirect costs involve the loss of productivity and the loss of income from patients. In most developing countries, there is a continually increasing economic burden caused by cardiovascular diseases (Neal *et al.,* 2002). Four percent of

the gross national income of the Chinese economy, estimated as €30.76 billion, is spent on cardiovascular diseases and its related factors. In South Africa, 25% of the total health care expenditure is spent on CVDs.

Due to the huge social and economic impact of CVDs, their prevention and accurate diagnosis has become one of the main priorities of public health-care (WHO, 2005; Schwappach *et al.,* 2007). CVD risk factors are the variables associated with an increased risk of CVD development. It was stated that approx. 75% of CVDs can be attributed to conventional risk factors. Risk factors are grouped into two categories, non-modifiable and modifiable. Non-modifiable factors are factors that cannot be altered or controlled, such as age, genetics, race and gender. Modifiable factors can be prevented and controlled by altering the lifestyle behaviors or getting medical treatment. People are exposed to more risk factors have the higher risk of developing CVDs. Lack of prevention of risk factors can consequently lead to the initiation of CVDs pathogenesis (Table 1.2).

Table 1.2. Modifiable risk factors and primary pathophysiological effects of CVDs

Modifiable risk factors	Initial pathogenesis effects	References
Poor dietary habits diet (high fat and cholesterol)	High levels of cholesterol	Sacks and Katan., 2002
Physical inactivity	Poor perfusion, adverse lipid profile	Ignarro, 2006
Obesity	Metabolic syndrome of insulin resistance	Grundy, 2004
Tobacco taking	Oxidative stress	Pasupathi *et al.*, 2009
Dyslipidaemia	Oxidative stress	Rizzo *et al.*, 2009
Hypertension (high blood pressure)	Oxidative stress, enhanced vasoconstriction	Harrison and Gongora, 2009
Infection	Inflammation	Lowe, 2001

1.1.2 Inflammation process of atherosclerosis

Atherosclerosis, the major cause of CVDs, refers to a chronic inflammation process affecting medium and large sized arteries, subsequently restricting blood flow by the formation of blood clots inside arteries. The development of atherosclerosis in humans starts as early as twenty years of age and progresses slowly over many years. The adhesion of endothelial cells (ECs) from the inner surface of the artery wall with leukocytes initiates the process of inflammation (Libby *et al.,* 2006). Healthy ECs lack the ability to adhere to leukocytes. However, common risk factors, physical damage and infection of the arteries trigger the interaction of the endothelium with monocytes and T lymphocytes, which are two types of leukocytes involved in the early stage of atherosclerosis. This causes the penetration of monocytes and T lymphocytes into the intima, which is an inner layer of the vessel wall. Monocytes express the scavenger receptors CD36 and SR-A, leading to their transformation into highly activated macrophages which take up low-density lipoproteins (LDL). These macrophages, which also called foam cells, combine with T cells in the intima to form the fatty streak.

The migration of smooth muscle cells to the site of inflammation is stimulated by cytokines and growth factors secreted by macrophages and T cells. Within the intima, macrophages also secrete inflammatory cytokines including tumour necrosis factor α (TNF α), interleukins and metalloproteinases. Collagen, synthesised by smooth muscle cells, becomes the predominant connective tissue of these inflammatory areas. The connective tissue deposits over the foam cells and macrophages, thus forming a fibrous cap. The foam cells and macrophages subsequently undergo apoptosis and the cell debris generated from apoptosis forms a 'lipid-rich' necrotic core. The fibrous cap containing the necrotic core finally develops into an atherosclerotic plaque. At the shoulder of the plaque, i.e. the junction of the fibrous cap with the endothelium, leukocytes continually transform into foam cells and deposit at the bottom of the

necrotic core, which results in the enlargement of the plaque. Meanwhile, T cells secrete cytokines such as interferon γ (IFN-γ), which restricts the production of collagen by smooth muscle cells. Macrophages also produce enzymes which digest the collagen and the prothrombotic substances within the plaque. These reactions lead to the activation of platelets, and cause the fibrous cap to reduce its strength. The fibrous cap undergoes thrombosis and ruptures in the blood vessel. The blood flow is interrupted by the contents released when the plaques rupture, finally leading to necrosis and acute myocardial infarction (AMI).

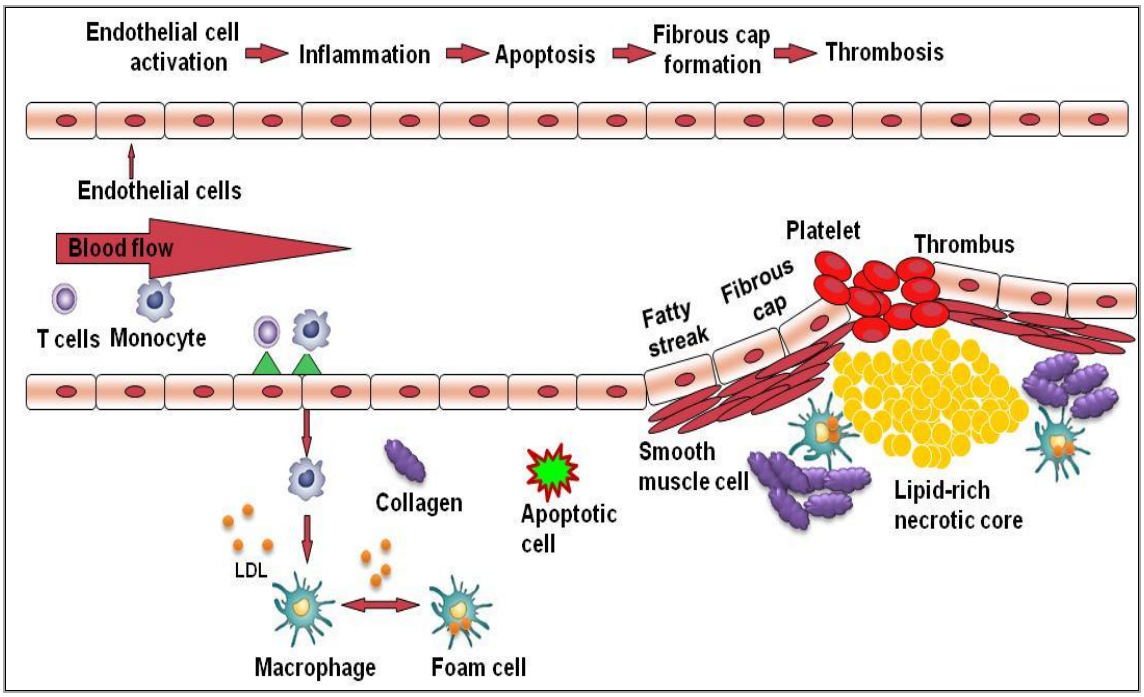

Figure 1.1. The process of atherosclerosis development. Low-density lipoprotein (LDL) undergoes chemical changes and activates the endothelial cells to adhere with the immune cells. These immune cells penetrate the intima and trigger the inflammation process, which encourage the transformation of macrophage into foam cells. Foam cells secrete a variety of cytokines and then undergo apoptosis. The fatty streak is subsequently formed due to the deposition of foam cells and their debris, and the fatty streak finally transforms into a fibrous cap. Substances released from foam cells destabilize the fibrous cap and cause rupturing of the fatty plaque (Based on references: Libby 2006; Full *et al.*, 2009).

1.2 Biomarkers for cardiovascular diseases

1.2.1 Current biomarkers for cardiovascular diseases

A biomarker is a measurable and evaluable substance which can indicate a specific biological state, including healthy and pathological biological processes and pharmacologic responses to a therapeutic intervention. Biomarkers can be used to identify risk stratification of diseases, to make a diagnosis, to assess the evolution of a disease and to detect a response to the toxicity of a disease treatment (Frank and Hargreaves, 2003; Phillips *et al.,* 2006; Christ-Crain and Opal, 2010).

Cardiac biomarkers are a class of biological analytes that are detectable in the bloodstream at elevated levels during the continuum of CVD. Current available CVD biomarkers for AMI detection have been extensively studied (Galvani *et al.,* 2001; Daniels *et al.,* 2009; McDonnell *et al.,* 2009). In general, each CVD biomarker is associated with types and stages of cardiac disease development (Fig 1.2). For instance, markers of inflammation are related to cardiac plaque formation and rupture. Coagulation factors and proteins are associated with intracoronary thrombus formation. Perfusion and functional imaging can detect reduced blood flow. Early ischemic biomarkers and classical CVD biomarkers indicate myocardial ischemia and necrosis.

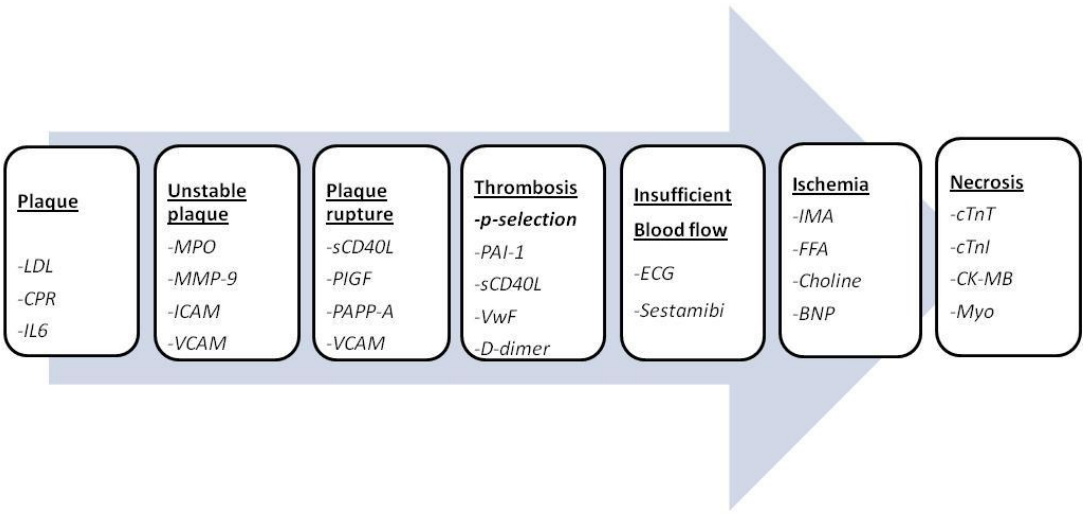

Figure 1.2. Biomarkers associated with stages of cardiovascular disease development. The arrow represents the progression of CVD from early stage (plaque formation) to late stage (necrosis). Biomarkers of inflammation indicate the stage of plaque formation and plaque rupture. Coagulation factors and proteins are biomarkers for thrombosis. Reduced blood flow can be detected by perfusion or functional imaging. Myocardial ischemia and necrosis can be diagnosed with early ischemic biomarkers and classical CVD biomarkers, respectively (Vasan, 2006).

Lactate dehydrogenase (LDH), Creatine Kinase (CK) and their isoenzymes and myoglobin are the classical biomarkers for CVD (O'Brien, 2006). LDH can be found in most tissues such as cardiac muscle, skeletal muscle, liver, lungs and brain. LDH has five isoforms, which are LDH-1, LDH-2, LDH-3, LDH-4 and LDH-5. Each isoform is comprised of combinations of two different subunits, which are M and H (Bansal *et al.,* 2005; Babaei *et al.,* 2007). LDH-1, mainly present in cardiac muscle, contains 4 H subunits. LDH-2, the predominant form in serum, contains 3 H subunits and 1 M subunit. The ratio of LDH-1 and LDH-2 levels can be used an indicator for CVD diagnosis (Chu *et al.,* 2002). Generally, LDH levels start to increase twelve to

twenty-four hours after myocardial infarction and reach a peak at forty-eight to seventy-two hours. The levels return to normal within 10 days. However, in most cases, skeletal muscle damage can also lead to the elevation of LDH levels. LDH, therefore, has low specificity for the CVD diagnosis.

In the second section of this thesis LDH is evaluated as a potential marker of mastitis. This links both sections of the thesis as the overall focus of the research was the evaluation of potential biomarkers related to inflammation for their applicability for early disease detection with relatively high specificity.

Myoglobin is a low molecular weight oxygen binging protein and it is also an early stage biomarker for myocardial infarction. Myoglobin levels are detectable as early as two hours after cardiac injury. Myoglobin is present in both skeletal and cardiac muscle and its levels increase with both skeletal and cardiac injury (O'Brien, 2008). Myoglobin, therefore, has to be used in conjunction with other serum markers to obtain accurate CVD diagnosis.

Creatine Kinase (CK) is one of the early used biomarkers for myocardial infarction. However, it also has low specificity due to its presence in slow-twitch muscle tissue. In comparison to CK, Creatine Kinase-MB (CK-MB), a derivative form of CK, is a more specific biomarker (Jaffe *et al.,* 2006). The CK-MB can be detected in the serum four to six hours after the onset of ischemia and its levels reach a peak at twelve to twenty-four hours. The levels return to normal within three days (Jaffe, 2005; Jaffe *et al.,* 2006). CK-MB levels can be elevated in a number of non-cardiac conditions such as pregnancy and parturition. It, therefore, cannot be used as a 'gold-standard' for AMI detection (Jaffe, 2005; Jaffe *et al.,* 2006).

Currently, cardiac troponins, either troponin T or troponin I, are the biomarkers of choice for the detection of cardiac injury (O'Brien, 2008; Conroy *et al.,* 2009). Cardiac troponin T levels increase in the immediate aftermath of myocardial damage. The elevation of cTnT levels can be monitored within minutes after myocardial injury and the peak occurs as early as two to six hours (O'Brien, 2008). Similarly, Lim and co-workers also reported cTnT level increased and showed a peak three to four hours after the occurrence of cardiac symptoms in patients with acute myocardial infarction action (AMI) (Lim *et al.,* 2005). Moreover, Inbar and Shoenfeld reported that cardiac troponins were detected in patients' serum within six hours after the initiation of CVD (Inbar and Shoenfeld, 2009). Due to the high cardiac sensitivity and specificity of troponin, the European Society of Cardiology and the American College of Cardiology (ESC/ACG) have recommended cardiac troponins as the preferred biomarkers since 2000. The diagnosis of acute myocardial infarction was redefined by ESC/ACG. It was recommended that the 99^{th} percentile of a reference control population (normal value) should be the 'cut-off' for the diagnosis of AMI as well as at least one of the these criteria: symptoms of ischaemia; ECG changes indicative of new ischaemia (e.g. new ST-segment depression or a new complete left bundle branch block); development of pathological Q-waves in the ECG and demonstration of a new area of infarction or disturbance of regional wall motility by imaging (Morrow, 2006; Giannitsis and Katus, 2010). From clinical studies, patients with an elevated cTnT level greater than 0.01 μg/L are considered as sub-clinical AMI (Morrow, 2001).

Table 1.3. Overview of serological markers used for myocardial necrosis detection

Biomarkers	MW (kDa)	Initial elevation	Peak level	Return to normal	Advantages	Disadvantages
Creatine kinase - MB (CK-MB)	85	3 to 12 h	12-24 h	2 to 3 days	More specific than CK alone; early detection marker; used for diagnosis of reinfarction	Low cumulative specificity; present in skeletal tissue; low discriminative value in coronary reperfusion
Lactate dehydrogenase (LDH)	35	12 to 24 h	48 to 72 h	10 days	High sensitivity when detected with isoforms ratios of LDH-1:LDH-2	Low specificity; present in most tissues;
Myoglobin (Myo)	17	2 h	6 to 12 h	1 to 2 days	Peaks rapidly; very early detection marker; high sensitivity; can determine the size of infarction	Low specificity; exists in skeletal tissue; returns to normal quickly
Heart Fatty acid binding protein (HFBP)	14.5	2 to 3 h	8-10 h	18-30 h	Early marker; estimate of infarction size; detects the re-perfusion of MI	Low specificity; present in muscle, brain and kidney
Troponin T (TnT)	35	4 to 6 h	12-24h	7 to 10 days	High sensitivity; high specificity, significant prognostic potential	Limited in detection of reinfarction; associated with end-stage renal disease
Troponin I (TnI)	23.5	4 to 6 h	12-24 h	6 to 8 days	High sensitivity and specificity; significant prognostic potential	Limited in detection of reinfarction; no accepted reference standards thus affecting assay reliability

(Based on references: Horak, 1999; Kemp *et al*., 2004; Bunk and Welch, 2006; Vasan, 2006; McDonnell *et al.*, 2009)

1.2.2 The biology of cardiac troponins

In 1963, Ebashi isolated a protein complex called 'natural tropomyosin' from rabbit skeletal muscle (Perry, 1998). The biological properties of the protein complex are similar to tropomyosin, therefore, the complex was named 'troponin' after tropomyosin (Tm) by Ebasi and Enda in 1968 (Ebashi and Endo, 1968). A number of groups performed the subsequent fractionation of the troponin complex and in 1972 the three components of troponin complex were separated and were named as troponin C (TnC), troponin I (TnI) and troponin T (TnT) (Fig. 1.3)(Greaser *et al.,* 1972).

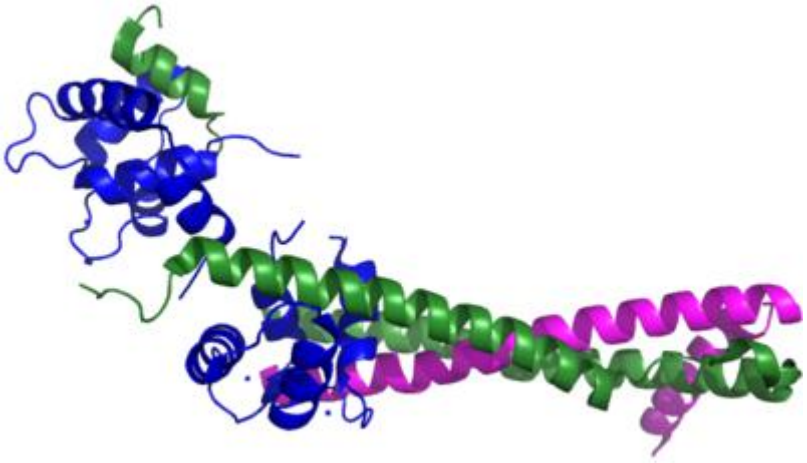

Figure 1.3. Structure of the human cardiac complex. The blue ribbon represents troponin C (TnC), the green ribbon represents troponin I (TnI), and the magenta ribbon represents troponin T (TnT).

The troponin complex plays a critical role in the regulation of striated muscle contraction. Striated muscle filaments consist of thick myosin filaments and thin actin filaments. The tropnin complex (Fig. 1.4) is attached to the tropomyosin protein forming the troponin/tropomyosin complex and is located within the groove of the thin actin filaments (Parmacek and Solaro, 2004; Ohtsuki and Morimoto, 2008). Typically, muscle contraction is accomplished by the sliding motion of the thick myosin filaments

along the thin actin filaments. In relaxed muscle, the heads of myosin filaments are attached to the actin molecules thus forming cross-bridges. When ATP interacts with a myosin head, it causes the detachment of the myosin head from the actin molecule. ATP then undergoes degradation and breakdown into ADP and inorganic phosphate. Calcium ions (Ca^{2+}) are stored in the sarcoplasmic reticulum of striated muscle. When the muscle contraction process initiates, Ca^{2+} ions are released from the reticulum and migrate to the sarcoplasm around the muscle filaments. After myosin detaches from the actin molecule, Ca^{2+} binds to troponin C which is located on the actin filaments thus leading to the shift of the tropomyosin-troponin complex (Fig.1.4). The shift of the complex allows the exposure of new myosin binding sites. The myosin head moves along the actin filaments and subsequently binds to a new actin molecules. This movement results in shortening of the muscle fiber thus causing muscle contraction (Szent-Gyorgyi, 1975; Krans, 2010).

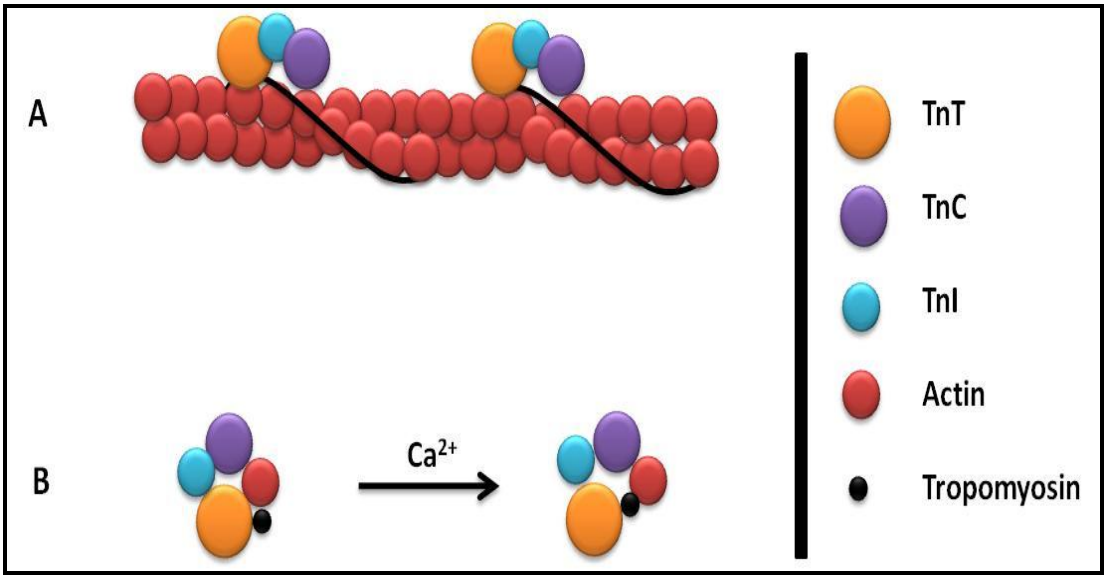

Figure 1.4. (A) Components of the troponin complex. Three troponin subunits, Troponin I (TnI), troponin C (TnC), and troponin T (TnT) interact with tropomyosin located along the actin filaments on the striated muscle. **(B) Cross-sectional view of the interaction between the striated muscle and calcium ions.** The interaction between myosin to actin is prevented by the tropomyosin-troponin complex when Ca^{2+} is absent. The binding of Ca^{2+} ions to TnC causes the movement of tropomyosin-troponin complex, thus initiating the interaction of myosin to actin and subsequently causing muscle contraction.

The TnC subunit, of approximately 18 kD molecular weight, consists of two globular domains and a central α-helix connecting the domains. The Ca^{2+} binding sites are located on both the N terminal and C terminal regions of the globular domains. Ca^{2+}-saturated TnC causes position shifting of the Tn–Tm complex, thus allowing the binding of actin with myosin. The Tn-Tm complex stimulates ATPase activity thus producing muscle contraction (Flicker *et al.,* 1982; Filatov *et al.,* 1999).

TnI, is a polar protein with positively charged residues that is responsible for inhibition of the actomyosin ATPase activity (Filatov *et al.,* 1999). In the presence of

Ca^{2+}-saturated TnC, the two peptide inhibition sites on cTnI interact with TnC instead of actin, resulting in the release of the actomyosin ATPase activity. TnT interacts with tropomyosin in the muscle contraction process thus regulating actomyosin ATPase activity. The binding of TnT with TnI and TnC in the presence of Ca^{2+} causes less inhibition of ATPase activity than in the absence of the Ca^{2+} and, therefore, assisting in muscular contraction (Filatov *et al.,* 1999).

Troponin T is an asymmetric 'comma'-shaped polypeptide. It has a globular domain at the C-terminus and an extended N-terminal end as the tail of the comma (Flicker *et al.,* 1982). Three homologous genes encode the three muscle-specific types of TnT: slow skeletal troponin T (ssTnT), fast skeletal troponin T (fsTnT) and cardiac muscle troponin T (cTnT) (Burlina *et al.,* 1994; Babuin and Jaffe, 2005). Each of the genes undergoes alternative mRNA splicing during development, resulting in different isoform expression at the N-terminus (Burlina *et al.,* 1994; Sumandea *et al.,* 2009). The gene fragment which encodes the N-terminus of the cTnT molecule is highly variable due to the alternative splicing of short exons 4 and 5 on mRNA. The variations of the genotype can lead to the variations of phenotype in the N-terminus (residue 1-70) (Ohtsuki, 1979; Filatov *et al.,* 1999). Troponin T has a molecular weight in the 31-36 kDa range and consists of about 250 to 300 amino acids. Four troponin T isoforms (cTnT1 to cTnT4) can be found in human cardiac muscle. All four isoforms are expressed in fetal cardiac muscle, and only one isoforms (cTnT2) predominantly exists in adult cardiac muscle (Anderson *et al.,* 1991). Snyder and co-worker found that rabbit cardiac TnT had a longer N-terminal region than its skeletal counterpart and was 20% more helical (Snyder *et al.,* 1996). Similarly, Townsend and co-workers compared the alignments of the TnT isoform from adult humans with other animal species and significant sequence variations were found between species in 67 residues at the N-terminal end (Townsend *et al.,* 1994). In addition, Dhoot and co-workers also

reported that the major isoforms of TnT in fast skeletal, slow skeletal and cardiac muscles are immunochemically distinct proteins (Dhoot *et al.,* 1979).

1.2.3 Immunoassay for Troponin T

Currently the Roche Elecsys® cTnT assay (Roche Diagnostics) is the only commercially available assay. This first generation of the Roche Elecsys® cTnT assay is based on a sandwich format using two monoclonal antibodies, with a detection capacity for cTnT of 0.1 μg/L (Katus *et al.,* 1991). However, the lack of cardiac specificity of the HRP-labeled 2nd monoclonal antibody caused 12% cross-reactivity with skeletal isoform of TnT, therefore, yielding false-positive diagnosis for patients with skeletal muscle injury (Wu *et al.,* 1994; Muller-Bardorff *et al.,* 1997; Hallermayer *et al.,* 1999). Katus and colleagues improved the assay by substituting the non-specific monoclonal antibody with a high-affinity cardiac antibody (Muller-Bardorff *et al.,* 1997). The new version of troponin T assay showed no binding against skeletal TnT and increased sensitivity with the detection level at 0.0123 μg/L. Both the first and second generation troponin T assays were compromised due to the use of recombinant cTnT purified from bovine sources as standard material (Hallermayer *et al.,* 1999). The recombinant bovine cTnT was found to be problematic for generating a linear calibration curve and thus the assays were not reliable. In the third generation cTnT assay, the bovine cTnT was replaced by recombinant human cardiac TnT (recHcTnT). The recHcTnT brings several advantages. Firstly, it can generate a high linear calibration curve which eliminates the non-linear dilution behavior caused by the use of bovine cTnT. Secondly, it has higher binding affinity to the monoclonal antibody. The fourth generation troponin assay uses the Fab fragments of two cardiac-specific monoclonal antibodies. A highly sensitive cardiac troponin T (hs-cTnT) was further developed by replacing the mouse constant C1 region with a human IgG C1 region, thus producinging to a mouse-human chimeric

detection antibody. This replacement can reduce the susceptibility to interferences by heterophilic antibodies (HAMAs) (Katus, 2008).

Using the Fab fragments, the sensitivities of the TnT assays have rapidly improved. The European Society of Cardiology and the American College of cardiology (ESC/ACG) have recommended the 99th percentile of the reference population as a 'cut-off' value for AMI diagnosis. Moreover, a 10% coefficient of variation (CV) is the level of precision. For clinical validation of the hs-cTnT assay, Koerbin and co-workers determined cTnT concentration of 104 samples from a cardio-healthy population using the hs-cTnT assay. Results showed that the hs-cTnT assay met the recommended criteria of a 10% CV at the 99th percentile of the population studied (Koerbin *et al.,* 2010). However, Tate (2008) reported that the fourth generation cTnT assay have a 20% CV at the 99th percentile in clinical validation. Thus, its imprecision has failed to meet the recommended level (Tate, 2008). Panteghini and co-workers also reported that the current troponin assay had not achieved the 10% CV at the 99th percentile by testing with eight serum pools (Panteghini, 2004). The development of new cTnT assays remains as a great challenge due to the limited number of available formats and their failure to meet recommended standards. Hence, it was hoped that the use of recombinant antibodies and a novel assay platform may introduce significant improvements for cTnT assay development.

1.3 Recombinant antibody technology

1.3.1 The immune system and antibodies

The immune system is the body's defence against infectious organisms and other foreign particles. It protects the body by using a network of cells, proteins, tissues and organs. Two fluid systems of the body, the blood system and lymph system, transport the agents of the immune system to various locations of the body. The blood system is

composed of liquid plasma and blood cells. These include erythrocytes (red blood cell), leukocytes (white blood cells) and thrombocytes (platelets). A subdivision of leukocytes, lymophocytes, consists of B and T cells. These cells circulate in both the blood and lymph system and generally are located in the lymphoid organs. The bean-shaped lymph nodes are often the location where the antigens are recognised by the immune system. Lymph organs include bone marrow, the thymus gland, adenoids, tonsils, spleen, lymph nodes and the appendix. The primary lymph organs, bone marrow and the thymus gland, are responsible to a large degree for the production of lymphocytes. Mature lymphocytes circulate in both the blood and lymph systems. Secondary lymph organs maintain mature naive lymphocytes and initiate an adaptive immune response allowing the activation of lymphocytes when foreign pathogens are encountered.

The classification of immune responses is based on their characteristics. For example, whether they are innate or acquired, have self or non-self recognition, are specific or general, cell mediated or humoral, primary or secondary. The innate and the acquired systems are two major divisions of the immune system although in reality they are very closely connected.

The innate immune system is a non-specific genetically derived system passed on from mother to offspring, which consists of physical barriers, mucous membranes, and internal mechanisms. Skin, as primary physical barrier, prevents the penetration of various micro-organisms by its physical presence, its acidic environment and secretions from hair follicles. Innate immunity involves a collection of immune cells including macrophages, neutrophils, eosinophils, natural killer cells, and dendritic cells. Each of these cells binds to antigens using pattern-recognition factors which results in the basic defence mechanisms of the innate response including phagocytosis and inflammation.

Phagocytosis is a process that involves engulfment and destruction of infectious organisms and other foreign particles by phagocytes. In cell-mediated immunity, phagocytes, such as macrophages, secrete lymphokines that encourage cytotoxic T cells and B cells to grow and divide. Lymphokines also attract neutrophils and increase the capacity of macrophages to engulf and destroy infectious organisms.

Acquired immunity is a specific immune response stimulated by a foreign substance. It is subdivided into cell-mediated immunity and humoral immunity. T lymphocyte precursors are produced in the bone marrow but mature in the thymus and constitute the basis of cell-mediated immunity. Cytotoxic T cells lyse antigens by secreting lymphotoxins and other factors or by inducing apoptosis. B lymphocytes are derived from the stem cells of the bone marrow and are selected for immune tolerance by clonal selection before maturing in the plasma. The mature plasma B cells can produce highly specific antibodies at a rate of 2000 molecules per second for four to five days.

Antibodies, also known as immunoglobins (Ig), are soluble glycoproteins, produced by the plasma B cells, to identify and inactive foreign substances, such as bacteria and viruses. Antibodies may inactivate antigens generally through four types of biochemical processes, i.e. complement fixation; neutralization; clumping of antigens by agglutination or in activation/removal by precipitation.

An immunoglobin monomer is the basic functional unit of each antibody. It is a 'Y' shaped molecule consisting of two identical heavy chains (V_H ~ 50 kD) and two identical light chains (V_L ~ 25 kD) linked by disulfide bonds and non-covalent interactions (Fig. 1.5). The heavy chains have one variable domain and three constant domains. The light chains consist of one variable domain and one constant domain. Antibodies of the same isotype have the same constant domain. Antibodies produced by

different B cells have different variable domains. The variable domain of each heavy chain consists of approximately 110 amino acids. The light chain consists of one variable domain and one constant domain. The variability of the antigen binding site is located in the complementary-determining regions (CDRs), subdivided into CDR-1, CDR-2, and CDR-3 (Janeway *et al.*, 2001).

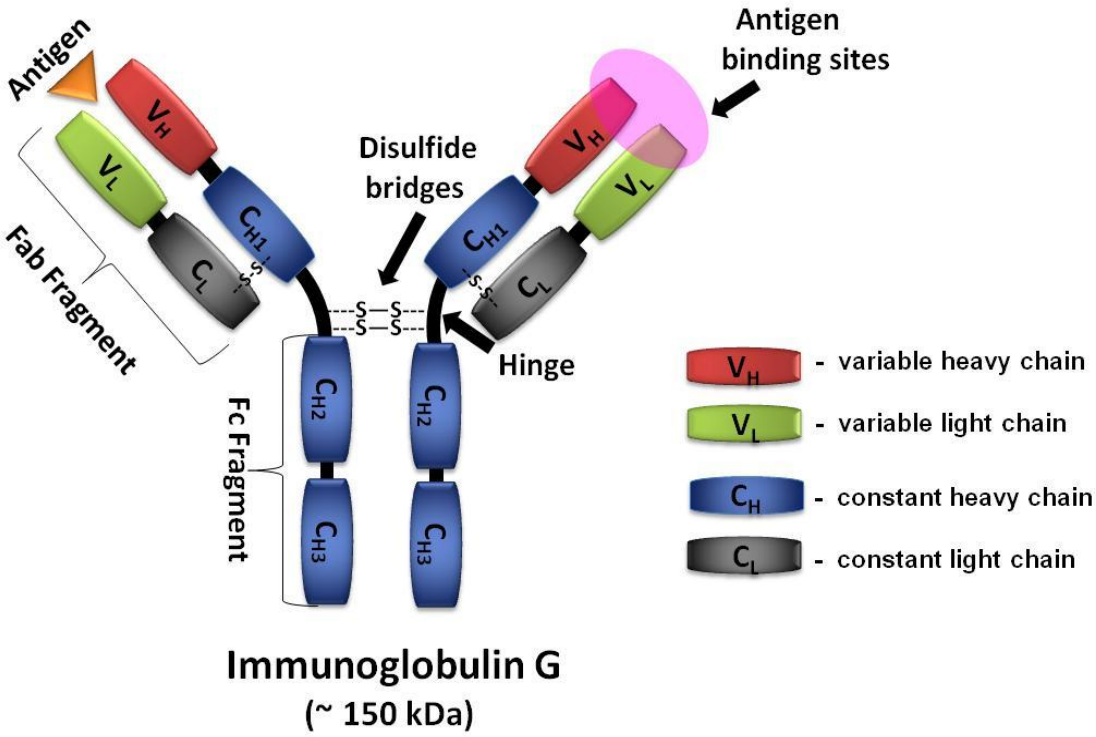

Figure 1.5. Structure of Immunoglobulin G (IgG). IgG (150 kD) consists of two heavy chains (50 kD) and two light chains (25 kD) which are linked by disulphide bonds. The light chain consists of a variable domain (V_L) and a constant domain (C_L). The heavy chain consists of a variable chain (V_H) and three constant chains (C_{H1}, C_{H2} and C_{H3}). The two heavy chains are linked by disulfide bonds in the hinge region. The antigen binding sites are located on the V_L and V_H domains (Gabrielli *et al.*, 2009).

Antibodies are divided into five groups based on the number of Y units and the type of heavy chain. The five groups are IgG, IgA, IgM, IgD and IgE (Table 1.4). IgG is a 150 kD monomer and it is the most common type of antibody in the blood. It constitutes approximately 75% of the total serum Ig and its relative abundance and excellent specificity toward the antigen has made it the principal antibody used in immunological research and clinical diagnosis. Human IgG consists of four subclasses, named IgG1, IgG2, IgG3 and IgG4. The four subclasses have 90% to 95% similarity with each other in the constant region. IgM is a 950 kD pentameric antibody and appears in the primary response after immunisation. It is the most effective 'complement-fixing' immunoglobin and comprises approximately 10% of normal human serum Ig content. IgA, comprising approximately 13% of the total serum Ig, can be monomeric or dimeric and is found in saliva, tears, nasal mucosa, prostatic fluid and many other bodily fluids. IgD is monomeric antibody and is found on the surface of B cells. IgE is 200 kD antibody in the monomeric form and triggers allergic reactions. Antibodies can be classified into subclasses based on the minor differences in the heavy chain type of each Ig class, in addition to the major antibodies classes (Alberts *et al.,* 2002).

Table 1.4. Antibody classification and characterisation

	Structure	Size	Constitution in serum	Subclasses (Isotopes)	Function
IgG	Monomer	150 kD	75% (12.5 mg/mL)	IgG1, IgG2, IgG3, IgG4	Entering tissue spaces and primarily binding antigens
IgA	Dimer	160 kD	13% (2.1 mg/mL)	-----	Concentrating in body fluids to guard the entrances of the body
IgM	Pentamer	950 kD	10% (1.25 mg/mL)	IgA1, IgA2	First appears during an immune response and first formed by developing foetus
IgD	Monomer	175 kD	< 1% (40 μg/mL)	-----	Regulating B cell's activities
IgE	Monomer	190 kD	< 0.003 % (0.4 μg/mL)	-----	Fc parts binds to mast cells and basophils and trigger allergic reactions; protection against parasitic worms

Both the light and heavy chains of an immunoglobin are encoded by multigene families located on the different chromosomes. The light chain family contains L (leader), V (variable), J (junctional) and C (constant) regions. The heavy chain family contains the same regions with an additional D (diversity) region. Antibody diversity is generated by the rearrangement of these segments in the developing B cells. There are slight differences of sequence rearrangements between light and heavy chains. In the light chains, the V and J segments are initially combined together, then preceded by an L segment and followed by an intron sequence and a C segment. However, in heavy chains, the D segment is combined with the J segment initially, and then this DJ segment is combined with the V segment to form the complete heavy chain VDJ

domain. The VDJ is finally joined to the C segment by RNA splicing after transcription (Fig. 1.6).

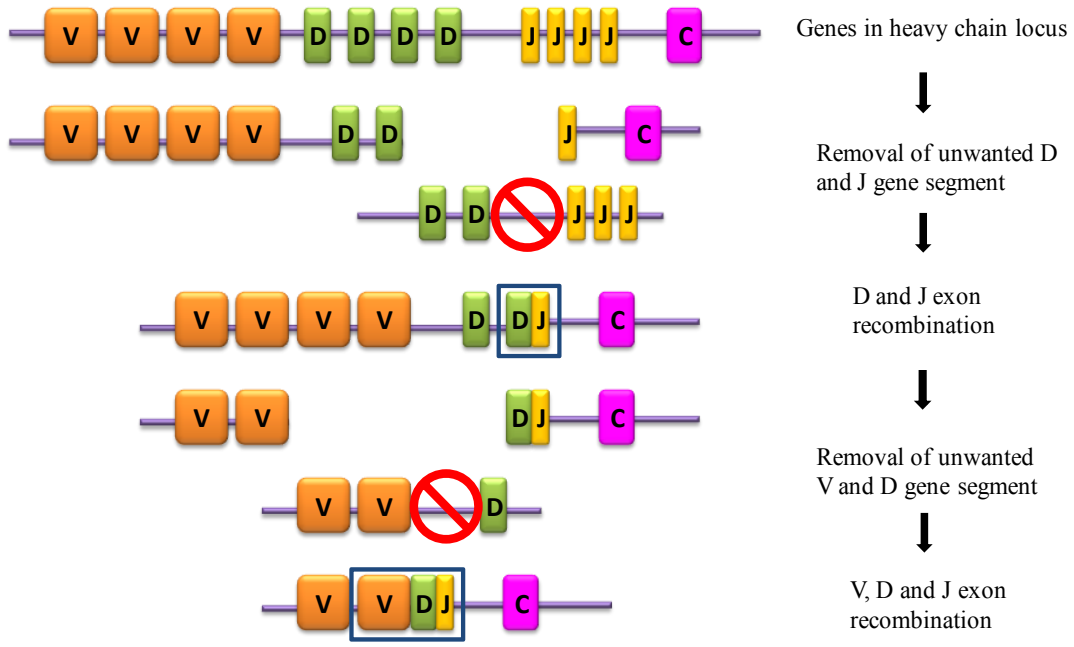

Figure 1.6. Recombinational arrangement of the DNA encoding variable (V), diversity (D), junction (J) and constant (C) regions of an immunoglobulin heavy chain. The rearranged chain is transcribed into messager RNA and translated into the heavy chain. (Based on references: Abbas and Lichtman, 2003; Costanzo *et al.*, 2009)

1.3.2 Polyclonal antibody generation

Antibodies have become vitally important as research tools for a range of applications due to their ability to bind, recognise and determine a range of different antigens including many biomarkers. Polyclonal and monoclonal antibodies are the basic forms of antibodies commonly used in analysis.

Polyclonal antibodies are generally purified direct from serum collected from animal hosts immunised with the desired antigens. The heterogeneous immunological response

elicited from an antigen produces different cell lines of B-lymphocytes which originated from common stem cells. Polyclonal antibodies produced by these different B-lymphocytes recognise different epitopes on an antigen. A number of different animal species can be used as hosts for polyclonal antibody production, such as rabbits, chicken, rats, goats, sheep, horses and guinea pigs. (Stills, 1994). For laboratory use, rabbits are excellent due to their capacity for producing sufficient antibody in a relative short period of time as well as the size which facilitates handing. Goats are also excellent hosts due to the large volume of serum generated as well as the ease and relatively low cost of maintaining goat herds for long periods of time. Chickens are suitable hosts owing to their phylogenetic distance from mammals, which may be beneficial for the production of antibodies to certain mammalian proteins. Chicken egg yolk contains large quantities of antibodies up to 60 mg per egg (Pauly *et al.,* 2011). Therefore, harvesting antibodies from eggs eliminates the need for invasive bleeding. The procedure for polyclonal antibody production is outlined in Figure 1.7. Polyclonal antibody preparations are used in a range of applications especially when labeled with an enzyme or chromophore (Waggoner, 2006).

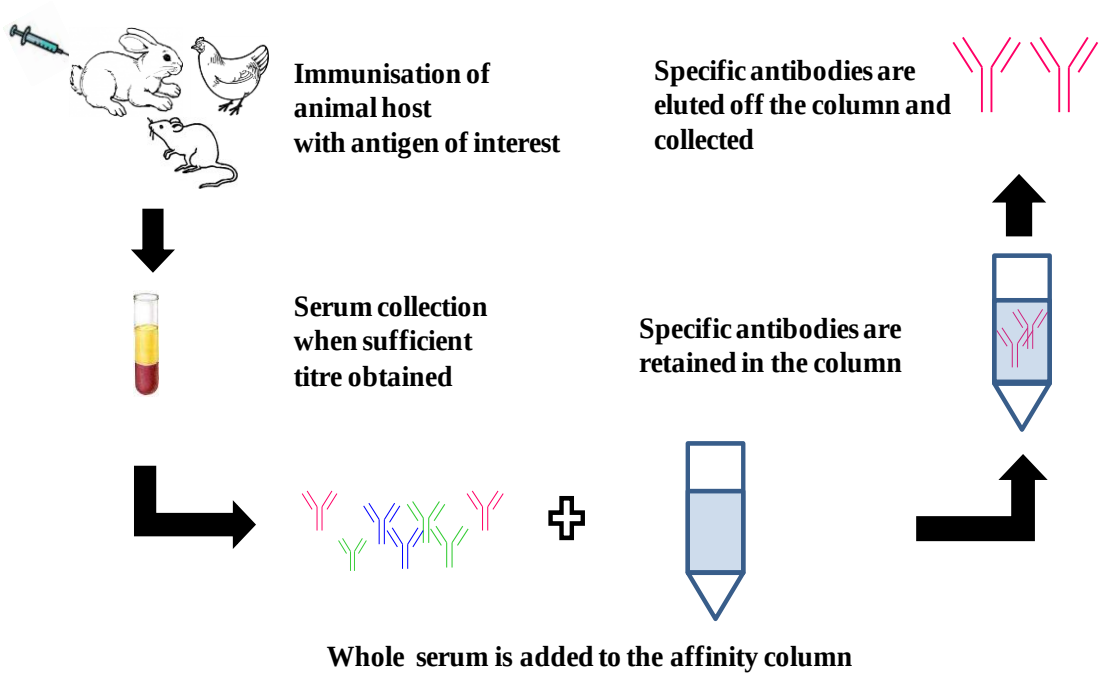

Figure 1.7. Polyclonal antibody generation and purification. Polyclonal antibody production requires the immunisation of animal hosts with the antigen of interest. Once a sufficient antibody immune response titre is obtained, serum containing polyclonal antibodies is collected. Polyclonal antibodies may be purified using affinity column chromatography.

1.3.3 Monoclonal antibody generation

Monoclonal antibodies are produced by an individual B-lymphocyte clone. They have a single defined specificity as they recognise and bind to the same unique epitope on the antigen. Cells from the spleen and lymph nodes from immunised animals are the sources used to isolate B-lymphocytes. The isolated B-lymphocytes are fused with myeloma cells creating a monoclonal hybrid cell line or hybridoma (Fig. 1.8). The production of antibodies using a monoclonal hybrid cell line ensures that the antibodies bind to the same epitope on antigens. In addition, the hybridoma is a constant and renewable antibody source so that antibodies produced from every batch are identical.

However, it is an expensive and time-consuming process, and the antibodies generated sometimes show cross-reactivity with unrelated antigens (Sun *et al.*, 2001).

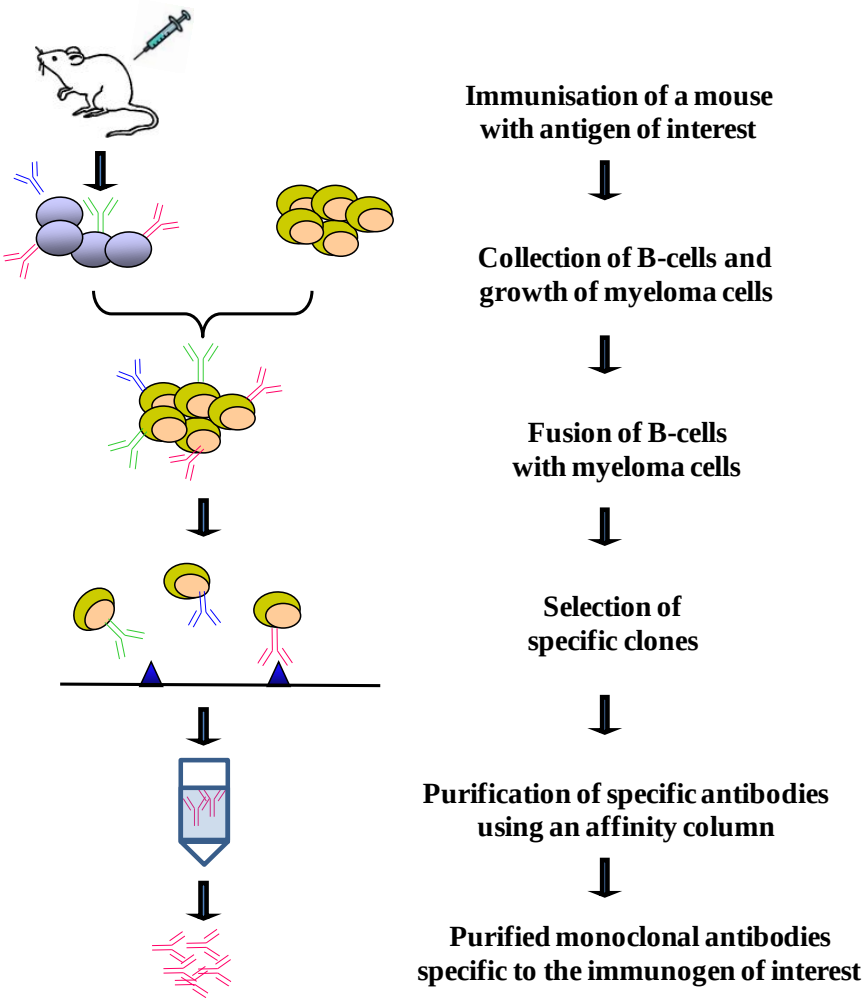

Figure 1.8. Monoclonal antibody generation using hybridoma technology. The production of monoclonal antibodies starts with the immunisation of mice with an antigen of interest. Antibody response is monitored throughout the immunisation process. B-lymphocytes are isolated when a sufficient serum antibody response is obtained. Addition of polyethylene glycol facilitates the fusion of B-lymphocytes with myeloma cells. Fused cells are grown in a selective media, selected and cloned out and monoclonal antibodies produced by selected fused cells can be purified using affinity chromatography with protein A or G.

1.3.4 Recombinant antibody generation

Recombinant antibodies are derived from the mRNA of B-lymphocytes, generating antibodies to immunised antigens, or from antibody libraries, using molecular biological techniques. They can be the whole IgG antibodies or fragments of antibodies. Nowadays, recombinant antibodies have become extremely important tools in various biomedical research applications. The antigen recognition binding sites are located in the complementary-determining regions (CDRs) on the variable regions of antibodies. By reformatting the heavy and light chain fragments of antibodies, recombinant antibodies with improved antigen-binding capacities can be constructed. Recombinant antibodies retain the recognition capacities of their parental antibody. Furthermore, due to the smaller molecular size, antibody fragments can often localise antigens more precisely than intact IgG. Antibody fragments are, therefore, widely used for both diagnosis and therapeutic purposes. Two commonly chosen formats of recombinant antibodies are the single chain fragment variable (scFv) and antigen binding fragment (Fab) (Fig. 1.9) (Hudson, 1998).

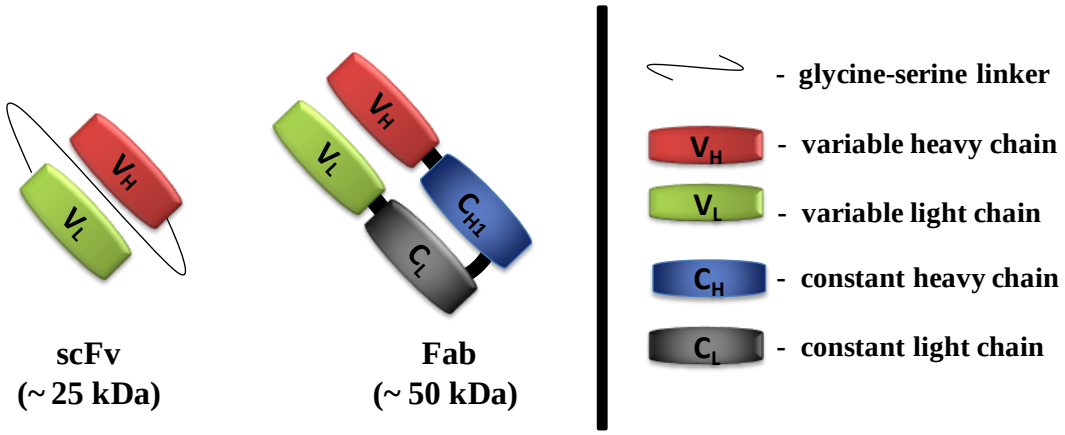

Figure 1.9 Commonly used recombinant antibody fragments. A scFv contains a V_H domain and a V_L domain linked by a peptide linker. The Fab contains a V_H domain and a fragment of the constant domain (C_HI) paired with V_L and the light chain constant domain (C_L).

Generation of recombinant antibodies requires the construction of antibody libraries and the selection of specific antibodies from those libraries. In general, three types of antibody libraries can be constructed: naive libraries, synthetic libraries and immune libraries. Naive libraries are produced from non-immunised animals. Theoretically, they can be used for the selection of antibodies against an unlimited range of antigens. However, a very large library size is required to obtain antibodies with high affinities (Carmen and Jermytus, 2002). Synthetic libraries are constructed by *in vitro* assembly of V_L and V_H genes thus introducing artificial CDR domains by altering the loop lengths using PCR and randomising oligonucleotide primers. Antibodies with moderate affinities are normally selected from synthetic libraries and a very large library size is also beneficial to enhance the likelihood for the selection of antibody with the required sensitivity and specificity (Hong and Kim, 2002). In contrast to non-immunised libraries, immune libraries require the immunisation of the target antigen into animal hosts. This approach is designed to increase the capacity of the libraries to possess high

affinity antibodies with the desired sensitivity for the target antigens (Carmen and Jermutus, 2002). An immune library should have at least 10^8 individual antibody-containing clones thus giving the possibility of selection of antibodies of the desired specificity. Phage display will subsequently allow selection of high affinity antibodies from millions of antibody variants (Fig. 1.10) (Okamoto et al., 2004).

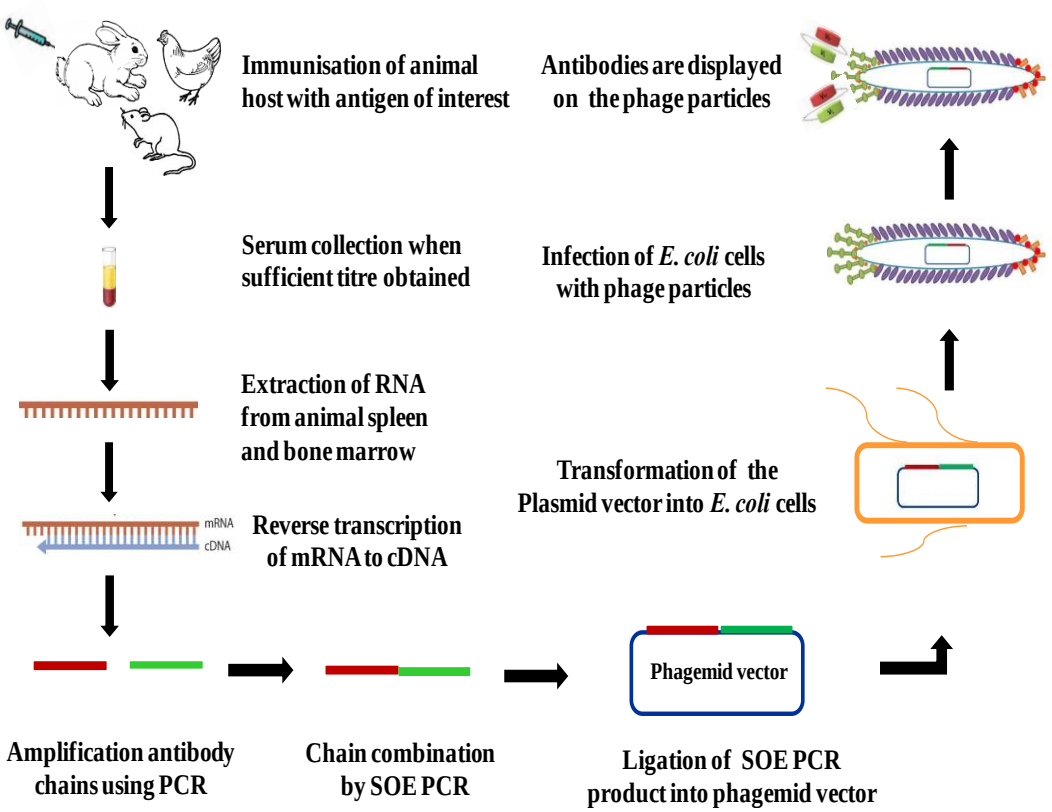

Figure 1.10. Construction of immune recombinant antibody library and selection of recombinant antibody by phage display. The production of recombinant antibodies starts with the immunisation of an animal host with the antigen of interest. Antibody responses are monitored throughout the immunisation process. Total RNA is extracted from the animal spleen and bone marrow once a sufficient antibody response is obtained. cDNA, which encodes antibody genes, are produced by reverse transcript of mRNA. Antibody chain genes are subsequently amplified using PCR followed by ligation into phagemid vectors. The ligation product is transformed into *E.coli* cells and phage particles are subsequently infected into the *E. coli* cells. Antibody fragments can be expressed and displayed on the surface protein of the phage particles (e.g. PIII) and specific antibody fragments can ultimately be selected by the biopanning process.

1.3.5 Phage display technology

Phage display is an extremely powerful tool for selecting peptides, proteins and antibodies with specific binding affinities from a large number of variants. This technique, first introduced by Smith in 1985, allows display of polypeptides on the surface of filamentous phage by fusing a foreign gene fragment on to gene III of filamentous phage (Smith, 1985; Winter *et al.,* 1994). Phage display provides a direct linkage between genotype and phenotype. While fusing a foreign DNA fragment with phage genome, the coat proteins of a phage particle must tolerate this foreign fusion without changing their properties. The foreign protein can thus be displayed on the phage particle with the aid of the coat proteins (Kay and Hoess, 1996; Bradbury and Marks, 2004). Phage displays allow the generation of vast numbers of variants. Typically, the infected phages number can reach to 10^{11} to 10^{12} per ml after continuous generations. This feature enables the construction of large antibody libraries with the required diversity, and an antibody with the required affinity can consequently be selected using biopanning.

1.3.5.1 Phage particles

Bacteriophages, first reported by Frederick in 1915 and Felix d'Herelle in 1917, are a class of viruses that contain a circular single-stranded DNA genome encased in a long protein capsid cylinder (Fig. 1.11). The Ff class phage (f1, fd and M13) is approximately 6.5 nm in diameter and 930 nm in length, containing a single-stranded DNA molecule of approximately 6400 nucleotides base pairs in length. The capsid cylinder contains about 2700 molecules of the geneVIII protein (pVIII). Other coat proteins such as gene VII (pVII) , gene IX (pIX), gene III (pIII) and gene VI (pVI) are present at the end of the phage particle. They use the tip of the F conjugative pilus as a receptor. Therefore, they are specific for *E. coli* containing the F pilus (Grossman *et al.,* 1990).

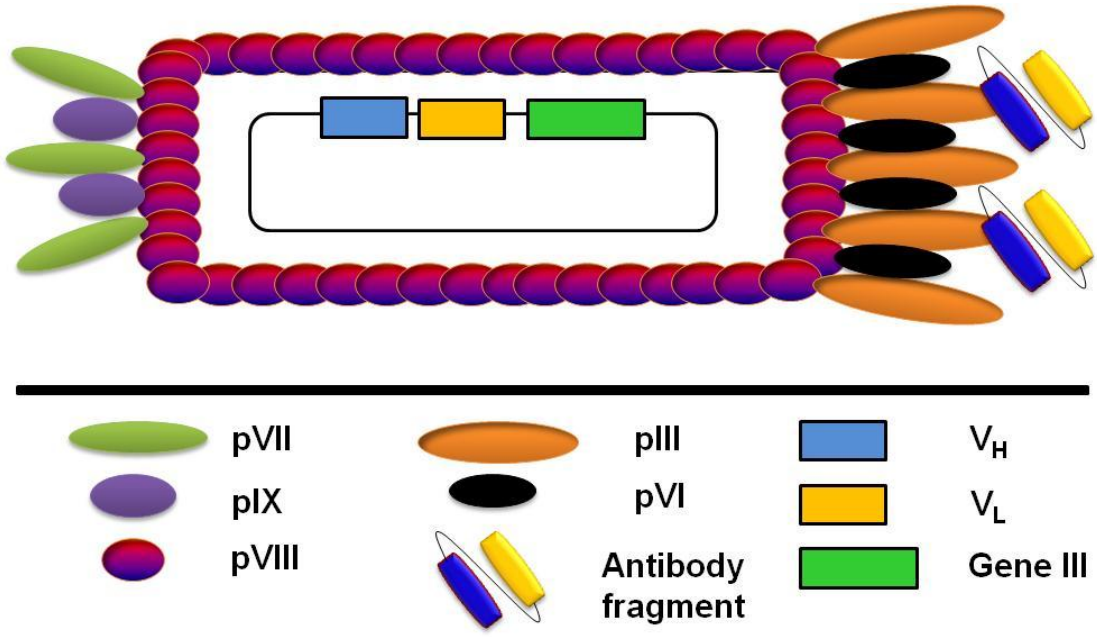

Figure 1.11. Structure of a filamentous phage particle. A filamentous phage particle contains a single strand DNA (gene III) encapsulated in major coat protein pVIII and manor coat proteins pIII, pVI, pVII and pIX. Antibody gene segments (V_H and V_L) are fused with gene III and antibodies can subsequently be expressed and displayed on the pIII coat protein.

pIII protein contains two N-terminal domains (N1 and N2) and one C-terminal domain (CT). N1 interacts with the TolA protein of the TolQRA complex located at the periplasmic space between the inner and outer *E. coli* membranes. The TolQRA complex is responsible for the phage infection and the translocation of single strand phage DNA into the cytoplasm. The infection of phage into bacteria cells is initiated by the binding of the tip of the F pilus to the N2 domain of the phage protein. Once the F pilus binds to the N2, N1 is isolated from N2 and interacts with the co-receptor for phage binding domain 3 of TolA (TolA-D3). Soluble TolA-D3 which is presented in the

periplasm inhibits the phage infection process. Due to the single strand phage DNA is translocated into the cytoplasm, other proteins, including the major capsid pVIII protein and minor proteins pVII and pIX, are subsequently disassembled into the cytoplasmic membrane. The complementary DNA strand of the phage DNA is synthesised and the phage DNA is subsequently converted into a supercoiled, double-stranded DNA. The double-stranded DNA serves as a template for phage gene expression. After protein synthesis and assembly processes, the coat proteins including the major capsid protein pVIII (as well as pVII and pIX) are fused with antibody light and heavy variable regions resulting in their display on the surface of phage particles. Consequently, biopanning allows the selection of phage particles with specific antibody fragments displayed on their surfaces through their binding with the immobilised target antigen (Gaskin *et al.,* 2001).

1.3.5.2 Phage vector systems

Phage vectors and phagemid vectors are two different systems which have been developed for the expression of gene III and antibody fusion proteins. The differences between the two vector systems include the types of coat protein used for protein display, the fractions of the protein to be displayed and the location where recombinant fusion occurs (Paschke, 2006). Phage vectors are directly derived from the phage genome encoding all proteins required for the replication and assembly of the phage particles. Using these vectors, libraries are cloned as a fusion with the coat protein originally present in the phage genome (Scott and Smith, 1990; Kay *et al.,* 1993) or inserted as fusion gene cassette with an additional copy of the coat protein. M13KE is a wild-type phage genome with a slight modification on the coat protein PIII, so that it can carry restriction sites to facilitate gene cloning (Zacher *et al.,* 1980). Phagemid vectors contain both phage and plasmid origins of DNA replication. The fusion protein expression is independent of the phage genome. They replicate as plasmids in *E. coli,* and

they can also be packaged as phage particles in the presence of helper phage. Helper phage provides the necessary structural proteins that encapsulate both the help-phage and phagemid genomes. The phagemid carries an expression cassette that encodes the fusion-coat protein to be displayed.

1.3.5.3 Biopanning process

In general, an antibody library contains millions of different antibodies. The selection against the desired target molecules is achieved by iterative cycles of biopanning (Fig 1.12). Biopanning is typically performed by re-amplifying a phage library by growing it in an appropriate media. The phage library, containing phage-displayed antibodies, is incubated with the target molecule of interest, which is immobilised on either a polystyrene plate or on paramagnetic beads. The phage-displayed antibodies are allowed to bind to the immobilised target. The unbound phage are washed away and the bound phage are eluted with an appropriate solution. The eluted phage are then re-amplified and subjected to next round of biopanning. A few additional cycles of binding and amplification are performed to enrich for higher affinity clones which have the ability to bind to the desired target. Typically, it takes from two to four rounds of biopanning to obtain a target with the desired affinity (Yuan *et al.*, 2006).

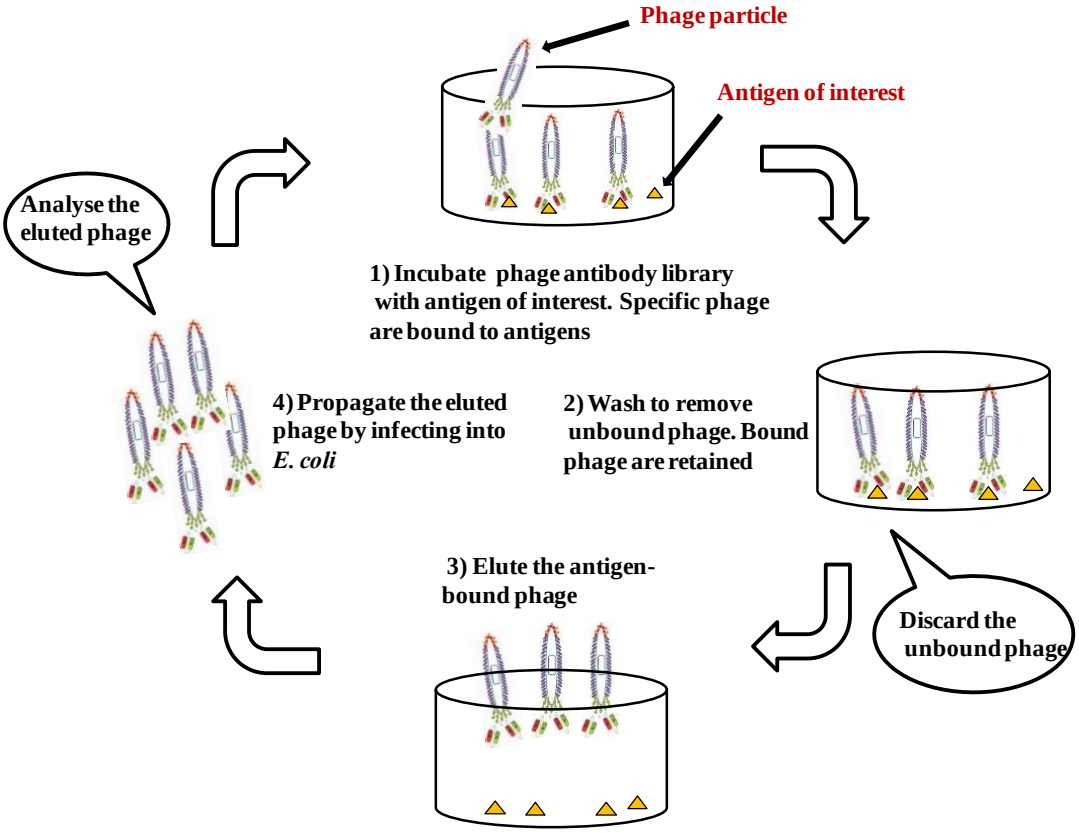

Figure 1.12 Biopanning cycle. Four steps are commonly involved in a biopanning cycle, labeled 1 to 4 in the Figure. In step 1, the phage library is incubated with the target antigen to allow binding of specific antibodies. In step 2, bound phage are retained and unbound phage particles are removed by washing. In step 3, antigen-bound phage particles are eluted and analysed. In step 4, eluted phage particles are infected into *E. coli* cells for propagation. Typically, four to six rounds of panning are required to obtain antigen-specific antibodies.

1.4 Mastitis

1.4.1 Introduction to mastitis

The second disease involved in this study is mastitis. Mastitis is an inflammation of the mammary gland and is the major disease affecting dairy cattle worldwide. This inflammation can be caused by microbial organisms or non-infectious sources such as physical injury. Organisms such as bacteria, viruses, fungi, mycoplasma and chlamydia have been found to be the causative agents (Watts, 1988; Radostits *et al.,* 1994). Over 159 different types of microbial species have been identified as pathogens for mastitis (Kuang *et al.,* 2009) and the majority are bacteria. The major infectious bacterial strains are *Streptococcus agalactiae*, *Staphylococcus aureus and Escherichia coli.* Fungi, viruses and yeast are also frequently found in infected udders (Wellenberg, 2002; Vimalraj *et al.,* 2006; Marques *et al.,* 2008). Although intensive studies have been performed on mastitis aetiology, up to 20 to 35% mastitis-causing pathogens have not yet been identified (Miltenburg *et al.,* 1996; Wedderkopp, 1997; Viguier *et al.,* 2009).

Mastitis affects approximately 30% of dairy cows worldwide annually. In addition, mastitis cost the EU dairy industry approximately €1.55 billion in 2005 (Hillerton and Berry, 2005). In the US, annual expenditure on mastitis is over $1.5 billion. In the UK, it was estimated that the average cost of a case of clinical mastitis dairy industry was £175 (Kossaibati, 2000). In Ireland, mastitis affects approximately 25% of Irish cows every year. Each mastitis incidence costs approximately €72 per cow (Berry and Amer, 2005). Mastitis is also the leading cause of death in adult dairy cows (Esslemont and Kossaibati, 1997). Bradley and Green reported that in the UK 0.6% of lactating cows died from mastitis (Bradley and Green, 2001a). In addition to the high economic losses and cow mortality, mastitis also lead to reduced productive-lives of cows, reduced milk yield, and altered milk composition which affects the quality of milk and its by-products.

1.4.2 Pathogenesis of mastitis

Mastitis starts when bacteria enter the mammary gland through the teat canal. Bacteria propagate in the udder and secrete toxins which can cause damage within the udder and leukocytes are then produced. These cause a change in milk composition and also affect milk quality and production.

Generally, the teat canal acts as the primary defence-line for mastitis infection. The teat is surrounded by a sphincter of smooth muscle which keeps the teat canal tightly closed and forms a physical barrier preventing bacterial invasion (Murphy *et al.,* 1988). Inside the teat canal, keratin also prevents the invasion of pathogens.

Once bacteria enter the teat canal, they start growing and multiplying. A number of enzymes are released by the bacterial cells and these enzymes cause leukocytes and epithelial cells to release factors, such as tumor necrosis factor-α, interleukin 8, interleukin 1, eicosanoids, oxygen radicals and acute phase proteins (Dohoo and Leslie, 1991). These chemoattactants then stimulate polymorphonuclear neutrophils (PMNs), attracting them to migrate to the sites of infection. At the sites of infection, PMNs release hydroxyl and oxygen radicals thus destroying the bacteria and some of the epithelial cells. Enzymes such as LDH and NAGase are also released by leukocytes and epithelial cells during this process (Viguier *et al.,* 2009).

1.4.3 Types of mastitis

Mastitis generally can be classified into two major groups: contagious mastitis and environmental mastitis. Contagious mastitis is the major type, which is caused by the infection by bacteria near the teat canal or inside the canal. This type of infection can be transmitted between cows during milking. In contrast, environmental mastitis is caused by pathogens from a contaminated environment, for example, from bedding or feeding

materials. This is a minor source of infection and it is only accounts for around 10% of the total incidence of mastitis.

Contagious mastitis can be subdivided into three groups: clinical mastitis, sub-clinical mastitis and chronic mastitis (Table 1.5). For clinical mastitis, visible indications can be observed from either the infected grand, the milk or from systemic symptoms (temperature, lost of weight), whereas, no obvious changes can be observed for sub-clinical mastitis and chronic mastitis. Clinical mastitis is further divided into pre-acute, acute and sub-acute mastitis based on the visible indications.

Table 1.5. Classification and characterisation of contagious mastitis

Contagious mastitis	Characterisation
Clinical mastitis - ***Pre-acute mastitis***	• Can be identified by the appearance of inflammation in the udder, such as redness and swelling • Changes in milk appearance (watery, flaky, clotting) • Symptoms of cows: fever, low appetite, lost of weight
- ***Acute mastitis***	• Still have visible signs of udder inflammation and alternations in milk appearance • Have less symptoms
- ***Sub-acute mastitis***	• Have minimum inflammation of udder • Have no visible symptoms
Sub-clinical mastitis	• Have no visible signs of udder inflammation • Have no visible systemic symptoms
Chronic mastitis	• Long-term infection process may last for months • No visible signs of udder inflammation, milk appearance and symptoms

(Based on references: Erskine *et al.,* 1988; Hogeveen, 2005; Abdel-Rady and Sayed, 2009)

1.4.4 Current detection approaches for sub-clinical mastitis

A number of approaches have been developed for the detection of sub-clinical mastitis and the majority of the approaches are based on the measurement of the number of somatic cells. Somatic cells, also termed white blood cells or leucocytes, play an important role in the immune response to infection with mastitis. Somatic cells can minimise bacterial infection and eventually eliminate the infection by phagocytosis. Somatic cell count (SCC) represents the number of somatic cells in milk samples, and it is reported as cells per ml of milk. SCC levels in milk can be used for detecting sub-clinical mastitis in cows (Fosmire and Timasheff, 1972). It is suggested that if the SCC exceeds 200,000 cells/mL in a milk sample, the udder quarter is likely to be infected by mastitis-causing pathogens (Fox and Kelly, 2006). Currently, a number of tests, base on SCC levels, are widely used for the diagnosis sub-clinical mastitic udders. These include, for example, the Portacheck® milk test, the Fossomatic™ SCC test and the California Mastitis Test (CMT).

The Portacheck® milk test is a portable assay kit. It contains the PortaSCC® digital reader that can be used to conduct a 'cow-side' determination of SCC within 45 minutes. In this test, enzymes found in the somatic cells can react with a dye on the test strip provided in the kit. The reaction turns the test strip from pink to blue; the darker the blue colour, the higher the SCC levels. The darkness of colour can then be determined using the PortaSCC® digital reader. The digital reader correlates the darkness of the colour to SCC and the reader output shows the SCC levels in milk samples. The Portacheck® milk test is widely used for the determination of SCC due to its low cost. However, it has limited sensitivity when SCC levels are low (Viguier *et al.*, 2009).

In comparison to Portacheck® milk test, the Fossomatic™ SCC has higher sensitivity. It is based on the measurement of optical fluorescence levels which are generated from the

interaction between ethidium bromide and nuclear DNA of somatic cells (Gonzalo *et al,* 2003). The detection is rapid and automated, however, the device is expensive and it is limited in relation to 'on-site' diagnosis.

The California Mastitis Test (CMT) is also based on the detection of SCC. The test reagents in CMT are bromocresol purple-containing detergents. They can disrupt the cell membrane of somatic cells, and subsequently interact with the DNA of somatic cells thus forming a 'gel-like' matrix. The size of the gel is proportion to the quantity of somatic cell present (Schalm and Noorlander, 1957). Although the gel-forming reaction only takes 10 seconds, the gel matrix disappears within 20 seconds. Therefore, the output data needs to be recorded immediately. This test is simple, inexpensive, rapid and is capable of being used 'on-site'. However, repeated tests may be required to obtain accurate data.

1.4.5 Enzymatic biomarkers for mastitis

Currently available assays for the detection of sub-clinical mastitis usually involve the determination of SCC as described in section 1.4.4. Compared to the SCC-based tests, antibody-based diagnostic approaches offer a number of distinct advantages. Antibodies involved in an immunoassay are developed against a specific antigen and, therefore, the assay is generally highly specific. Furthermore, a wide range of detection methods can be applied in the immunoassay, including enzymatic, radioactive-labeling, fluorescence, luminescence and electrochemical approaches. The antibody-antigen interactions can also be incorporated into different assay platforms such as lateral flow strips, ELISA, Biacore^{TM} chips or immuno-PCR. N-acetyl-β-D-glucosaminidase (NAGase) and Lactate dehydrogenase (LDH) are enzymes released by damaged epithelial cells and leukocytes from the mammary gland. Both the LDH and NAGase may have potential as biomarkers for detection of sub-clinical mastitis (Zank and Schlatter, 1998).

NAGase hydrolyses N-acetyl-β-D-glucosamine residues from N-acetyl-β-D-glucosaminides, including glycoproteins and fragments of chitin. NAGase has two isoforms Hex A and Hex B. Hex A has a molecular weight 118 kDa and Hex B has a molecular weight 234 kDa (Friggens *et al.,* 2007). NAGase activity in milk was determined using a fluorometric assay (Guilbault, 1975; Kitchen *et al.,* 1984). However, Chagunda and co-workers (2006) found that NAGase may be less reliable than LDH as a marker of mastitis (Chagunda *et al.,* 2006).

1.4.6 Lactate dehydrogenase (LDH)

LDH is a ubiquitous enzyme which can be found in the cytoplasm of all cells and tissues in animals, as well as in yeasts and bacteria. It has five isoforms (LDH-1 to LDH-5) which are composed of combinations of two different subunits (Babaei *et al.,* 2007), each with a molecular weight of 35 kDa (Bakuev *et al.,* 1972, Huston *et al.,* 1972). The two forms of subunits of LDH are M and H (Bansal *et al.,* 2005). They are encoded by two different genes. Gene *LDHA* located on chromosome 11p15.4 encodes subunit M. Gene *LDHB* located on chromosome 12p12.2-p12.1, encodes subunit H. LDH-1 contains 4H subunits and is found in the heart. LDH-2 contains 3H subunits and 1M subunit and is the predominant form in serum. LDH-3 contains 2H subunits and 2M subunits and is found in the lungs. LDH-4 consists of 1H and 3M subunits and is found in the kidneys and LDH-5 consists of 4M subunits and is found in the liver. The isoforms differ in catalytic, physical and immunological properties (Chagunda *et al.,* 2005).

In living cells, LDH catalyses the reversible conversion of pyruvate to lactic acid in the absence of oxygen using nicotinamide-adenine dinucleotide (NADH) as a co-substrate. The equilibrium of this reaction strongly favours the reduction reaction, where pyruvate is converted to lactate (Drent *et al.,* 1996)

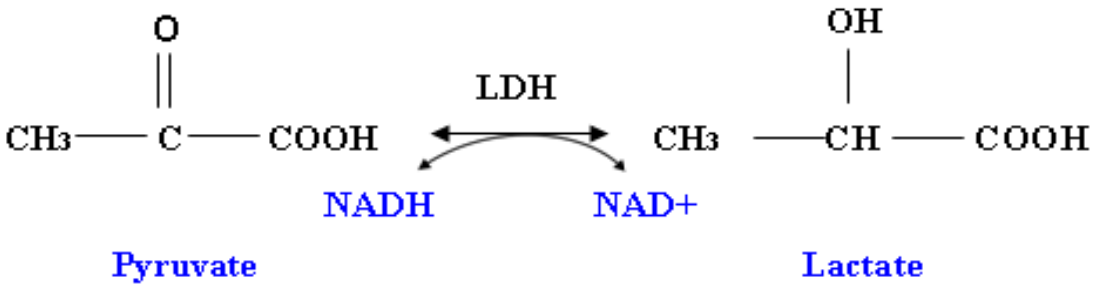

Normally, damage of body tissues can cause the increase of LDH levels in serum. LDH and its isoforms have been used as biomarkers for the detection of a number of diseases, such as cardiac necrosis (section 1.2.1) and lung inflammation (Drent *et al.,* 1996).

The stability of LDH in serum was studied by Jacobs and co-workers (Jacobs *et al.,* 1986). They found LDH-1 was stable at 25°C, 4°C and −20°C with less than 10% loss of activity. In contrast, LDH isoforms, -2 to 5, were stable at 4°C. Interestingly, they also reported that LDH-containing serum should be stored either frozen or at room temperature but not in a refrigerator (Jacobs *et al.,* 1986). Milk is a different matrix to serum, so the effects of storage temperature and storage time period on LDH stability in milk samples were investigated in this study.

1.5 Research aims

The first aim of the project was to generate and characterise recombinant antibodies against cardiac troponin T. Chickens were selected as the host for immunisation due to their phylogenetic distance from humans in order to generate a diverse anti-troponin T antibody library. Both phage display selection and automated high throughput screening technologies were used for the selection of specific antibodies and their characterisation. Affinity maturation of selected antibodies by heterogeneous chain shuffling yielded novel panels of recombined fragments with improved binding characteristics that were analysed by biomolecular interaction analysis technology. Antibodies produced in this project will eventually be integrated, with other anti-CVD biomarker antibodies, for the development of a multi-analyte CVD point-of-care device (e.g. an array or biochip).

The standard method for diagnosis of mastitis is to measure the somatic cell count in milk. However, this technique is limited in detection sensitivity for routine use in herds. In recent decades, indigenous L-lactate dehydrogenase (LDH) in milk has attracted much attention as a potential indicator of mastitis. The second aim of this project was to identify the effectiveness of LDH as a mastitis biomarker by measuring its levels in both healthy and mastitic milk samples using a standardized fluorescence-based assay. The correlation of LDH levels with other markers of mastitis (SCC and NAGase) in milk samples was also to be analysed. Moreover, the effect of storage and handling on LDH activity in milk samples was also investigated.

Chapter 2
Materials and Methods

2.1 Materials

The materials section consists of reagents, consumable labware, commercial kits, culture compositions, buffer compositions and bacterial strains.

2.1.1 Reagents

All reagents were of analytical grade and purchased from Sigma-Aldrich Ireland Ltd. (Dublin, Ireland). Reagents were purchased from other suppliers are listed in Table 2.1.

Table 2.1. Reagents used and their suppliers

Reagents	Suppliers
Human cardiac troponin T **Human skeletal troponin T** **Human cardiac troponin I** **Human skeletal troponin I**	Life Diagnostics, Inc., West Chester PA 19380, USA.
Mouse anti-cTnT **monoclonal antibody**	HyTest Ltd., Joukahaisenkatu 6, 20520, Turku, Finland.
Mouse anti-M13 monoclonal **antibody, HRP conjugated**	GE Healthcare Bio-Sciences AB, SE-751 84 Uppsala, Sweden.
Mouse anti-HA monoclonal **antibody, HRP conjugated**	Roche Diagnostics Ltd., Grenzacherstrasse 124, Basel 4070, Switzerland.
Rabbit anti-HA epitope tag **polyclonal antibody**	Thermo Fisher Scientific, 25/28 North Wall Quay, Dublin 1, Ireland.
Bacteriological agar **Yeast extract**	Cruinn Diagnostics Ltd., Hume Center, Parkwest Business Park,

Typtone	Nangor Road, Dublin 12, Ireland.
Chicken PCR primers	Eurofins MWG Operon, 318 Worple Road, Raynes Park, London, SW 20, 8QU, UK.
T4 DNA ligase **M13KO7 Helper phage** ***Alu*I/*Sfi*I restriction enzymes**	ISIS Ltd., Unit 1 & 2, Ballywaltrim Business Centre, Boghall Road, Bray, Co. Wicklow, Ireland.
Deoxynucleotide Triphosphates (dNTP) **Go Taq® DNA polymerase** **Fusion Taq® DNA polymerase**	Medical Supply Company Ltd., Damastown, Mulhuddart, Dublin 15, Ireland.
RNaseZAP® solution **Sodium acetate (3M, pH 5.2)**	Applied Biosystems/Ambion. Inc., Lingley House, 120 Birchwood Boulevard, Warrington, WA3 &QH, UK
Pellet paint® NF co-precipitant	Merck Millpore Ltd., 4045 Kingswood Road, Citywest Business Campus, Dublin 24, Ireland.
Industrial methylated spirits (IMS)	Lennox Laboratory Supplies Ltd., John F. Kennedy Drive, Naas Road, Dublin 12, Ireland.
PageRuler™ Plus Prestained **Protein ladder**	VWR International Ltd., Orion Business Campus, Northwest Business Park, Ballycoolin, Dublin 15, Ireland.
Platinum HIFI™ Taq DNA polymerase **TRIzol® reagent**	Bio-sciences, Crofton, Dun Laoghaire, Co. Dublin, Ireland.

Ni-NTA agarose resin	Qiagen, 28159 Avenue Stanford, Valencia, CA 91355, USA.

2.1.2 Consumables

Consumables section describes disposable labware and the supplier information.

Table 2.2. Laboratory consumables and suppliers

Consumables	Suppliers
Plastic labware, **(Eppendorf tubes, PCR tubes,** **Sterile polypropylene centrifuge** **tubes, Pipette tips, Petri dishes)**	Sarstedt, Sinnottstown, Drinagh, Co. Wexford.
'RNase-free' Oakridge tubes	Applied Biosystems/Ambion. Inc., Lingley House, 120 Birchwood Boulevard, Warrington, WA3 &QH, UK.
Immuno 96 MicroWell™ **solid plates**	Nunc, Kamstrup DK, Roskilde, Denmark.
F96 MicroWell™ polystyrene **black plates**	Bio-Sciences Ltd., Dun Laoghaire, Co. Dublin, Ireland.
Biacore™ CM5 sensor chips, **Vivaspin™ concentrators**	GE Healthcare Bio-Sciences AB, SE-751 84 Uppsala, Sweden.

2.1.3 Commercial kits

Various commercial kits used for recombinant antibody library generation and their suppliers are listed in Table 2.3.

Table 2.3. Commercial kits and suppliers

Commercial kits	Suppliers
Superscript™ III reverse transcriptase kit	Invitrogen Corporation, 5791 Van Allen Way, Carlsbad, CA 92008, USA .
Perfectprep Gel Cleanup Kit	Eppendorf AG, Barkhausenweg 1, Hamburg 22339, Germany.
Wizard Plus SV Miniprep™ kit Wizard™ PCR clean-up kit	Promega, 2800 Woods Hollow Road, Madison, WI 53711, USA.
QIAquick™ gel extraction Kit	Qiagen, 28159 Avenue Stanford, Valencia, CA 91355, USA.
Amine coupling kit	GE Healthcare Bio-Sciences AB, SE-751 84 Uppsala, Sweden.

2.1.4 Composition of culture media

Culture media and their components are listed in Table 2.4.

Table 2.4. Components of culture media

Super Broth (SB) Media	Mops	10 g/L
	Yeast Extract	30 g/L
	Tryptone	20 g/L
Terrific Broth (TB) Media	Tryptone	12 g/L
	Yeast Extract	24 g/L
	Glycerol	4 mL
The constituents were dissolved in 900 mL of molecular grade water and autoclaved. The final volume was adjusted to 1 L with 100 mL of a sterile filtered solution of 0.17 M KH_2PO_4 and 0.72 M K_2HPO_4.		
SOC Media	Tryptone	20 g/L
	Yeast Extract	5 g/L
	NaCl	0.5 g/L
	KCl	2.5 mM
	$MgCl_2$	20 mM
	Glucose	20 mM
2 x Tryptone-Yeast Extract (TYE) Media	Tryptone	16 g/L
	Yeast Extract	10 g/L
	NaCl	5 g/L
100 x 5O5 media	Glycerol	50% (v/v)
	Glucose	5% (w/v)

2.1.5 Composition of buffers

This section describes the constituents of various buffers used in this study.

Table 2.5. Components of buffers

Phosphate buffered saline (PBS)	NaCl	8 g/L
The pH of the solution was adjusted to 7.4	Na_2HPO_4	1.44 g/L
with 1M HCl, and it with then filtered and	KH_2PO_4	0.24 g/L
degassed prior to use	KCl	0.2 g/L
Phosphate buffered saline Tween (PBST)	NaCl	8 g/L
	Na_2HPO_4	1.44 g/L
The pH of the solution was adjusted to 7.4	KH_2PO_4	0.24 g/L
with 1M HCl, and it then filtered and	KCl	0.2 g/L
degassed prior to use	Tween 20	0.05% (v/v)
Hepes buffered saline (HBS)	HEPES	2.38 g/L
The pH of the solution was adjusted to 7.4	NaCl	8.77 g/L
with 1M HCl, and it was then filtered and	EDTA	1.27 g/L
degassed followed by addition of Tween 20	Tween 20	0.5 mL

Table 2.6. Components of buffers for SDS-PAGE and Western blotting

1M Tris-HCl solution	Trizma base	121.14 g /L
	Molecular grade water	to 1L
Trizma base was dissolved in 1 L of molecular grade water and it was aliquoted into three clean bottles. The pH of each solution was adjusted to 6.8, 8.3 or 8.8, and they were then filtered and degassed prior to use		
0.5 M Tris-HCl solution	Trizma base	60.57 g /L
	Molecular grade water	to 1L
Trizma base was dissolved in 1 L of molecular grade water. The pH was adjusted to 6.8 with 1M HCl , and it was then filtered and degassed prior to use		
12.5% (v/v) Separation gel	1 M TrisHCl (pH 8.8)	1.5 mL
	30% (w/v) acrylamide (Acrylagel)	2.5 mL
	2% (w/v) methylamine bisacrylamide	1.0 mL
	10% (w/v) sodium dodecyl sulfate (SDS)	30 µL
	10% (w/v) ammonium persulphate (APS)	30 µL
	TEMED	6 µL
	Molecular grade water	934 µL
5% (v/v) Stacking gel	1 M TrisHCl (pH 6.8)	250 µL
	30% (w/v) acrylamide (Acrylagel)	375 µL
	2% (w/v) methylamine bisacrylamide	150 µL
	10% (w/v) sodium dodecyl sulfate	25 µL
	10% (w/v) ammonium persulphate (APS)	25 µL
	TEMED	5 µL
	Molecular grade water	1.67 mL

10 x electrophoresis buffer	1M Tris HCl (pH 8.3)	30 g/L
	Glycine	144 g/L
	SDS	10 g/L
	Molecular grade water	to 1L

Transfer buffer	1M Tris HCl (pH 8.3)	30 g/L
	Glycine	144 g/L
	SDS	10 g/L
	20% (v/v) methanol	200mL
	Molecular grade water	to 1L

SDS - PAGE gel loading buffer (4 x)	**10 mL**
0.5M Tris HCl (pH 6.8)	2.5 mL
20% (v/v) glycerol	2.0 mL
5% (v/v) 2-mercaptoethanol	0.5 mL
20% SDS (w/v)	2.5 mL
Bromophenol blue	20 ppm
Molecular grade water	2.5 mL

Coomassie stain dye	**500 mL**
Coomassie blue R-250	1 g
45% (v/v) methanol	225 mL
Acetic acid (17.46 M, 1.05g/mL)	50 mL
Molecular grade water	225 mL

Coomassie destain	**1 L**
Acetic acid (17.46 M, 1.05g/mL)	250 mL
20% (v/v) methanol	250 mL
Molecular grade water	500 mL

Table 2.7. Components of buffers used for immobilised metal ion affinity chromatography (IMAC)

100mM Sodium Hydroxide (NaOH)	NaOH	4 g/L
NaOH (0.4 g) was dissolved in 10 mL of molecular grade water and the solution was filtered and degassed prior to use		

100mM Sodium Acetate (pH 4.4)	CH_3COONa	8.2 g/L
Sodium Acetate (0.82 g) was dissolved in 100 mL of molecular grade water. The pH was adjusted to 4.4 with 1 M HCl, and it was filtered and degassed prior to use		

Sonication buffer	100 mL
150 mM PBS	100 mL
NaCl (0.03g/mL)	2.92 g
Imidazole (1.36g/L)	0.136 g

Running buffer	100 mL
150 mM PBS	99 mL
NaCl (0.03g/mL)	2.92 g
Imidazole (1.36g/L)	0.136 g
1% (v/v) Tween-20	1 mL

Elution buffer	1 mL
100 mM NaOH	500 µL
10 x PBS (pH 7.4)	500 µL

2.1.6 Bacterial strains

This section describes two bacterial strains used for cloning and expression. Both strains were purchased from Stratagene, La Jolla, California, USA (Table 2.8).

Table 2.8. *E.coli* strains used for antibody cloning and expression

***E. coli* XL1-Blue strain: recA1 endA1 gyrA96 thi-1 hsdR17 supE44 relA1 lac *[F′* proAB lacI^{q}Z∆M15 *Tn*10 (*Tet*^{R})*]*.**
***E. coli* TOP10 F strain: {*lac*I^{q}, Tn*10*(Tet^{R})} *mcr*A *ara-leu*)7697 *gal*U *gal*K *rps*L (Str^{R}) *end*A1 *nup*G**

2.2 Equipment

The standard equipment used in this study and supplier information are listed in Table 2.9.

Table 2.9. Laboratory equipment and the suppliers

Equipment	Supplier
Balances (Chyo JK-180, Mettler PJ300)	Medical Supply Company Ltd., Damastown, Mulhuddart, Dublin 15, Ireland.
Biacore ™ 3000 **Biacore ™ 4000**	GE Healthcare Bio-Sciences AB, SE-751 84 Uppsala, Sweden.
Biometra $T_{GRADIENT}$ PCR machine, **Sanyo Gallenkamp orbital shaker** **(D070022)**	ABG Scientific Ltd., Orion Business Campus, Northwest Business Park, Ballycoolin, Dublin 15, Ireland.
DNA gel electrophoresis apparatus	Alpha Technologies, The Leinster Technology Centre, Blessington Industrial Estate, Co. Wicklow, Ireland.
Gene Pulser Xcell ™ electroporation system	Alpha Technologies, The Leinster Technology Centre, Blessington Industrial Estate, Co. Wicklow, Ireland.
Nanodrop™ ND-1000	NanoDrop Technologies, Inc., 3411 Silverside Rd 100BC, Wilmington, DE19810-4803, USA.

PortaSCC® digital reader	PortaCheck Inc., 1 Whittendale Drive, Suite E Moorestown, NJ 08057, USA.
PX2 thermal cycler	Thermo Electron Corporation, 81 Wyman Street, Waltham, Massachusetts (MA), 02454, USA.
Roller mixer SRT1	Sciencelab, Inc., 14025 Smith Road, Houston, Texas 77396, USA.
Safire2™ microplate reader	Tecan Group Ltd., Seestrasse 103, CH-8708 Männedorf, Switzerland.
SDS Bio Rad min-Protean® 3 cell, **Trans-Blot® SD Semi-Dry Transfer,** **Bio-Rad Powerpac™ (Basic)**	Alpha Technologies, The Leinster Technology Centre, Blessington Industrial Estate, Co. Wicklow, Ireland.
Vibra Cell™ sonicator (VC50)	Sonics and Materials Inc., 53 Church Hill Road, Newtown, CT 06470-1614, USA.
Eppendorf benchtop centrifuge (5810R), **Eppendorf microcentrifuge (5417R)**	VWR International Ltd., Orion Business Campus, Northwest Business Park, Ballycoolin, Dublin 15, Ireland.

2.3 Methods

2.3.1 Generation of avian anti-cTnT scFv antibody fragments

2.3.1.1 SDS-PAGE analysis of commercial cTnT antigen

SDS-PAGE gel analysis was used to detect the purity of commercial preparations of cTnT antigen. Human cTnT (1.92 mg/mL) was purchased from Life Diagnostics Inc. (USA). The cTnT antigen was diluted 1 in 10, 1 in 20 or 1 in 40 with 1 x PBS (pH 7.4). SDS-PAGE gel loading buffer was added to the cTnT samples followed by boiling at 95^{o}C for 5 minutes. The samples were then analysed on a 12.5% (v/v) SDS-PAGE gel. The remaining cTnT was aliquoted into sterile PCR tubes and stored at -80^{o}C.

2.3.1.2 Immunisation of chicken with cTnT antigen

The animal handing procedure was approved by the Ethics Committee at Dublin City University (Dublin, Ireland) and licensed by the Irish Department of Health and Children (Dublin, Ireland). All experiments were performed ensuring that the animals suffered minimum stress.

A white male Leghorn chicken, aged 4-5 weeks, was injected with cTnT antigen over a period of two months. A pre-bleed was collected 7 days prior to the immunisations. The chicken was initially injected with a final concentration of 200 µg/mL cTnT, mixed in a 1:1 ratio with Freund's complete adjuvant. The immunogen was vigorously shaken to ensure the formation of a completely homogenous emulsion. Subsequent immunisations with 100 µg/mL cTnT mixed with equal volume of Freund's incomplete adjuvant were given at two weeks intervals. A bleed was taken from the chicken 7 days after the fourth boost and the serum anti-cTnT titre was determined by ELISA. The chicken was given the final boost when the titre reached a sufficient level; it was sacrificed 7 days after the last immunisation.

2.3.1.3 Determination of the serum anti-cTnT antibody titres

The avian polyclonal serum was analysed using a direct ELISA to determine its titre against cTnT antigen. An immuno 96 MicroWell™ solid plate (Nunc, Denmark) was coated with 1µg/mL cTnT for 1 hour at 37°C. The plate was blocked with 5% (w/v) Milk Marvel in 1 x PBS (pH 7.4) for 1 hour at 37°C. The plate was washed once with 1 x PBST (pH 7.4) and once with 1 x PBS (pH 7.4). A series of chicken serum dilutions from neat to 1 in 1,000,000 was prepared in 1xPBST (pH 7.4). Each dilution (100 µL) were added to the ELISA plate in triplicate and incubated for 1 hour at 37°C. The plate was washed twice with 1 x PBST (pH 7.4) followed by twice with 1 x PBS (pH 7.4). Rabbit anti-chicken IgY conjugated to horseradish peroxidase (HRP) was diluted 1 in 2000 with 1 x PBS and 100µL of the dilution was added to the plate. After a 1 hour incubation at 37°C, the plate was washed 3 times with 1 x PBST (pH 7.4) and 1 x PBS (pH 7.4). HRP TMB substrate (100 µL) was added to each well and the plate was incubated for 10 minutes at 37°C. The reaction was stopped by the addition of 100 µL of 10% (v/v) HCl. The absorbance levels of the wells were determined at 450 nm using a Safire2™ microplate reader (Tecan, Switzerland).

2.3.1.4 Extraction of total RNA from the immunised chicken

A Laminar flow hood (Gelaire BSB 4) was thoroughly cleaned with 70% (v/v) industrial methylated spirits (IMS, Lennox, Ireland) and RNaseZAP® (Ambion, UK) to create an 'RNA-free' environment. Surgical tools and a homogeniser (Ultra-Turrax, model TP 18/10, IKA® Werke GmbH & Co. KG, Germany) were autoclaved and baked overnight at 180°C to ensure sterility. The immunised chicken was sacrificed by cervical dislocation. The spleen was transferred into 10 mL pre-chilled TRIzol® reagent (Invitrogen, USA) and thoroughly homogenised at 50% power output for 1 minute. The bone marrow from the chicken was washed out with 10 mL of chilled TRIzol® reagent using a sterile needle and syringe. Both samples were incubated at room temperature for 5 minutes followed by centrifugation (Eppendorf benchtop centrifuge 5810R, VWR,

Ireland) at 5,500 g for 10 minutes at 4°C in a pre-chilled rotor. The supernatants were carefully transferred to 'RNase-free' Oakridge tubes (Ambion, UK) and 3 mL of chloroform was added into each tube. Both samples were mixed vigorously and incubated at room temperature for 15 minutes followed by centrifugation (Eppendorf microcentrifuge 5417R, VWR, Ireland) at 19,500 g at 4°C for 15 minutes. The samples were separated into a lower phenol/chloroform phase, an interphase containing DNA and protein and an upper aqueous phase containing RNA. The upper aqueous phase was carefully transferred to a fresh 'RNase-free' Oakridge tube and 15 mL of propan-2-ol was added into each sample. The tubes were shaken vigorously for 15 seconds and incubated at room temperature for 10 minutes for RNA precipitation. Samples were centrifuged at 19,500 g at 4°C for 30 minutes, resulting in a white 'gel-like' RNA pellet. The pellet was washed with 30 mL of 75% (v/v) ethanol and centrifuged at 19,500 g at 4°C for 10 minutes in a pre-chilled rotor. The supernatant was carefully removed and the RNA pellet was air-dried for 5 minutes in a laminar hood. The pellet was finally resuspended in 250 μL of 'RNase-free' water. RNA concentrations were measured by spectrophotometric measurement at 260 nm with a NanoDrop™ spectrophotometer ND-1000 (Thermo Fisher Scientific, USA).

2.3.1.5 Reverse transcription of total RNA to cDNA

A fresh aliquot of the total RNA was immediately reverse transcribed into cDNA using an oligo-(dT) primer and a SuperScript™ III First-Strand Synthesis System (Invitrogen, USA). All components were kept on ice throughout the experiments. A 10 x master mixture 1 was prepared with the components listed below (Table 2.10). Mixture 1 (25 μL) was aliquoted into 8 'RNAase-free' PCR tubes followed by incubation at 65°C for 5 minutes (Biometra $T_{GRADIENT}$ PCR machine, Labrepco, USA). The mixture was then incubated on ice for 1 minute. Mixture 2 (25 μL) (Table 2.11) was added to the 8 tubes containing mixture 1 and then incubated at 50°C for 50 minutes, followed by 85°C for 5 minutes. RNase H (5 μL) was then added to each tube. The tubes were

incubated at 37°C for 20 minutes. The cDNA was aliquoted into sterile tubes and stored at −20°C.

Table 2.10. Composition of mixture 1 for reverse transcription reaction

Mixture 1 - components	Stock concentration	Volume per reaction
RNA	15.5 µg/µL	0.32 µL (to give 5 µg)
Oligo-dt	50 µM	1 µL
dNTPs	10 mM	1 µL
Sterile H_2O	------	7.68 µL
Total Volume		**10 µL**

Table 2.11. Composition of mixture 2 for reverse transcription reaction

Mixture 2 - components	Stock concentration	Volume per reaction
RT buffer	10 x	2 µL
$MgCl_2$	25 mM	4 µL
DTT	10 mM	2 µL
RNase OUT	40 U/µL	1 µL
Superscript™ III RT	200 U/µL	1 µL
Total Volume		**10 µL**

2.3.1.6 PCR primers for the generation of avian scFv antibodies

The sets of primer sequences listed in Table 2.12 were used to generate a chicken scFv library with a 15 amino acid residue $(Gly_4Ser)_3$ linker. All primers were purchased from Eurofins MWG Operon (London, UK) and were immediately aliquoted into sterile tubes after delivery and subsequently stored at -20°C.

Table 2.12. Primer sequences for the amplification of avian scFv gene fragments

Variable heavy chain (V_H) primers	
CSCHo-F (sense), long Linker	5′ GGT CAG TCC TCT AGA TCT TCC GCC GTG AC GTT GGA CGA G 3′
CSCG-B (reverse)	5′ CTG GCC GGC CTG GCC ACT AGT GGA GGA GAC GAT GAC TTC GGT CC 3′
Variable light chain (V_L) primers	
CSCVK (sense)	5′ GTG GCC CAG GCG GCC CTG ACT CAG CCG TCC TCG GTG TC 3′
CKJo-B (reverse)	5′ GGA AGA TCT AGA GGA CTG ACC TAG GAC GGT CAG G 3′
Overlap extension primers	
CSC-F (sense)	5′ GAG GAG GAG GAG GAG GAG GTG GCC CAG GCG GCC CTG ACT CAG 3′
CSC-B (reverse)	5′ GAG GAG GAG GAG GAG GAG GAG CTG GCC GGC CTG GCC ACT AGT GGA GG 3′

2.3.1.7 Amplification of variable chains for the generation of avian anti-cTnT scFv antibodies

The PCR components of the V_H and V_L amplification listed in Table 2.13. The volume of one reaction was 50 µL. Four amplification reactions were performed to ensure sufficient V_H and V_L genes for the SOE-PCR (section 2.3.1.9).

Table 2.13. Composition of PCR reaction mixture used for the amplification of the variable domains

PCR component	Concentration in 50 µL reaction	Volume of each component
cDNA template		1µL
5 x Go Taq® buffer	1x	5µL
V_L/V_H sense primer	60pM	0.6µL
V_H/V_L reverse Primer	60pM	0.6µL
dNTP (10 mM)	0.2mM	1µL
Go Taq® Polymerase	1U/µL	0.25µL
$MgCl_2$ (25 mM)	2mM	4µL
H_2O	------	37.55µL
Total volume		**50µL**

The amplification of the V_H and V_L domains was performed in a Biometra $T_{GRADIENT}$ PCR machine under the following conditions:

Stage	Cycle	Temperature (^oC)	Time (sec)
1) Initial denaturation	1	94^{o}C	300
2) Denaturation	30	94^{o}C	15
Annealing		56^{o}C	90
Extension		72^{o}C	90
3) Final extension	1	72^{o}C	600

2.3.1.8 Isolation of the variable heavy and variable light gene fragments

The amplified PCR products were evaluated on a 1% (w/v) agarose gel and extracted with the QIAquick™ gel extraction Kit (Qiagen, USA) and Wizard® PCR 'clean-up' system kit (Promega, USA). The gel fragments of V_H (~ 400 bp product) and V_L (~ 350 bp product) were carefully separated using sterile scalpels and weighed in 1.5 mL eppendorf tubes.

Three volumes of binding buffer were added to 1 volume of gel fragment and the gel slices were fully dissolved in the binding buffer by incubating at 50°C for 10 to 20 minutes. The guanidine isothiocyanate contained in the buffer enhances DNA binding to the silica membrane columns. The mixture (700 µL) was transferred to a collection column and centrifuged (Eppendorf microcentrifuge 5417R, VWR, Ireland) at 19,500 g for 1 minute to remove any residual buffer. After the removal of 'flow-through', wash buffer (750 µL) was added onto the membrane of the QIAquick™ spin column and centrifuged at 19,500 g for 1 minute. The washing step was repeated once to ensure the maximum removal of salts and other buffer residuals. The DNA was eluted with 30 µL molecular grade water by centrifuging at 19,500 g for 1 min. The purified DNA concentration was measured at 260 nM using the Nanodrop™ ND-1000

2.3.1.9 Splice by Overlap Extension (SOE) PCR for the construction of anti-cTnT scFv gene fragments

Splice by overlap extension (SOE) primers listed in Table 2.12 were used to link the purified V_H and V_L fragments with a glycine-serine linker $(Gly_4Ser)_3$. The fragment was analysed on a 1% (w/v) agarose gel and purified as described in section 2.3.1.8.

Table 2.14. Components of SOE-PCR reaction mixture used for the amplification of scFv fragments

PCR component	Concentration in 50 µL reaction	Volume of each component
5 x Go Taq® buffer	1x	5 µL
V_L gene	100 pM	1µL
V_H gene	100 pM	1µL
$MgCl_2$ (25mM)	3 mM	6 µL
dNTP (10mM)	0.2 mM	1µL
CSC-F Primer	60 pM	0.6 µL
CSC-B Primer	60 pM	0.6 µL
Go Taq® Polymerase	1U/µL	2 µL
H_2O	------	32.8 µL
Total volume		**50 µL**

The SOE-PCR was performed in a Biometra $T_{GRADIENT}$ PCR machine under the following conditions:

Stage	Cycle	Temperature (^oC)	Time (sec)
1) Initial denaturation	1	94^oC	240
2) Denaturation	24	94^oC	30
Annealing		56^oC	45
Extension		72^oC	120
3) Final extension	1	72^oC	600

2.3.1.10 SOE-PCR restriction digestion and ligation into pComb3XSS vector

The cloning vector pComb3XSS and the puried scFv fragment were quantified using the NanoDrop™ ND1000 spectrophotometer with UV absorbance at 260 nM. The *Sfi*I restriction enzyme was used to digest both the cloning vector pComb3XSS and the puried scFv fragment. It recognises the nucleotide sequence 5′ggccnnnn ^ nggcc3′. The restriction digestion site within the nucleotides is indicated by the '^'symbol. The reactions (Table 2.15) were incubated at 50°C for 5 hours.

Table 2.15. Reaction mixture for restriction digestion of pComb vector and SOE-PCR product

pComb vector	***Sfi*I digest**
Component	Volume
pComb vector	4 µL
10 x Buffer 2	20 µL
10 x BSA	20 µL
***Sfi*I**	1.2 µL
H_2O	154.8 µL
Total volume	**200 µL**

SOE-PCR product	***Sfi*I digest**
Component	Volume
SOE-PCR product	116 µL
10 x Buffer 2	20 µL
10 x BSA	20 µL
***Sfi*I**	23.4 µL
H_2O	20.6 µL
Total volume	**200 µL**

The digested pComb3XSS vector (~ 3400 bp) and the scFv fragment (~ 750 bp) were evaluated on a 1% (w/v) agarose gel and purified, as described in section 2.3.1.8. DNA concentrations of both samples were determined using the NanoDrop™ ND1000 spectrophotometer by measuring O.D. at 260 nm. The scFv fragment was ligated into the pComb3XSS vector with a mass ratio of 2:1. The reaction (Table 2.16) was incubated overnight at room temperature.

Table 2.16. Reaction mixture for ligation of SOE-PCR product into pComb vector

Digest component	Concentration in 200 µL volume	Volume of each component
Digested pComb3XSS vector	1.4 µg/rxn	34.7 µL
Digested scFv gene	0.7 µg/rxn	4.4 µL
5 x Ligase buffer	1 x	40 µL
T4 DNA Ligase	400 U/µL	10 µL
H_2O	------	110.9 µL
Total volume		**200 µL**

The ligation mixture was precipitated by adding 20 µL sodium acetate (pH 5.2), 400 µL 100% ethanol and 2 µL of pellet paint® NF co-precipitant. After overnight precipitation at -20°C, the solution was centrifuged (Eppendorf microcentrifuge 5417R, VWR, Ireland) at 19,500 g for 20 minutes in a pre-chilled rotor. The supernatant was discarded and the pellet was washed with 70% (v/v) pre-chilled ethanol. The sample was centrifuged at 19,500 g for 10 minutes at 4°C and the pellet was resuspended in 10 µL of molecular grade water. The ligation product was stored at 4°C.

2.3.1.11 Electroporation of XL-1 blue *E. coli* cells with a scFv-containing plasmid

The scFv-containing pComb3XSS plamid was electro-transformed into electrocompetent XL-1 blue *E. coli* cells (Stratagene, USA) using a Gene Pulser Xcell electroporation system (Alpha Technologies, Ireland). The apparatus was set at 25 µF, 1.25 kV and the Pulse Controller at 200 Ω. Electrocompetent *E. coli* cells (50 µL) were slowly thawed in ice. The ligated product (2 µL) was carefully added to the *E. coli* cells. The mixture was incubated on ice for 1 minute and then immediately transferred to a pre-chilled electroporation cuvette (Alpha Technologies, Ireland). The cuvette was then

securely placed in the ShockPod. One pulse was passed through the mixture in the cuvette chamber and the mixture was immediately flushed with 1 mL of pre-warmed SOC medium. The time before addition of SOC medium to the cells was kept to a minimum, as a delay of 1 minute can result in a 3-fold decrease in transformation efficiency. The mixture was transferred to a 20 mL sterile tube containing 2 mL of pre-warmed SOC media and incubated (Sanyo orbital incubator D070022, ABG, Ireland) for 1 hour at 37^{o}C while shaking at 220 rpm. The pComb3XSS transformants were spread on TYE plates which were supplemented with 100µg/ml carbenicillin and 1% (v/v) glucose. Commercial XL-1 blue *E. coli* cells with no transformants were plated out in parallel on agar plates containing 100 µg/mL carbenicillin and 1% (v/v) glucose as negative controls. The plates were incubated overnight at 37^{o}C. The pComb3XSS transformant colonies were scraped off the plates and amplified in super broth media. The amplified library was then subjected to the selection of specific anti-cTnT antibody through biopanning.

2.3.1.12 Rescue of anti-cTnT scFv-displaying phage

In the phage rescue process, all glassware and centrifuge tubes were autoclaved and baked overnight at 60^{o}C to ensure all containers were completely sterile and dry. A total of 200 µL of the potential anti-cTnT scFv library suspension was immediately inoculated into two conical flasks after being scraped from overnight plates. Each conical flask contained 100 mL pre-warmed sterile Super Broth (SB) media with 100 µg/mL carbenicillin. These library-containing cultures were incubated at 200 rpm and 37^{o}C until mid-exponential phase of growth (O.D. ~ 0.400 at 600 nm) was reached. The M13KO7 helper phage was then added to the culture to a final concentration of 1 x 10^{11} plaque-forming units (pfu)/mL. The cultures were incubated at 37^{o}C for 30 minutes while stationary followed by incubation at 200 rpm and 37^{o}C for 2 hours. Subsequently, kanamycin (50 µg/mL) was added and the cultures were grown overnight at 30^{o}C while shaking at 200 rpm. The culture was transferred into sterile sorval tubes and centrifuged

(Eppendorf benchtop centrifuge 5810R, VWR, Ireland) at 5,500 g (4°C) for 15 minutes and the bacterial pellet was discarded. For phage propagation, the supernatant was transferred into 'RNase-free' Oakridge tubes and the phage particles precipitated by the addition of 4% (w/v) polyethylene glycol (PEG) 8,000 and 3% (w/v) NaCl. The mixture was shaken at 200 rpm for 10 minutes at 37°C to allow the PEG/NaCl to completely dissolve. The mixture was precipitated on ice for 1 hour in the cold room (4°C) and centrifuged (Eppendorf microcentrifuge 5417R, VWR, Ireland) at 14,000 g for 20 minutes in a pre-chilled rotor with an extended break for 15 minutes. The phage-containing bacterial pellet was resuspended in 2 mL of 1% (w/v) BSA in 1 x PBS (pH 7.4) solution and then centrifuged at 19,500 g for 10 minutes at 4°C to remove cell debris. Sodium azide (0.05%, w/v) was added to the supernatant as preservative to prevent antibody degradation. Sodium azide is a toxic material and hence the handing of the sodium azide solution was performed in the fumehood throughout this study. The antibody-containing supernatant was stored at 4°C.

2.3.1.13 Selection of avian scFv phage library via biopanning against immobilised cTnT

Eight wells of an immuno 96 MicroWell™ solid plate (Nunc, Demark) were coated overnight at 4°C with 100 µL of 50 µg/mL cTnT in 1 x PBS (pH 7.4). The plate was blocked with 200 µL of 5% (w/v) Marvel in 1x PBS (pH 7.4) for 1 hour at 37 °C and the plate was washed once with 1 x PBST (pH 7.4) and once with 1 x PBS (pH 7.4). Rescued phage (100 µL) were added into each well and incubated at 220 rpm for 2 hours at room temperature. Non-bound phage were washed away with 3 times 1x PBST (pH 7.4) and 3 times 1 x PBS (pH 7.4) for round one panning. The numbers of washing steps were increased for the following 4 rounds of panning to increase the stringency of phage-infected antibody selection. For antigen-binding phage elution, a total of 100 µL of 10 mg/mL type II porcine trypsin in 1x PBS (pH 7.4) solution was added into the plate and incubated at 37°C for 30 minutes. Sodium azide (2%, w/v) was added into 400

µL of the eluted phage as preservative and stored at 4°C. The remaining 400 µL of phage were infected into 2 mL of mid-exponential phase XL-1 blue *E. coli* cells (O.D.600 nm ~ 0.4). The cells were incubated for 30 minutes at 37°C without shaking. A serial dilution of the phage infected cells ranged from 10^{-1}-10^{-10} was prepared in sterile 2xTY media and spread on 2xTY agar plates, containing 100 µg/mL carbenicillin, and incubated overnight at 37°C. The remaining culture was further propagated at 200 rpm for 1 h at 37°C. Cells were harvested by centrifugation (Eppendorf benchtop centrifuge 5810R, VWR, Ireland) at 5,500 g for 10 minutes at 4°C. Antibody library were prepared by resuspending the cell pellet in 400 µL of fresh 2xTY media. The mixture was then spread on TYE plates containing 1% (w/v) glucose and 100 µg/mL carbenicillin. Plates were incubated overnight at 37 °C. Input titres were determined by infecting mid-exponential growth phase XL-1 blue *E. coli* cells (180 µL) with 20 µL of precipitated phage (stored at 4°C) for 15 minutes at 37°C. Serial dilutions were performed (10^{-1}-10^{-12}) and spread on TYE agar plates containing 100 µg/mL carbenicillin and incubated overnight at 37°C.

In the subsequent rounds of biopanning (rounds 2-5), growth media (100 mL) was used for cell propagation. The concentrations of immobilised antigen on the Immuno 96 MicroWell™ solid plate surface were reduced. The number of washing steps by 1 x PBST (pH 7.4) and 1 x PBS (pH 7.4) were increased. These strategies were employed to select specific antigen-binding clones. For the generation of soluble scFv antibodies, scFv-phage particles from round four were infected to *E. coli* Top10-F cells. Volume of media for phage propagation, antigen coating concentrations and the number of washing steps are shown in Table 2.17.

Table 2.17. Biopanning conditions for the selection of anti-cTnT scFvs

Biopanning round	Volume of media (mL)	Immobilised antigen (µg/mL)	No. of wash steps	Infected cell strains
1	200	50	3 x PBST, 3 x PBS	*E. coli* XL1-blue
2	100	25	5 x PBST, 3 x PBS	*E. coli* XL1-blue
3	100	10	5 x PBST, 5 x PBS	*E. coli* XL1-blue
4	100	5	7 x PBST, 5 x PBS	*E. coli* XL1- blue
5	100	2	7 x PBST, 7 x PBS	*E. coli* Top10-F

2.3.1.14 Soluble expression of anti-cTnT scFv antibodies using a simple 'on-plate' screening method

Output phage, from the 5th round of biopanning, were infected into *E. coli* Top 10F' cells. The cells were then diluted in media and spreaded on agar plates supplemented with 50 µg/mL carbenicillin. After 20 hours incubation at 37^{o}C, a total of 96 single colonies from the output titer plates were inoculated into microtitre plate wells containing 200 µL of SB broth (10 g/L MOPS, 30 g/L Tryptone and 20 g/L yeast extract) supplemented with 50 µg/mL carbenicillin and 10 µg/mL tetracycline and grown while shaking at 37^{o}C for 6-8 hours. The culture from each well (20 µL) was removed as a master stock and 20 µL of 10 mM IPTG added to the remaining 180 µL of culture. The induced culture was immediately transferred to an ELISA plate (Immuno 96 MicroWell^{TM} solid plate) previously coated with 100 µL/well of a 1 µg/mL cTnT solution for 1 h at 37^{o}C and blocked with 3% (w/v) BSA for 1 h at 37^{o}C. The culture-containing ELISA plate was incubated overnight at 30^{o}C with agitation. Following overnight 'on-plate' expression, the cells and culture media were removed by washing with PBST (pH 7.4). For the detection of bound antibody, HRP-labelled mouse anti-HA monoclonal antibody (Roche) of a concentration of 25 ng/mL (100 µL) was

added to each well for 1 h at 37°C and the wells were washed five times with PBST prior to the addition of the HRP TMB substrate. This method was published in Journal of Immunological Methods (Guo *et al.*, 2010) (see Appendix I).

2.3.1.15 Analysis of anti-cTnT scFv antibodies using direct and inhibition ELISAs

A direct ELISA was performed to determine the titre of anti-cTnT scFv antibodies against cTnT antigen. It was carried out by coating an immuno 96 MicroWell™ solid plate overnight at 4°C with 100 µL of 1 µg/ml cTnT and blocked with 200 µL 5% (w/v) Marvel in 1 x PBS (pH 7.4) for 1 hour at 37°C. The plate was washed once with 1 x PBST (pH 7.4) and once with 1 x PBS. A series of dilutions of crude lysate extracted from antibodies (neat, 1 in 5, 1 in 10, 1 in 20, 1 in 16, 1 in 32, 1 in 64, 1 in 128, 1 in 256 and 1 in 5,120) were prepared in 1 x PBS (pH 7.4) and 100 µL of each was added into wells in duplicate. The plate was incubated at 37°C for 1 hour. The plate was washed twice with 1 x PBST (pH 7.4) and twice with 1 x PBS (pH 7.4). HRP-labelled mouse anti-HA monoclonal antibody (25 µg/mL) were diluted in 1 x PBS (pH 7.4) and added into the plate for 1 hour at 37°C. HRP TMB substrate (100 µL) was added to each well and the plate was incubated for 10 minutes at 37°C. The absorbance reading was determined at 450 nm using a Safire2™ microplate reader.

Inhibition ELISA was performed by coating an immuno 96 MicroWell™ solid plate overnight at 4°C with 100 µL of 1 µg/mL cTnT and blocked with 200 µL 5% (w/v) Marvel in 1 x PBS (pH 7.4) for 1 hour at 37°C. Various concentrations of cTnT (1 µg/mL, 500 ng/mL, 250 ng/mL, 125 ng/mL, 62.5 ng/mL, 31.25 ng/mL, 15.63 ng/mL and 7.81 ng/mL) were prepared in 1 x PBS (pH 7.4) and incubated with a fixed dilution of scFv clone for 1 hour at 37°C. HRP-labelled mouse anti-HA monoclonal antibody was diluted 1 in 2000 in 1 x PBS (pH 7.4) and added to the plate for 1 hour at 37°C. HRP TMB substrate (100 µL) was added to each well and the plate was incubated for

10 minutes at 37^{o}C. The absorbance values were determined at 450 nm with a Safire2^{TM} microplate reader.

2.3.1.16 Purification of anti-cTnT scFv fragments using immobilised metal affinity chromatography (IMAC)

An overnight culture containing scFv (300 mL) was centrifuged (Eppendorf benchtop centrifuge 5810R, VWR, Ireland) at 5,500 g for 20 minutes. The cell pellet was resuspended in 10 mL of sonication buffer. The mixture was then sonicated at 40% amplitude with 6 seconds pulse for 2 minutes and then centrifuged at 19,500 g at 4^{o}C to remove cell debris. The clear lysate was filtered with a 2 μm filter consists of nitrocellulose membrane (Merck Millipore, Ireland). A 2 mL aliquot of Ni-NTA agarose resin (Qiagen, USA) was added to a 20 mL column and equilibrated with 20 mL running buffer. The filtered lysate was then applied to the equilibrated column and the 'flow-through' collected in a 50 mL tube. The column was then washed with 30 mL of running buffer to remove any loosely bound non-specific proteins and once again the 'flow-through' was collected in a 50 mL tube. The scFv fragment was eluted using 8 mL of 100 mM NaAc, pH 4.4, and collected in a 50 mL tube containing 2 mL of 100 mM NaOH and 2 mL of 10 x PBS (pH 7.4). The 12 mL scFv-containing elution fragment was then thoroughly buffer exchanged against filtered 1 x PBS (pH 7.4) using a 5 kDa cut-off Vivaspin™ concentrators column (GE healthcare, Sweden). The buffer-exchanged scFv was then quantified using the Nanodrop™ ND-1000 at 280 nm and aliquoted into clean PCR tubes and stored at -20°C.

2.3.1.17 Preconcentration analysis of rabbit anti-HA polyclonal antibody on a Biacore^{TM} CM5 sensor chip

Preconcentration studies was performed to indentify the optimal pH value of sodium acetate allowing the maximum immobilisation level of rabbit anti-HA epitope tag polyclonal antibody (Thermo Fisher, Ireland) to the carboxy-methylated dextran CM5

sensor chip surface (GE healthcare, Sweden). A total of six different sodium acetate buffer (10 mM) solutions (pH 5.0, pH 4.8, pH 4.6, pH 4.4, pH 4.2 and pH 4.0) were mixed with anti-HA polyclonal antibody for a final antibody concentration of 12.5 µg/mL. A CM5 sensor chip was activated by passing over a mixture of 400 mM 1-ethyl-3-[3-dimethylaminopropyl] carbodiimide hydrochloride (EDC) (GE Healthcare, Sweden) and 100 mM *N*-hydroxysuccinimide (NHS) (GE Healthcare, Sweden). The diluted antibodies were subsequently passed over the surface at a flow rate of 10 µL/min for 30 seconds.

2.3.1.18 Immobilisation of rabbit anti-HA polyclonal antibody on a Biacore™ CM5 sensor chip

A Biacore™ CM5 sensor chip surface was immobilized with rabbit anti-HA epitope tag polyclonal antibody (Thermo Fisher, Ireland) using amine coupling reagents. Hepes buffered saline buffer (HBS, pH 7.4) was used as the running buffer throughout the experiment. HBS was filtered and degassed before running through the Biacore™. The dextran surface with initially activated by an injection of the fresh prepared mixture of EDC (0.4 M) and NHS (0.1 M), at 1:1 ratio, for 10 minutes. Anti-HA antibody was prepared in sodium acetate buffer (pH 4.0) to a final concentration of 25 µg/mL and injected over flow cells 1, 2, 4, 5 for 10 minutes at a flow rate of 10 µL/min. Flow cell 3 was left unmodified as a reference. The residual reactive sites (unbound material) were then deactived by injection of 1 M ethanolamine hydrochloride (GE Healthcare, Sweden), pH 8.5. The chip surface was regenerated by five injections of 20 mM NaOH.

2.3.1.19 SPR-based kinetic studies of anti-cTnT scFv antibodies

The kinetic studies were performed on anti-cTnT scFv to assess its antigen binding affinity. Anti-HA antibody was diluted in sodium acetate buffer (pH 4.0) and immobilised on a Biacore™ CM5 sensor chip surface (section 2.3.1.18). Anti-cTnT scFv antibodies were diluted in 1x HBS and then passed over the chip surface at a rate

of 10 µL/min for 2 minutes. CTnT, at a series of concentrations (50 nM, 25 nM, 12.5 nM, 6.25 nM, 3.125 nM and1.56 nM), was subsequently injected over the chip surface. The association phase was processed for 2 minutes and the dissociation phase was processed for 10 minutes. The 12.5 nM concentration was run in duplicate. All sensorgrams were subjected to fit globally to a 1:1 binding model. The assay format is illustrated in Fig.2.1.

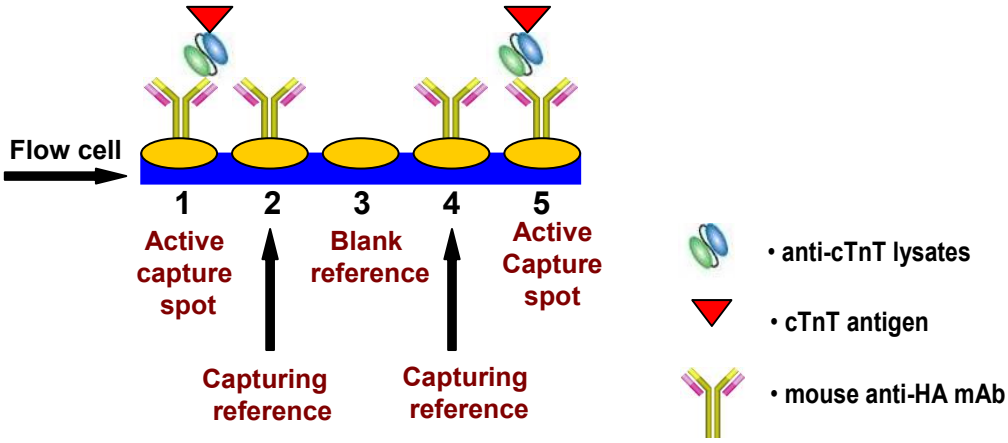

Figure 2.1. Assay format used for the characterisation of anti-cTnT scFv antibody. The five gold circles represent five flow cells (1-5). Flow cells 1, 2, 4, 5 were immobilised with anti-HA antibody. The active binding sites of flow cells 2 and 4 were deactived using ethanolamine hydrochloride; they are used as capturing references. Antibody-containing lysate was passed over flow cells 1 and 5 followed by injecting with cTnT antigen. Flow cell 3 was used as blank reference.

2.3.2 Affinity maturation of avian anti-cTnT scFv clones by chain-shuffling

2.3.2.1 Amplification of variable domains of plamids extracted from anti-cTnT scFv libraries

The primers used for the construction of light chain-shuffled antibody library are listed in Table 2.18. The variable light (V_L) chains were amplified using the plasmid pooled from the unpanned library; and variable heavy (V_H) genes were amplified using the plasmid pooled from the 5th biopanning round. The variable heavy (V_H) chains were amplified using the plasmid extracted from the unpanned library and variable light (V_L) genes were amplified using the plasmid pooled from 5th biopanning round. The PCR components for V_H and V_L amplification are described in Tables 2.18 and 2.19, respectively.

Table 2.18. Composition of PCR reaction mixture used for the amplification of the V_H domain

PCR component	Concentration in 50 µL reaction	Volume of each component
Plasmid DNA	50 ng	1 µL
5 x Go Taq® buffer	1 x	5 µL
V_H sense primer	60 pM	0.6 µL
V_H reverse primer	60 pM	0.6 µL
dNTP (10 mM)	0.2 mM	1 µL
Go Taq® Polymerase	5U/µL	0.25 µL
$MgCl_2$ (25 mM)	0.75mM	1.5 µL
H_2O	------	40.05 µL
Total volume		**50 µL**

The amplification of the V_H gene was performed in a Biometra $T_{GRADIENT}$ PCR machine under the following conditions:

Stage	Cycle	Temperature (^oC)	Time (sec)
1) Initial denaturation	1	94^{o}C	300
2) Denaturation	30	94^{o}C	15
Annealing		58^{o}C	15
Extension		72^{o}C	90
3) Final extension	1	72^{o}C	600

Table 2.19. Composition of PCR reaction mixture used for the amplification of the V_L domain

PCR component	Concentration in 50 µL reaction	Volume of each component
Plasmid DNA	50 ng	1 µL
10 x HIFI buffer	1 x	5 µL
V_L sense primer	60 pM	0.6 µL
V_L reverse Primer	60 pM	0.6 µL
dNTP (10 mM)	0.2 mM	1 µL
Platinum HIFI ™ Taq	5 U/µL	0.2 µL
$MgCl_2$ (25 mM)	4 mM	8 µL
H_2O	------	33.6 µL
Total volume		**50 µL**

The amplification of the V_L gene was performed in a Biometra $T_{GRADIENT}$ PCR machine under the following conditions:

Stage	Cycle	Temperature (^oC)	Time (sec)
1) Initial denaturation	1	94^{o}C	300
2) Denaturation	30	94^{o}C	15
Annealing		57^{o}C	15
Extension		72^{o}C	90
3) Final extension	1	72^{o}C	600

2.3.2.2 Splice by Overlap Extension (SOE) PCR for the construction of chain-shuffled anti-cTnT scFv gene fragments

Splice overlapping extension (SOE) primers listed in section 2.3.1.6 were used to link the purified V_H and V_L fragments with a long glycine-serine linker $(Gly_4Ser)_3$. The light chain-shuffled SOE was generated by linking V_L amplified from an unpanned library with V_H amplified from the 5th biopanning round. The heavy chain-shuffled SOE was generated by linking V_L amplified from pan 5 library with V_H amplified from an unpanned library. The PCR components are presented in Tables 2.20 and 2.21.

Table 2.20. Composition of SOE-PCR reaction mixture used for the amplification of the heavy chain-shuffled scFv fragments

PCR component	Concentration in 50 µL reaction	Volume of each component
V_H (unpanned)	100 ng	2.5 µL
V_L (5^{th} round)	100 ng	2.5 µL
SOE sense primer	60 pM	0.6 µL
SOE reverse primer	60 pM	0.6 µL
5 x Go Taq® buffer	1 x	10 µL
dNTP (10 mM)	0.2 mM	1 µL
Go Taq® Polymerase	5 U/µL	0.25 µL
$MgCl_2$ (25 mM)	3 mM	6 µL
H_2O	------	26.55 µL
Total volume		**50µL**

The SOE-PCR for heavy chain-shuffling was performed in a Biometra $T_{GRADIENT}$ PCR machine under the following conditions:

Stage	Cycle	Temperature (^oC)	Time (sec)
1) Initial denaturation	1	94^{o}C	300
2) Denaturation	30	94^{o}C	15
Annealing		58^{o}C	15
Extension		72^{o}C	90
3) Final extension	1	72^{o}C	600

Table 2.21. Composition of SOE-PCR reaction mixture used for the amplification of the light chain-shuffled scFv fragments

PCR component	Concentration in 50 µL reaction	Volume of each component
V_L (unpanned)	102 ng	0.6 µL
V_H (5^{th} round)	100 ng	2.5 µL
SOE sense primer	60 pM	0.6 µL
SOE reverse primer	60 pM	0.6 µL
5 x Go Taq® buffer	1 x	10
dNTP (10 mM)	0.2 mM	1 µL
Go Taq® Polymerase	5 U/µL	0.25 µL
$MgCl_2$ (25 mM)	3 mM	6 µL
H_2O	------	28.45 µL
Total volume		**50µL**

The SOE-PCR for light chain-shuffling was performed in a Biometra $T_{GRADIENT}$ PCR machine under the following conditions:

Stage	Cycle	Temperature (^oC)	Time (sec)
1) Initial denaturation	1	94^{o}C	300
2) Denaturation	30	94^{o}C	15
Annealing		58^{o}C	15
Extension		72^{o}C	90
3) Final extension	1	72^{o}C	600

2.3.2.3 Construction of chain-shuffled anti-cTnT scFv libraries and rescue of anti-cTnT scFv-displaying phage

The purified SOE products were digested by the *Sfi*I restriction enzyme and then ligated into the pComb3XSS vector followed by transforming into *E. coli* XL1-blue cells for library construction, using the protocol described in section 2.3.1.11. Digestion and ligation conditions are given in Tables 2.22 and 2.23.

Table 2.22. Reaction mixture for restriction digestion of pComb vector and the SOE-PCR product

pComb vector	***Sfi*I digest**
Component	Volume
pComb vector	5 µL
10 x Buffer 2	20 µL
10 x BSA	20 µL
***Sfi*I**	1.2 µL
H_2O	153.8 µL
Total volume	**200 µL**

SOE-PCR product	***Sfi*I digest**
Component	Volume
SOE-PCR product	102 µL
10 x Buffer 2	20 µL
10 x BSA	20 µL
***Sfi*I**	23.4 µL
H_2O	34.6 µL
Total volume	**200 µL**

Table 2.23. Reaction mixture for ligation of the heavy chain-shuffled SOE-PCR product into pComb vector

Digest component	Concentration in 200 µL volume	Volume of each component
Digested pComb3XSS vector	1.4 µg/rxn	81.36 µL
Digested scFv gene	0.7 µg/rxn	61 µL
5 x Ligase buffer	1 x	20µL
T4 DNA Ligase	400 U/µL	10 µL
H_2O	------	27.64 µL
Total volume		**200 µL**

Table 2.24. Reaction mixture for ligation of pComb vector and the light chain-shuffled SOE-PCR product

Digest component	Concentration in 200 µL volume	Volume of each component
Digested pComb3XSS vector	1.4 µg/rxn	81.36 µL
Digested scFv gene	0.7 µg/rxn	75 µL
5 x Ligase buffer	1 x	20µL
T4 DNA Ligase	400 U/µL	10 µL
H_2O	------	13.64µL
Total volume		**200 µL**

The biopanning process for selection of chain-shuffled antibodies was described in section 2.3.1.12. More stringent panning conditions were used, including a decrease in antigen coating concentration and an increase in the number of washing steps (Table 2.25).

Table 2.25. Biopanning conditions for the selection of chain-shuffled anti-cTnT scFv antibodies

Biopanning round	Volume of media (mL)	Immobilised antigen (µg/mL)	No. of wash steps	Infected cell strains
1	200	20	3 x PBST, 3 x PBS	*E. coli* XL1-blue
2	100	10	5 x PBST, 3 x PBS	*E. coli* XL1-blue
3	100	5	5 x PBST, 5 x PBS	*E. coli* XL1-blue
4	100	2	7 x PBST, 7 x PBS	*E. coli* XL1-blue
5	100	1	9 x PBST, 9 x PBS	*E. coli* Top10-F

2.3.2.4 DNA fingerprinting of anti-cTnT scFv antibodies

DNA fingerprinting was performed to analyse antibody diversity. Anti-cTnT scFv clones were grown in 5 mL SB media overnight at 37^{o}C. The overnight culture was subjected to plasmid purification using a Wizard Plus SV Miniprep™ kit (Promega, USA). The cell culture was harvested by centrifugation (Eppendorf benchtop centrifuge 5810R, VWR, Ireland) at 3,200 g for 20 minutes. The supernatant was discarded and the pellet was resuspended in 250 µL cell resuspension buffer. Cell lysis buffer was then added to lyse the cells and release periplasm proteins. The mixture was then incubated at room temperature for 5 minutes followed by addition of 300 µL of neutralisation solution. Cell debris were then pelleted by centrafugation at 22,000 g for 10 minutes. The supernatant, which contained the plasmid DNA, was transferred to a spin column allowing the plasmid DNA to bind to the spin column. Wash buffer (700 µL) was then

added to the spin column and centrifuged at 19,500 g for 1 minute. The washing step was repeated once to resure the maximum removal of salts and other buffer residuals. The plasmid DNA was eluted with 50 µL of molecular grade water. The scFv gene fragments were then amplied from the DNA plasmid. The PCR components are listed in Table 2.26.

Table 2.26. Composition of PCR reaction mixture for the amplification of scFv plasmid DNA

PCR component	Concentration in 50 µL reaction	Volume of each component
Plasmid DNA	100 ng	1 µL
SOE sense primer	60 pM	0.6 µL
SOE reverse primer	60 pM	0.6 µL
5 x Go Taq® buffer	1 x	10
dNTP (10 mM)	0.2 mM	1 µL
Go Taq® Polymerase	5 U/µL	0.25 µL
$MgCl_2$ (25 mM)	3 mM	6 µL
H_2O	------	30.55 µL
Total volume		**50µL**

The PCR was performed in a Biometra $T_{GRADIENT}$ PCR machine under the following conditions:

Stage	Cycle	Temperature (^oC)	Time (sec)
1) Initial denaturation	1	94^{o}C	300
2) Denaturation	30	94^{o}C	15
Annealing		58^{o}C	15
Extension		72^{o}C	90
3) Final extension	1	72^{o}C	600

The PCR products were subsequently digested using an *Alu*I restriction enzyme using the conditions outlined in Table 2.27. The mixture was digested at 37°C for 2 hours and then resolved on a 3% (w/v) agarose gel.

Table 2.27. Reaction mixture for restriction digestion of scFv plasmid DNA using *Alu*I restriction enzyme

scFv gene	***Alu*I digest**
Component	Volume
PCR product	8 µL
10 x Buffer 4	2.4 µL
100 x BSA	0.24 µL
***Alu*I**	0.5 µL
H_2O	12.86 µL
Total volume	**24 µL**

2.3.2.5 Preparation of crude bacterial lysates of anti-cTnT scFv for Biacore™ 4000 analysis

A total of 384 anti-cTnT antibodies including 192 light-chain-shuffled scFv antibodies and 192 heavy-chain-shuffled antibodies were randomly picked and inoculated into 100 µL sterile SB medium containing 100 µg/mL carbenicillin and incubated overnight at 220 rpm at 37°C. The overnight culture was subcultured into a sterile 96-deep well plate containing 750 µL SB with 1 x 5O5 solution and 100 µg/mL carbenicillin. The plates were left shaking at 220 rpm 37°C until the cell density reached an O.D. ~ 0.400 at 600 nm. The cells were then induced with 1 mM sterile filtered IPTG solution and incubated overnight at 30°C. The overnight cells were pelleted by centrifuging (Eppendorf

benchtop centrifuge 5810R, VWR, Ireland) at 5,500 g for 15 minutes and the pellets were then resuspended in 500 µL 1x HBS. The lysates from cells were extracted by placing the plates at -80^{o}C for 10 minutes followed by thawing at 37 ^{o}C for 10 minutes. This step was repeated three times. The plates were centrifuged at 5,500 g for 15 minutes to pellet the cell debris and the supernatant was transferred into fresh 96-well plates.

2.3.2.6 Characterisation of anti-cTnT scFv clones using the Biacore^{TM} 4000

The binding ability of anti-cTnT scFv against cTnT antigen was assessed with the previously prepared anti-HA sensor chip (section 2.3.1.18). The assay format used for the analysis was previously described in section 2.3.1.19. One in three dilutions of the crude bacterial lysate, prepared in 1x HBS, were simultaneously passed over flow cells 1 and 5 of the sensor chip at a flow rate of 10 µL/min for 10 minutes. The antigen, cTnT, at a concentration of 1 µg/mL was subsequently injected at a flow rate of 10 µL/min for 2 minutes followed by dissociation in buffer for 10 minutes. Flow cells 2 and 4 were used as capturing references whereas flow cell 3 was used as a blank reference.

2.3.2.7 Analysis of the cross-reactivity of anti-cTnT scFv antibodies

Cross-reactivity analysis was performed to assess the specific of anti-cTnT antibodies. It was carried out in a direct ELISA assay format using crude bacterial lysate extracted from 10 anti-cTnT scFv antibodies. The capacity of the anti-cTnT scFv antibodies to cross-react with other isoforms of troponins including skeletal troponin T (sTnT), cardiac troponin T (cTnI) and skeletal troponin I (sTnI) was tested. Two negative controls were incorporated in this assessment to eliminate false-positive responses. The first negative control excluded the antigen-coating step. The second negative control only contained 5% (w/v) Marvel blocking solution.

2.3.2.8 Checkboard ELISA using different cTnT coating concentrations

Checkboard ELISA was performed to select the optimal cTnT concentrations for inhibition assay development. A 96 MicroWell™ solid plate was coated overnight at 4°C with 100 µL of cTnT with a series of concentration (3, 1.5, 1, 0.5, 0.25, 0.125, 0 µg/ml) and blocked with 200 µL 5% (w/v) Marvel in 1 x PBS (pH 7.4) for 1 hour at 37°C. The plate was washed once with 1 x PBST (pH 7.4) and once with 1 x PBS (pH 7.4). A series of dilutions of crude lysate extracted from 8C2 antibody (1 in 100, 1 in 250, 1 in 500, 1 in 1,000, 1 in 2,000, 1 in 4,000, 1 in 8,000, 1 in 16,000, 1 in 32,000, 1 in 64,000, 1 in 128,000) were prepared in 1 x PBS (pH 7.4) and 100 µL of each was added into wells. The plate was incubated at 37°C for 1 hour. The plate was washed twice with 1 x PBST (pH 7.4) and twice with 1 x PBS (pH 7.4). HRP-labelled mouse anti-HA monoclonal antibody was diluted 1 in 2,000 in 1 x PBS (pH 7.4) and 100 µL of the dilution was added into the plate for 1hour at 37°C. HRP TMB substrate (100 µL) was added to each well and the plate was incubated for 10 minutes at 37°C. The absorbance reading was determined at 450 nm using a Safire2™ microplate reader.

2.3.2.9 Optimisation of the 8C2 scFv antibody dilution for ELISA inhibition assay

To ensure the best performance of the inhibition assay, the concentration of 8C2 used for antigen detection was optimised. An immuno 96 MicroWell™ solid plate plate was coated overnight at 4°C with 100 µL of 1 µg/mL cTnT and blocked with 200 µL 5% (w/v) Marvel in PBS (pH 7.4) for 1 hour at 37°C. A number of concentrations of cTnT (1 µg/mL, 500 ng/mL, 250 ng/mL, 125 ng/mL, 62.5 ng/mL, 31.25 ng/mL, 15.63 ng/mL and 7.81 ng/mL) were prepared in 1 x PBS (pH 7.4) and incubated with four different dilutions of the scFv 8C2 clone (1 in 1,000, 1 in 2,000, 1 in 3,000 and 1 in 4,000) for 1 hour at 37°C. HRP-labelled mouse anti-HA monoclonal antibody was diluted 1 in 2,000 in 1 x PBS (pH 7.4) and 100 µL of the dilution was added to the plate for 1 hour at 37°C. HRP TMB substrate (100 µL) was added to each well and the plate was incubated

for 30 minutes at 37°C. The absorbance reading was determined at 450 nm using a Safire2™ microplate reader.

2.3.3 Generation of avian anti-cTnT Fab antibody fragments

2.3.3.1 Amplification of variable domains for the generation of avian anti-cTnT Fab antibodies

The primer sequences listed below were used to generate a chimeric chicken/human Fab library (Table 2.28). The primers were compatible with the pComb3XSS vector. All primers were purchased from Eurofins MWG Operon (London, UK) and were immediately aliquoted into sterile tubes and stored at -20°C after arrival.

Table 2.28. Primer sequences for the amplification of avian Fab gene fragments

Variable heavy chain (V_H) primers	
ChybVH (sense)	5′ GCT GCC CAA CCA GCC ATG GCC GCC GTG ACG TTG GAC GAG TCC 3′
ChybIg-B (Reverse)	5′ CGA TGG GCC CTT GGT GGA GGC GGA GGA GAC GAT GAC TTC GGT CCC 3′
Variable light chain (V_L) primers	
CSCVK (sense)	5′ GTG GCC CAG GCG GCC CTG ACT CAG CCG TCC TCG GTG TC 3′
CHybL-B (Reverse)	5′ AGA TGG TGC AGC CAC AGT TCG TAG GAC GGT CAG GGT TGT CCC GGC 3′
Primers for amplification of the Human C_HI chain from a cloned Human Fab	
HKC-F (sense)	5′ CGA ACT GTG GCT GCA CCA TCT GTC 3′
dpseq (reverse)	5′ AGA AGC GTA GTC CGG AAC GTC 3′
Primers for amplification of the Human $C_κ$ chain from a cloned Human Fab	
HKC-F (sense)	5′ CGA ACT GTG GCT GCA CCA TCT GTC 3′
Lead-B (reverse)	5′ GGC CAT GGC TGG TTG GGC AGC 3′

Primers for PCR assembly of chicken V_H sequences with the Human C_HI PCR product	
LeadVH (sense)	5′ GCT GCC CAA CCA GCC ATG GCC 3′
dpseq (reverse)	5′ AGA AGC GTA GTC CGG AAC GTC 3′
Primers for PCR assembly of chicken V_L sequences with the Human $C_κ$ PCR product	
CSC-F (sense)	5′ GAG GAG GAG GAG GAG GAG GTG GCC CAG GCG GCC CTG ACT CAG 3′
Lead-B (reverse)	5′ GGC CAT GGC TGG TTG GGC AGC 3′
Primers for PCR assembly of chimeric light-chain sequence with chimeric heavy-chain sequence	
CSC-F (sense)	5′ GAG GTG GCC CAG GCG GCC CTG ACT CAG 3′
dep-EX (reverse)	5′ GAG AGA AGC GTA GTC CGG AAC GTC 3′

The chicken variable domains (V_H and $V_λ$) were amplified using previously produced chicken cDNA as template. The sense primer CHybVH and reverse primer CHyblg-B were used to amplify the V_H domain. The amplification of the V_H was optimised by using three $MgCl_2$ concentrations (2 mM, 3 mM, 4 mM). The annealing temperature was 56^{o}C. However, there was no significant product yield under these PCR conditions. Further optimisation was performed using an increased annealing temperature (58^{o}C). The optimised PCR components for V_H amplification are listed in Table 2.29. The sense primer, CSCVK, and reverse primer were used to amplify the $V_λ$ domain. The PCR components are listed in Table 2.30.

Table 2.29. Composition of PCR reaction mixture used for the amplification of the V_H domain

PCR component	Concentration in 50 µL reaction	Volume of each component
cDNA template	50 ng	1 µL
5 x Go Taq® buffer	1x	5 µL
CHybVH	60 pM	0.6 µL
CHyblg-B	60 pM	0.6 µL
dNTP (10 mM)	0.2 mM	1 µL
Go Taq® Polymerase	5 U/µL	0.25 µL
$MgCl_2$ (25 mM)	2 mM	4 µL
H_2O	------	37.55 µL
Total volume		**50 µL**

Table 2.30. Composition of PCR reaction mixture used for the amplification of the V_λ domain

PCR component	Concentration in 50 µL reaction	Volume of each component
cDNA template	50 ng	1 µL
5 x Go Taq® buffer	1 x	5 µL
CSCVK	60 pM	0.6 µL
CHybl-B	60 pM	0.6 µL
dNTP (10 mM)	0.2 mM	1 µL
Go Taq® Polymerase	5 U/µL	0.25 µL
$MgCl_2$ (25 mM)	1 mM	2 µL
H_2O	------	39.55 µL
Total volume		**50 µL**

Both V_H and V_λ amplifications were performed with the same PCR profile as below:

Stage	Cycle	Temperature (^oC)	Time (sec)
1) Initial denaturation	1	94^{o}C	300
2) Denaturation	30	94^{o}C	15
Annealing		58^{o}C	15
Extension		72^{o}C	90
3) Final extension	1	72^{o}C	600

The amplification of the human constant domains (C_HI and C_κ) was performed using the pComb3XTT vector as template. The sense primer HIgGCH1-F and reverse primer dpseq were used for the PCR scale-up of the C_HI fragment. Table 2.31 shows the components of the PCR mix for the amplification of the C_HI fragment.

Table 2.31. Composition of PCR reaction mixture used for the amplification of the C_H1 domain

PCR component	Concentration in 50 µL reaction	Volume of each component
pComb3XTT	20 ng	0.2 µL
5 x Go Taq® buffer	1 x	5 µL
HIgGCH1-F	60 pM	0.6 µL
dpseq	60 pM	0.6 µL
dNTP (10mM)	0.2 mM	1 µL
Go Taq® Polymerase	5 U/µL	0.25 µL
$MgCl_2$ (25mM)	2 mM	4 µL
H_2O	------	38.35 µL
Total volume		**50 µL**

The amplification of the C_H1 domain was performed in a Biometra $T_{GRADIENT}$ PCR machine under the following conditions:

Stage	Cycle	Temperature (^oC)	Time (sec)
1) Initial denaturation	1	94^{o}C	300
2) Denaturation	30	94^{o}C	15
Annealing		58^{o}C	15
Extension		72^{o}C	90
3) Final extension	1	72^{o}C	600

The human Cκ domain amplification was performed with the sense primer, HKC-F, and the reverse primer, Lead-B, using the pComb3XTT as template. The amplification of the Cκ domain was performed using the following PCR mixture composition (Table 2.32).

Table 2.32. Composition of PCR reacture mixture used for the amplification of the Cκ domain

PCR component	Concentration in 50 µL reaction	Volume of each component
pComb3XTT	20 ng	0.2 µL
5 x Go Taq® buffer	1 x	5 µL
HKC-F	60 pM	0.6 µL
Lead-B	60 pM	0.6 µL
dNTP (10 mM)	0.2 mM	1 µL
Go Taq® Polymerase	5 U/µL	0.25 µL
$MgCl_2$ (25 mM)	2 mM	4 µL
H_2O	------	38.35 µL
Total volume		**50 µL**

The amplification of the Cκ domain was performed in a Biometra $T_{GRADIENT}$ PCR machine under the following conditions:

Stage	Cycle	Temperature (^oC)	Time (sec)
1) Initial denaturation	1	94^{o}C	300
2) Denaturation	30	94^{o}C	15
Annealing		56^{o}C	15
Extension		72^{o}C	90
3) Final extension	1	72^{o}C	600

The PCR product was pooled and concentrated by ethanol precipitation. The precipitated PCR products were evaluated on a 1% (w/v) agarose gel and the correct-sized bands (V_H / Cκ ~ 400bp) (V_λ / C_HI ~ 350 bp) were carefully cut out and the DNA was purified, as described in 2.3.1.8.

2.3.3.2 Amplification of the chimeric heavy and light chains using overlap extension PCR

The construction of the chicken chimeric heavy chain (Fd) fragment was achieved by joining the purified V_H and the C_HI fragments generated from the previous PCR amplification. The amplification was performed using the sense primer LeadVH and the reverse primer, dpseq. The amplification of the PCR components was optimised using both $MgCl_2$ concentration gradients (1 mM, 2 mM, 3 mM, 4 mM) and temperature gradients (56^{o}C, 58^{o}C, 60^{o}C, 62^{o}C). The optimised PCR components are shown in Table 2.33.

Table 2.33. Composition of PCR reaction mixture used for the amplification of the chimeric heavy chain

PCR component	Concentration in 50 µL reaction	Volume of each component
V_H	50 ng	1 µL
C_H	50 ng	1 µL
LeadVH	60 pM	0.6 µL
dpseq	60 pM	0.6 µL
5 x Go Taq® buffer	1 x	5 µL
dNTP(10 mM)	0.2 mM	1 µL
Go Taq® Polymerase	5 U/µL	0.25 µL
$MgCl_2$ (25 mM)	4 mM	8 µL
H_2O	------	32.55 µL
Total volume		**50 µL**

The amplification of the chimeric heavy chain was performed in a Biometra $T_{GRADIENT}$ PCR machine under the following conditions:

Stage	Cycle	Temperature (^{o}C)	Time (sec)
1) Initial denaturation	1	94^{o}C	300
2) Denaturation	15	94^{o}C	15
Annealing		60^{o}C	15
Extension		72^{o}C	120
3) Final extension	1	72^{o}C	600

For the generation of the chicken chimeric light chain, the purified chicken V_L and human Cκ fragments were amplified using the sense primer, CSC-F, and the reverse primer, Lead-B. The PCR components are shown in Table 2.34.

Table 2.34. Composition of PCR reaction mixture used for the amplification of the chimeric light chain

PCR component	Concentration in 50 µL reaction	Volume of each component
V_L	50 ng	1 µL
Cκ	50 ng	1 µL
CSC-F	60 pM	0.6 µL
Lead-B	60 pM	0.6 µL
5 x Go Taq® buffer	1x	5 µL
dNTP(10 mM)	0.2 mM	1 µL
Go Taq® Polymerase	5 U/µL	0.25 µL
$MgCl_2$ (25 mM)	2 mM	4 µL
H_2O	------	36.55 µL
Total volume		**50 µL**

The amplification of the chimeric light chain was performed in a Biometra $T_{GRADIENT}$ PCR machine under the following conditions:

Stage	Cycle	Temperature (^{o}C)	Time (sec)
1) Initial denaturation	1	94^{o}C	300
2) Denaturation	30	94^{o}C	15
Annealing		56^{o}C	15
Extension		72^{o}C	90
3) Final extension	1	72^{o}C	600

The PCR products from the amplification of the chimeric Fd and light chain fragments were subject to ethanol precipitation and analysed on a 1% (w/v) agarose gel. Both chains were then extracted from the gel (section 2.3.1.8).

2.3.3.3 Splice by Overlap Extension (SOE) PCR for the construction of Fab gene fragments

The final splice overlap extension (SOE) PCR combined the purified chicken/human chimeric Fd fragment and the light chain fragment. The fragments were mixed equally in the overlap PCR reaction and amplified with the sense extension primer, CSC-F, and the reverse extension primer, dp-EX. The amplification was optimsed using three PCR polymerases (Go Taq®, Fusion Taq® and Platinum HIFI™ Taq polymerases), two types of magnesium compound ($MgCl_2$, $MgSO_4$) and a number of Mg^{2+} concentrations (0 mM, 1mM, 0.5 mM, 1 mM, 2 mM, 2.5 mM). The optimised PCR components are listed in Table 2.35.

Table 2.35. Composition of SOE-PCR reaction mixture used for the amplification of the Fab gene fragments

PCR component	Concentration in 50 µL reaction	Volume of each component
Chimeric heavy chain	60 ng	1 µL
Chimeric light chain	60 ng	1 µL
HIFI buffer (10 x)	1x	5 µL
CSC-F	60 pM	0.6 µL
dep-EX	60 pM	0.6 µL
dNTP(10mM)	0.2 mM	1 µL
Platinum HIFI ™ Taq	5 U/µL	0.2 µL
$MgSO_4$ (50 mM)	2.5 mM	2.5 µL
H_2O	------	38.1 µL
Total volume		**50 µL**

The SOE-PCR was performed in a Biometra $T_{GRADIENT}$ PCR machine under the following conditions:

Stage	Cycle	Temperature (^oC)	Time (sec)
1) Initial denaturation	1	94^oC	120
2) Denaturation	15	94^oC	15
Annealing		56^oC	30
Extension		72^oC	120
3) Final extension	1	72^oC	300

2.3.3.4 SOE-PCR restriction digestion and ligation into pComb3XSS vector

The purified SOE-PCR product and pComb 3XSS vector were digested using *Sfi*I restriction enzyme (section 2.3.1.10). The digestion conditions are shown in Table 2.36.

Table 2.36. Reaction mixture for restriction digestion of pComb3XSS vector and the SOE-PCR product

pComb3XSS vector ***Sfi*I *digest***	
Component	Volume
pComb3XSS plasmid	95 µL
10 x Buffer 2	20 µL
10 x BSA	20 µL
***Sif*I**	10 µL
H_2O	55 µL
Total volume	200 µL

SOE fragment ***Sfi*I *digest***	
Component	Volume
SOE product	53 µL
10 x Buffer 2	20 µL
10 x BSA	20 µL
***Sif*I**	5.5 µL
H_2O	101.5 µL
Total volume	200 µL

The digestion mixtures were incubated for 5 hours at 50°C and ethanol-precipitated followed by gel purification, as described in section 2.3.1.8. The purified Fab fragment (~ 1500 bp) was then ligated into the pComb3XSS vector (~ 3400 bp) using the conditions given in Table 2.37.

Table 2.37. Reaction mixture for the ligation of pComb3XSS vector and the Fab fragments

Component	Volume
10 x T4 Ligase buffer	20 µL
pComb3XSS vector (1.4 µg)	26 µL
Fab insert	28 µL
T4 DNA ligase	10 µL
H_2O	116 µL
Total Volume	200 µL

The ligation mixture was incubated overnight at room temperature and then subjected to ethanol precipitation.

2.3.3.5 Rescue of anti-cTnT Fab-displaying phage

For the construction of anti-cTnT Fab libraries, the Fab-containing pComb3XSS plasmid was electro-transformed into commercial *E. coli* XL1-blue cells using the method described in section 2.3.1.11. The 'overnight-grown' transformants (200 µL) were scraped from 2xTY agar plates and propagated in 200 mL sterile SB medium contain 100 µg/mL carbenicillin and 10 µg/mL tetracycline. The culture was incubated at 220 rpm at 37°C until the cells reached exponential growth phase (O.D. ~ 0.4). The Fab library was rescued by adding 1ml of commercial M13KO7 helper phage and then incubated at 37°C for 30 minutes, to allow phage infection of cells. The culture was then left at 37^{o}C for 2 hours, while shaking at 220 rpm, before the addition of 50 µg/mL kanamycin. The rescued library was incubated overnight at 37°C at 220 rpm. The method for selection of specific anti-cTnT Fab clones was described in section 2.3.1.13.

2.3.3.6 Optimisation of Fab antibody expression conditions

Fab expression conditions were optimised in order to improve antibody expression levels. Each of the overnight culture of four Fab clones (A1, C5, C7 and D3) was inoculated into 500 mL TB media containing 1 x 5O5 solution with 100 µg/mL carbenicillin and 10 µg/mL tetracycline. The culture was incubated at 37°C, while shaking at 220 rpm, until the cells reached exponential growth (O.D. ~ 0.4). IPTG concentration gradients and time-course optimisition were performed. Each of the Fab cultures were divided into four sterile flaskes. Four different IPTG concentrations (0.05 mM, 0.1 mM, 0.25 mM and 0.5 mM) were added into each of the four flasks and then incubated at 30^{o}C at 220 rpm. Samples were collected from each flask after 2, 4 and 6 hours and overnight induction. Antibody-containing cell lysates from each culture was extracted by repeated freeze-thaw cycles at -80^{o}C/37^{o}C. The antibody expression levels were assessed by analysing the lysate using an direct ELISA format. The absorbance values indicated the expression levels of each of the samples.

2.3.4 Studies on lactate dehydrogenase levels in normal and mastitic milk

2.3.4.1 Description of LDH fluorescence assay

The detection of LDH activity was based on two reactions (Huston *et al.*, 1972). The primary reaction was the conversion of L-lactate into pyruvate by oxidation. In this reaction L-lactate was oxidised by LDH, using nicotinamide adenine dinucleotide (NAD^+), as a co-substrate, thus producing pyruvate and NADH + H^+. In the secondary reaction, NADH + H^+ produced from primary reaction quantitatively reduced the non-fluorescent resazurin to the highly fluorescent substance resorufin. Diaphorase was the enzyme necessary to catalyse the secondary reaction (Joyce *et al.*, 1992).

$$\text{L-Lactate} + NAD^+ \xrightarrow{\text{LDH}} \text{Pyruvate} + NADH + H^+ \quad \text{Primary reaction}$$

$$NADH + H^+ + \text{Resazurin} \xrightarrow{\text{Diaphorase}} \text{Resorufin} + NAD^+ \quad \text{Secondary reaction}$$

2.3.4.2 Determination of the optimal assay conditions for LDH measurement in milk

The aim of this section was to determine the optimal reaction time for LDH detection in milk samples. This assay reaction was based on the two oxidation/reduction reactions described in section 2.3.4.1. The time used for a known amount of commercial LDH (0.248 mg/mL) to convert a known amount of lactate (350 mM) to pyruvate was measured as described below:

Reaction set-up

1. The reagent mixture was prepared as shown in Table 2.38.

Table 2.38. Reagent mixture for LDH assay

Component	Stock concentration	Volume added (µL)	Final concentration
Tris HCl, pH 8.9	750 mM	20	75 mM
β-NAD	10 mM	20	1 mM
Resazurin	480 µM	20	48 µM
KCl	1 M	20	100 mM
Triton X-100	40 ppm	20	4 ppm
Diaphorase	10 U/mL	20	1 U/mL
H_2O	-------	53.4	-------
L-lactate	350 mM	20	35 mM
Total volume		**193.4**	

2. The reagent mixture (193.4 µL) was added into each well of a 96 Microwell™ polystyrene black plate containing 6.6 µL of LDH (0.248 mg/mL). Assays were performed in triplicate. 200 µL of 5 mM resorufin was added into one well in the plate as a background control in the fluorescence assay.

3. The production of resorufin was determined by fluorometry. Fluorescence was measured with excitation at 544 nm and emission at 590 nm. The Safire2^{TM} microplate reader was set under the following conditions:

- 37^{o}C
- Fluorescence detection
- Excitation at 544 nm, emission at 590 nm, and a bandwidth of 20 nm
- The gain at 44 and the Z position at 11200, (Z position has no units)
- The bandwidth value, gain value and Z position value were automatically set by the plate reader

The fluorescent readings were recorded every 30 seconds for a time period of 330 seconds. The fluorescent readings were plotted against time for determination of the optimal reaction time.

2.3.4.3 Determination of LDH levels in milk

The aim of this section was to determine LDH activity in untreated milk samples. Since the optimal reaction time was determined from the curve (Fig. 6.1) to be 180 seconds this time period was used throughout as the standard time for the detection of LDH.

Reaction set-up

The reagent mixture (193.4 µL) (section 2.3.4.2) was added into each well of a 96 Microwell^{TM} polystyrene black plate containing 6.6 µL of milk.

Safire2^{TM} microplate reader set-up

The Safire2^{TM} microplate reader was set up to read the plate, with the parameters described in section 2.3.4.2. Fluorescence values were recorded at time 0 seconds. Samples were incubated at 37^{o}C for 180 seconds, and fluorescence values were recorded again. Experiments were carried out in triplicate.

Controls

The master mix (193.4 µL) and 6.6 µL 1 x PBS (pH 7.4) was used as the negative control in this fluorescence assay.

Commercial LDH solution (6.6 µL) with a known concentration was added to 193.4 µL of the master mix as a positive control for the fluorescence assay.

Resorufin (200 µL) was added to the plate as a background control for the fluorescence assay.

Calculation

1) Mean values of the fluorescence readings were calculated for all the milk samples and the LDH controls.

2) Net values of the milk samples and the LDH controls were obtained by taking 0 minute mean values away from 3 minutes mean values. Table 2.39 below shows the calculation of net fluorescent value.

Table 2.39. Fluorescence produced in milk samples and LDH control solutions

	Fluorescent reading Mean: 0 minute	Fluorescent reading Mean: 3 minutes	Net
Milk sample	A	B	E = B-A
LDH solution	C	D	F = D-C

A and B represented the mean fluorescent values of the milk samples at 0 and 3 minutes, respectively. C and D represented the mean fluorescent values of the LDH solution at 0 and 3 minutes, respectively. E and F represented the net values for milk sample and LDH solution, respectively.

3) The enzymatic activity of the LDH solution, according to the manufacturer, was 659 enzyme units per mg. Therefore, the enzymatic activity of the LDH solution can be determined by multiplying the LDH concentration (mg/mL) by the enzymatic activity

value (659 units/mg) to get enzyme units per mL, then multiply by 1000 to give enzyme units per L * (represented by Y)

For example: 0.1 mg/mL LDH solution x 659 units per mg = 65.9 units per mL = 65,900 units per L (U/L)*

*in previous publications, LDH activity was presented in units per L (Larsen, 2005; Hiss *et al.*, 2007)

The LDH fluorescence unit (F) was correlated with LDH enzymatic activity (Y) by dividing F by Y. This correlation value represented by Z equals LDH activity (U/L) per fluorescence unit.

$$Z = Y\ (U/L) / F$$

For example: F= 1000 fluorescence unit, Y=65900 U/L

$$Z = 65900/1000 = 65.9$$

4) The net fluorescence value (E) of the milk samples were converted into LDH activity U/L (X) by multiplying Z by E.

$$\text{LDH activity in milk } X\ (U/L) = Z \times E$$

For example: E = 20 fluorescence unit, Z= 65.9

$$X = 65.9 \times 20 = 1318\ U/L$$

Statistical analysis was performed on all milk samples using PASW statistics 18 (formerly SPSS Statistics) for Windows. Pearson's Product Moment Correlation Analysis was used to compare the mean levels of LDH, NAGase and SCC. The correlation value (r) can fall between 0 (no correlation) and 1.00 (perfect correlation). PASW statistics 18 software sets r values greater than 0.80 as a good correlation. One-way ANOVA was used to determine significance. Data was considered statistically significant at p value < 0.05.

Chapter 3
Generation of avian anti-troponin T antibody scFv fragments

3.1 Introduction

This chapter outlines the production and characterisation of recombinant avian anti-cTnT scFv antibody fragments. It contains an in-depth description of the construction of an avian antibody phage library; the screening and selection of antigen-specific antibodies; the analysis of antibodies using the SPR technique and the inhibition assay development of the selected antibody. The main focus of this chapter is the use of phage display for antibody production and selection.

Recombinant antibody fragments have become essential tools in several fields, including biomedical research, disease diagnostics and therapeutics (Smith *et al.,* 2004). More than 30% of all biological proteins used in clinical trials for both diagnosis and therapeutics are recombinant antibody fragments (Hudson, 1998). The Fv fragment is the smallest functional antibody fragment and is comprised of single V_L and V_H domains that maintain the monovalent binding affinity of the parent antibody. In solution, the association of individual V_L and V_H domains of the Fv fragment is weak. The two variable domains can dissociate into its individual domains due to the low affinity interaction between them (Glockshuber *et al*., 1990; Hudson, 1998., Bronzino., 2000). In contrast, in a recombinant format, the V_L and V_H domains are often tethered to each other using a flexible polypeptide linker to form a stable scFv antibody fragment, thus allowing for the co-secretion of both variable domains in the periplasm of bacteria cells (Freund *et al.,* 1993). A 15 amino acid residue $(Gly_4Ser)_3$ linker is a common choice, in which glycine and serine provide flexibility and solubility to the antibody fragments (Hudson and Winter, 1991). The 15 amino acid residue length also provides each of the variable domains with enough freedom of movement and space to bind the antigen, thus ensuring there is no steric interference between each section of the scFv (Shan *et al.,* 2011).

The production of recombinant antibody and antibody fragments involve systems such as mammalian cell culture, microbial cell culture (i.e. bacteria, yeast and fungi) and plant cells (Table 3.1). Mammalian cell systems are particularly useful in antibody production for therapeutic purposes. However, the process is time consuming and expensive. In this study, the simple and cost-effective bacterial cell systems are the choice for recombinant antibody production.

Table 3.1. Recombinant antibodies production systems

	Advantages	Disadvantages
Mammalian system	• Extensively used for full length IgG production • Glycosylation pattern is similar to *in vivo* glycoprotein • Particular useful for therapeutic protein production	• Low production due to low cell growth rate • Production costly • High risk of contamination
Microbial system – *bacteria*	• High transformation efficiency • Rapid production due to high growth rate • Simple production due to simple compositions of media and easy cultivation • Robustness and scalability of fermentation process • Cost effective	• Limited range of therapeutic products as protein glycosylation does not normally occur in bacterial hosts • Risk of contamination by endotoxins
Yeast	• Organisms are typically free of pyrogens and infectious viruses • These hosts can produce glycosylated protein as well as full length IgG and antibody fragments • Antibody domains fold and associate properly	• Long fermentation time • Modest yield of antibodies • Lack full mammalian glycan pattern • High levels of proteolysis caused by host proteases
Fungi	• Efficient production and secretion capacity • Higher growth rates than plant and mammalian cells • Proteins are glycosylated	• High risk of antibody proteolysis • High culture viscosity • No reports of therapeutic protein production

Plant	• Low risk of viral contamination • Moderate cost and time-scale of production • 'Human-like' glycosylation in transgenic plant cells	• Plant harvest, handling and storage are not convenient

(Based on references: Pluckthun, 1991; Nyyssönen *et al.,* 1993; Keranen and Penttila, 1995; Shusta *et al.,* 1998; Freyre et al., 2000; Peeters *et al.,* 2001; Ma *et al*., 2003; Wiebe, 2003; Rahbarizadeh *et al.,* 2006; Liddell, 2009).

The generation of recombinant antibody libraries using the avian system as the animal host offers a number of distinct advantages. Chickens are phylogenetically more distance from humans than other commonly used laboratory animal species, such as mice and rats. Importantly, the generation of antibodies from the avian immune system can achieve better immune responses to conserved mammalian proteins (Narat, 2003; Zhang, 2003). This may offer significant benefit for the development of diagnostic assays for human diseases.

Interestingly, the avian immune system contains two sets of germ line genes named V (variable) and J (joining), which form the heavy and light chains of the antibody. The re-arrangement of the V and J segments in the avian systems leads to the generation of a large repertoire of different antibodies (Cohn and Moldave, 1993). In contrast, in mammalian species, such as rabbit and mouse, an extra D (diversity) segments is involved in repertoire production. Although the extra segment may generate greater repertoire diversity than in the avian species, the antibody library construction requires more procedures than in the avian systems, such as the need for extra sets of primers and PCR amplifications. Recombinant avian antibody generation is, therefore, easier and simpler, owing to the need of only two sets of primers and two amplification processes.

Despite limited gene rearrangements, the avian immune system possesses a unique Bursa B cell development process. During this process, gene conversion leads to sequence change in CDRs which result in a high level of antibody diversity. It was suggested that this mechanism has the potential to develop more diverse antibodies than those found in either humans or rodents (Thompson, 1992). In addition, the avian host offers other benefits for antibody generation. These include low animal-housing and feeding costs, a rapid and sustained antibody response, and the capability of simultaneously responding to up to seven distinct immunogens (Hof *et al.,* 2008).

Using the phage display technique, recombinant antibodies can be produced from the avian system and subsequently characterised using Surface Plasmon Resonance (SPR). SPR is a non-invasive optical phenomenon that monitors molecular interactions

between ligands in 'real-time'. SPR detects the change of refractive index of a thin metal film caused by the binding of mobile molecules to immobilised molecules on the metal film (Drescher *et al.,* 2009). The molecular interactions lead to a change in the angle of reflected light, which is generated when the polarised light is impinging on the metal film (Rich and Myszka, 2000; Gopinath, 2010). The SPR response is dependent on the mass of biomolecules bound on the film surface, and is independent of the nature of that biomolecule. Therefore, both the quantity of ligands immobilised on the sensorchip surface and the quantity of molecules bound to the ligands can be determined with the same mass-dependent principle (Myszka, 2004). Moreover, the mass-dependent detection does not require protein-labeling, and this eliminates any possible changes that may occur to the properties of the protein during the process of labelling.

The Biacore^{TM} 3000 instrument is an SPR-based biosensor system which uses chips in analysis. The CM5 sensor chip has a thin layer of gold to which is attached to a carboxy-methylated dextran polymer. Biomolecules can be linked to the dextran layer with a variety of established chemical methods. The amount of bound analytes can be detected down to picogram levels per square millimeter on the gold surface. The major applications performed on this system include: biosample concentration measurements; binding analysis between biomolecular partners; multiple binding pattern analysis; enzymatic process monitoring; antibody-antigen epitope mapping and kinetic analysis. The principle of SPR is given in Figure 3.1.

A.

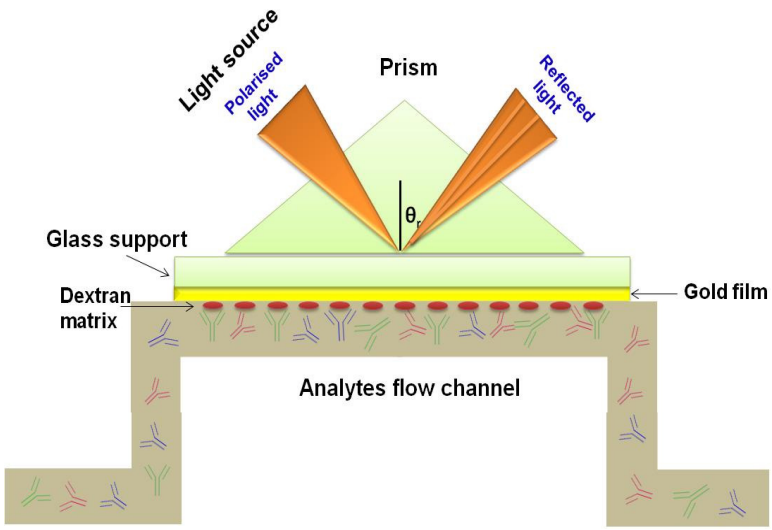

B.

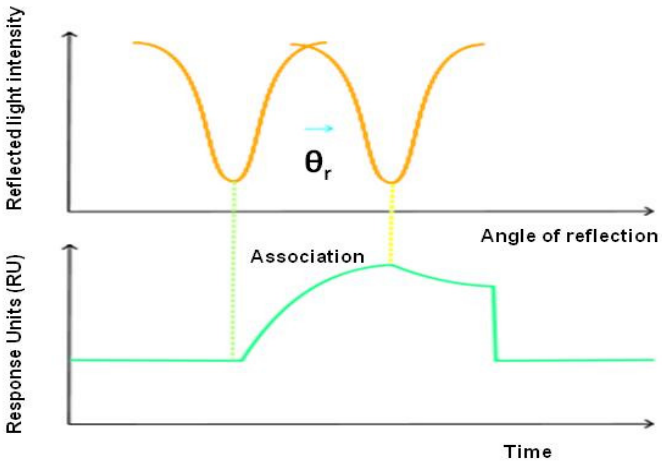

Figure 3.1. The principle of SPR detection. (A) A CM5 sensor chip is made up of a glass support coated with a thin gold film to which a covalently bound carboxy-methyl dextran matrix is attached. When a light source (polarised light) passes through a prism and strikes the gold film, the light is totally reflected (reflected light). The θr value represents the angle change of reflected light. (B) Correlations between the change of refractive index and SPR response. The SPR response represented by the response unit (RU) is a direct measurement of the angle of minimum reflected intensity. A change in the angle of reflected light of approximate 10^{-4} degrees correlates to a change of refractive index of 10^{-6} and this is also equivalent to one RU.

(Based on references: BIAtechnology handbook, 1998; Gomes and Audreu, 2002).

Although the principle of concentration measurements using SPR-based assays is similar to conventional ELISA, the SPR technique has a number of distinct advantages. For example, SPR continuously monitors the interaction at each time-point in each step; in contrast, ELISA only measures the end-point level of the final interactant. Moreover, SPR-based assays do not require washing steps, multiple secondary reagents or protein-labeling. The elimination of these steps and reagents means that SPR-based assays are simplified. In addition, they often display increased assay sensitivity.

A key application of SPR is kinetic and affinity studies on analyte-ligand interactions. Kinetic analysis is time-dependent and is used to describe how fast an interaction occurs, whereas affinity measurements describe the strength of complex formation (Fig. 3.2). Major parameters involved in kinetic studies are the association rate constant (k_a) and the dissociation rate constant (k_d). Affinity levels are represented by the equilibrium association constant (K_A) and the equilibrium disassociation constant (K_D). K_A is the ratio between k_a and k_d whereas K_D is the inverse of K_A (Crescenzo *et al.,* 2008).

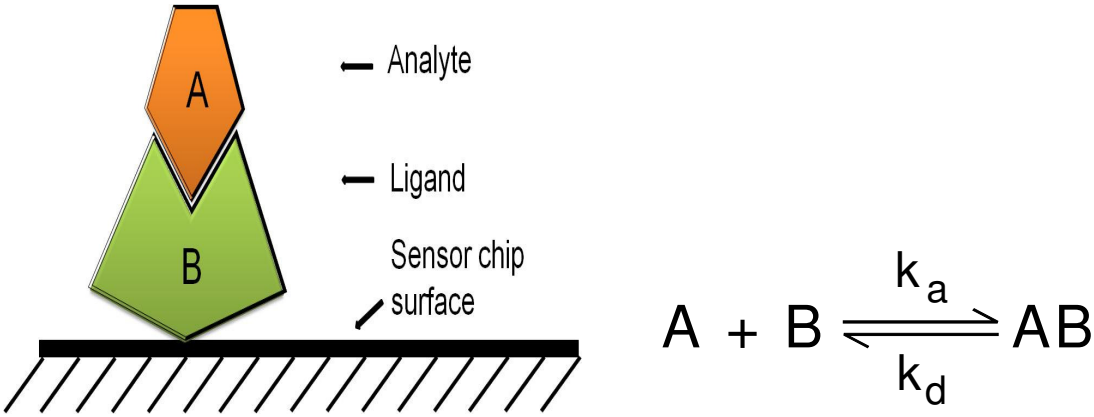

Figure 3.2. Formation of protein-protein complex in a 1:1 interaction. A represents the analyte to be measured which is free in a solution. B represents the ligand which is immobilised on a chip surface. AB in the complex formed by the interation between the analyte and ligand. Complex formation is a reversible process, and the terms k_a and k_d describe the association rate constant and dissociation rate constant, respectively. So the equilibrium association constant (K_A) and the equilibrium disassociation constant (K_D), descrbing the affiniteis of the complex, can be calculated using k_a and k_d values.

3.1.1 Work summary for the generation of avian anti-cTnT scFv antibodies

This chapter describes the use of phage display to produce recombinant anti-cTnT scFv antibody fragments. Before the immunisation procedure, the amino acid sequence of human cardiac troponin T (cTnT) was compared to its skeletal counterpart (sTnT). In addition, the sequence of human cTnT was also aligned with cTnT from other animal species including rabbit, mouse and chicken. It was found that cTnT from chicken was evolutionarily more distant to human than other species. Therefore, chicken was an optimal system for anti-cTnT antibody production. Commercial cTnT protein was analysed using SDS-PAGE to determine its purity and was subsequently used to inject a chicken host. For antibody production, the antibody RNA was isolated from chicken spleen and bone marrow when a sufficient immune response was obtained.

The scFv antibody genes were amplified from cDNA and then ligated into phagemid pComb3XSS vectors. The antibody phage library was subsequently constructed by transforming the antibody gene-containing plasmids into *E.coli* XL-blue cells. The selection of specific antibodies was achieved by performing five biopanning cycles. Antibodies with high cTnT binding levels were detected using a simple ELISA-based 'on-plate' screening method (Appendix I) and eleven antibodies were selected. Inhibition ELISA analysis was then performed using the crude bacterial lysates extracted from the eleven clones and clone F1 showed the highest antigen-detecting sensitivity. The F1 clone was then isolated and characterised using SPR-based kinetic studies. Finally, an inhibition assay was developed based on a purified F1 antibody. The precision of the inhibition assay was also investigated.

3.2 Results

3.2.1 Sequence alignment of cardiac troponin T with skeletal troponin T

As previously described in section 1.2.1, most classical cardiac markers are low in cardiac tissue specificity as they also exist in skeletal tissues. Therefore, skeletal tissue damage can also cause the elevation of their levels. In contrast, cardiac TnT is highly specific to cardiac tissue due to its distinct structural difference from its skeletal isoform (sTnT). In this section, the sequence of cardiac form of TnT (cTnT) was aligned with the sTnT to compare their structures. The aligment of the amino acid squence of both forms is shown in Figure 3.3.

The functional N-terminal region of the cTnT protein is the first 91 amino acids of the sequence (Sumandea *et al.,* 2009). The amino acid alignment showed a shorter N-terminal region for human sTnT compared to cTnT. Within the first 91 amino acid residues of the cTnT sequence, only 57 amino acids of sTnT were aligned. ClustalW version 2 software also determined that the similarity score between cTnT and sTnT was 59%. This indicated that both isoforms were significantly different.

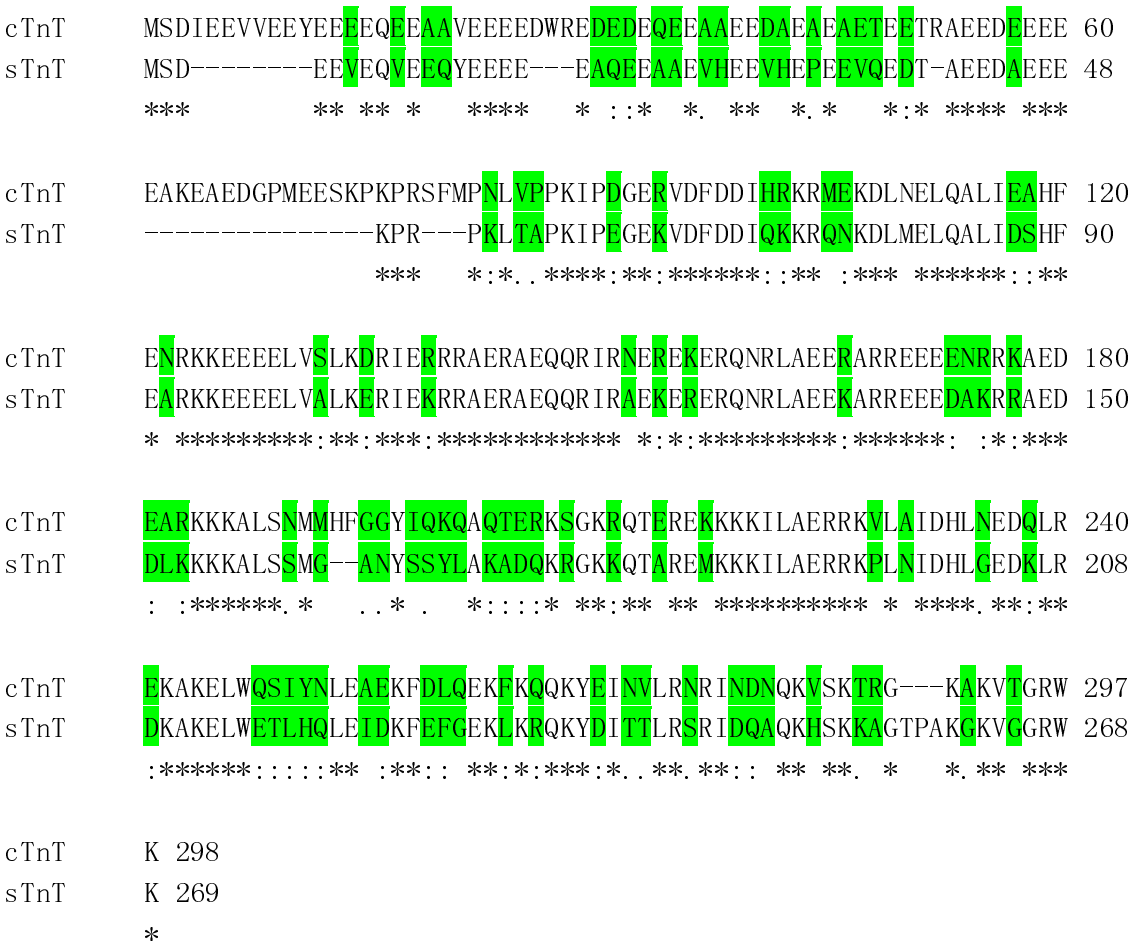

Figure 3.3. Protein sequence alignment between human cardiac TnT and skeletal TnT.

The amino acid sequences were aligned using ClustalW version 2 software. The variations in amino acids between the two sequences are highlighted in green. The dash line (‘-‘) indicates no amino acid at that position.

3.2.2 Sequence alignment of cTnT from human and other species

In order to examine if chicken would be a more suitable host than other animal species, the protein sequence of human cTnT was aligned with cTnT from rabbit, mouse and chicken (Fig. 3.4). The sequences similarity score between cTnT from human and other cTnTs were also determined by ClustalW version 2 software (Table 3.2).

It is shown in Table 3.2 that human and rabbit cTnT had 91% homology, and the similarity score between human and mouse was 87%, whereas human and chicken only had 78% homology. Therefore, cTnT from chicken is evolutionarily more distant from human than from other species.

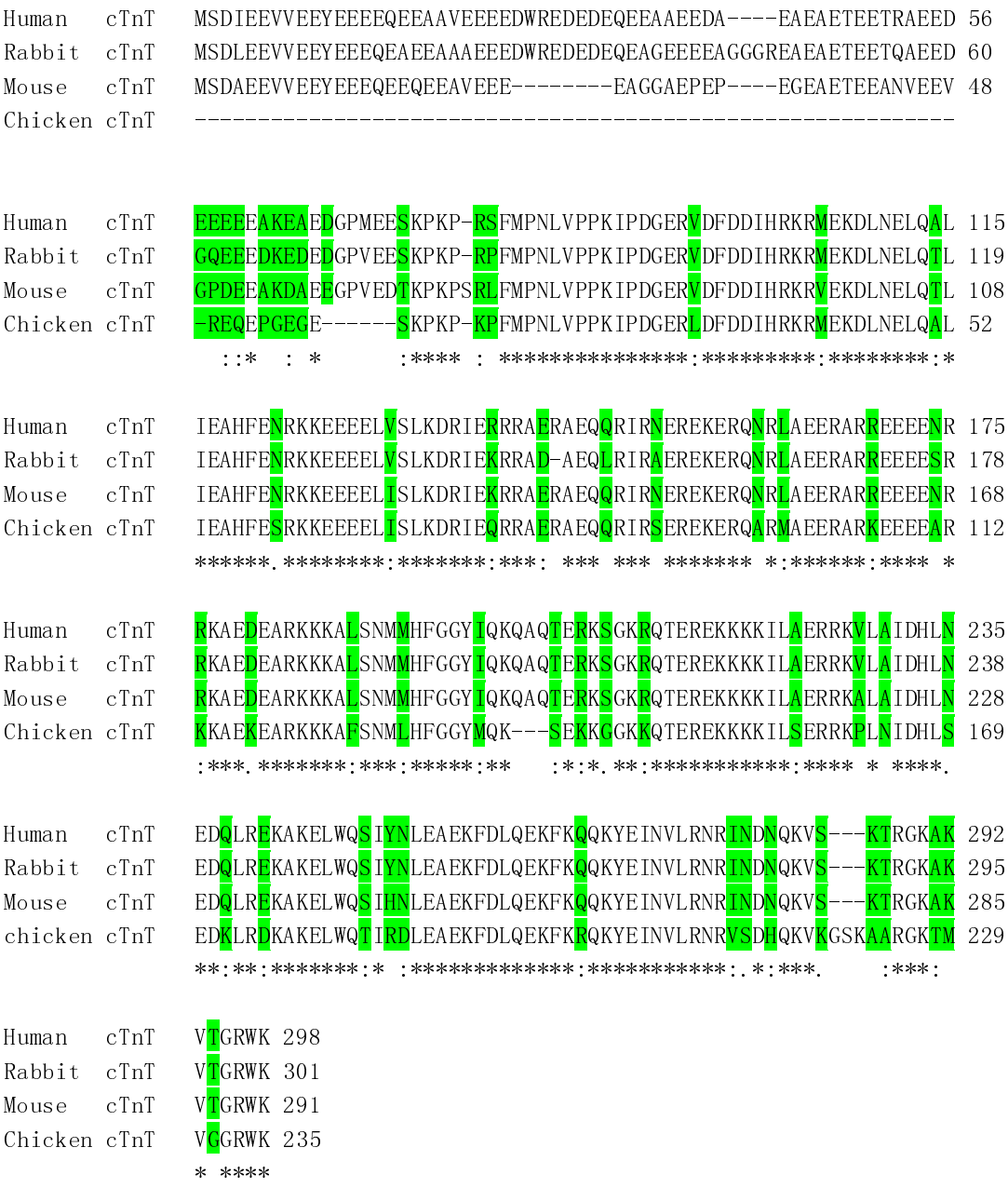

Figure 3.4. Protein sequence alignment of cTnT between human and other species. The variations of amino acids between human cTnT and other species are highlighted in green. The number at the end of each row represents the length of the sequence. The dash line (‘-‘) indicates no amino acid at that position.

Table 3.2. Similarity score between cTnT from human and other species

	Human vs Rabbit	Human vs Mouse	Human vs Chicken
Similarity score	**91%**	**87%**	**78%**

3.2.3 Verification of immunogen purity by SDS-PAGE

The purity of an immunogen is vitally important for producing an antibody with high antigenic specificity. The commercial human cTnT protein was analysed using SDS-PAGE to determine its purity. Human cTnT protein (~ 35 kD) with a concentration of 1.92 mg/mL was purchased from Life diagnostics, Inc. (USA). The cTnT protein was diluted in 1 x PBS buffer and analysed for purity on SDS-PAGE (Fig. 3.5).

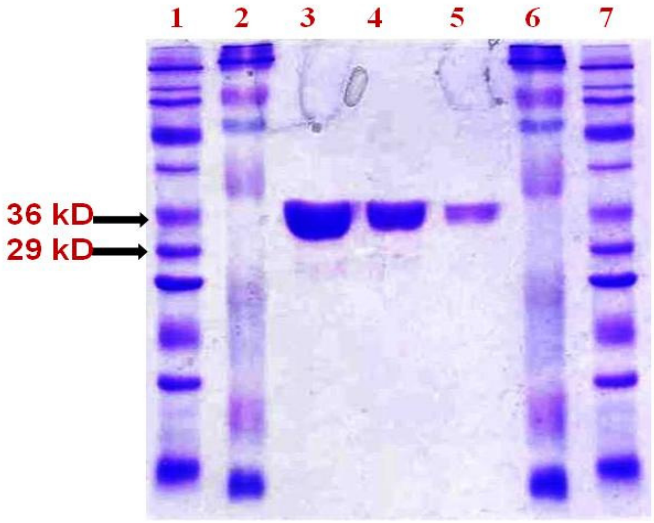

Figure 3.5. SDS-PAGE analysis of commercial cTnT protein.

Lanes 1 and 7 contained a Sigma-wide protein marker. Lanes 2 and 6 contained a Page-ruler prestain protein marker. Lanes 3, 4, 5 show a 1 in 10, a 1 in 20 and a 1 in 40 cTnT protein dilution in 1 x PBS buffer, respectively. Each of the lanes 3, 4 and 5 contained a single protein band at a size of approximately 35 kD, which indicated the presence of cTnT. No non-specific bands were observed in any of the three lanes. This suggested that the cTnT protein had high purity. The commercial cTnT protein was subsequently used as antigen for animal immunisation.

3.2.4 Determination of the antibody titre against cTnT in avian sera

Human cTnT was injected into a chicken host and four immunisations were performed. A bleed was taken seven days after the final immunisation. The serum anti-cTnT titre was performed using a direct ELISA format to detect the antibody response. A series of dilutions ranging from neat to 1 in 128,000 of the chicken serum diluted in 1 x PBST were tested. An antibody titre between 1/10,000 and 1/100,000 of antigen was observed from the ELISA, which indicated a sufficient immune response for cTnT.

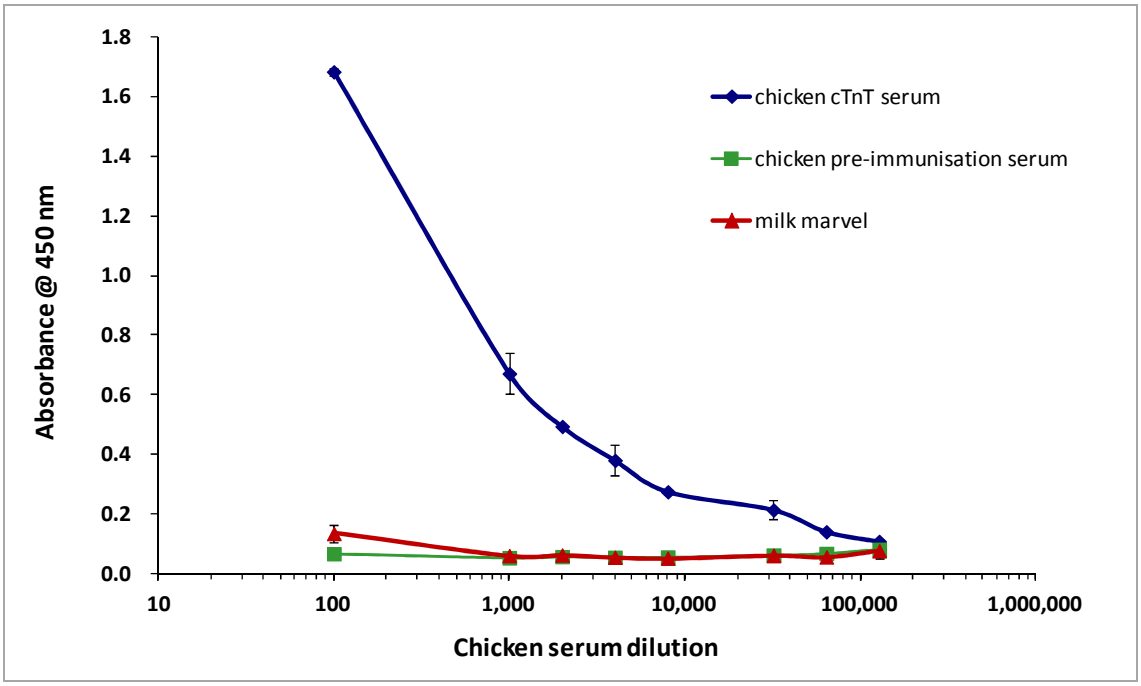

Figure 3.6. Determination of avian serum titre against cTnT. An ELISA plate was coated with 1µg/mL of the cTnT and blocked with 5% (w/v) Marvel in PBS. A 1 in 2,000 dilution of HRP-conjugated rabbit anti-chicken antibody was used as the secondary antibody to detect any positively binding antibodies to cTnT. A series of dilutions of the chicken pre-immunisation serum in 5% (w/v) Marvel in PBS, were used as negative controls. The serum titre was greater than 1/10,000 but less than 1/100,000. No antibody response was seen in the pre-immunised chicken serum.

3.2.5 PCR amplification of chicken variable heavy and light chain genes

The spleen and bone marrow were harvested from the chicken and total RNA was extracted. The concentration of total RNA extracted from the chicken spleen was 139.5 µg as determined by the Nanadrop^{TM} ND-1000. In contrast, only 11.7µg of total RNA was extracted from the bone marrow. Due to the low quantity of bone marrow RNA, only RNA from chicken spleen was used as template for the cDNA synthesis.

The first round PCR involved the amplification of V_H and V_L (Fig. 3.7). Agarose gel analysis showed that neither the V_H or V_L was amplified at a low $MgCl_2$ concentration, i.e. 0 mM, 0.5 mM and 1 mM. The V_L amplification was optimised using a concentration of 2 mM $MgCl_2$. At this concentration, the PCR reaction produced a strong band of ~ 350 bp. At the same $MgCl_2$ concentration, a clear strong band at ~ 350 bp with a small number of non-specific amplifications (greater than 350 bp) was also observed for the V_H chain. Large-scale amplifications were performed with 2 mM $MgCl_2$ for both variable genes. The PCR products were extracted, as detailed in section 2.3.1.8.

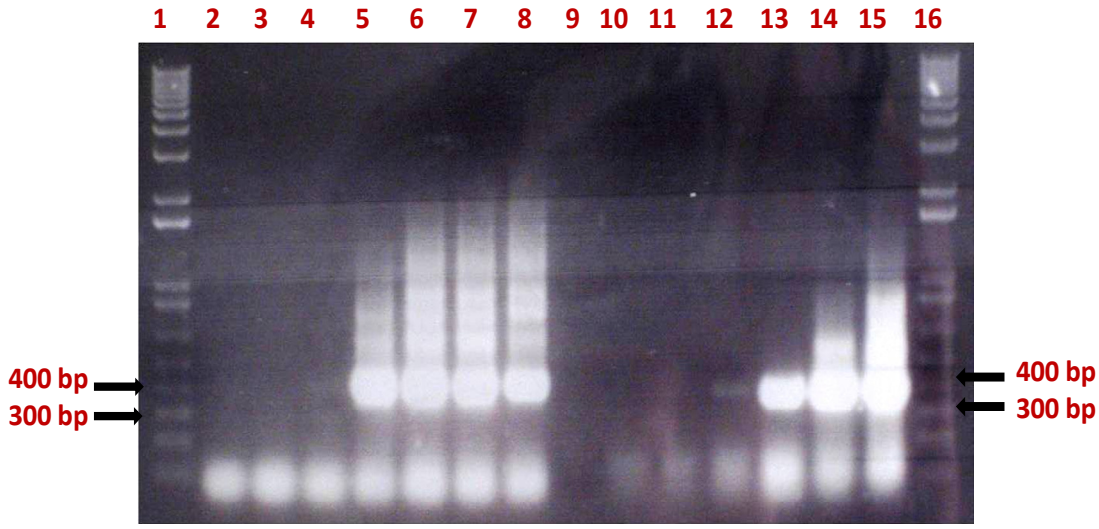

Figure 3.7. Optimisation of the amplification of the V_H and V_L genes using different magnesium concentrations.

Lanes 1 and 16 represent a 1 kb plus DNA molecular weight ladder (Invitrogen, USA). Lanes 2 to 8 represent amplifications of V_H with a series of $MgCl_2$ concentrations (0 mM, 0.5 mM, 1 mM, 2 mM, 3 mM, 4 mM, 5 mM, respectively). Similarly, lanes 9 to 15 represent amplifications of V_L with various $MgCl_2$ concentrations (0 mM, 0.5 mM, 1 mM, 2 mM, 3 mM, 4 mM, 5 mM, respectively). Lane 9 was intentionally left blank.

3.2.6 Anti-cTnT scFv-Splice by Overlap Extension (SOE) PCR

The SOE primers, CSC-F and CSCB (section 2.3.1.9), were used to link the purified V_H and V_L fragments with a glycine-serine linker $(Gly_4Ser)_3$. The SOE-PCR was optimised using different Mg^{2+} concentrations. In addition, the pComb3XSS vector was digested using a *Sfi*I restriction enzyme (see section 2.3.1.10). The digested pComb3XSS vector (~ 3400 bp) and stuffer fragments (~ 1400 bp), as well as the SOE-PCR product, were resolved on a 1% (w/v) agarose gel (Fig. 3.8).

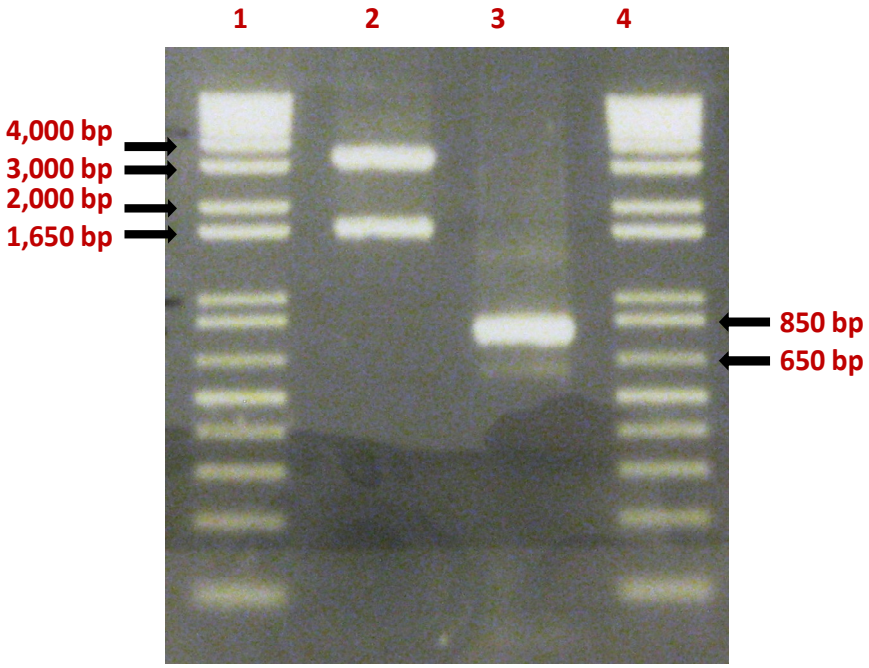

Figure 3.8. Optimised SOE-PCR and the digestion of the pComb3XSS vector. Lanes 1 and 4 contained a 1 kb plus DNA molecular weight ladder. Lane 2 contained the *Sfi*I digested pComb3XSS vector and stuffer fragment. Lane 3 contained the gel-purified SOE-PCR product. The PCR optimisation was performed by using a series of Mg^{2+} concentrations (0 mM, 0.5 mM, 1 mM, 2 mM, 3 mM, 4 mM). The optimal condition was selected as 3 mM $MgCl_2$. A large-scale SOE-PCR was performed and the PCR product was extracted, as described in section 2.3.1.8. A clear band (~ 750 bp) in lane 3 indicated the success of the SOE-PCR. In addition, the upper band between 3,000 bp and 4,000 bp shows the fully digested pComb3XSS, whereas, the lower band, near the 1,650 bp marker, is the vector's stuffer fragment.

3.2.7 Avian anti-cTnT scFv library construction and enrichment via biopanning

The gel-purified SOE-PCR product was extracted from a 1% (w/v) agarose gel and concentrated by ethanol precipitation. The PCR product and pComb3XSS vector were digested with the *Sfi*I restriction enzyme followed by overnight ligation with T4 DNA ligase. The ligated product was ethanol-precipitated and transformed into electrocompetent *E. coli* XL1-Blue cells by electroporation, as described in section 2.3.1.11. The transformed avian anti-cTnT scFv library had a size of 2.6×10^8 cfu/mL. Recombinant anti-cTnT scFv clones were selected from this library by performing five rounds of phage display biopanning against immobilised cTnT antigen, as described in section 2.3.1.12. The number of phage (phage titre) before and after each round of biopanning is shown in Table 3.3.

Table 3.3. Phage input and output titres over the 5 rounds of biopanning of the avian anti-cTnT scFv library

Biopanning round	Input (cfu/mL)	Output (cfu/mL)
1	1.3×10^{12}	1.0×10^5
2	1.7×10^{12}	9.0×10^4
3	1.5×10^{12}	5.2×10^5
4	1.0×10^{11}	5.0×10^4
5	1.6×10^{11}	1.3×10^4

3.2.8 Soluble expression of avian anti-cTnT scFv antibodies

A total of 96 anti-cTnT scFv antibodies were selected from biopanning round 5 output plates. These clones were subsequently analysed using a simple 'on-plate' monoclonal ELISA screening method (section 2.3.1.14). Positive clones were selected based on their absorbance. Generally, the threshold is set at three times the background signal (Updegraff and Anderson, 1991). In this study, the ELISA threshold was set at three times the absorbance of the blank sample.

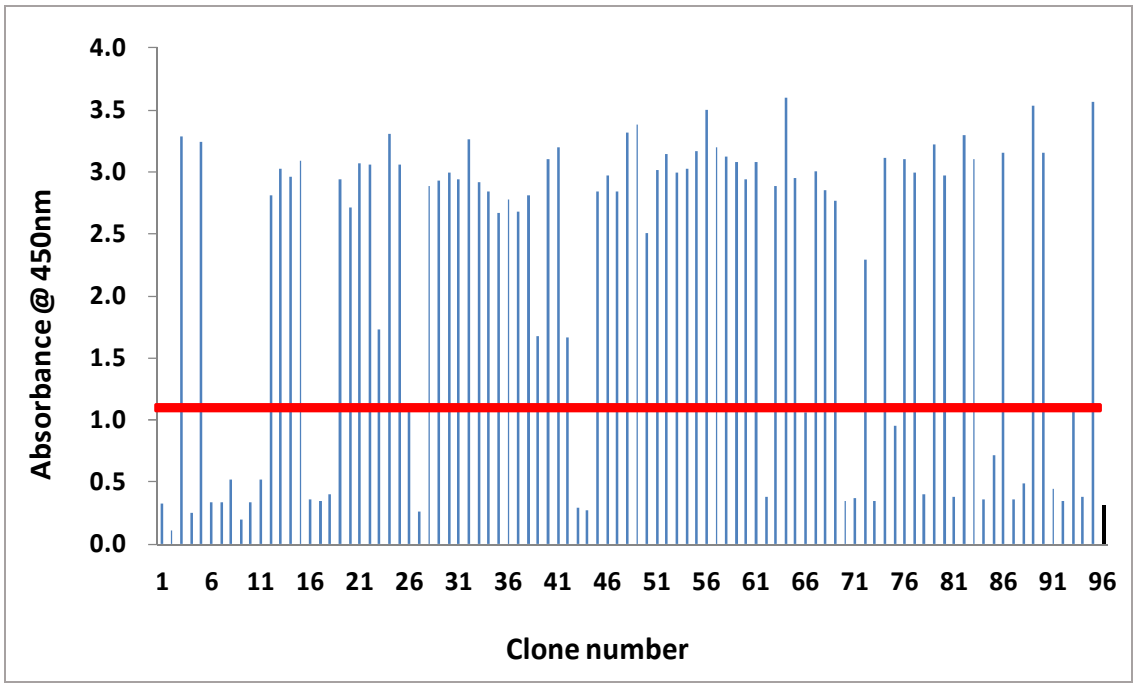

Figure 3.9. Screening of anti-cTnT scFv phage clones from round five of biopanning. Each of the blue bars represents the absorbance reading of each scFv antibody. A blank reference was also included in the analysis, which is represented by the black bar (96). To identify the positive antigen-binding clones, a red horizontal line which indicates the ELISA threshold was drawn at the absorbance level (~ 1.1). The threshold is three times of the absorbance value of the blank reference.

3.2.9 Titration ELISA analysis of anti-cTnT scFv antibodies

A total of eleven scFv clones that had significant binding reactivity against cTnT, as determined from monoclonal ELISA analysis, were grown up and expressed overnight. Crude bacterial lysates were prepared and subjected to a titration ELISA. Analysis revealed that individual anti-cTnT scFv clones had large differences in antibody expression. The midpoint of the linear range of the antibody titre was selected as the dilution value for a subsequent inhibition ELISA (Fig. 3.10).

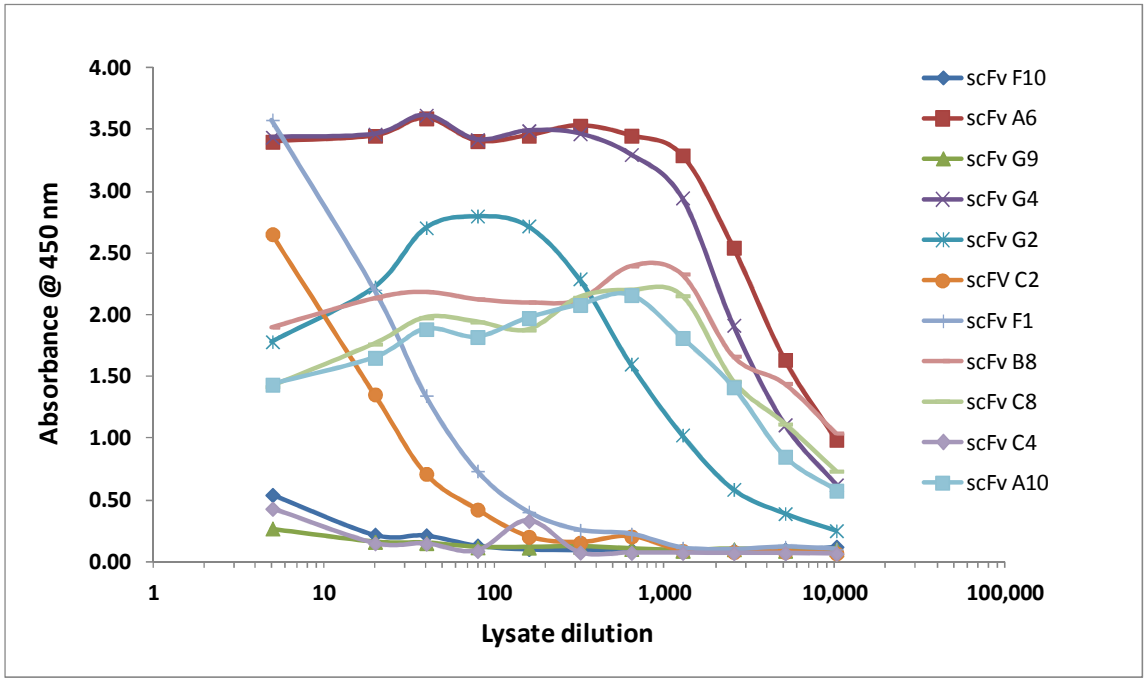

Figure 3.10. Antibody titre determination of anti-cTnT scFv antibodies. An ELISA plate was coated with 100 µL of 1 µg/mL cTnT and blocked with 200 µL 5% (w/v) milk Marvel in PBS. A series of dilutions of crude antibody lysates (1 in 5, 1 in 10, 1 in 20, 1 in 40, 1 in 80, 1 in 160, 1 in 320, 1 in 640, 1 in 1280 and 1 in 2,650) were prepared and 100 µL of each dilution was added into separate wells. The scFv antibodies were detected using HRP-labeled mouse anti-HA monoclonal antibody. The ELISA was developed with TMB substrate and the absorbance was read at 450 nm.

3.2.10 Inhibition ELISA analysis of anti-cTnT scFv antibodies

Inhibition ELISAs were performed with the same set of clones previously described in section 3.2.9. The dilution factors of the crude lysates of each clone were based on the midpoint value obtained from the titration ELISA (Fig 3.10). An A_0 standard, which is the absorbance of antibody lysate dilution without any inhibition of free antigen, was also included in the analysis. The degree of inhibition was calculated by dividing the absorbance value at each cTnT concentration (A) with the A_0 absorbance value. The data were fitted into a four parameter equation using SigmaPlot version 11.0 software. Out of the eleven clones tested, clone F1 had the lowest IC_{50} value of 214 ng/mL (Fig. 3.10).

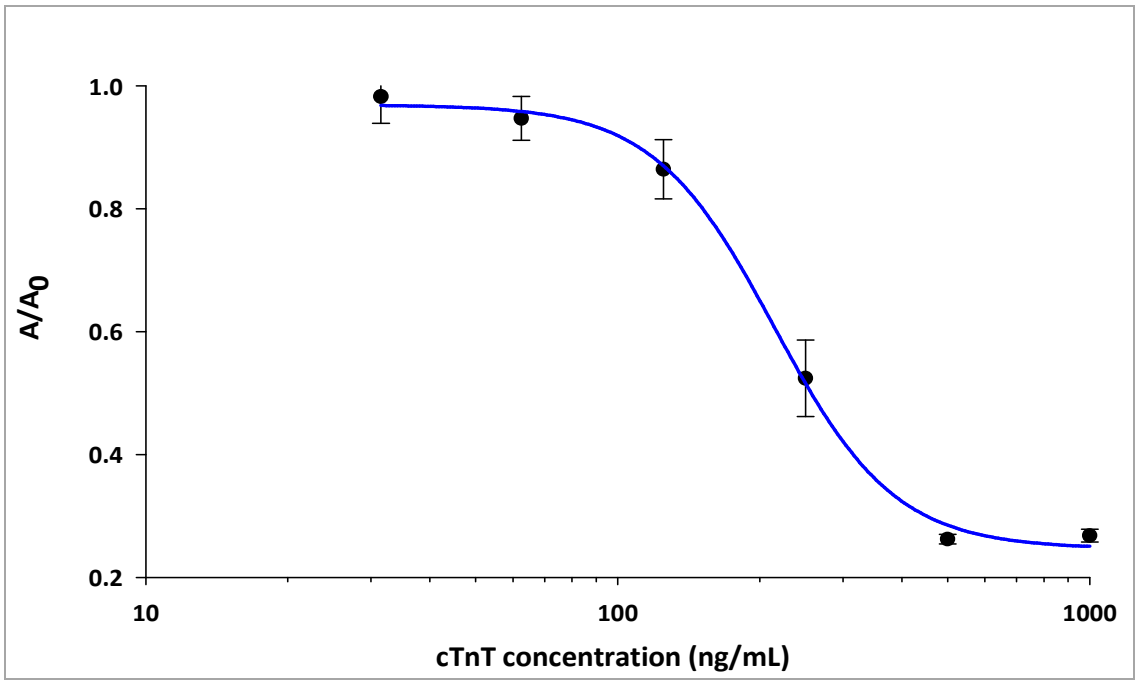

Figure 3.11. Inhibition ELISA analysis of anti-cTnT scFv antibodies.

An ELISA plate was coated with 1 µg/mL cTnT and blocked with 200 µL of 5% (w/v) Marvel in PBS. Various concentrations of cTnT (1,000, 500, 250, 125, 62.5, 31.25 and 15.63 ng/mL) were incubated with a 1 in 40 dilution of the scFv clone F1, for 1 h at 37°C. ScFv binding was detected using HRP-labeled mouse anti-HA monoclonal antibody. The ELISA was developed with TMB substrate and the absorbance was read at 450 nm.

3.2.11 Purification of Anti-cTnT F1 scFv antibody using immobilised metal affinity chromatography (IMAC)

The F1 antibody demonstrated the lowest the IC_{50} value, as determined through the antibody selection process, and it was subsequently purified using the IMAC protocol, as described in section 2.3.1.16. The fractions from the different purification stages were analysed by SDS-PAGE and Western blotting (Fig. 3.12).

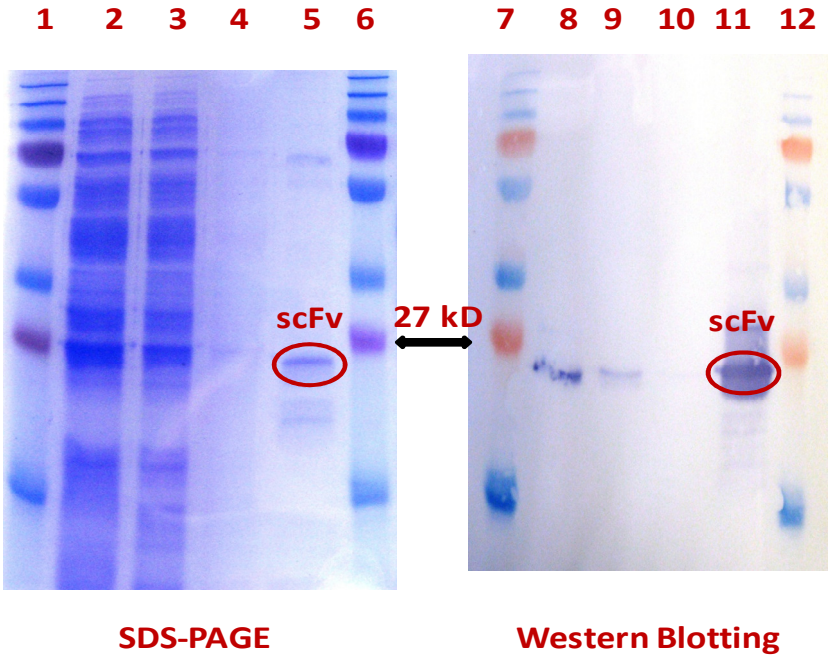

Figure 3.12. SDS-PAGE and Western blotting analysis of the F1 scFv.
Lanes 1, 6, 7 and 12 contained a set of page-ruler prestain protein markers. Lanes 2 and 8 contained crude lysates, extracted by sonication. Lanes 3 and 9 contained 'flow-through' that was obtained after passing the *E. coli* cell lysate through a Ni-NTA agarose resin. Lanes 4 and 10 contained the washed fractions. Lanes 5 and 11 contained the eluted fractions.

Lanes 2 and 3 contained a large number of contaminant proteins of various sizes. No significant protein banding differences were observed between the crude lysates in lane 2 and the 'flow-through' solution in lane 3. In contrast, lanes 4 and 10, which contained wash fractions collected after passing washing buffer through the column, had little or no protein bands. This indicated the removal of non-specific proteins from the column

resin. A clear strong band just below 27 kDa was observed in lane 5 (marked by a red circle) and this indicated the successful purification of the F1 scFv antibody (25 kD). In addition, a small number of non-specific bands were also observed in the eluted sample. The SDS-PAGE analysis was performed in duplicate. A second gel was used for Western blotting verification, and a single band just below 27 kDa was observed in each of the lanes 8 and 9, thus indicating the presence of specific anti-cTnT scFv antibodies. No protein bands were observed in lane 10 thus indicating that non-specific proteins were removed. Lane 11 contained the elution fragment. The major band (marked by a red circle) was present just below the 27 kDa marker, thus verifying the identity of the F1 scFv. However, a number of non-specific bands (smeary bands) close to the major band were also present in lane 11. These may be due to the concentration of the secondary antibodies being too high, or the incubation with the secondary antibodies being too long. The protein concentration of the highly purified F1 scFv was 0.74 mg/mL (a total of approximately 0.37 mg antibody) as determined by the Nanodrop^{TM} ND-1000. An ELISA was subsequently performed to determine the titre of the purified F1 scFv (Fig. 3.13).

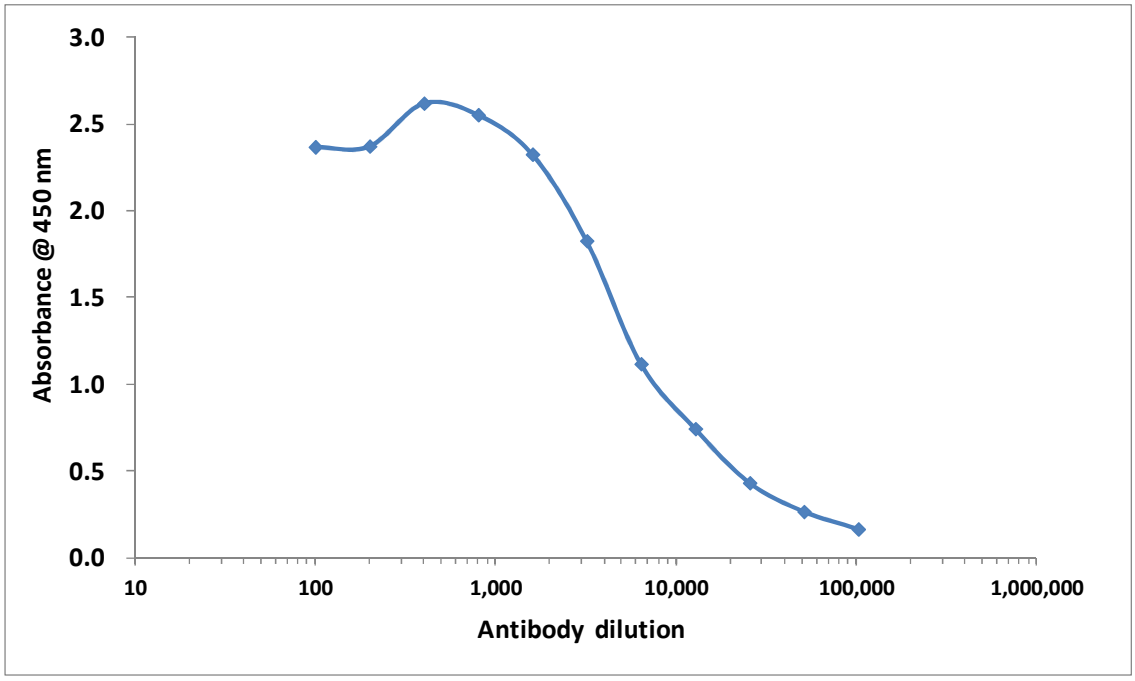

Figure 3.13. Antibody titre determination of purified anti-cTnT scFv F1 antibody. An ELISA plate was coated with 100 µL of 1 µg/mL cTnT and blocked with 200 µL 5% (w/v) Marvel in PBS. A series of dilutions of purified F1 antibody (1 in 100 to 1 in 102,400) was prepared and 100 µL of each was added into the wells. The scFv antibodies were detected using HRP-labeled mouse anti-HA monoclonal antibody. The ELISA was developed with TMB substrate and the absorbance was read at 450 nm.

The midpoint of the linear range (1 in 6,400) of the titration ELISA was selected as the optimal dilution for an inhibition ELISA. Kinetic studies and inhibition studies were then performed using the purified F1 scFv.

3.2.12 Preconcentration analysis of rabbit anti-HA polyclonal antibody for immobilisation on a dextran chip surface

A CM5 dextran chip surface was prepared for kinetic studies of the F1 scFv using the Biacore™ 3000. The preparation process involved a preconcentration study and ligand immobilisation (section 3.2.13). This section describes the preconcentration on a CM5 dextran chip surface.

Preconcentration allows the identification of the optimal conditions for ligand immobilisation on the chip surface. A suitable pH value is selected from this step and this maximises the amount of ligand that is covalently linked to the dextran surface. Sodium acetate buffer solution has a low ionic capacity and its use favours the electrostatic attraction between the negatively charged dextran matrix and the positively charged ligand, which is dissolved in the sodium acetate solution. A preconcentration study was performed using a rabbit anti-HA epitope tag polyclonal antibody as a capture ligand mixed with sodium acetate buffer solutions at six different pH values (Fig. 3.14). Initially, a desorb procedure was performed on the Biacore^{TM} instrument to clean the microfluidic tubes, chamber, and injection port. A CM5 dextran was then docked and primed five times with 1 x HBS buffer prior to the preconcentration run.

Figure 3.14 shows increased RU with decreased pH values. The lowest RU level was obtained at pH 5.0 whereas the highest RU level was observed at pH 4.0. In general, the optimal pH value is the one which can generate the maximum surface binding response. This value should also be lower than the isoelectric point (pI) of the immobilised ligand. Due to the negatively charged chip surface, the lower pH can maintain the positive charge of the ligand solution thus keeping the electrostatic attraction pattern between the ligand and the chip surface. pH 4.0 was selected as optimal for the immobilisation of anti-HA antibodies.

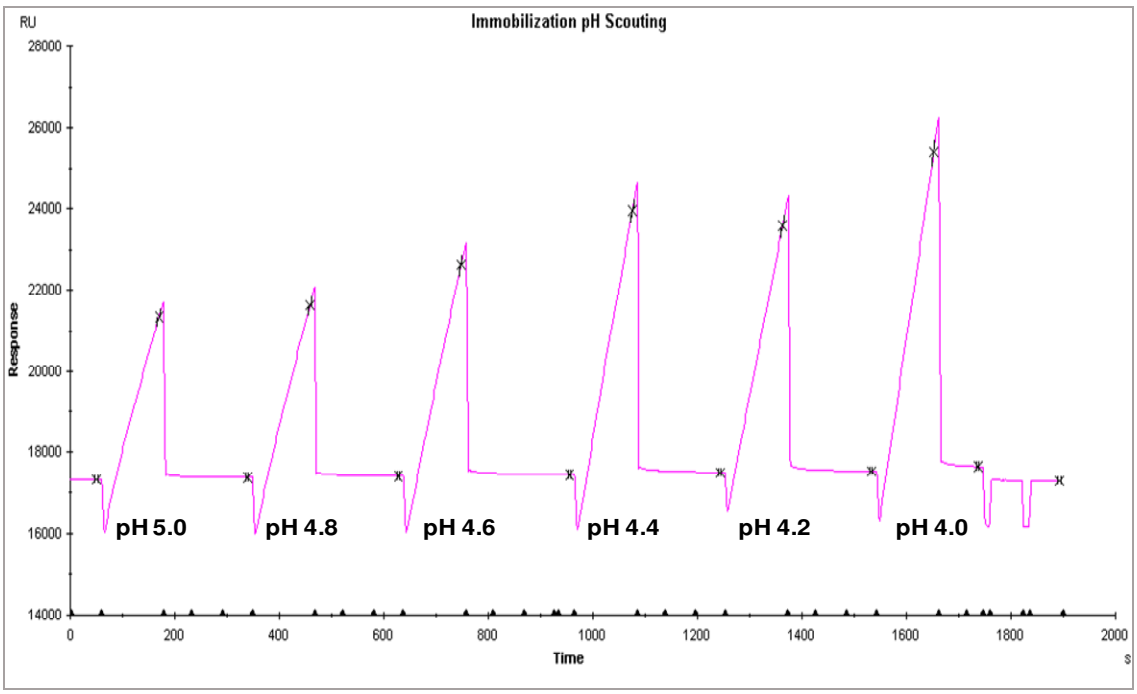

Figure 3.14. Preconcentration profile of an anti-HA polyclonal antibody for immobilisation on a CM5 chip. Six different sodium acetate buffer (10 mM) solutions (at pHs of 5.0, 4.8, 4.6, 4.4, 4.2 and 4.0) were mixed with anti-HA polyclonal antibody to give a final antibody concentration of 12.5 µg/mL. The experiment was set-up using the Biacore™ 3000 surface preparation wizard. The levels of ligand binding were indicated by response units. The highest level of binding occurred at pH 4.

3.2.13 Immobilisation of rabbit anti-HA polyclonal antibody on a dextran chip surface

Many different chemistries for surface coupling of protein to a metal surface have been developed (Karlsson and Larsson, 2004; Rich and Myszka, 2005). Amino coupling is a common approach for attaching the ligand covalently to the dextran matrix (Rich and Myszka, 2005). Using a mixture of equal volumes of EDC (0.4 M) and NHS (0.1 M), the carboxymethylated dextran matrix can be activated resulting in the formation of functional succinimide ester groups. Primary amine groups on a ligand can be covalently linked with succinimide ester groups thus enabling the immobilisation of the ligand on the chip surface. The unbound functional groups on the chip surface are inactivated with ethanolamine-HCl (1M). Subsequent regeneration steps remove non covalently linked substances from the coupling process. The RU difference between the

end of regeneration step and the beginning of activation step indicates the level of immobilisation obtained (Fig. 3.15). The final RU is correlated with the amount of antibodies immobilised, which was approximately 7,120 RU.

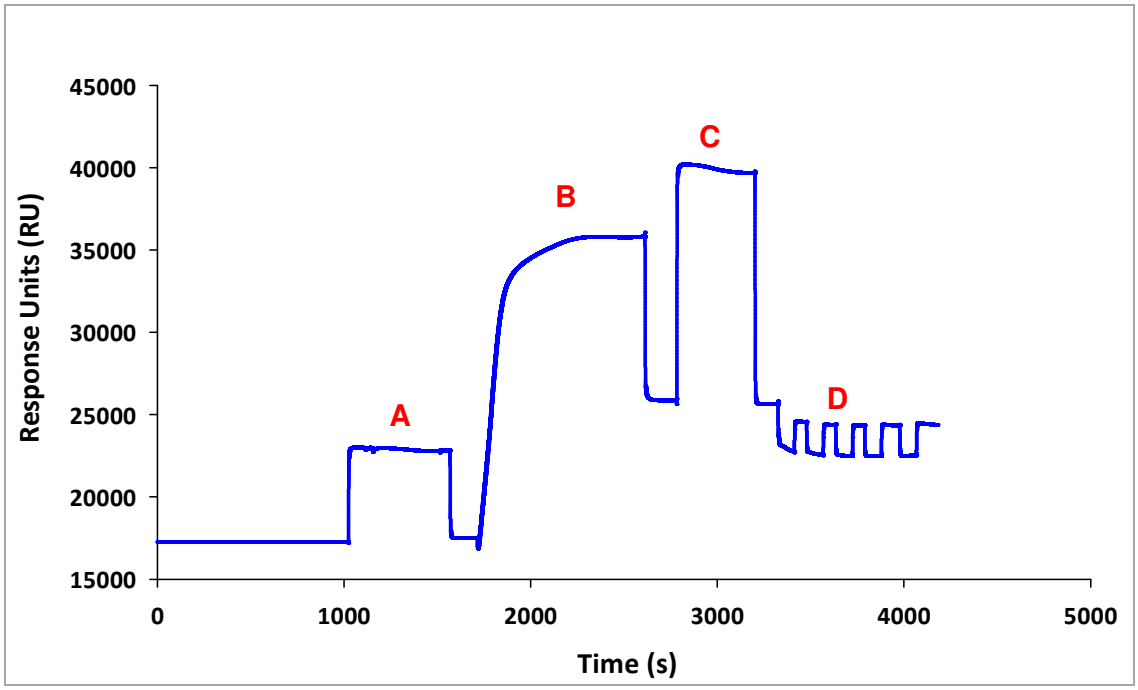

Figure 3.15. Immobilisation of anti-HA antibodies on a Biacore™ CM5 chip surface. Anti-HA antibody was diluted in 10 mM sodium acetate buffer (pH 4.0) to a final concentration of 25 ng/mL. Four main steps, indicated by letters A to D in Figure 3.15, show the sequential steps involved in the immobilisation process. Step A: surface activation occured when a mixture of EDC and NHS was passed over the dextran surface. Step B: antigen was covalently bound to the activated dextran via the amine groups. In step C, ethanolamine-HCl was used to block unreacted groups on the surface. Finally, in step D, the chip surface was regenerated using five injections of 20 mM NaOH, which was found to be the optimal procedure for surface regeneration.

3.2.14 Kinetic studies of anti-cTnT scFv F1 antibody

'Real-time' monitoring of protein-protein interactions on Biacore™ 3000 can be applied to antibody kinetic studies. The data collected over a specified time are used for the determination of both the association rate constant (k_a) and the disassociation rate constant (k_d). The equilibrium association rate constant (K_A) and the equilibrium

dissociation rate constant (K_D) can be calculated subsequently. Kinetic studies on F1 antibody were performed using a capture assay format (see section 2.3 .1.19). A range of cTnT antigen concentrations were selected for binding studies and the experimental binding curves were fitted to the theoretical curves (binding model). A number of factors were involved for choosing a suitable model for the anti-cTnT scFv studies. For example, for efficient estimation of the binding constant, the binding model is required to be as simple as possible. In this study, the interaction between cTnT antigen and anti-cTnT scFv was a homogeneous 1:1 interaction, therefore, complicated heterogenous binding models did not suit. In addition, the model selected should allow analysis of a wide range of ligands and analyte concentrations. The 1:1 Langmuir binding model is a simple classical model which can be used for the majority of protein-protein interaction studies. It assumes that both the analyte and ligand are homogeneous. It also assumes that the analyte is monovalent, which is particularly useful for antigen-specific antibody studies. Moreover, a range of analyte concentration can be used for this model. Therefore, the F1 kinetic curves were fitted to a 1:1 Langmuir binding model. Association and disassociation information was recorded throughout the process (Fig. 3.16).

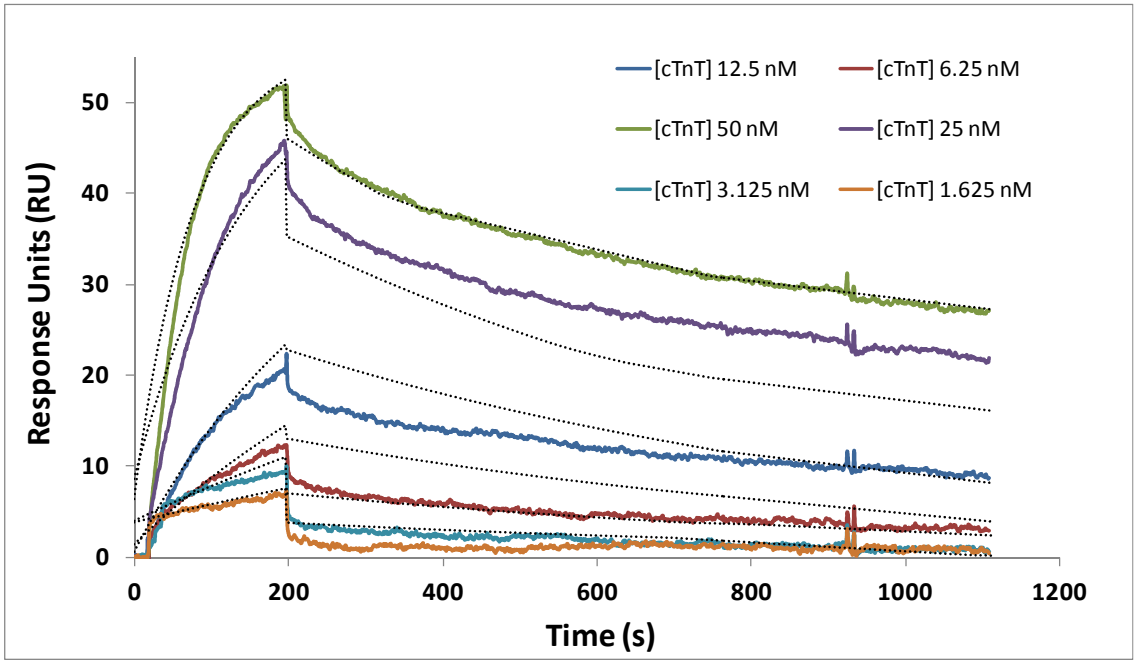

Figure 3.16. Kinetic characterisation of anti-cTnT F1 scFv antibody on Biacore™ 3000. The F1 scFv antibodies were passed over the anti-HA antibody surface. Then cTnT, at concentrations of 50, 25, 12.5, 6.25, 3.125 and 1.625 nM, were passed over the chip surface. The analysis of cTnT binding at a concentration of 12.5 nM was carried out in duplicate. The curves (in color) represent the six different cTnT concentrations and were fitted to a 1:1 Langmuir binding model (black dotted line). Kinetic parameters were evaluated using the Biaevaluation 4.1 software. Poor fitting of the experimental curves with the binding model was observed.

Table 3.4 lists the kinetics constants obtained from the evaluation. The affinity of F1 was determined as 2.4 nM. However, this data was not reliable due to poor curve fitting.

Table 3.4. Parameters determined from scFv F1 kinetic analysis

k_a ($M^{-1}s^{-1}$)	k_d (s^{-1})	K_A(M^{-1})	K_D (M)
2.7×10^5	**6.5×10^{-4}**	**4.2×10^8**	**2.4×10^{-9}**

3.2.15 Inhibition assay analysis of anti-cTnT scFv F1 antibody

In order to obtain accurate data to determine the antigen detection capacity of F1 antibody, an inhibition assay was performed. An inhibition assay is based on the capacity of analyte binding to free molecules in solution, resulting in an inhibition binding of the analyte to the ligand which is linked on a surface. It is an effective method for measuring the concentration of free molecules in solution. Assay performance generally can be validated by its precision, specificity and accuracy. Precision of an assay refers to the agreement between data collected from replicate measurements on the same sample, which can be represented by the standard deviation (SD) and coefficient of variation (CV). Assay specificity refers to the capacity of the assay to measure the analyte without the interference from other substances present in the sample. Assay accuracy describes the agreement of measured concentrations with accepted reference value. Data collected from a standard reference assay are required for assay accuracy validation. Terms such as limit of detection (LOD), limit of quantification (LOQ) and IC_{50} often used to describe the performance of an assay.

3.5. Description of parameters in an inhibition assay

Parameters	Description
LOD	Lowest analyte concentration in a sample that can be detected
LOQ	Valid range of analyte concentrations (from lowest to highest) within which the assay performance is acceptable
IC_{50}	The concentration of analyte which gives 50% of the maximum response

(Based on references: Armbruster *et al.,* 1994; Armbruster and Pry, 2008)

The inhibition assay of F1 was performed using an ELISA format. The purified F1 antibody was diluted 1 in 6,400 in PBS (see section 3.2.11) and then incubated with different concentrations of free cTnT antigen. The mixture was added into a cTnT-coated ELISA plate thus allowing competitive binding of F1 antibody with free cTnT and cTnT bound on ELISA plate. Intra-day assays (three assays on the same day) were also performed to assess the assay performance. The collected data were fitted in a four-parameter calibration curve using SigmaPlot version 11.0 software (Fig. 3.17).

Figure 3.17 shows all the five data points are in the linear range of the inhibition assay, thus, the precision of the assay was determined using the data of the five points.

The precision (repeatability) of the F1 inhibition assay was assessed using the coefficient of variation in percentage (% CV) values. Percentage for CV was determined from the ratio between the Standard deviation (SD) and mean then multiplying by one hundred. Table 3.6 shows the mean of A/A_0 values, SD and % CV for the intra-day assays. The % CV values showed a precision ranging from 1.9% to 11.6%.

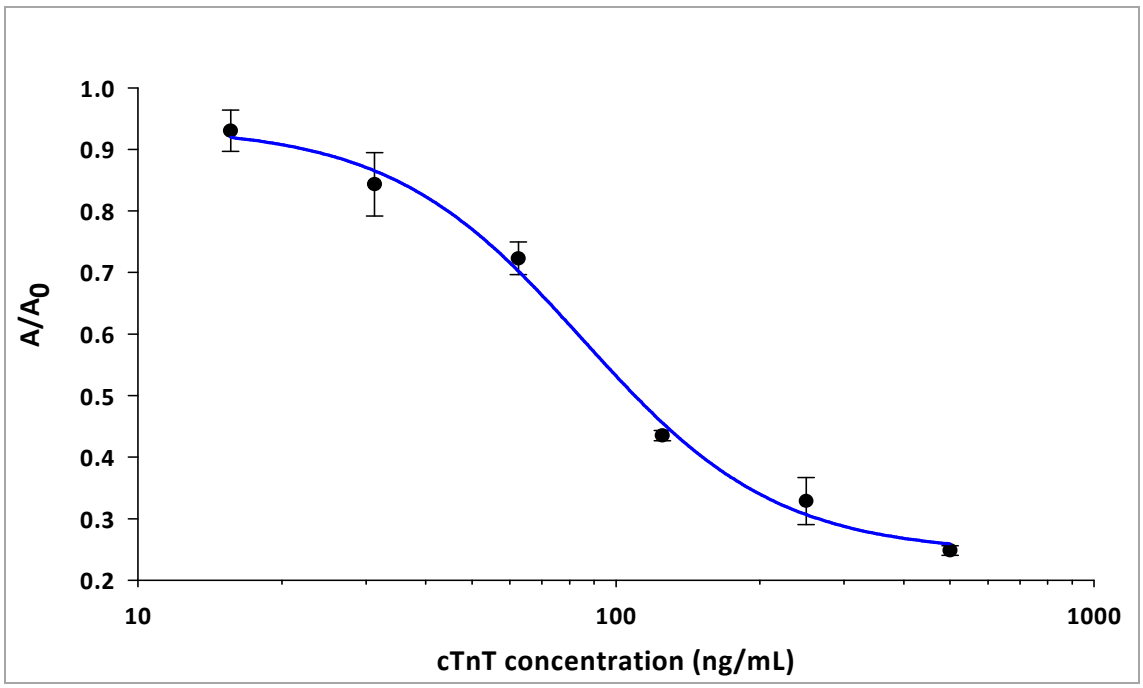

Figure 3.17. Inhibition ELISA analysis of purified anti-cTnT scFv F1 antibody. An ELISA plate was coated with 1 µg/mL cTnT and blocked with 200 µL of 3% (w/v) BSA in PBS. Various concentrations of cTnT (500, 250, 125, 62.5, 31.25, 15.63 ng/mL) were incubated with the F1 scFv antibodies for 1 hour at 37°C. The scFv antibodies were detected using HRP-labeled mouse anti-HA monoclonal antibody. The ELISA was developed with TMB substrate and the absorbance was read at 450 nm. A four-parameter fitted curve was plotted using SigmaPlot version 11.0 software. The IC_{50} value of purified F1 antibody was determined as 85 ng/mL. The error bars represent the mean values +/- the standard deviation.

Table 3.6. Parameters determined for the evaluation of inhibition assay precision

[cTnT] ng/mL	Mean	SD	%CV
500	0.25	0.01	3.1
250	0.33	0.04	11.6
125	0.44	0.01	1.9
62.50	0.73	0.02	3.7
31.25	0.84	0.05	6.1
15.63	0.93	0.03	3.6

3.3 Discussion

This chapter described the generation of recombinant antibody fragments against cTnT, a 'gold standard' for CVD diagnosis. It was focused on the construction of an avian immune antibody library using a chicken host and the selection of a cTnT-specific scFv using the phage display technique. Antibody purification, characterisation and assay development were also described.

Cardiac TnT is unique to cardiac muscle due to the fact that it possess unique epitopes not found in the skeletal isoform (sTnT) (Mair *et al.,* 1992). In order to obtain an in-depth understanding of their structural differences, the amino acid sequence between cTnT and sTnT was aligned and compared. It was found that sequence homology was 59% (Fig. 3.3). The dissimilarity value is higher than described by Mair. He reported that cardiac troponin T was 10% to 30% structurally different from its skeletal form (Mair, 1997). In addition, Perry also reported the structural differences between cTnT and sTnT, where cTnT always contains more amino acid residues than sTnT (Perry, 1998). Furthermore, a longer N-terminal portion of cTnT than present in sTnT was also observed from sequence alignment. Only 57 amino acid residues of sTnT were aligned with the first 91 amino acid residues of the cTnT sequence (Fig. 3.4). This observation concurs with Perry's study, which reported the N-terminal of TnT from rabbit cardiac muscle was approximately 50 Å longer than its skeletal isoform (Perry, 1998). Similarly, Gusev also indicated that TnT isoforms synthesized from skeletal and cardiac muscles vary in length and amino acid composition of the N-terminal 40-60 member peptides (Gusev *et al.,* 1983). Therefore, the high levels of structural difference enabled the production of specific antibodies binding solely to cTnT.

In order to ensure that a chicken was a suitable host for antibody generation, its cTnT sequence was aligned with cTnT from other animal species. The similarity score revealed that human and chicken only had 78% homology. This score was lower than that found in human and rabbit (91%) and between human and mouse (87%). The low similarity confirmed that cTnT from chicken species was in evolutionary terms, more distant from human and therefore, the production of antibody in chickens should achieve a better immune response than in rabbits and mice.

For antibody production, both a suitable animal host and a antigen of good quality are important. An immunogen of low purity (containing contaminating proteins) can lead to the animal host responding to non-related proteins thus producing antibodies with low antigenic specificity. Human cTnT was used as an immunogen in this study and was purchased from Life Diagnostics Inc. (USA). The purity of immunogen was verified by SDS-PAGE analysis. As shown in Figure 3.5, a single clean protein band indicated that the cTnT immunogen had a high level of purity (Fig. 3.5). This commercial cTnT protein was subsequently used to immunise a chicken. After the 4th immunisation, the chicken serum had a titre in excess of 1 in 10,000 against the cTnT antigen, which indicated the chicken host had generated a sufficient polyclonal response. A preliminary inhibition ELISA showed that the crude bacterial lysates from the F1 scFv antibody had an IC_{50} value of 214 ng/mL (Fig 3.11). Crude lysate solutions are routinely extracted from cells by destroying the cell membrane, using freeze-thaw cycles or sonication. During cell lysis, the desired proteins and a large quantity of non-specific substances are released. Due to the simplicity of the technique, crude lysates are widely used in immunoassay development. For example, Yin and colleagues successfully developed an assay for the quantification 'collagen-like' polymer based on crude cell lysates (Yin *et al.,* 2002). An ELISA assay was also reported for the detection of a blood coagulation factor XIII subunit A using crude cell lysates (Katona *et al.,* 2001). However, non-specific substances can interfere the performance of the assay. For instance, the target recombinant protein fragment can be easily degraded by proteolytic enzymes in the cell lysates. Therefore, purified antibody is still the choice for protein characterisation studies and assay development. In this study, the F1 scFv antibody was purified prior to kinetic analysis and assay development.

The Biacore^{TM} 3000 biosensor system used the 'real-time' and 'label-free' approach for SPR-based protein-protein interaction studies. Pre-concentration pH analysis revealed that sodium acetate buffer, pH 4.0, was optimal for immobilisation of rabbit anti-HA polyclonal antibody onto a CM5 sensorchip surface (Fig. 3.14). In contrast, Leonard and co-workers reported that a sodium acetate buffer with a pH 4.5 was optimal for anti-HA antibody immobilisation (Leonard *et al.,* 2011). The difference in pH may be due to the variation between chip surfaces or the sources of anti-HA antibodies used. An

RU level of 7,120 was obtained after the immobilisation of anti-HA antibodies onto the CM5 sensor chip. This amount was considered sufficient for subsequent SPR studies.

Kinetics analysis was performed on the purified F1 scFv antibody using the previously prepared anti-HA sensor chip. A 1:1 Langmuir binding model was chosen for curve fitting (section 3.2.14). The kinetic study showed the anti-cTnT F1 antibody had an affinity (K_D) of 2.4 nM (Table 3.4). However, figure 3.16 displayed that all six of the experimental curves poorly overlaid the binding model curves. Significant deviations were observed in both the association phase and the disassociation phase (Fig. 4.11). A number of factors may have affected the accuracy of this kinetic study and thus impacted on the curve fitting. One key factor was the amount of ligand (F1 antibodies) captured on the sensorchip surface. Generally, a low ligand capture level can prevent the rebinding of the analyte during the disassociation process (Karlsson and Larsson, 2004). In this study, the amount of F1 antibodies captured on the sensorchip surface generated a low cTnT binding level (52 RU), hence indicating a relative low ligand capture level.

It is possible that mass transport may have negatively impacted the kinetic study. Mass transport describes the movement of antibody molecules from the buffer solution to the sensorchip surface. Mass transfer can be influenced by the flowrate of buffer solution hence affecting ligand-analyte binding (Goldstein *et al.,* 1999). It is possible that the kinetic experiment was mass transport limited, either due to the excess levels of immobilised anti-HA or captured scFv antibodies. It is also possible that the scFv solution was heterogeneous and consisted of monomers, dimers and other multimers, therefore, avidity effects on the sensorchip surface prevented the accurate determination of the kinetic rate constants.

In order to obtain more reliable data to interpret the antigen binding capacity of the F1 antibody, an inhibition assay was developed (Fig. 3.17). It was shown that the F1 had an IC_{50} of 85 ng/mL and this value was lower than that observed from the crude lysate analysis (214 ng/mL). Elimination of interferences from non-specific protein in crude lysate may have improved the antigen detection levels of the F1 scFv. Analysis of the

linear range of the F1 antibody intra-day assays, showed that the assay precision (1.9% to 11.6%) was within an acceptable range (< 20%), as reported by Reed and co-workers. They demonstrated that CV levels in an immunoassay that exceed 20% are expected to cause a loss of precision. Such large variations in CV are often seen when quantifying samples at the extreme ends of an assay's range (Reed *et al.,* 2002). In contrast, Makin demonstrated that the acceptable assay precision of an immunoassay was less that 10% (Makin, 2010). Using highly purified F1 antibodies may improve the cTnT ELISA inhibition assay.

In conclusion, recombinant anti-cTnT scFv fragments were successfully produced and SPR-based kinetic analysis indicated that this recombinant antibody fragment had nanomolar cTnT binding affinity. However, this data was not reliable as the theoretical and experimental SPR sensorgrams differ significantly from each other. A successfully developed ELISA-based inhibition assay revealed that the purified F1 scFv had an IC_{50} value of 85 ng/ml for the cTnT antigen. In addition, the assay precision was within an acceptable range. Further improvements are required for the anti-cTnT scFv antibodies in order to meet the recommended criteria for CVD diagnosis. Protein engineering strategies such as random or site-direct mutagenesis can increase the affinities of antibody. Such an approach is described in the next chapter, where a shuffling method was applied to the construction of heavy and light chain-shuffled libraries for the selection of anti-cTnT antibodies with enhanced affinities.

Chapter 4
Affinity maturation of avian anti-cTnT scFv antibody fragments by chain shuffling

4.1 Introduction

This chapter outlines the application of mutagenesis for the generation of improved avian anti-cTnT scFv antibodies. It contains an in-depth description of the mutagenesis used for the production of new chain-shuffled scFv antibodies. In addition, the isolation, SPR-based characterisation and the development of an inhibition assay for new mutant anti-cTnT scFv antibodies are also described.

Although recombinant antibody technology is useful for the generation and isolation of many different proteins, it is still has a number of limitations. For instance, many enzymes produced by recombinant technology have limited utilities due to their degradation when exposed to unsuitable reaction conditions, such as high temperature, high pH and chemical solvents (Shaw, 1987). Furthermore, some recombinant antibodies may have limited use in diagnostic assays due to poor specificity and low antigen affinity (Gronwall and Stahl, 2009).

Protein engineering allows the researcher to alter the properties of a recombinant protein in order to meet the required criteria. In protein engineering, genetic manipulations are used to modify the coding sequence of a gene, and this can lead to an improvement in the required traits of the protein encoded by that gene. Examples include improving protein thermal tolerance, enhancing enzymatic activities, increasing protease resistance, strengthening reactivity in organic solvents, increasing pH stabilities, eliminating cofactor requirements or altering the binding specificity of antibodies. These improvements can be achieved using a number of approaches, such as adding disulfide bonds, replacing labile amino acids or altering the CDRs of antibodies (Chen *et al.,* 1991; Wilson and Agard, 1991; Zoller, 1991,1992; Markert *et al.,* 2001; Eijsink *et al.,* 2004 and Mathieu *et al.,* 2010).

So far, the properties of a number of industrial enzymes have been successfully modified by protein engineering (Goodenough, 1995; Rubingh, 1997). The thermal stability of Xylanase, an enzyme used for paper bleaching, was improved two fold after incorporation of a disulfide bond into the enzyme (Wakarchuk *et al.,* 1994; Gruber *et al.,* 1998). A second example includes subtilisins which are essential agents in detergents as they can degrade proteins by hydrolysis. In natural extracellular environments, subtilisins are stabilized by binding with calcium. However, in an industrial environment, there are a large number of metal-chelating agents that can bind to calcium ions (Strausberg *et al.,* 1995). To overcome this problem, calcium-independent subtitisins were generated by protein engineering. This was achieved by deleting the amino acids which were responsible for calcium binding (Kumar and Takagi, 1999; Bryan, 2000).

In general, protein engineering is performed by indirectly modifying the encoded gene rather than direct modification of the protein. The modification of the gene allows continuous production of the modified product by the host organism. However, if the mutation is performed directly on the protein, every single batch of protein has to be modified, which can be time-consuming and expensive. Mutagenesis can be divided into two major categories: random mutagenesis and site-directed mutagenesis. Random mutagenesis refers to mutations that can occur at any site within the DNA, whereas, site-directed mutagenesis targets mutations to particular sites (Carter, 1986; Cadwell and Joyce, 1994). Generally, a large number of variants are produced from random mutagenesis and this eliminates the need to know the detailed gene information of the protein. In contrast, site-directed mutagenesis requires specific knowledge of the gene sequence which encodes the target protein. This method generates mutant proteins with fewer amounts of variants, thus saving time on analysis. A wide range of mutagenesis

strategies have been developed and several strategies may be used for either site-directed mutagenesis or random mutagenesis (Fig. 4.1).

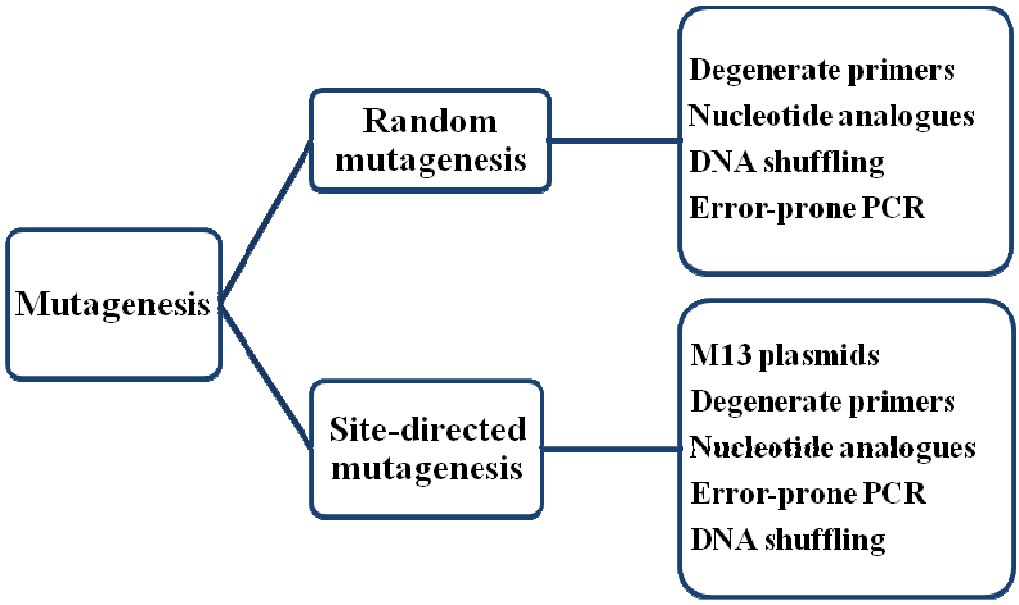

Figure 4.1. Strategies for random mutagenesis and site-directed mutagenesis. Both random mutagenesis and site-directed mutagenesis are often used in protein engineering. (Based on references: Carter, 1986; Wilson and Keefe, 2001; Chusacultanachai and Yuthavong, 2004; Antikainen and Martin, 2005)

DNA shuffling, invented by Stemmer in 1994, can be used in both random and site-directed protein mutagenesis (Joern, 2003). This method can be used to recombine pools of homologous genes by random fragmentation and PCR reassembly (Stemmer, 1994a). Typically, three-experimental steps are used. In the first step, the gene fragments are digested into small DNA fragments. Next, these fragments are randomly ligated together to form recombinant gene fragments and finally, the new fragments are amplified using PCR (Stemmer, 1994a). This technique has been applied to the improvement of activity of TEM-1 β-lactamase toward cefotaxime. Stemmer reported that the mutant TEM-1β-lactamase had a 32,000 fold increase in activity over the original enzyme (Stemmer, 1994b).

An alternative approach is 'chain shuffling' which is often used to improve the affinities of recombinant antibodies (Bacher *et al.,* 2002; Finlay *et al.,* 2006). Chain-shuffling is a method for *in vitro* recombination of pools of antibody chain genes by random fragmentation and PCR reassembly (Fig.4.2). Generally, a mutant antibody library can be generated by assembly of antibody chain genes from an original library (library prior to biopanning), with antibody genes from an antigen-specific library (library post biopanning). Subsequently, the new mutant antibody library can undergo biopanning and screening procedures for the selection of antibodies with higher antigen-binding capacities.

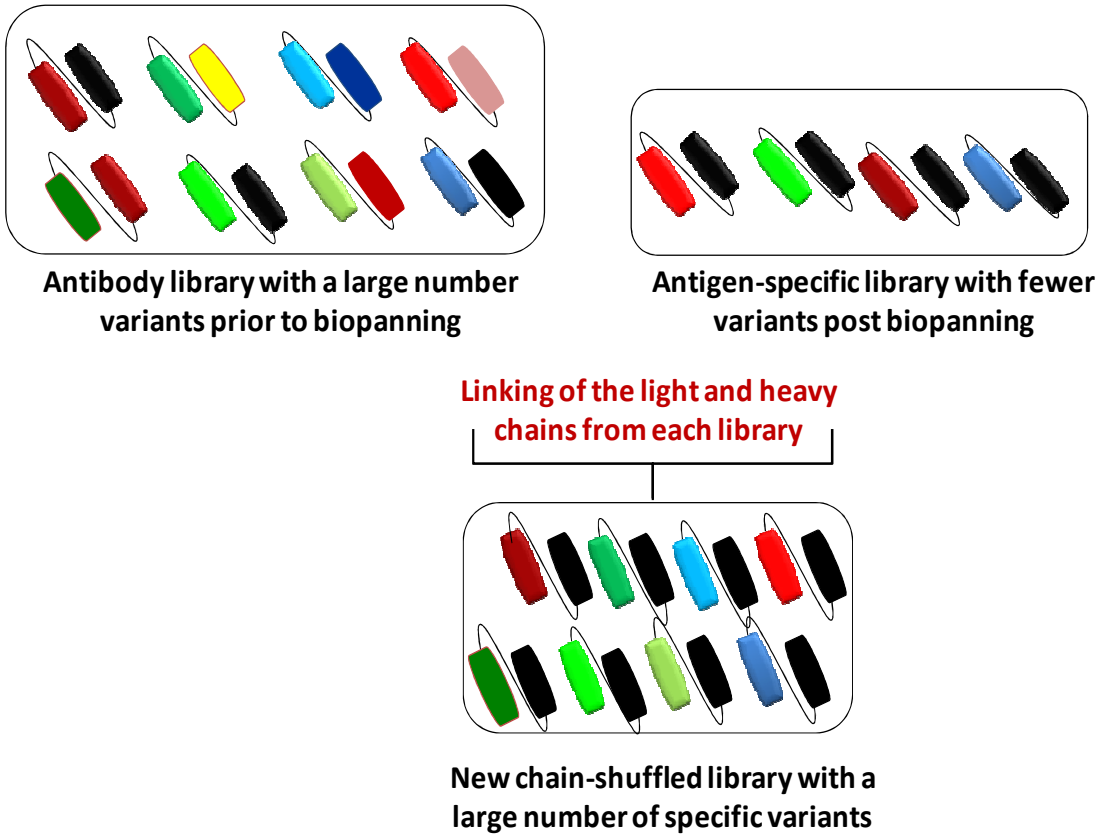

Figure 4.2. Antibody chain shuffling strategy. Antibody chain genes were amplified from the original antibody library (library prior to biopanning) and antigen-specific library (library post biopanning). The amplicons from the two libraries are assembled by PCR thus generating a new chain-shuffled library.

A number of studies have shown that the affinity of antibodies can be improved using the chain shuffling approach. For example, Fitzgerald and colleagues showed that the halofuginone detection level of an anti-halofuginone scFv antibody was increased 185 fold using the light-chain shuffling approach (Fitzgerald *et al.,* 2011). Similarly, Tachibana and co-workers used chain shuffling to improve the affinity of a lectin Fab fragment, CP33. The affinity of the Fab fragment was increased either 4.8 or 1.7 fold with single amino acid modifications to the light chain (Tachibana *et al.,* 2004). Moreover, Yoshinaga and co-workers also improved the affinity of anti-human MCP-1 antibody by 15 fold (Yoshinaga *et al.,* 2008). In this work, both light chain and heavy chain shuffling were performed in order to achieve a greater number of variants for biopanning of the anti-cTnT scFv library.

4.1.1. Work summary for the generation of chain-shuffled avian anti-cTnT scFv antibodies

In this chapter, mutant avian antibody libraries (light chain-shuffled and heavy chain shuffled) were constructed. Variable antibody chain genes were amplified from the original avian anti-cTnT scFv antibody library (section 3.2.7). In addition, variable antibody chain genes were also amplified from the fifth round of the biopanning of the anti-cTnT scFv library. The amplified variable chain genes were assembled by SOE-PCR and ligated into a phagemid pComb3XSS vector. The mutant antibody phage libraries were subsequently constructed by transforming the antibody gene-containing plasmids into *E.coli* XL-Blue cells. The enhancement of specificity of anti-cTnT scFv antibodies was achieved by performing five separate rounds of biopanning and positive scFv clones were selected using a simple ELISA-based ‘on-plate’ screening method.

DNA fingerprinting was used to assess the variety of anti-cTnT scFv antibodies generated in the libraries. In addition, 384 anti-cTnT scFv clones were analysed using a

SPR-based ranking method. From the ranking results, ten antibodies were selected and subjected to kinetic studies. Four clones, showing high affinity levels, were assessed for cross reactivity and temperature stability. From the kinetic analysis, the experimental curves of clone 8C2 had closer fitting with the theoretical binding curves and hence it was selected for further study. This 8C2 clone was subsequently purified and incorporated into an inhibition assay. Following chain shuffling, the 8C2 clone showed improved antigen-binding capacity compared to the wild-type F1 clone.

4.2 Results

4.2.1. PCR amplification of the avian cTnT variable heavy and light chain genes

Two types of mutant antibody libraries were produced; a light chain-shuffled library and a heavy chain-shuffled library. For the construction of the light chain-shuffled antibody library, the variable light (V_L) chain genes were amplified from the original unpanned cTnT library. In addition, the variable heavy (V_H) chain genes were amplified using the DNA plasmids extracted from the fifth round of biopanning of the cTnT library. In contrast, for heavy chain shuffling, the V_H genes were amplified from the original unpanned cTnT library. In addition, the V_L genes were amplified from the fifth round of biopanning of the cTnT library (section 2.3.2.1). After PCR optimisation, amplicons were analysed on a 1% (w/v) agarose gel (Fig. 4.3) and, as shown in the gel image below, the variable genes were successfully amplified.

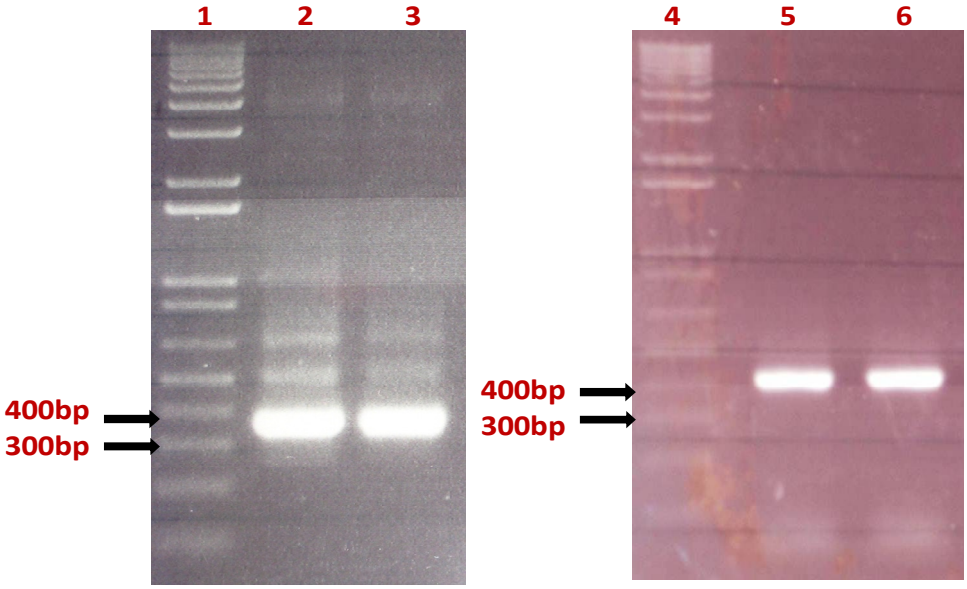

Figure 4.3. PCR amplification of the avian cTnT variable heavy and light chain genes. Lanes 1 and 4 contained 1kb plus DNA molecular weight ladders (Invitrogen, USA). Lane 2 contained V_L (~ 350 bp) genes from the original unpanned library. Lane 3 contained V_L (~ 350 bp) genes from the fifth round biopanned library. Lane 4 and 5 contained V_H (~ 400 bp) genes from the original unpanned library and the fifth round biopanned library, respectively.

4.2.2. Anti-cTnT chain-shuffled scFv-Splice by Overlap Extension (SOE) PCR

The cTnT light chain-shuffled SOE-PCR was generated by linking the V_L amplified from the unpanned library with the V_H fragment from the fifth round of biopanning. The cTnT heavy chain-shuffled SOE-PCR was generated by linking the V_H amplified from the unpanned library, with the V_L fragment from the fifth round of biopanning. The pComb3XSS plasmid was subsequently digested using a *Sfi*I restriction enzyme. Both the vector and the stuffer was gel-purified and resolved on a 1% (w/v) agarose gel, in addition to the SOE-PCR products (Fig. 4.4). The gel image shows the pComb3XSS vector was successfully digested. Both the V_L and the V_H genes were also successfully amplified.

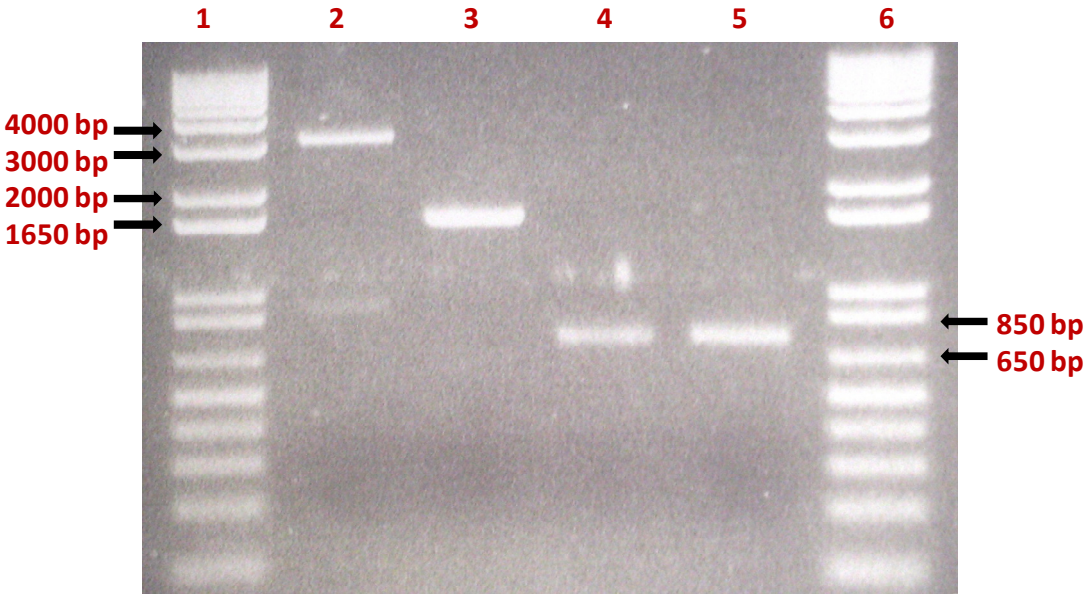

Figure 4.4. SOE-PCR amplification of chain-shuffled fragments and *Sfi*I digested pComb3XSS vector. Lanes 1 and 6 contained 1 kb plus DNA molecular weight ladders. Lanes 2 and 3 contain *Sfi*I digested pComb3XSS vector and stuffer, respectively. Lanes 4 and 5 contained light chain-shuffled and heavy chain-shuffled SOE-PCR products, respectively.

4.2.3. Avian anti-cTnT chain-shuffled scFv library construction and enrichment via biopanning

Large-scale amplifications for both the light chain-shuffled and heavy chain-shuffled SOE-PCRs were carried out and the SOE-PCR products were resolved on a 1% (w/v) agarose gel. After gel electrophoresis, these PCR products were extracted and concentrated by ethanol precipitation. The PCR products and pComb3XSS vector were subsequently digested with a *Sfi*I restriction enzyme, and ligated overnight with T4 DNA ligase. The ligated product was ethanol precipitated and subsequently electroporated into electrocompetent *E. coli* XL1-Blue cells, as described in section 2.3.1.11. The sizes of the transformed avian anti-cTnT light chain-shuffled and heavy chain-shuffled libraries were 1.5 x 10^8 cfu/mL and 3.6 x 10^7 cfu/mL, respectively. Recombinant anti-cTnT scFv clones were selected from these libraries by performing five rounds of biopanning against immobilised cTnT antigen, as described in section 2.3.1.12. Table 4.1 (A) and (B) show the input and output titres for each of the 5 rounds of biopanning of the heavy and light chain-shuffled scFv anti-cTnT libraries.

Table 4.1 (A). Input and output titres of light chain-shuffled anti-cTnT scFv library over five rounds of biopanning

Biopanning round	Input (cfu/mL)	Output (cfu/mL)
1	9.0×10^{11}	1.1×10^{6}
2	5.0×10^{11}	7.5×10^{5}
3	1.6×10^{11}	1.3×10^{5}
4	1.7×10^{12}	5.0×10^{5}
5	4.8×10^{11}	2.9×10^{5}

Table 4.1 (B). Input and output titres of the heavy chain-shuffled anti-cTnT scFv library over five rounds of biopanning

Biopanning round	Input (cfu/mL)	Output (cfu/mL)
1	6.0×10^{11}	4.7×10^{6}
2	2.4×10^{11}	5.6×10^{6}
3	5.4×10^{11}	1.2×10^{5}
4	1.4×10^{12}	1.5×10^{5}
5	1.6×10^{12}	8.0×10^{4}

4.2.4. Soluble expression of avian anti-cTnT chain-shuffled scFv antibodies

To identify clones with high cTnT binding levels from the biopanned libraries, thirty two clones from the chain shuffled-library were picked from biopanning rounds three, four and five and analysed using the 'on-plate' ELISA screening method, described in section 2.3.1.14. The ELISA threshold was set as three times of the absorbance value of the blank sample, as described in section 3.2.8. Figures 4.5 (A) and (B) revealed a number of light and heavy chain-shuffled scFv clones that appeared to bind strongly to the cTnT antigen.

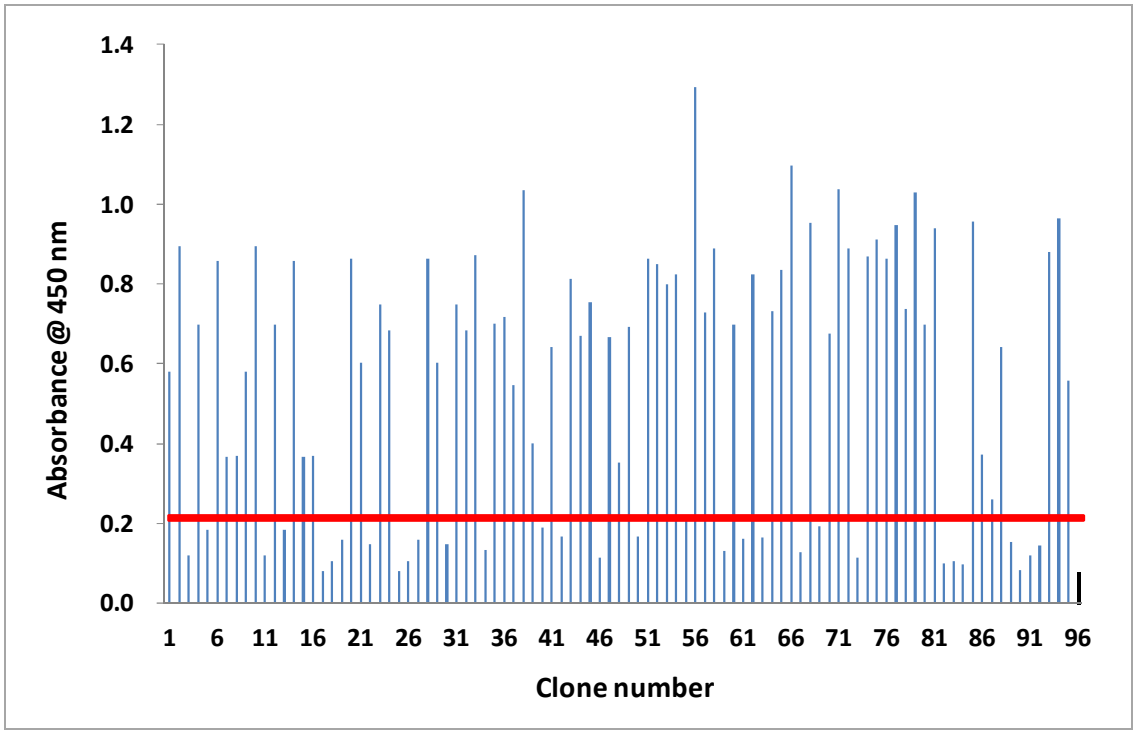

Figure 4.5 (A). Screening of the light chain-shuffled anti-cTnT scFv clones from rounds three, four and five of biopanning. Each blue bar represents the absorbance reading of a scFv antibody. A blank reference was also included in the analysis, which is represented by the black bar (96). To identify positive antigen-binding clones, a red horizontal line, which indicates the ELISA threshold, was drawn at the absorbance level of ~ 0.2. The threshold value is three times the blank reference absorbance.

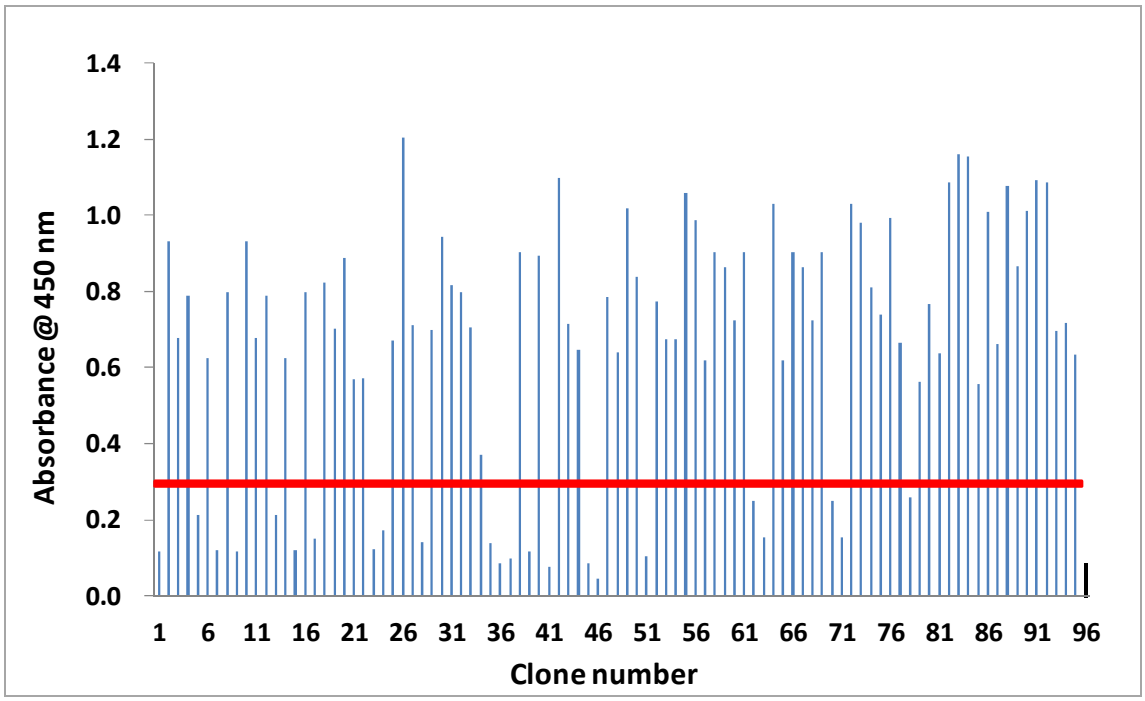

Figure 4.5 (B). Screening of heavy chain-shuffled anti-cTnT scFv phage clones from rounds three, four and five of biopanning. Each blue bar represents the absorbance reading of an individual scFv antibody. A blank reference was also included in the analysis, which is represented by the black bar (96). A red horizontal line drawn at background absorbance level of ~ 0.3 marks the ELISA threshold. It is three times the blank reference absorbance.

4.2.5. Comparison of the number of positive parental and chain-shuffled anti-cTnT scFv fragments

The binding reactivity of clones to cTnT from both the heavy and light chain shuffled libraries were recorded and the percentages of positive clones were calculated. These data were then compared with the data obtained from the parental anti-cTnT library (Table 4.2). It was shown that the overall percentage of positive clones isolated from the parental scFv cTnT library was 56.3%. In contrast, an overall higher level of positive clones was isolated from both the heavy chain-shuffled (66.7%) and light chain-shuffled (75%) scFv cTnT libraries. Interestingly, the light-chain-shuffled library had the highest number of positive clones. The increase in the number of cTnT-binding clones indicates

that the chain-shuffling approach can generate a superior library by the elimination of non-specific clones.

Table 4.2. Parental and chain-shuffled anti-cTnT scFv clones isolated from biopanning rounds 3, 4 and 5

Biopanning Round	Parental scFv cTnT library		V_H shuffled scFv cTnT library		V_L shuffled scFv cTnT library	
	No. of positive clones	Percentage of positive clones	No. of positive clones	Percentage of positive clones	No. of positive clones	Percentage of positive clones
Round 3	9/32	28.1 %	20/32	62.5 %	22/32	68.8%
Round 4	14/32	43.8%	22/32	68.8%	22/32	68.8%
Round 5	67/96	69.8%	22/32	68.8%	28/32	87.5%
Overall	**90/160**	**56.3%**	**64/96**	**66.7%**	**72/96**	**75%**

4.2.6. DNA fingerprinting analysis of anti-cTnT scFv clones

In comparison to DNA sequencing, DNA fingerprinting is a relatively inexpensive and effective technique for the identification of gene diversity. In this technique, restriction enzymes are used to digest the antibody gene fragments which are then resolved on an agarose gel. Based on the gene fragments pattern presented on the agarose gel, different clones can be identified. This approach is extremely useful when dealing with a large number of clones. *Alu*I and *BstN*I are commonly used restriction enzymes (Cai and Garen, 1997; Stahl *et al.,* 2010; Chang *et al.,* 2011). In general, genes with different restriction mapping patterns represent different clones.

Plasmids of eighteen scFv antibodies which showed positive binding against cTnT from monoclonal ELISA analysis were PCR-amplified. The genes were digested using the restriction enzyme, *Alu*I. The digested products were analysed on a 3% (w/v) agarose gel (Fig. 4.6). The analysis of the eighteen scFv antibodies exhibited six different restriction map patterns, which indicated a moderate diversity level of scFv. However, two clones (in lanes 14 and 16) had no clear restriction digest profile, perhaps due to the poor quality of isolated plasmid DNA which was not amplified by PCR.

Figure 4.6. Restriction digestion profile of anti-cTnT scFv clones. Lanes 1 and 20 contained a 100 bp DNA molecular weight ladder. Lanes 2 to 19 contained 18 anti-cTnT scFv clones which were digested by the restriction enzyme, *Alu*I. Six different DNA patterns, indicated by the letters A to F, were observed. Seven scFv antibodies, located in lane 1, 2, 3, 7, 8, 10 and 13 showed the same restriction profile (A). Four scFv antibodies, located in lane 5, 6, 9 and 12 showed the same restriction profile (B). Lanes 11, 15 and 17 had the restriction profiles C, D and F, respectively. Lanes 18 and 19 showed the same restriction profile (F). Lanes 14 and 16 did not show any clear restriction profiles.

4.2.7. Characterisation of avian anti-cTnT chain-shuffled scFv clones using the Biacore™ 4000 system.

The SRP-based Biacore™ 4000 system (GE healthcare, Sweden) was used to rank the cTnT-binding capacities of scFv clones. The Biacore™ 4000 system has four independent flow cells with five detection spots on each flow cell. Up to 16 ligands can be immobilised on the chip surface, therefore, this system can analysis 16 analytes in one single run (Safsten *et al.,* 2006). A total of 384 anti-cTnT chain–shuffled scFv clones which included 192 light chain-shuffled and 192 heavy chain-shuffled clones were analysed on the Biacore™ 4000 system using the format depicted by Figure 2.1.

In SPR analysis, a number of parameters can be used to characterise the clones, such as antibody capture levels; antigen binding early level; antigen binding late level; antibody-antigen complex stability early level; antibody-antigen complex stability late level and complex percentage left level. Antibody capture levels indicate the amount of scFv antibodies captured on the anti-HA surface. The antigen binding early value describes the amount of cTnT antigen bound to scFv antibodies just after the start of the cTnT injection. In contrast, the binding late value represents the amount of cTnT antigen bound to scFv antibodies just before the end of cTnT injection. ScFvs that have high binding late values indicate good antigen association. The stability early represents the amount of antigen binding just after the end of the sample (cTnT) injections. In contrast, the stability late represents the amount of antigen binding after a fixed period of dissociation. In addition, the binding stability can be represented by percentage left value (left %), which is the ratio of stability late and stability early. The sensorgram curves from the mutant scFv analysis are shown in Figure 4.7. A representative number of the sensorgram curves from the light and heavy chain-shuffled scFv analysis are shown in Figure 4.7. Three different stages (A, B and C) were observed through the

scFv-cTnT interaction process. Figure 4.7 reveals the anti-cTnT scFv clones had different surface capture and antigen binding levels.

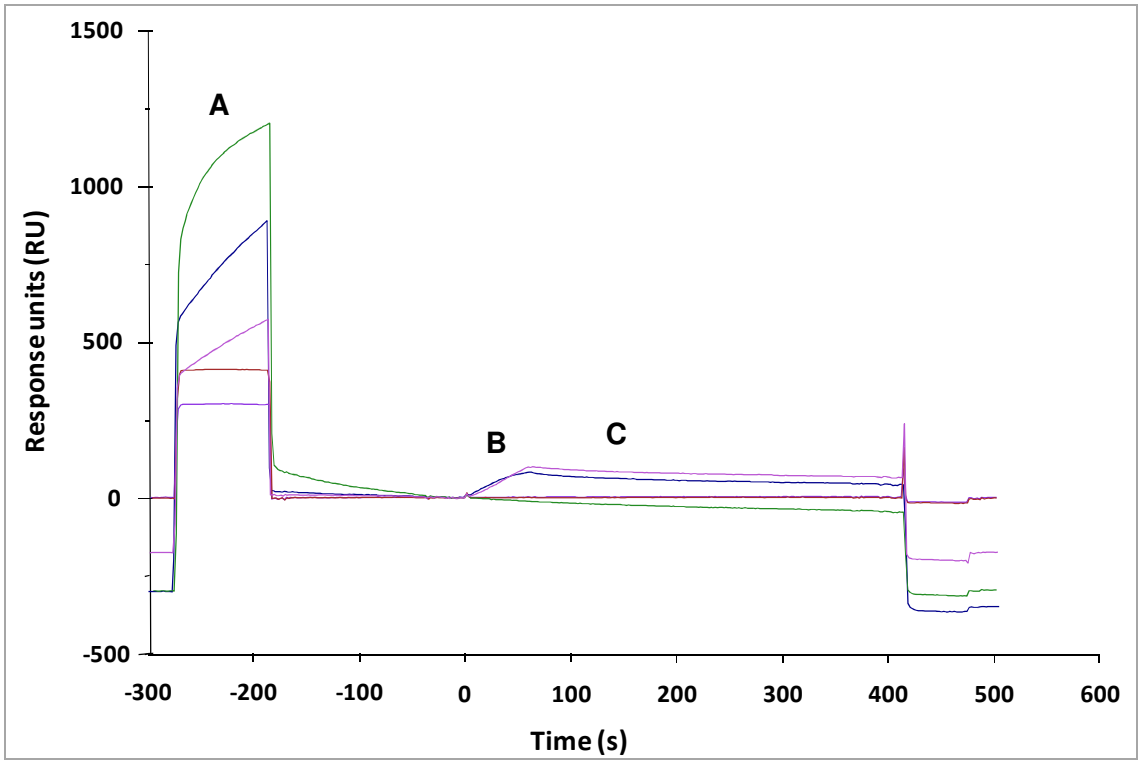

Figure 4.7. Sensorgram profiles of anti-cTnT scFv antibodies using the Biacore™ 4000 system. The X axis represents time in seconds, and the injection of the cTnT antigen occurred at time 0 seconds. Each line represents the capture and binding profile of different anti-cTnT scFv antibodies. Stage A shows the level of scFv captured. Stage B showed the association between cTnT antigen and the captured scFv antibodies. Stage C represents the disassociation between the cTnT antigen and the scFv antibodies.

4.2.8. Ranking of avian anti-cTnT chain-shuffled scFv clones by antibody captured on the CM5 sensorchip surface

Based on the values obtained from the binding analysis, the 384 clones were ranked by plotting the capture levels versus the binding late levels (Fig. 4.8). In Figure 4.8, clones were classified into three groups. Data points within or close to region A indicated low capture levels and low binding levels, which can be regarded as representing negative clones. Clones within or close to region B were captured onto the chip surface but had very low binding levels to the cTnT antigen. These clones can be used as negative antigen-binding controls. Clones within or close to region C show both high capture levels and high antigen-binding levels.

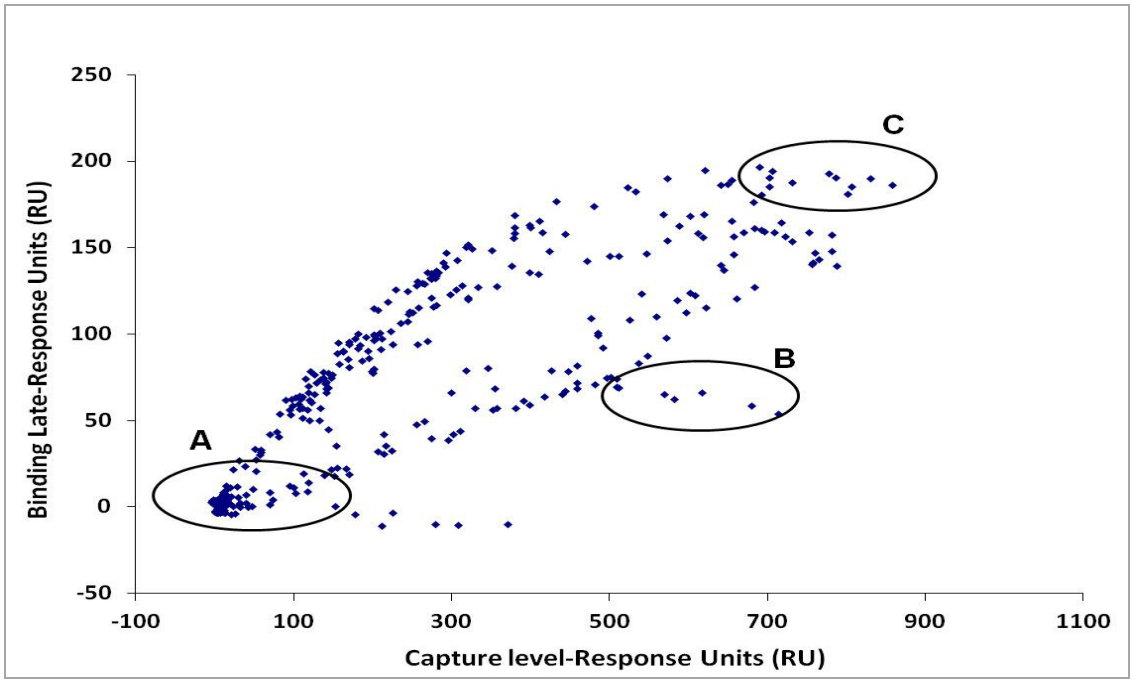

Figure 4.8. Anti-cTnT light and heavy chain-shuffled scFv antibodies ranked by capture level. Each individual blue point represents a scFv antibody. The X-axis represents the response units of antibody captured on the anti-HA immobilized chip surface. The Y-Axis represents the response unit at the stage just before the end of sample (cTnT) injection (i.e. the binding late levels). Three regions (A, B, C) marked with black circles represented clones with different capture and binding capacities.

4.2.9. Ranking of the anti-cTnT chain-shuffled scFv clones by percentage left

Capture level-based ranking only indicates the amount of antigen which binds to the captured antibodies. However, it does not show how strong or stable the antibody-antigen interaction is. Whereas, percentage left indicates the stability of the antigen-antibody interaction. This percentage left value was calculated by dividing the stability late level by the stability early level. The anti-cTnT scFv clones were hence ranked by the percentage left (% left) (Fig. 4.9 (A) and (B)). A wide range of % left levels (from 7.2 to 76%) was observed.

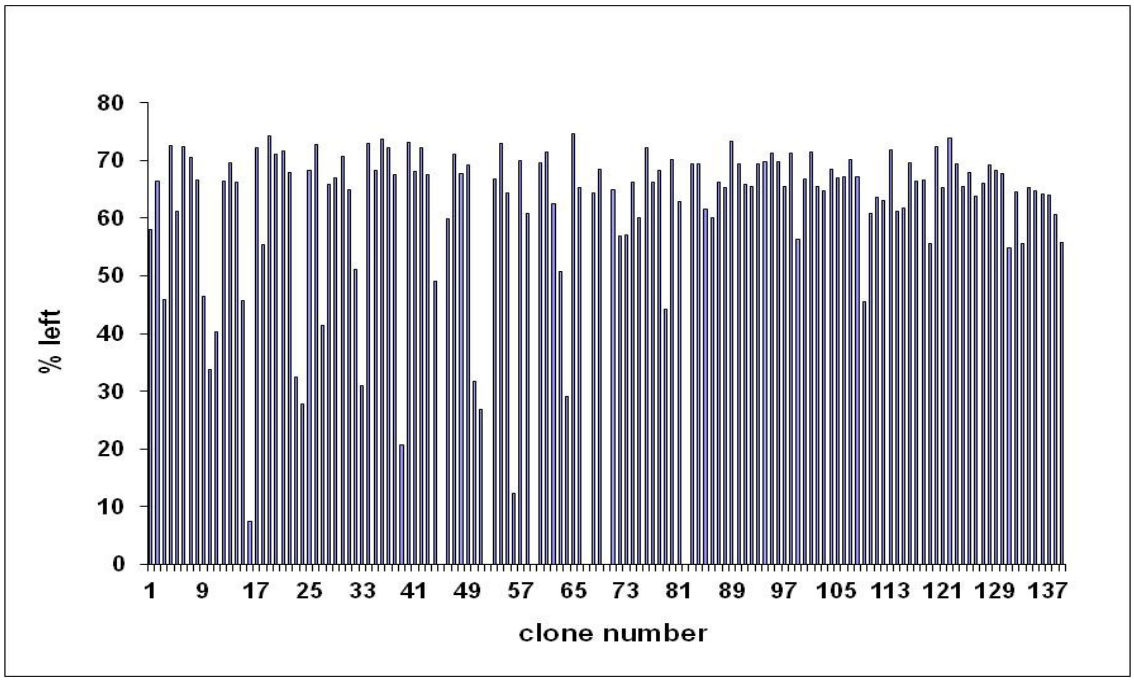

Figure 4.9 (A). Ranking of anti-cTnT light chain-shuffled scFv clone by % left. The X axis shows the anti-cTnT scFv clone number. Y axis represents the % left level of each clone. A wide range of % left values was observed, varying from 7.2 to 75.71%.

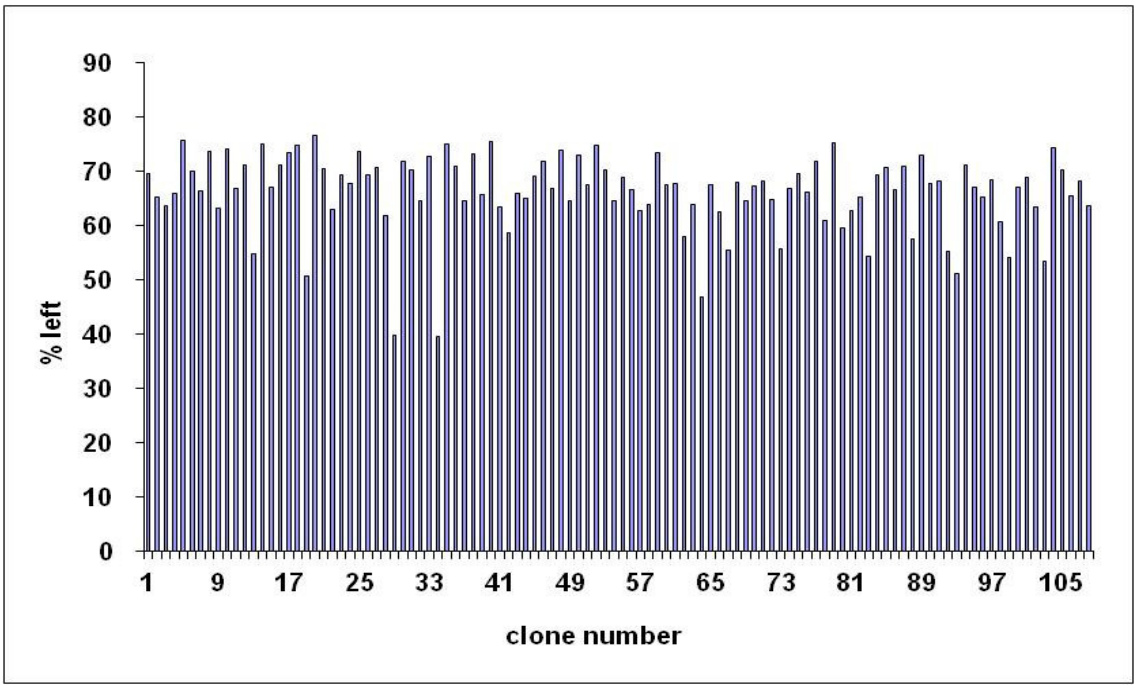

Figure 4.9 (B). Ranking of anti-cTnT heavy chain-shuffled scFv clone by % left. The X axis shows the anti-cTnT scFv clone number. The Y axis represents the % left level of each clone. A moderate range of % left values was observed, varying from 39.92 to 76%.

As the % left values for the clones with high stabilities were very similar i.e. between 70% to 76%, it was possible that these clones were genetically identical. Therefore, to avoid choosing the same clones, ten antibodies with various antigen-binding stabilities (from 33.75 to 76%) (Fig. 4.9 (A) and (B)) were selected for further precision kinetic studies (Table 4.3).

Table 4.3. Antigen binding stability levels of ten avian anti-cTnT scFv antibodies

Clone name	Stability early (RU)	Stability late (RU)	% left
7D8	**182.1**	**138.4**	**76.00**
8C2	**162.8**	**120.7**	**74.14**
8C10	**145.6**	**106.3**	**73.01**
7D6	**148.9**	**108.6**	**72.93**
8A6	**131.8**	**94.9**	**72.00**
8D2	**145.3**	**103.4**	**71.16**
8F5	**135.8**	**74.2**	**63.07**
7H8	**179.4**	**107.4**	**59.86**
8H6	**206.5**	**80.2**	**39.93**
7G2	**63.7**	**21.5**	**33.75**

4.2.10 Kinetic studies of ten anti-cTnT chain-shuffled scFv antibodies

For kinetic analysis, a total of six different cTnT antigens concentrations were tested (section 2.3.1.19). The kinetic curves were fitted in a 1:1 Langmuir binding model and kinetic parameters were generated using Biaevaluation 4.1 software. The kinetic curves of four clones which revealed higher affinities levels were shown in Figure 4.10. The experimental curves of a heavy chain-shuffled clone, 8C2, had a better overlay with the 1:1 Langmuir binding model than other three clones (7D8, 8C10 and 7H8).

In addition, the kinetic constants for each of the four clones were calculated by Biaevaluation 4.1 software (Table 4.4). Interestingly, all four antibodies had subnanomolar affinities. However, 8C2 displayed the lowest Chi^2 value. The Chi^2 value indicates the goodness of the curve fit, thus describing the accuracy of kinetic

parameters generated. A low Chi^2 value generally indicates that the kinetic analysis is more reliable.

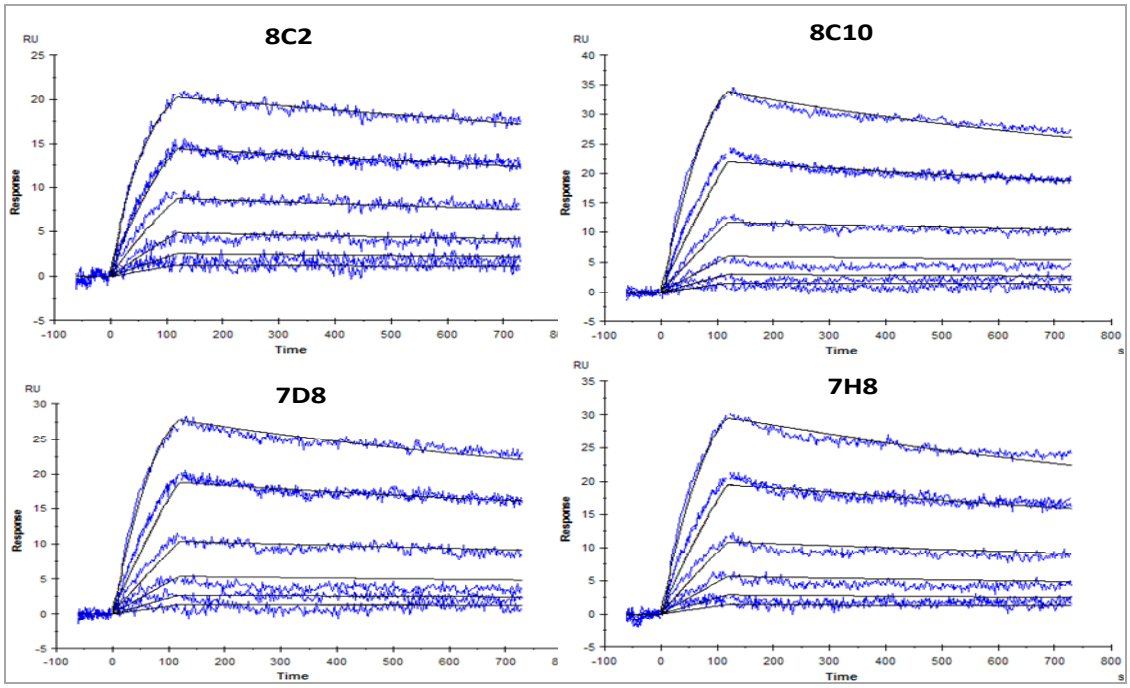

Figure 4.10. Kinetic characterisation of anti-cTnT scFv antibodies. The blue curves represented the experimental curves of the four anti-cTnT scFv antibodies (8C2, 8C10, 7D8, and 7H8) with six cTnT concentrations (50 nM, 25 nM, 12.5 nM, 6.25 nM, 3.12 nM and 1.56 nM). They were fitted using a 1:1 Langmuir binding model (in black). In addition, the analysis of cTnT with 12.5 nM concentration was carried out in duplicate.

Table 4.4. Parameters determined from scFv kinetic studies

Clone	k_a (1/Ms)	k_d (1/s)	K_A(1/M)	K_D (M)	Chi^2(RU^2)
***8C2**	**6.90×10^6**	**2.73×10^{-4}**	**2.53×10^{10}**	**3.95×10^{-10}**	**0.29**
8C10	**2.17×10^6**	**7.11×10^{-4}**	**3.05×10^9**	**3.28×10^{-10}**	**0.85**
7D8	**1.76×10^6**	**5.37×10^{-4}**	**3.27×10^9**	**3.05×10^{-10}**	**0.70**
7H8	**1.28×10^6**	**6.17×10^{-4}**	**2.07×10^9**	**4.82×10^{-10}**	**0.79**

*8C2 has the best kinetic curve fit

4.2.11 Cross reactivity analysis of anti-cTnT chain-shuffled scFv antibodies

Cross reactivity studies are used for the determination the capacity of an antibody binding site to cross react with non-target proteins. Often cross reactivity occurs when a protein shares a common epitope with the target antigen, or it has an epitope which is structurally similar to the desired antigen (Porrozzi *et al*., 2004).

To assess the cross reactivity of anti-cTnT scFv antibodies, all four clones were analysed with other troponin isoforms: Skeletal troponin T (sTnT), Cardiac troponin I (cTnI) and skeletal troponin I (sTnI). The sTnT protein is a major type TnT isoform that exists in skeletal muscle tissue. In addition, cTnI and sTnI are also very common troponin isoforms. The cross reactivity study of the anti-cTnT scFv antibodies were performed using the troponin isoforms (sTnT, cTnI and sTnI) in a direct ELISA format (section 2.3.1.15). Figure 4.11 revealed all four clones displayed high specificity for cTnT with no significant cross reactivity to any of the sTnT, cTnI or sTnI isoforms.

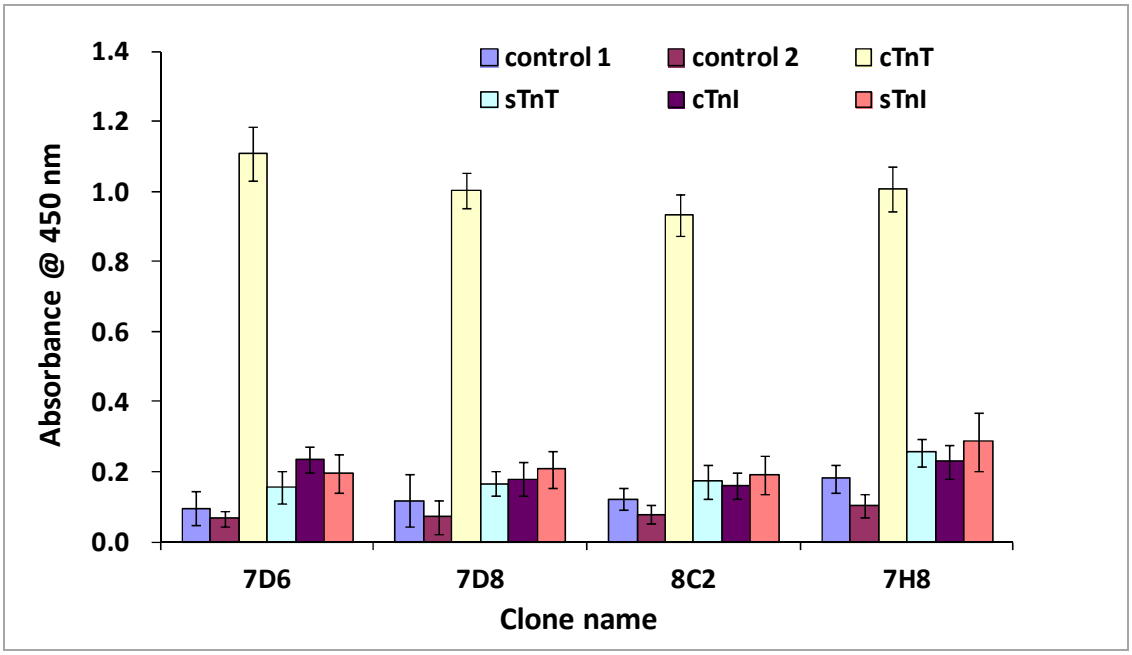

Figure 4.11. Cross reactivity studies of anti-cTnT scFv antibodies. The yellow bar represents the absorbance from the binding analysis between scFvs with cTnT protein. The light blue, black and red bars represent the absorbance from the binding analysis between scFvs with sTnT, cTnI and sTnI, respectively. The dark blue bar represents control 1 with no antigens coated in the plate wells. The dark red bar represents control 2 which contained only blocking solutions Marvel (5% (w/v)). The analysis was performed in triplicate. The error bars represent the standard deviation.

4.2.12 Temperature stability studies of anti-cTnT chain-shuffled scFv antibodies

The four scFv antibodies (8C2, 7D6, 7D8 and 7H8) were further assessed for their temperature stability. An antibody that exhibits high stability levels over a range of temperature has added value as a diagnostic reagent. The anti-cTnT scFv antibodies were analysed using the Biacore^{TM} 4000 at three different temperatures (30^{o}C, 25^{o}C, 20^{o}C). The same assay format used for the analysis was illustrated by Figure 2.1. Figure 4.12 shows the affinities levels of each scFv antibodies at three temperatures. This data was generated by plotting the association rate constant (k_a) against dissociation rate constant (k_d).

Over three different temperatures, the four clones displayed a very narrow range of cTnT affinity (0.427 nM to 2.74 nM). In addition, clone 7H8 and 7D8 had subnanomolar affinities at all three temperatures (less than 1 nM). In contrast, clone 8C2 and 7D6 only revealed subnanomolar affinities at 30^{o}C or 25^{o}C. At 20^{o}C, their affinity levels were greater than 1 nM. Although clones 8C2 and 7D6 showed greater variations in affinity levels than 7H8 or 7D8, the variations were not significant due to the narrow affinity range. All four clones remained stable over the three temperatures.

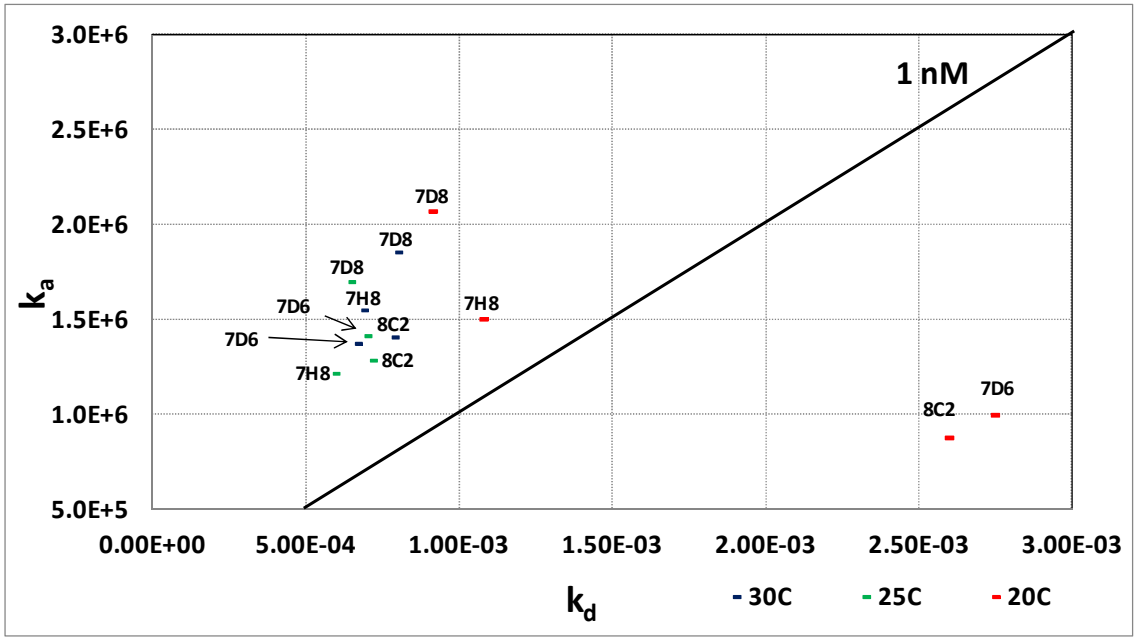

Figure 4.12. Temperature stability studies of anti-cTnT scFv antibodies. The X-axis represents the dissociation constant K_d (1/s). The Y-Axis represents the association constant K_a (1/Ms). The blue, green and red points represent three different assay temperatures (30°C, 25°C, 20°C), and each point was labeled with the clone name (8C2, 7H8, 7D6 and 7H8). The black straight line which crosses the plot indicates an affinity level of 1 nM. Data points above the straight line have an affinity less than 1 nM, whereas, the data points below have an affinity greater than 1 nM.

4.2.13 Purification of anti-cTnT 8C2 scFv antibody using immobilised metal affinity chromatography (IMAC)

As the 8C2 scFv displayed high cTnT affinity, the best kinetic curve fit and the antigen-binding was stable over a range of temperatures, the 8C2 scFv was chosen for further analysis. The 8C2 was firstly purified using the IMAC protocol as previously described in section 2.3.1.16. Subsequently, an inhibition ELISA was performed using the IMAC-purified antibodies. The fractions from the different purification stages were analysed by SDS-PAGE and Western blotting (Fig. 4.13 (A) and (B)). The protein concentration of the purified scFv was 0.5 mg/mL as determined using the Nanodrop™

ND-1000. A total of 0.3 mg of 8C2 antibody was purified. The purified antibody was then used for inhibition assay development.

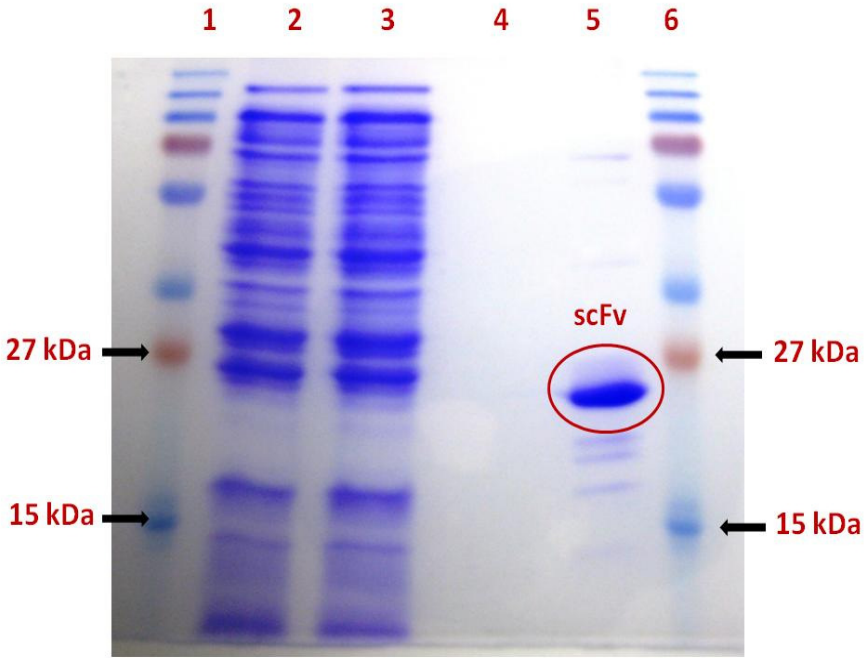

Figure 4.13 (A). SDS-PAGE analysis of the IMAC-purified 8C2 scFv antibody. Lanes 1 and 6 contained a page-ruler prestain protein marker. Lane 2 contained crude lysates extracted by sonication. Lane 3 contained 'flow-through' that was obtained after passing the *E. coli* cell lysates through a Ni-NTA agarose resin. Lane 4 contained a wash fraction, and lane 5 contained the elution fraction. Both lanes 2 and 3 contained a large number of irrelevant proteins with various sizes. In contrast, lane 4, which contained the column wash eluent, had no protein bands. This indicated the removal of non-specific proteins from the column resin. A clear strong band just below 27 kDa marker was observed in lane 5 (marked by a red circle), and this indicated the successful purification of the 8C2 scFv antibody. In addition, a minor number of non-specific bands were also observed in the eluted sample. The SDS-PAGE analysis was performed in duplicate and a second gel was used for Western blotting (Fig. 4.13 (B)).

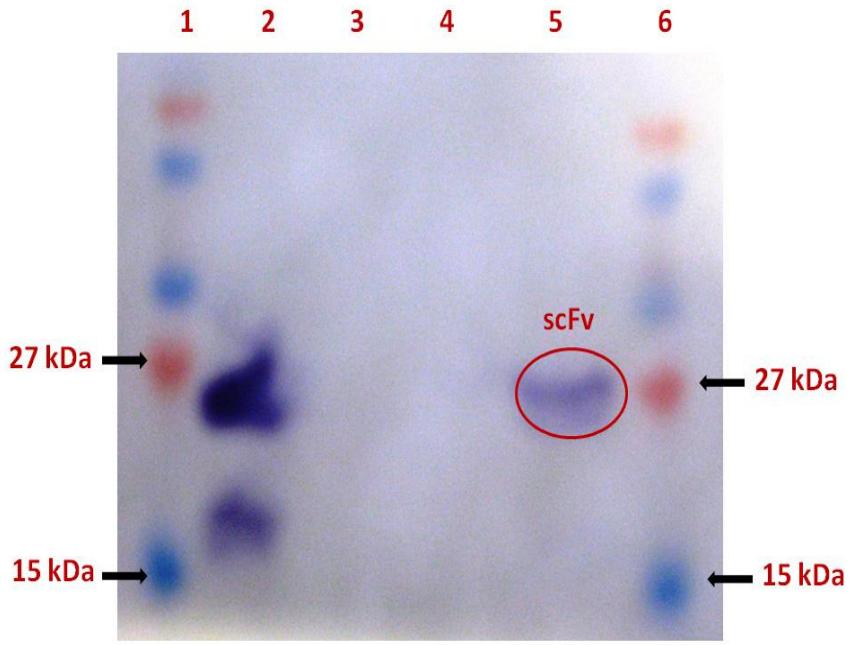

Figure 4.13 (B). Western blotting analysis of the IMAC-purified 8C2 scFv antibody. Lanes 1 and 6 contained a page-ruler prestain protein marker. Lane 2 contained crude lysates extracted by sonication. Lane 3 contained 'flow-through' that was obtained after passing the *E. coli* cell lysates through a Ni-NTA agarose resin. Lane 4 contained a wash fraction, and lane 5 contained the eluted antibody fraction. A strong band just below 27 kDa was observed in lane 1, thus indicating the presence of specific anti-cTnT scFv antibodies. However, a second non-specific band was also observed just above 15 kDa, which could have occurred due to the degradation of the 8C2 antibody in unstable lysates. In contrast, the 'flow-through' fraction (lane 4) had no protein bands and thus indicates that non-specific proteins were removed during this step. Lane 5 contained the eluted fragment; a clear strong band (marked by a red circle) at approximately 25 kDa was observed.

4.2.14 Checkerboard ELISA analysis of the 8C2 scFv antibody

A checkerboard ELISA analysis was performed to indentify an optimal cTnT coating concentration for the inhibition assay. Seven different concentrations of the cTnT antigen were coated on an immuno 96 MicroWell^{TM} solid plate and detected by the addition of a series of 8C2 antibody dilutions. The ELISA profiles were shown in Figure 4.14. It was shown that cTnT concentrations 1, 1.5 and 3 μg/mL generated higher detection signals than other concentrations. The IC_{50} values at these three concentrations were very close. However, in order to minimize the consumption of cTnT protein (due to its cost), a concentration of 1,000 ng/mL was selected as the optimal coating concentration for the inhibition assay.

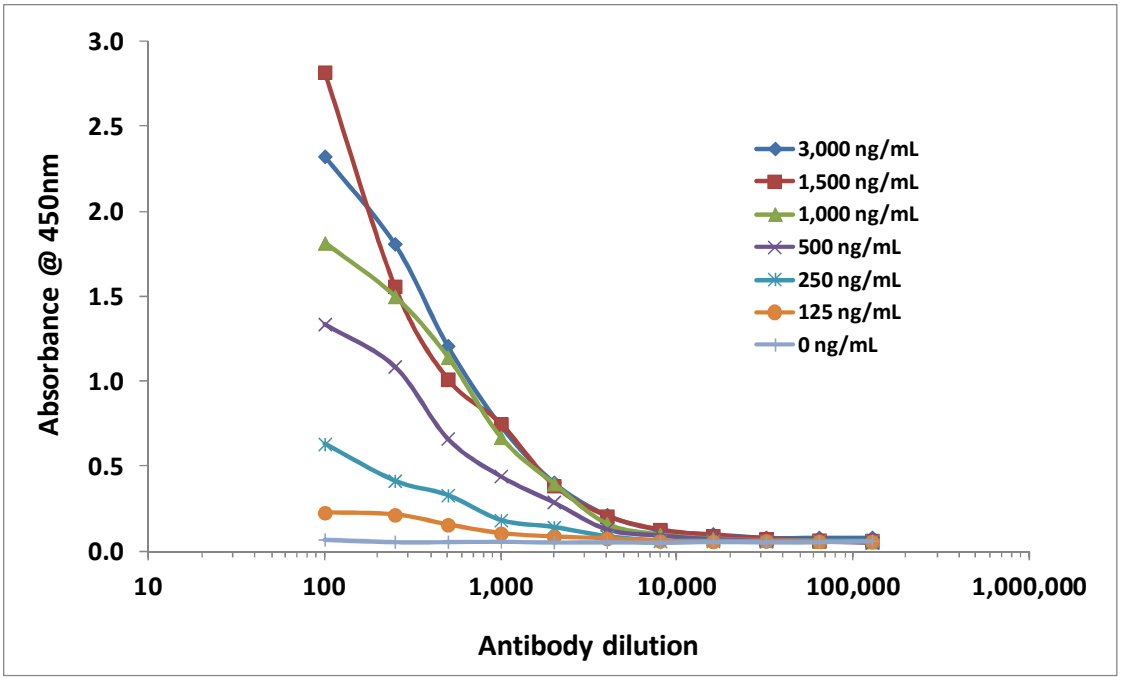

Figure 4.14. Checkerboard ELISA using different cTnT coating concentrations. A range of cTnT concentrations (0, 125, 250, 500, 1,000, 1,500 and 3,000 ng/mL) were coated on an immuno 96 MicroWell^{TM} solid plate. A series of dilutions of the 8C2 scFv antibodies (1 in 100, 1 in 250, 1 in 500, 1 in 1,000, 1 in 2,000, 1 in 4,000, 1 in 8,000, 1 in 1,6000, 1 in 32,000, 1 in 64,000 and 1 in 128,000) were added to the plate. Binding of the scFv antibodies was detected using HRP-labeled mouse anti-HA monoclonal antibody. The ELISA was developed with TMB substrate and the absorbance read at 450 nm.

4.2.15 ELISA optimisation of the 8C2 scFv antibody

A second optimisation procedure was performed to detect the optimal concentration of the 8C2 scFv to be used in the assay. This was achieved by using different 8C2 antibody dilutions in an inhibition ELISA. The 8C2, which had an original concentration of 0.5 mg/mL, was diluted 1 in 1,000 (500 ng/mL), 1 in 2,000 (250 ng/mL), 1 in 3,000 (166.77 ng/mL) and 1 in 4000 (125 ng/mL) in PBS (pH 7.4). The ELISA profiles are shown in Figure 4.15. It was observed that antibody at a 1 in 1,000 dilution showed a

significantly higher IC_{50} value than at any of the other three concentrations. In contrast, no significant variations of the IC_{50} values were observed for the 1 in 2,000, 1 in 3,000 and 1 in 4,000 dilutions. To minimise the antibody consumption, a 1 in 4000 dilution, equivalent to 125 ng/mL 8C2 antibody, was chosen as the optimal concentration.

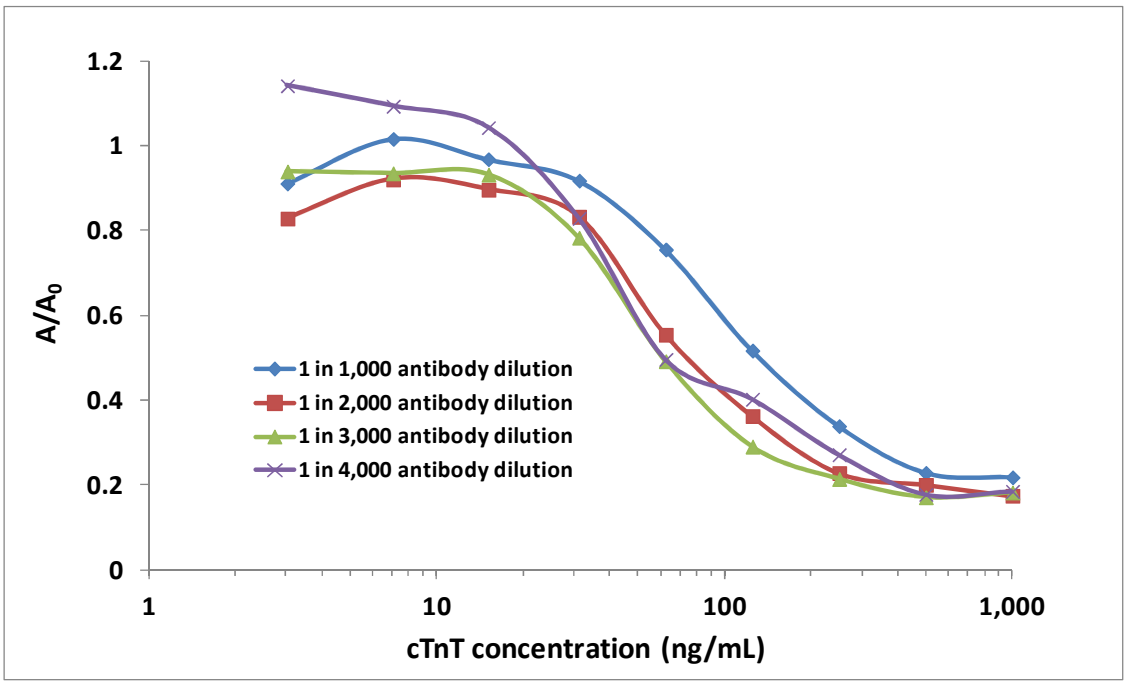

Figure 4.15. Optimisation of 8C2 scFv concentrations for use in an inhibition ELISA assay. The immuno 96 MicroWell™ solid plate was coated with a previously determined optimal cTnT concentration of 1,000 ng/mL. The blue, red, green and purple lines represent four antibody dilutions: 1 in 1,000, 1 in 2,000, 1 in 3,000 and 1 in 4,000, respectively. The scFv antibodies were detected using HRP-labeled mouse anti-HA monoclonal antibody. The ELISA was developed with TMB substrate and the absorbance was read at 450 nm.

4.2.16 ELISA inhibition assay of the 8C2 scFv antibody

An inhibition cTnT assay was developed with the purified 8C2 scFv in order to determine its cTnT antigen detection capacity. The assay used an optimal cTnT coating concentration 1,000 ng/mL and the optimal 8C2 concentration of 125 ng/mL. Intra-day assays (three assays on the same day) were performed to validate the cTnT inhibition assay. The collected data were fitted in a four-parameter calibration curve using the SigmaPlot version 11.0 software (Fig. 4.16). The IC_{50} value of purified 8C2 scFv was determined as 38 ng/mL.

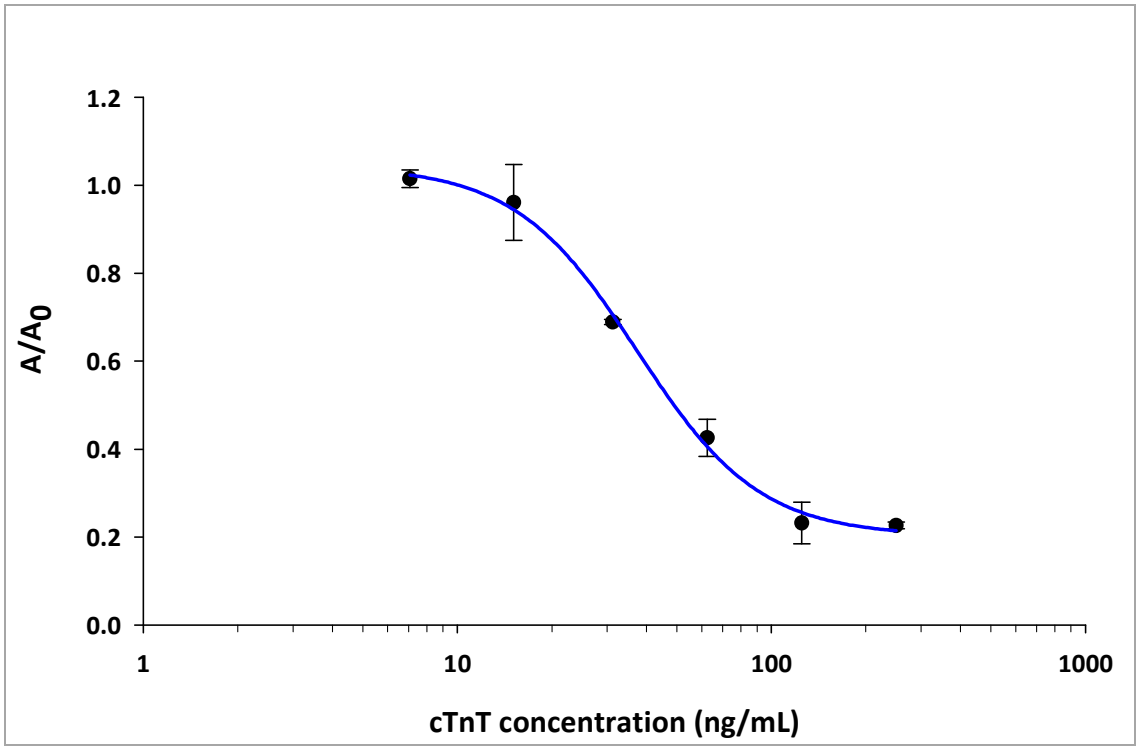

Figure 4.16. Inhibition assay of purified anti-cTnT 8C2 scFv antibody. An ELISA plate was coated with 1 µg/mL cTnT and then blocked with 200 µl of 5% (w/v) Marvel in PBS (pH 7.4). Different concentrations of cTnT (250, 125, 62.5, 31.25, 15.63 and 7.81 ng/mL) were incubated with the 8C2 scFv (at a final concentration 125 ng/mL) for 1 hour at 37°C. The scFv antibodies were detected using HRP-labeled mouse anti-HA monoclonal antibody. The ELISA was developed with TMB substrate and the

absorbance was read at 450 nm. The assay was performed in triplicate. The error bars represent the mean values +/- the standard deviation.

In an inhibition assay, an A_0 standard indicates the absorbance of antibody lysate dilution without any inhibition of free antigen. The A/A_0 value indicates the degree of inhibition which is calculated by dividing the absorbance value at each cTnT concentration (A) with the A_0 absorbance value. The precision of the assay can be evaluated using the coefficient of variation in percentage (% CV) values. Table 4.5 shows the mean of A/A_0 values, SD and % CV of the intra-day analysis. The assay precision had a range from 0.8% to 20.4%.

Table 4.5. Parameters used to determine the precision of the cTnT inhibition assay

[cTnT] ng/mL	Mean	SD	%CV
250	0.23	0.01	3.3
125	0.23	0.05	20.4
62.50	0.43	0.04	10.0
31.25	0.69	0.01	0.8
15.63	0.96	0.09	9.0
7.81	1.01	0.02	2.0

4.2.17 Comparison of antigen-binding capacities of chain-shuffled 8C2 and wild-type anti-cTnT F scFv antibodies

The heavy chain-shuffled 8C2 scFv was compared to the wild-type scFv F1. The IC_{50} values obtained from inhibition assays and affinity levels obtained from kinetics studies were compared (Fig. 4.17). The 8C2 had an improved IC_{50} value of 38 ng/mL, in contrast, the wild-type scFv F1 had an IC_{50} value of 85 ng/mL. The heavy chain shuffled 8C2 showed an improvement of approximately 2.2 fold compared to the

wild-type F1. In addition, kinetic analysis showed that 8C2 had an affinity level of 0.39 nM, whereas, F1 had an affinity level of 2.40 nM. The 8C2 showed an improvement of approximately 6 fold in comparison to F1.

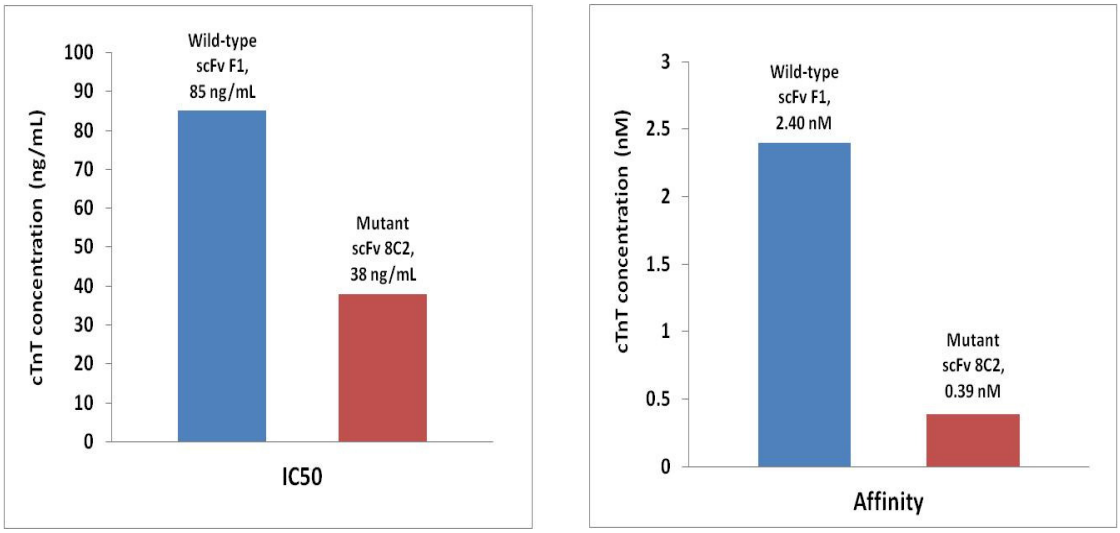

Figure 4.17. Comparison of cTnT-binding capacities between wild-type scFv F1 and chain-shuffled scFv 8C2. The blue bars represent the IC_{50} value (85 ng/mL) and affinity level (2.4 nM) of scFv F1; the red bars represent the IC_{50} value (38 ng/mL) and affinity level (0.39 nM) of scFv 8C2.

4.3 Discussion

This chapter describes the use of the chain shuffling approach for the generation of an affinity-enhanced avian anti-cTnT scFv antibody. In addition, the construction of new chain-shuffled antibody libraries and the selection of an antigen-specific antibody using the phage display technique is also described. DNA fingerprinting, antibody cross reactivity studies, SPR-based kinetic analysis and inhibition assay development are also discussed.

Using the previously constructed wild-type anti-cTnT scFv library, new heavy and light chain-shuffled libraries were generated. After five rounds of biopanning, it was shown

that both the heavy and light chain-biased scFvs have an increase in the number of positive cTnT-binding clones. A total of 66.7% of the heavy chain-shuffled clones and 75% of the light chain-shuffled clones demonstrated positive binding to the cTnT antigen. In comparison, only 56.3% of the wild-type clones were cTnT binders. This may indicate that a chain-shuffling approach can generate a larger number of positively binding clones. Therefore, the chain shuffling approach would enhance the production of antibodies especially when the parental library has a very low number of positive antigen-binding clones. This observation is in agreement with the work of Yuan and co-workers who reported that gene recombination from library pools enable a substantial increase in the number of positive mutants that had phenotypic improvement. (Yuan *et al.*, 2005).

DNA fingerprinting was used to assess the diversity of the scFv antibodies. Analysis of eighteen antibodies revealed six different restriction mapping profiles, which indicated a moderate level of clonal diversity (Fig. 4.6). Although two clones did not show any restriction profiles this may have been due to the poor quality of DNA plasmids. Overall, however, this method still gave a good indication of the diversity of the scFv antibodies generated.

In order to identify scFv antibodies that had high cTnT binding stability, a total of 384 heavy and light chain-shuffled antibodies were assessed using SPR. The Biacore™ 4000 system facilitated the rapid analysis of the clones (less than 10 hours), which saved valuable experimental time and costs. Furthermore, lower volumes of reagents were required by the Biacore™ 4000 than conventional ELISA. In addition, the experimental conditions were consistent for each clone, as the analysis was completed in one single run; therefore, the data obtained were more reliable and accurate. The % left value-based ranking revealed that the scFv antibodies had a broad stability range

(7.2% to 76%). Although the highest value, 76%, for an anti-cTnT antibody was less than what was reported by Leonard and co-workers for an anti-CRP scFv antibody (92%). However, this value is still considered to be a relatively good stability level as is discussed previously by Leonard and co-workers (Leonard *et al.,* 2007). Leonard and co-workers used 75% as a 'cut-off' value for the ranking of anti-CRP antibodies; therefore, the anti-cTnT scFvs in this study displayed good stability levels.

It is crucial that the selected antibodies are highly specific for cTnT. Therefore, cross-reactivity studies were performed against different troponin isoforms present in the troponin complex (sTnT, cTnI and sTnI). Four scFv antibodies showed high specificity towards cTnT with no significant cross reactivity to the other troponin isoforms. These scFv antibodies can be the potential candidates for CVD diagnosis.

Antibodies with high levels of temperature stability are often preferred in clinical diagnostics and therapeutics. The affinity levels of four anti-cTnT scFv antibodies were determined at 20, 25 and 30^{o}C to investigate its variation with temperature. Two scFvs had affinity levels less than 1 nM over the three temperatures (Fig. 4.12). Overall, clones showed a very narrow range of affinity level (0.427 to 2.74 nM). Therefore, temperature changes did not appear to affect the antigen-binding capacities of these anti-cTnT scFv antibodies to any significant extent.

Another important feature of an antibody is its affinity level, which indicates association and disassociation of the antibody-antigen complex. Ten scFv antibodies with various % left values were subjected to kinetic studies. The curves were fitted to the 1:1 Langmuir binding model. Kinetic analysis showed that four clones had subnanomolar affinity levels (Table 4.4). Since all four clones had very close subnanomolar affinities, the curve fits were examined in order to select a clone for further analysis. Visual

inspection of the experimental curve (blue curves) of 8C2 clone showed closer fitting with the theoretical binding curves (black curves) than for the other three clones. There were no significant deviations in both the association phase and disassociation phase. Moreover, the quality of curve fitting was also assessed and is represented by the Chi^2 value. Generally, smaller Chi^2 values indicate better data fitting to the chosen binding model (Poduslo *et al.,* 2010). In Table 4.4, 8C2 had the lowest Chi^2 (0.29) compared to the other three clones (0.70, 0.79 and 0.85) and it was, therefore, chosen for further studies.

The purified 8C2 antibody was subsequently incorporated in an inhibition immunoassay. A checkerboard ELISA was performed to identify both the optimal cTnT coating concentration and the optimal 8C2 antibody concentration. The ultimate goal was to use the least amount of reagents while maintaining the highest assay sensitivity. Similar IC_{50} values were observed for the cTnT concentrations of 1, 1.5 and 3 μg/mL (Fig. 4.14). For least antigen consumption, the lowest concentration (1 μg/mL) was selected. The optimal 8C2 antibody concentration (125 ng/mL) was also determined for inhibition assay development (Fig. 4.15).

An inhibition assay was successfully developed using the previously selected optimal conditions. 8C2 was determined to have a cTnT IC_{50} value of 38 ng/mL (Fig. 4.16). The assay precision analysis showed the CV% had a range of 0.8% to 20.4%. In this range, six data points had the CV% less than 10%, showed that the assay precision was in an acceptable range (< 20%) (Reed *et al.,* 2002). Although large variations in CV are often seen when quantifying samples at the extreme ends of an assay's range (Reed *et al.,* 2002). At the extreme ends of an assay curve, sample concentrations are relative high or low, thus, a minor variation in these concentrations can cause large variations in the precision analysis. However, an unexpected CV% value of 20.41 (at 125 ng/mL cTnT

concentration) was observed in this study. It exceeded the acceptable range (< 20%). The high CV% value may be due to uneven sample mixing, it also may due to sample was not homogeneous which might contain higher order of antibody structures (dimers, trimers or multimers).

To assess the efficiency of chain-shuffling for the enhancement of antibody affinity, the antigen detection capacity of mutant 8C2 and wild-type F1 antibody were compared (Fig. 4.17). The 8C2 had an IC_{50} value of 38 ng/mL, which showed an improvement of approximately 2.2 fold compared to the wild-type F1 (85 ng/mL). In addition, the mutant scFv, 8C2 had a K_D value of 0.39 nM, which indicated an improvement of approximately 6 fold compared to the wild-type F1 (2.40 nM). These results indicated that chain shuffling can be successfully applied to produce affinity enhanced anti-cTnT scFv. Using a light chain shuffling approach, the detection level for halofuginone of an anti-halofuginone scFv antibody was improved by 185 fold (Fitzgerald *et al.,* 2011). Similarly, Park and co-workers showed an increase in affinity of two natural antibodies (1C2 and 1E4), against preS1 of hepatitis B virus (HBV), by factors of 2.8 and 6.5 compared to the parental clones (Park *et al.,* 2000), whereas, Lou and colleagues improved affinities of botulinumb neurotoxin scFv antibodies from 9 to more than 77 fold using the chain-shuffling approach (Lou *et al.,* 2010). Thus, chain shuffling is an effective approach for enhancing antibody- antigen binding capacity.

In conclusion, using the chain shuffling approach, the antigen binding capacity of the anti-cTnT antibody was successfully enhanced. A 2.2 fold improvement in affinity and a 6 fold improvement in the IC_{50} were shown by the mutant 8C2 scFv compared to the wild type F1. In the next chapter, the production of a second avian anti-cTnT fragment, the Fab fragment, will be described.

Chapter 5
Generation of avian anti-troponin T Fab antibody fragments

5.1 Introduction

This chapter describes the production and expression of avian anti-cTnT Fab recombinant antibodies. It contains an in-depth description of the properties of Fab fragments. The focus of this chapter is the generation the Fab antibodies using phage display. In addition, the optimisation studies for the improvement of Fab antibody expression levels are also described.

Both scFv and Fab are commonly used recombinant antibody fragments. They share a number of similar features. For examples, both of them have the same antigen-binding sites as their parental antibodies.In addition, the small molecular size of both scFv (~25 kD) and Fab (~50 kD) can facilitate tissue penetrability.

In comparison to the scFv, the Fab antibody antibody fragment has a number of distinct advantages (Table 5.1). Lee and co-workers reported that the intra-molecular disulfide bonds in Fab fragments lead to higher stability than the corresponding scFv fragments (Lee *et al.,* 1998). The additional domains within the Fab structure contribute to the interaction between the light and heavy chains, hence leading to increased structural stability. Rothlisberger and co-workers compared the neutralisation capacity of Fab and scFv fragments against *Centruroides noxius.* They found that the Fab antibody fragments had greater neutralisation capacity for *Centruroides noxius* (Rothlisberger *et al.,* 2005). Similarly, Quintero-Hernandez and co-workers showed that a mouse Fab antibody (BCF2), to a scorpion toxin (Cn2), had improved neutralisation capacity and stability compared to equivalent scFv formats (Quintero-Hernandez *et al.,* 2007).

Table 5.1 Comparison of Fab and scFv antibody fragments

	Advantages	Limitations
Fab	• Small size (~50 kD) facilitates high mobility and tissue penetration • Can be simply generated using the papain and pepsin proteases • Exist as monomers and tend not to aggregate • Stable over long-term storage • Can be humanised for therapeutic purposes • Crystallisation process is easier than IgG	• Short half-life in blood circulation • Lower expression levels in *E. coli* cells compared to scFv
scFv	• Small size (~25 kD) facilitates high mobility and tissue penetration • High expression levels in *E. coli* cells • Crystallisation process is easier than IgG	• Cannot be generated using proteolysis • Unstable over long-term storage • Aggregates can form higher order structures (dimmers and trimers)

(Based on references: Bird and Walker, 1991; Marks *et al.,* 1991; Kramer *et al.,* 2002; Hust and Dubel, 2004; Daniela *et al.,* 2005 and Jordan *et al.,* 2007)

Enzymatic digestion and recombinant techniques are being routinely used for the generation of Fab antibody fragments. In the late 1950s, Porter digested IgG into three fragments using papain. The Fab fragments were then purified using ion exchange chromatography (Porter, 1958). Papain is an enzyme extracted from papaya. It is routinely used for proteolysis of IgG antibodies, thus producing Fab fragments. Fab' and $F(ab')_2$ are derivative forms of Fab fragments, that are widely used for research and clinical purposes. The production of Fab' involves use of an aspartic acid protease, pepsin, which cleaves the hinge region of the IgG molecule and forms an $F(ab')_2$ with a molecule weight of 100 kD. The $F(ab')_2$ can be subsequently reduced, using reducing reagents such as dithiothreitol. This process yields two Fab' fragments with free cysteine residues near the C-terminus (Fig. 5.1). Although enzymatic digestion is often used as a routine method for Fab generation, the generation of antibody fragments by

recombinant technology has a number of distinct advantages. For example, recombinant technology allows the production of antibodies in *E. coli* cells, which can generate high yields at a reduced cost, provided the conditions are optimized. Moreover, mutagenesis can be used to improve the affinity and the expression levels of Fab fragments. Furthermore, small peptide affinity tags, such as His, can be incorporated to the C-terminus of the heavy chain or the light chain thus facilitating purification. The production of recombinant Fab antibodies can be achieved using an immune antibody library and the phage display approach (Fig. 5.2).

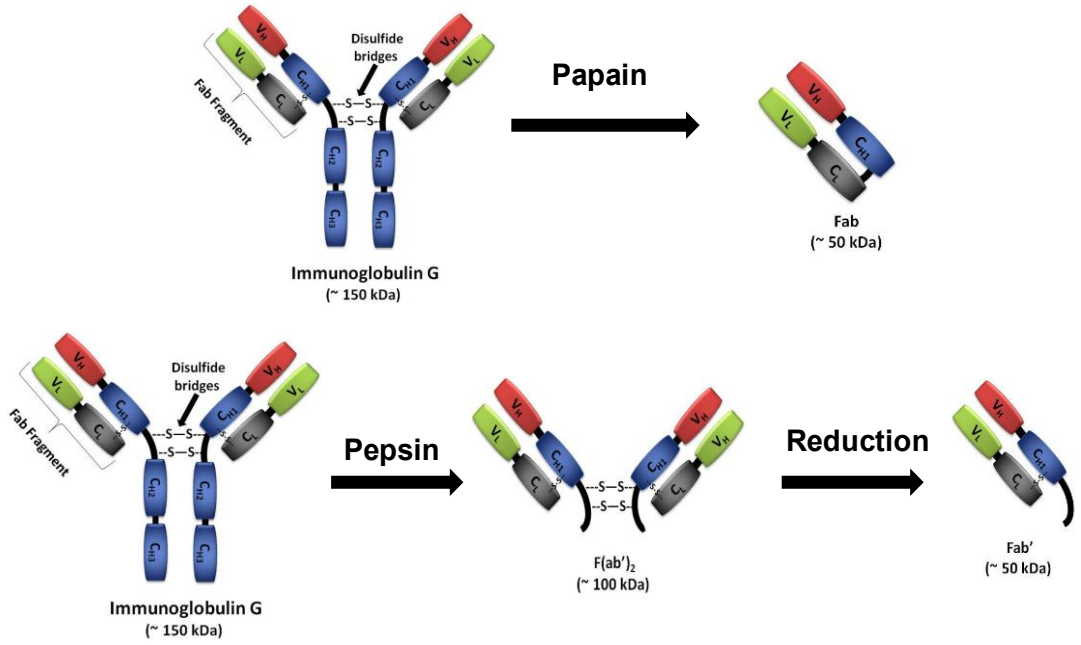

Figure 5.1. Generation of Fab and its derivative fragments using enzymatic proteolysis. Papain cleaves the IgG molecule to form Fab molecules. Pepsin cleaves the IgG molecule to form a $F(ab')_2$ fragment, which can then reduced to a Fab' fragment using reducing reagents.

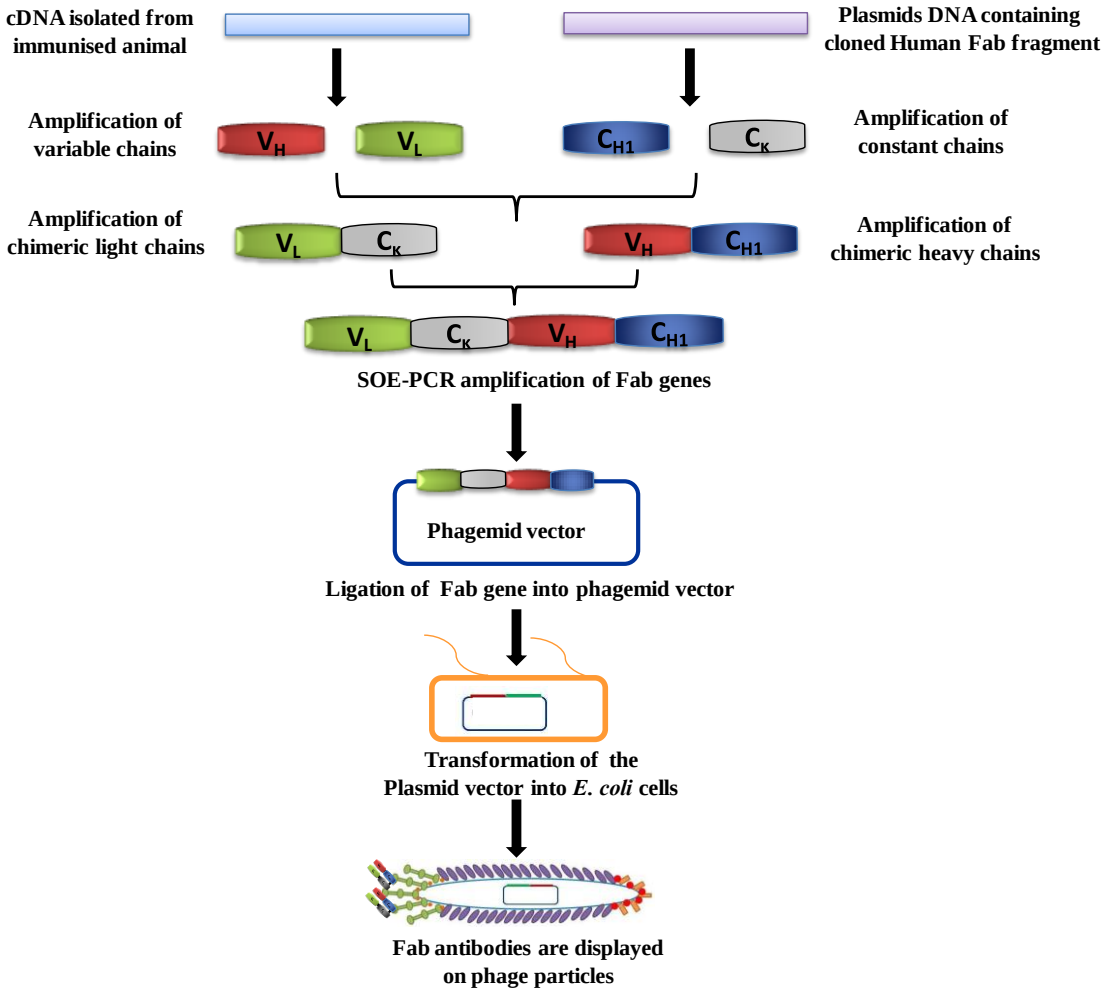

Figure 5.2. Generation of recombinant Fab antibody using phage display. The production of Fab antibody involves initial immunisation of an animal host with the antigen of interest. Total RNA is extracted from the animal spleen and bone marrow, once a sufficient antibody response is obtained. cDNA is subsequently generated by reverse transcription of mRNA. In the first round of PCR, variable and constant chains (V_H, V_L, C_κ and C_H1) are amplified. In the second round of PCR chimeric heavy and light chains are assembled, and the Fab genes are finally amplified using Splice by Overlap Extension (SOE) PCR. The Fab genes are subsequently ligated into phagemid vectors. The ligation product is transformed into *E. coli* cells and the cells are then infected by phage particles. Fab fragments are expressed in *E. coli* and subsequently displayed on the surface of the phage particles (Lee *et al.*, 1998).

The expression of Fab antibodies in *E. coli* cells involves the production of V_H, V_L, C_κ and C_H1 regions as well as an inter-chain disulfide bond. The disulfide bond is required for the connection of the variable and constant regions. In *E. coli* cells, the reducing environment in the cytoplasm prevents the formation of the disulfide bond. Therefore, Fab expression takes place in the periplasm where the four heavy and light chains are secreted independently. The disulfide bond is subsequently formed and associated with the C_H1 and C_κ chains to form the Fab fragments. The periplasm provides an oxidising environment and it also contains thiol-disulfide oxidoreductases, which catalyse the formation of the disulfide bond. Fab fragments are most often purified from the periplasm of *E. coli* rather than the cytoplasm, due to the lower protein concentration and smaller number of proteins found in periplasm (Rader 2009).

Protein expression in *E coli* systems is a complex process and a number of factors can affect the levels of expression, for example, the types of media used for *E. coli* cultivation, the induction concentrations of IPTG, the period of incubation the incubation temperature and culture agitation conditions.

5.1.1 Work summary for the generation of avian anti-cTnT Fab antibody fragments

Phage display was used to produce recombinant avian anti-cTnT Fab fragments. The avian cDNA which was used to generate the scFv antibodies, was also used for Fab production. The amplification of Fab genes involved optimisation steps such as the use of a range of magnesium concentrations, different annealing temperatures and different types of DNA polymerases. For antibody phage library construction, the Fab genes were ligated into the pComb3XSS vector and transformed into *E. coli* XL1 blue cells. The library was subjected to five rounds of biopanning against the cTnT antigen, and phage particles were infected into *E. coli* Top10 F' cells for soluble expression. Positive

Fab clones were selected using an ELISA-based ‘on-plate’ screening method. ELISA analysis revealed the positive cTnT-binding Fab clones had low expression levels. Therefore, in order to improve the expression levels, optimisation was performed using different types of media for cell cultivation, different IPTG concentrations and different periods of incubation. It was demonstrated that the expression levels of three Fab antibodies (A1, C5 and D3) were successfully optimised.

5.2 Results

5.2.1. PCR amplification of avian variable domains and human constant domains

In comparison to scFv library generation, more PCR amplification steps are required for the construction of a Fab library. Four gene fragments were amplified in the first round of PCR, including the chicken variable chains (V_H, V_λ) and human constant chain (C_HI, C_κ). In the second round of PCR, chicken/human chimaeric heavy chain and light chains were amplified. In the final SOE-PCR, one PCR amplification step was used to assemble the Fab fragment. This section describes the first round of PCR amplifications.

In the chapter 3 and 4, the generation of avian anti-cTnT scFv antibodies was outlined. Chicken cDNA, harvested from the immunised chicken, was used for the amplification of Fab genes. PCR optimisation of V_H, V_λ, C_HI and C_κ was performed using different concentrations of $MgCl_2$ (Fig. 5.3 (A)). The gel image shows that the C_κ chains were successfully amplified at three $MgCl_2$ concentrations (2, 3 and 4 mM). Although some non-specific bands were observed for the V_λ amplifications, these were far distant from the amplified V_λ genes (~ 350 bp). Therefore, the V_λ genes could be extracted by carefully cutting out the large-scale product bands. A concentration of 2 mM $MgCl_2$ was chosen for the PCR amplification of V_λ and C_κ genes, since high magnesium concentrations may increase the error rate of Taq DNA polymerase (Eckert and Kunkel, 1990). Neither the V_H or C_HI genes were amplified under the three different $MgCl_2$ concentrations (2, 3 and 4 mM). Further optimisation was performed using different annealing temperature as well as different $MgCl_2$ concentrations.

For further PCR optimisation of V_H and C_HI gene amplifications, the annealing temperature was increased from 56°C to 58°C, and a series of $MgCl_2$ concentrations (1, 2, 3 and 4 mM) were also tested. Figure 5.3 (B) shows that the optimal $MgCl_2$

concentration for the V_H amplification was 2 mM. In addition, the C_HI gene was successfully amplified at all $MgCl_2$ concentrations tested. The amplification of V_H/C_HI (2 mM IPTG at 58°C) and V_λ/C_κ (2 mM IPTG at 56°C) were performed on a large-scale,. The PCR products were resolved on a 1% (w/v) agarose gel and the PCR products were extracted. The purified PCR products are shown in Figure 5.3 (C).

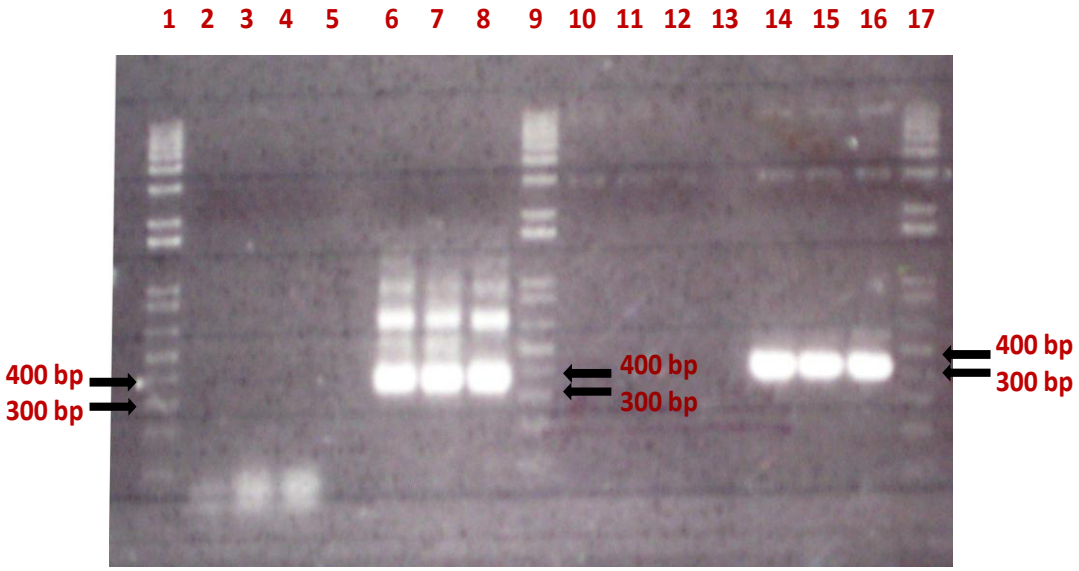

Figure 5.3 (A). Optimisation of the amplification of avian variable chain (V_H ,V_λ) and human constant chain (C_HI, C_κ) using different Mg^{2+} concentrations. Lanes 1, 9 and 17 contained 1kb plus DNA molecular weight markers. Lanes 2, 3 and 4 contained the V_H gene amplified with 2, 3 and 4 mM $MgCl_2$, respectively. Similarly, lanes 6, 7 and 8 contained the V_λ gene amplified with 2, 3 and 4 mM $MgCl_2$, respectively. In addition, Lanes 10, 11, 12 contained the C_HI genes amplified with 2, 3 and 4 mM $MgCl_2$, respectively, whereas, lanes 14 to 16 contained the C_κ genes amplified with 2, 3 and 4 mM $MgCl_2$, respectively. Lanes 5 and 13 were left blank.

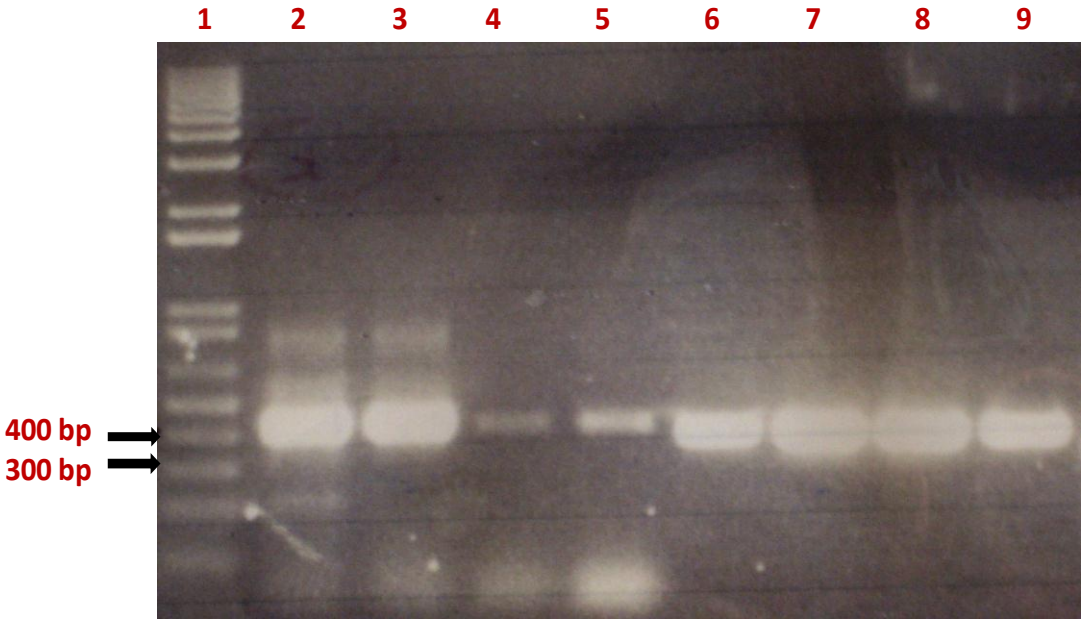

Figure 5.3 (B). Optimisation of the amplification the chicken variable heavy chain (V_H) and human constant heavy chain (C_HI). Lane 1 represents a 1kb plus DNA molecular weight ladder. Lanes 2 to 5 represent the amplification of V_H with a series of $MgCl_2$ concentrations (1, 2, 3, and 4 mM) using 58^oC as the annealing temperature. Similarly, Lane 6 to 9 represent the amplification of C_HI with a series of $MgCl_2$ concentrations (1, 2, 3 and 4 mM) using 58^oC as the annealing temperature.

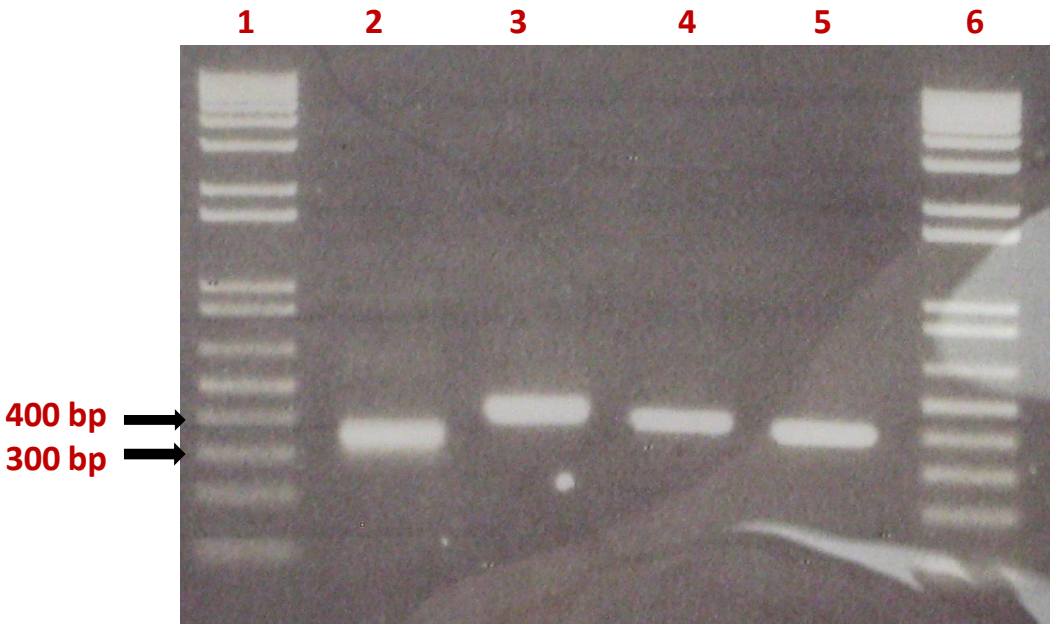

Figure 5.3 (C). Agarose gel analysis of purified PCR product of chicken variable chain (V_H, V_λ) and human constant chain (C_HI, C_κ). Lanes 1 and 6 contained a 1kb plus DNA molecular weight ladder. Lanes 1 to 4 contained the purified PCR product of the V_λ (~ 350bp), V_H (~ 400bp), C_HI (~ 400bp) and C_κ (~ 350bp), respectively.

5.2.2. PCR amplification of chicken/human chimeric heavy and light chain genes

The generation of the chicken/human chimeric heavy chain (Fd) fragment, was achieved by assembling the avian V_H and human C_H1 fragments. In addition, the chicken/human chimeric light chain region was assembled using the avian V_L fragment and human Cκ fragments. The chimeric heavy and light chain PCRs were optimised using different $MgCl_2$ concentrations (1, 2, 3 and 4 mM) and different temperatures (56, 58, 60 and 62^oC). The optimal conditions for the amplification of the chimeric heavy chain were 4 mM $MgCl_2$ with an annealing temperature of 60^oC. Similarly, the optimal PCR conditions for the amplification of chimeric light chains were 2 mM $MgCl_2$ with an annealing temperature of 57^oC. Both the chimeric light chain (~ 750 bp) and heavy chain (~ 800 bp) were successfully amplified and the PCR products were resolved on a 1% (w/v) agarose gel (Fig. 5.4).

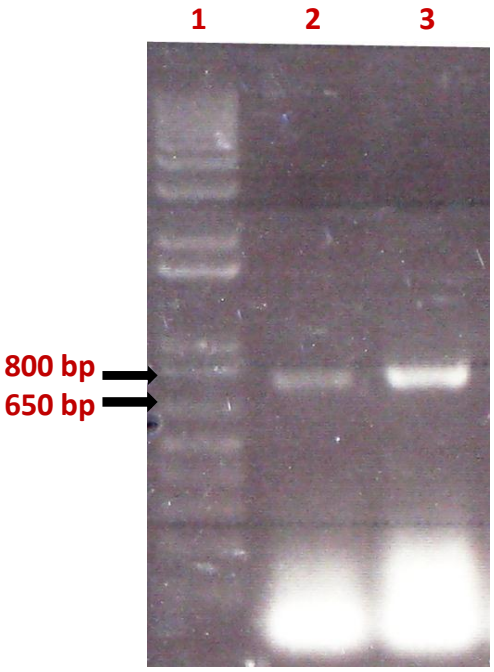

Figure 5.4. Amplification of the chicken/human chimeric heavy chain and light chains. Lane 1 contained a 1kb plus DNA molecular weight ladder. Lanes 2 and 3 contained the amplified chicken/human chimaeric light (~ 750 bp) and heavy chains (~ 800 bp), respectively.

5.2.3 Anti-cTnT Fab-Splice by Overlap Extension (SOE) PCR

The final splice by overlap extension (SOE) PCR involved assembling the chicken/human chimaeric heavy chain fragment with the light chain fragment. A number of optimisation steps were performed. These included testing different PCR polymerases (Go-Taq® polymerase, Fusion Taq® and Platinum HIFI™ Taq polymerase) and optimisation of magnesium chloride (0, 0.5, 1, 2 and 2.5 mM) and magnesium sulfate (0, 0.5, 1, 2 and 2.5 mM) concentrations. The PCR was optimised using platinum HIFI™ Taq polymerase and a concentration of 2.5 mM magnesium sulfate (Fig 5.5).

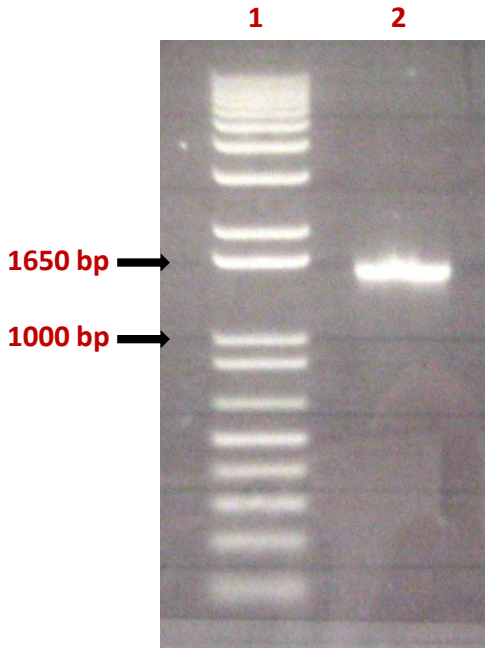

Figure 5.5. SOE-PCR amplification of Fab fragment using optimised PCR conditions. Lane 1 represents a 1kb plus DNA molecular weight ladder. Lane 2 represents SOE-PCR fragment (~ 1500 bp).

5.2.4. Avian anti-cTnT Fab library construction and enrichment via biopanning

A large-scale amplification of the SOE-PCR was subsequently performed. The PCR product was extracted from a 1% (w/v) agarose gel and concentrated by ethanol precipitation. The PCR product and pComb3XSS vector were digested using a *Sfi*I restriction enzyme followed by overnight ligation at room temperature with T4 ligase. The ligated product was ethanol-precipitated and transformed into electrocompetent *E. coli* XL1-Blue cells by electroporation, as described in section 2.3.1.10. The transformed avian anti-cTnT scFv library had a size of 1.2 x 10^7 cfu/mL. Recombinant anti-cTnT Fab clones were selected from this library by performing five rounds of phage display biopanning against immobilised cTnT antigen, as described in section 2.2.1.12. Table 5.2 shows the input and output titres for each of the 5 rounds of biopanning of the avian Fab anti-cTnT libraries.

Table 5.2. Input and output titres of anti-cTnT Fab clones over five rounds of biopanning.

Biopanning round	Input (cfu/mL)	Output (cfu/mL)
1	1.7×10^{12}	4×10^{6}
2	1.2×10^{12}	3×10^{6}
3	1.5×10^{12}	5×10^{5}
4	9.5×10^{11}	1.2×10^{5}
5	3.2×10^{11}	3.9×10^{4}

5.2.5. Expression of soluble chicken anti-cTnT Fab antibodies

A total of 96 anti-cTnT Fab antibodies were picked from biopanning round 5 output plates. These clones were subsequently analysed using a simple 'on-plate' monoclonal ELISA screening method (section 2.3.1.14). Figure 5.6 shows a small number of soluble Fab antibodies (13 out of 96) that were specific to the cTnT antigen.

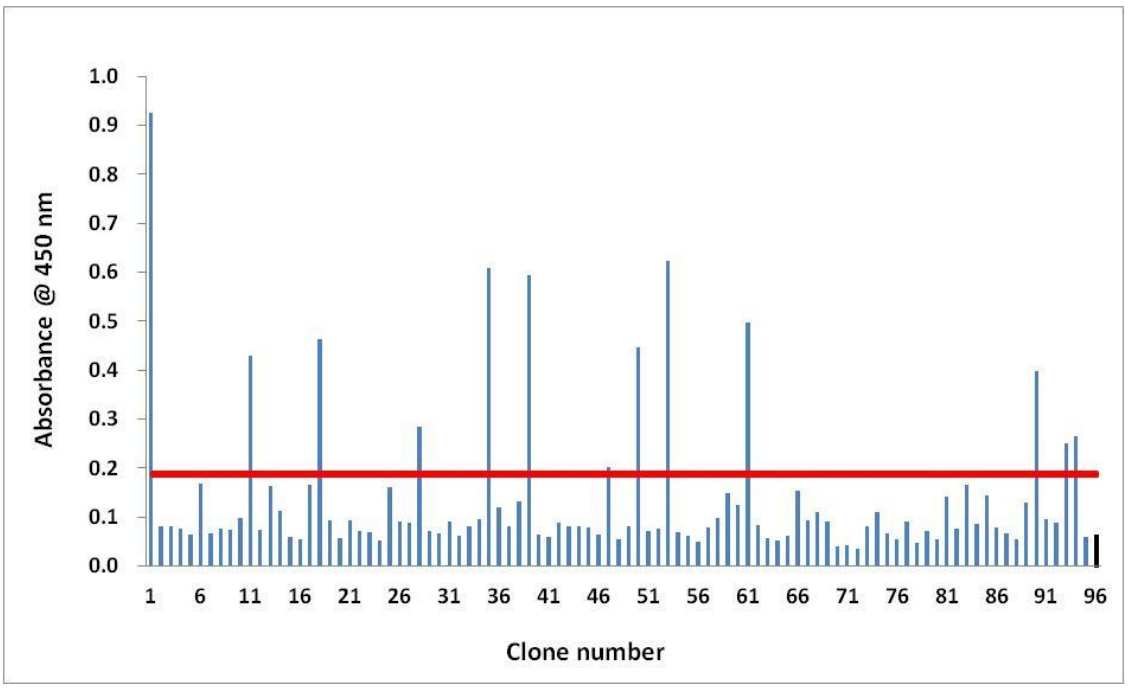

Figure 5.6. Screening of anti-cTnT Fab phage clones from round five of biopanning. Each of the blue bars represents the absorbance readings from each Fab clone. A black bar (Number 96) represents the absorbance reading of a blank reference. A red horizontal line drawn at background absorbance level (~ 0.18) marks the ELISA threshold. The threshold value was set at three times the absorbance value of the blank reference.

5.2.6. Titre determination of anti-cTnT Fab antibodies by ELISA

A total of eight Fab clones that had previously displayed high cTnT-binding levels from monoclonal ELISA analysis were selected for further studies. These clones were grown in a 5 mL SB media and expressed overnight at 30°C, and induced with 1 mM IPTG. Crude bacterial lysates were prepared and subsequently analysed by ELISA (Fig. 5.7). All eight clones had very low levels of antibody expression. The clone D3 had a maximum absorbance of only approximately 0.3.

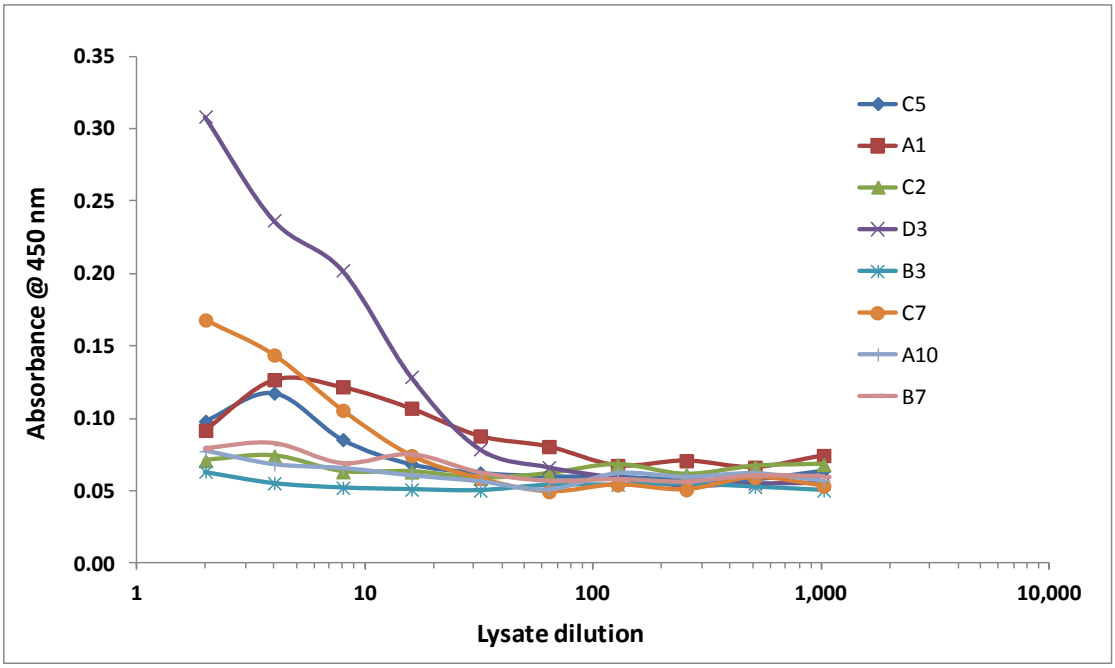

Figure 5.7. Antibody titre determination of anti-cTnT Fab antibodies. An ELISA plate was coated with 100 µL of 1 µg/mL cTnT and blocked with 200 µL 5% (w/v) Marvel in PBS. A series of dilutions of the crude antibody lysates (1 in 2, 1 in 4, 1 in 8, 1 in 16, 1 in 32, 1 in 64, 1 in 128, 1 in 256, 1 in 512 and 1 in 1,024 dilutions) were prepared and 100 µL of each dilution was added into the wells. The Fab antibodies were detected using HRP-labeled mouse anti-HA monoclonal antibody. The ELISA was developed with TMB substrate and the absorbance was read at 450 nm.

5.2.7. Optimisation of Fab antibody expression conditions

In orde to improve the expression levels of the Fab clones in the *E.coli* system, a number of optimsation steps were performed. Protein expression in *E.coli* is a complex process and depends on a wide number of parameters such as the type of growth media used, IPTG concentration used induction, expression temperature, culture shaking speed and the period of incubation. In this study, the optimistaion process involved the substitution of SB media for TB media; optimisation of the IPTG induction concentration and selection of the optimal period for incubation. The expression levels of four Fab clones (A1, C5, C7 and D3) were optimised (Fig. 5.7). The Fab cultures were induced with four different IPTG concentrations (0.05, 0.1, 0.25 and 0.5 mM), and subsequently incubated at 30^{o}C. After IPTG induction, samples from each culture were collected after 2 hours, 4 hours, 6 hours and overnight (~ 16 hours) incubation. The ELISA absorbance values, which indicated the expression levels of each of the samples, are shown in Figure 5.8.

Figure 5.8 reveals that the expression levels of clone A1, C5 and D3 were successfully optimised. Clone A1 had a maximum Fab expression level after 2 hours induction using a IPTG concentration of 0.05 mM. Similarly, both the clones C5 and D3 had a maximum Fab expression level after 6 hours induction using a IPTG concentration of 0.5 mM. Interestingly, the expression levels of clones A1, C5 and D3 were significantly decreased after overnight incubation (~ 16 hours). Furthermore, the expression levels of clone C7 were low across all the conditions tested and, therefore, this clone was excluded from further studies.

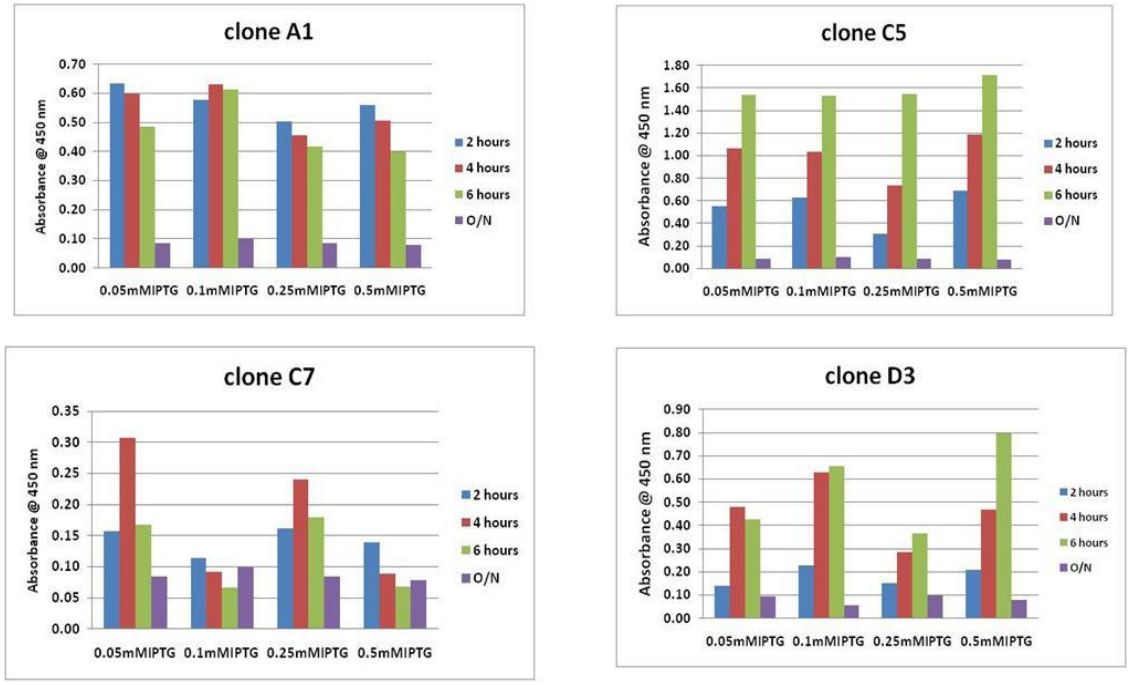

Figure 5.8. Optimisation of Fab antibody expression levels. Each bar chart represents the expression levels of different Fab antibody (A1, C5, C7 and D3). Cultures were incubated at 30^{o}C and induced with 0.05, 0.1, 0.25 and 0.5 mM IPTG. Samples were collected over a period of 2, 4, 6 hours and overnight (~ 16 hours). Fab antibody expression levels were determined using a direct ELISA.

5.3 Discussion

This chapter describes the generation of avian anti-cTnT Fab antibodies using phage display. In addition, selection of cTnT-specific Fab antibodies and optimisation of their expression levels is also described.

In comparison to scFv antibodies, Fab antibodies have a number of distinct advantages, as described in section 5.1. Fab format was, therefore, also chosen for the generation of anti-cTnT antibodies. Using the previously isolated avian cDNA, an anti-cTnT Fab library was generated. After five rounds of biopanning, only 25% (13 out of 96) bound specifically to cTnT. This figure is significantly less than that found from the selection of the scFv antibodies (section 4.2.5, Table 4.3). Table 4.3 shows up to 56.3% of the wild-type clones, 66.7% of heavy chain-shuffled clones and 75% of light chain-shuffled clones were selected as positive cTnT-binding clones. The smaller number of positive Fab clones may indicate that the Fab antibodies had lower displaying efficiency in comparison to the scFv antibodies. It is possible that the more complex *E. coli* expression process negatively impacted on the levels of Fab antibodies. For scFv antibodies, *E. coli* expression only involves two variable chains (V_H, V_L), whereas, the expression of Fab requires the production of four chains (V_H, V_L, C_L and C_H1) and a disulphide bond for the connection of the two Fab chimeric regions. Thus, the folding and assembly of Fab fragments in the periplasm of *E. coli* is more complex than for scFv antibodies. This observation is consistent with the work of Skerra and co-workers. They found that the display of Fab on the phage particles due to its large molecule size (50 kD) (Skerra *et al.,* 1993). Moreover, Pluckthun also reported Fab antibodies had a slower folding rate than scFvs in *E. coli* cells (Pluckthun, 1990; Pluckthun, 1991).

E. coli systems have been utilised for the production of recombinant proteins for more than two decades (Hudson *et al.,* 1988; Skerra and Pluckthun, 1988; Bird *et al.,* 1998;

Graumann and Premstaller, 2006). A total of eight Fab clones having positive binding for cTnT were analysed by a titration ELISA. However, all eight antibodies had low expression levels (Fig. 5.7). In order to improve the Fab expression level, the type of growth media, the IPTG induction concentration and the period of inculation were optimised. It was shown that three Fab clones (A1, C5 and D3) were successfully expressed (Fig. 5.8). Using the TB media, clone A1 showed a maximum expression level when using 0.05 mM IPTG and incubating for a period of 2 hours. Clones C5 and D3 required 0.5mM IPTG and incubation for 6 hours for optimal expression. Although both SB and TB are highly enriched media often used in the cultivation of *E. coli*, TB contains glycerol which provides an extra carbohydrate source for *E. coli* growth. In addition, the potassium phosphates in TB may enhance protein expression. For example, Manderson and co-workers compared SB and TB as growth media for the production of recombinant hydatid vaccine (Eg95). They reported a higher biomass of the Eg95 vaccine was produced using TB media (Manderson *et al.,* 2006).

In conjunction with media type, IPTG concentration was also optimised. IPTG triggers the *lac* operon required for the metabolism of lactose in *E.coli.* As an expensive reagent, the minimum concentration of IPTG which can fully induce the *lac* promoter is the optimal condition. In addition, excessive IPTG concentrations may reduce cell viability and diminish Fab expression. Generally, the concentration of IPTG required to fully induce the *lac* promoter can vary widely depending on the clone. Figure 5.8 shows A1 and C7 had the highest Fab expression levels with 0.05 mM ITPG induction, whereas, C5 and D3 showed the highest expression levels at 0.5 mM IPTG. These IPTG concentrations are less than those reported by Mohkam and co-workers. They found the maximal expression level of recombinant Fab against human leptin receptor was achieved with a 1 mM IPTG concentration (Mohkam *et al.,* 2011). In addition, Robbens and co-workers used 2 mM IPTG to achieve high levels of recombinant murine

interleukin-2 protein (Robbens *et al.,* 1995). In contrast, a four-fold lower IPTG concentration (0.05 mM) was used by Donovan and co-workers to increase the yield of a monoclonal antibody Fab fragment (Donovan *et al.,* 2000). Furthermore, IPTG concentrations of between 0.1 mM and 2 mM have also been used to induce the *lac* promoter for recombinant proteins (Yee and Blanch 1993; Bhattacharya and Dubey 1997; Li *et al.* 1999; Madurawe *et al.* 2000). Therefore, the optimal IPTG concentration for maximum expression is strongly dependent on the individual clone.

Period of induction is another parameter affecting antibody expression. The expression levels of anti-cTnT Fab antibodies were analysed after 2, 4, 6 hours and overnight (~ 16 hours) incubation. Interestingly, clone A1 had a maximum expression level after a short period of incubation (2 hours) incubation with a low IPTG (0.05 mM) induction, whereas, clones C5 and D3 requried a longer period for induction (6 hours) with a higher IPTG (0.5 mM) induction. This observation is contrary to that found by Azaman and co-workers. They showed for the production of interferon-α2b in *E. coli*, high yield occurred when using longer induction time and lower IPTG concentrations or shorter induction time and higher IPTG concentrations (Azaman *et al.,* 2010). This may be due to using different *E. coli* strains for protein expression, using different types of growth media or incubation temperatures. However, the different inherent protein structure between Fabs and interferon-α2b may well be the major factor.

In conclusion, chicken anti-cTnT Fab antibodies were successfully generated. Expression conditions for Fab antibodies were also successfully optimised. Further work will involve SPR-based characterisation and affinity chromatographic purification of the selected anti-cTnT Fab antibodies. The ultimate goal is to develop a highly sensitive cTnT immunoassay that incorporates either the anti-cTnT scFv or the Fab antibody fragments, or both in a sandwich format.

Chapter 6
Determination of LDH levels in milk samples

6.1 Introduction

This chapter outlines an investigation of the effectiveness of LDH as a biomarker for the detection of sub-clinical mastitis. It contains an in-depth description of the standardisation and optimisation of a fluorescence-based 'end-point' assay and the use of this assay for the determination of LDH in various milk samples.

Enzymatic assays for the determination of LDH activity can use either a kinetic or an 'end-point' method. A kinetic method involves monitoring the change of parameters, such as fluorescence or absorbance, at short time intervals. The change of parameter is normally related to the amount of product formation and substrate consumption. An enzyme's progress curve (rate curve) is a plot of absorbance or fluorescence as a function of time. The best fit enzyme progress curve allows estimation of the reaction rate therefore allowing determination of the initial concentrations of reagents participating in the reaction. An 'end-point' assay measures the change of parameters caused by the quantity of substrates consumed or products formed over a fixed period of time. During this time period, normally at the steady-state of an enzyme-based reaction, the rate of substrate converted and products generated are linear. This linearity allows quantitative analysis of the initial concentrations of substrates based on the parameter changes at the end of the reaction (Rose and Warms, 1987; Bravo *et al.*, 2004).

Kinetic analysis is sometimes considered as a more sensitive analytical method than 'end-point' analysis. Monitoring the change of parameters in 'real-time' may increase the assay accuracy. However, it also has a number of disadvantages. The assay performance is a time-consuming and expensive process especially with large numbers of samples. Plotting of rate curves for reaction rate estimation can be problematic and considerable judgment is required for interpretation (Hicks *et al.,* 1973). In comparison to kinetic assays, an 'end-point' assay can be easily developed, with monitoring of changes of parameters only at two time points throughout the assay. Therefore, it is a rapid, convenient and cost effective approach (Srisawasdi *et al.,* 2007). These features are particularly useful when analysing a large number of samples, as for example, in the determination of LDH levels in 12 batches of milk samples used in this project. In addition, Srisawasdi and co-workers reported that an 'end-point' assay had better

precision for the determination of serum cholesterol than kinetic analysis (Srisawasdi *et al.,* 2007). The 'end-point' assay was, therefore, chosen for the determination of LDH levels in milk samples.

6.1.1 Work summary for the determination of LDH levels in milk samples

Using a fluorescence-based 'end-point' assay, the LDH levels in various milk samples were determined. The correlation of LDH levels with other markers of mastitis (SCC and NAGase) in milk samples was also investigated. Moreover, the analysis of the effectiveness of using composite milk samples for mastitis diagnosis is examined. In addition, the effects of the lactation stage, storage and handling on LDH activity in milk samples were also investigated.

6.2 Results

6.2.1 Optimal reaction conditions for LDH levels determination in milk samples

The aim of this section is to determine an optimal 'end-point' reaction time where the reaction rate of the conversion of LDH to pyruvate can reach a maximum level. A known amount of LDH (0.248 mg/ml) was used to convert a known amount of lactate (350 mM) to pyruvate. The fluorescence was measured at 30 second intervals for 330 seconds, as described in section 2.4.3.2. A time curve was generated by plotting fluorescence values against time (Fig. 6.1).

Figure 6.1 shows the fluorescence values started increasing as soon as the incubation began. The increase of fluorescence values is due to the formation of the highly fluorescent substance, resorufin. The values stayed constant from approx. 250 seconds to 300 seconds. A sixth order polynomial rate curve was fitted to the data which had a R-square value of 1, thus showing a very good fit. In addition, the estimated rate from 0 second to 300 seconds was found to be 205 FU/s from the sixth order polynomial equation. However, this value only indicates the reaction rate at 330 seconds; the optimal 'end-point' reaction time where the reaction rate can reach a maximum level was still yet to be determined.

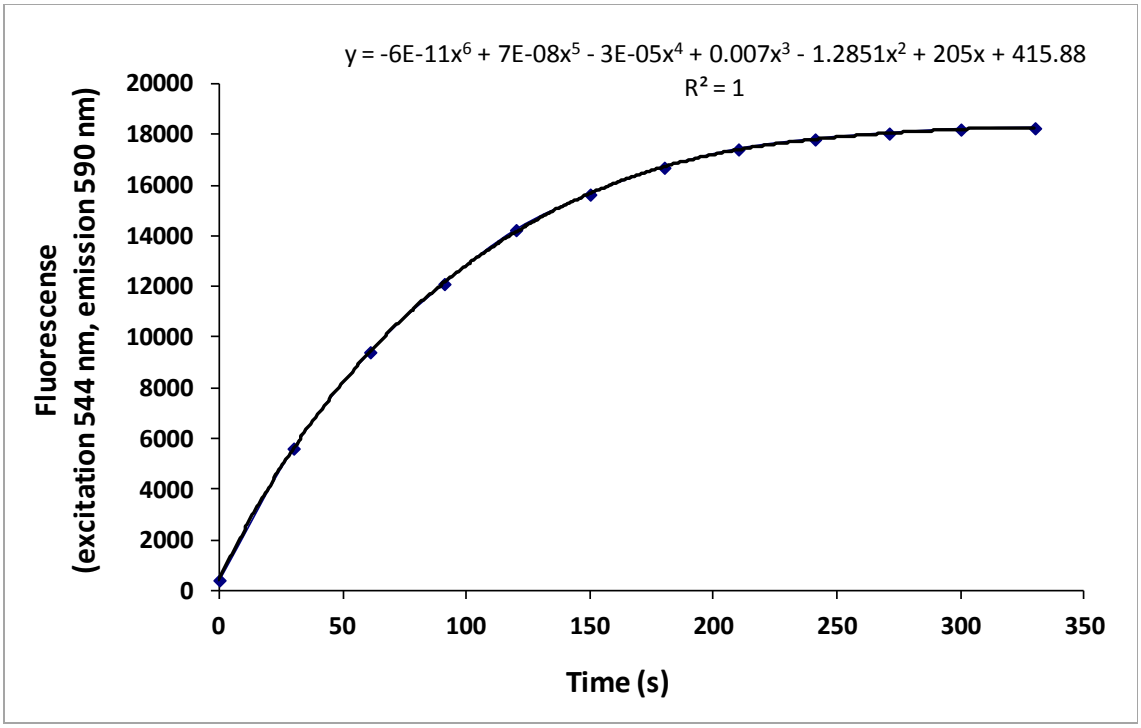

Figure 6.1. Measurement of fluorescence values produced by a reduction reaction catalysed by LDH. Measurements started at time zero (0 seconds) and finished at time 330 seconds. A rate curve was plotted with the data points to estimate the rate of the reaction.

Generally, the rate of an enzymatic reaction reaches its maximum level at the steady-state or exponential phase of the reaction. To determine an optimal 'end-point' reaction time where the rate has a maximum value, different orders of polynomial rate curves were fitted to the data at time points of 120, 150, 180, 210, 240, 270, 300 and 330 seconds. The estimated reaction rates are listed in Table 6.1.

Table 6.1 shows the overall estimated reaction rates of converting L-lactate to pyruvate following the formation of the final product, resorufin, are in a range from 177 to 215 FU/s. The maximum rate 215 FU/s was found at time 180 seconds, which may suggest the reaction was at its exponential reaction phase. In addition, a rate curve of the reaction from 0 seconds to 180 seconds is shown in Figure 6.2, a fifth order polynomial equation show that at 180 seconds the reaction rate reached the maximum level (215

FU/s). Therefore, 180 seconds was selected as an optimal 'end-point' reaction time for the determination of LDH levels in the enzymatic assay for use in milk samples.

Table 6.1. Estimation of reaction rate at each time point by fitting rate curves

Estimated Rate (FU/s)* / Time (s)	3rd order polynomial fit	4th order polynomial fit	5th order polynomial fit
120	203	204	------
150	196	210	199
180	191	202	215
210	188	198	209
240	185	196	203
270	182	194	202
300	180	191	200
330	177	190	197

* FU/s stands for fluorescent units per second

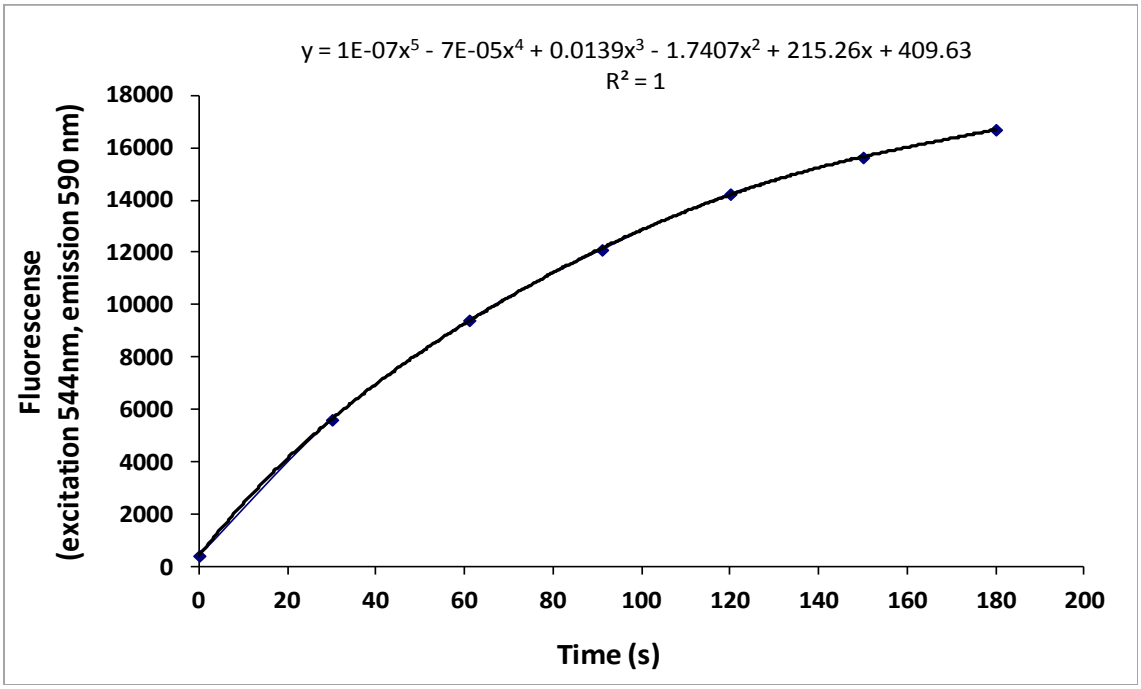

Figure 6.2. Rate curve of the reduction reaction catalysed by LDH at 180 seconds. A rate curve was plotted with the data points from 0 to 180 seconds, and the fifth order polynomial equation shows the reaction rate reached its maximum level of 215 FU/s.

6.2.2 Linearity study of resorufin produced using different LDH concentrations at 180 seconds

A linearity study was performed to show that the formation of fluorescent product, resorufin, was proportionally related with LDH concentration at 180 seconds. A series of LDH dilutions was prepared with a range of concentrations from 0.13 to 17 µg/mL. The assay was performed as described in section 2.3.4.2. Fluorescence readings were obtained at time 0 seconds and 180 seconds. The linearity between net fluorescence readings and LDH concentrations is shown in Figure 6.3.

It is shown that when 180 seconds was used as the 'end-point' for LDH activity determination by the fluorescence assay, the amount of resorufin formation was linearly proportional with LDH concentrations. The 'end-point' of 180 seconds was, therefore, suitable for the determination of LDH in milk samples.

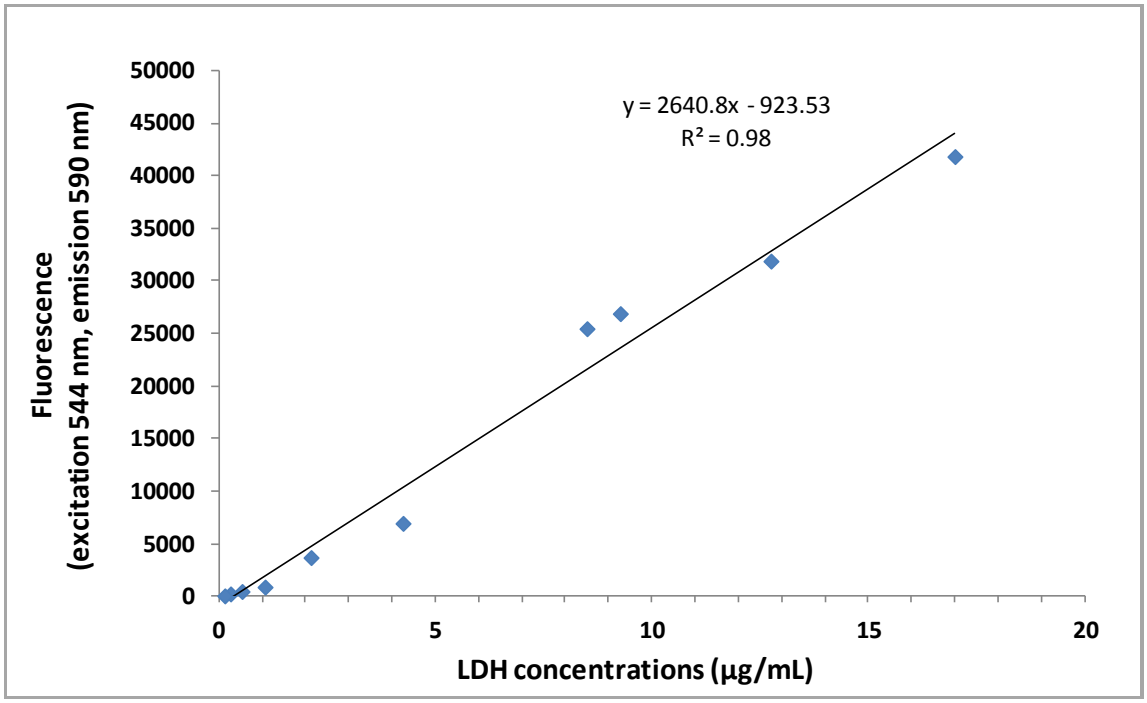

Figure 6.3. Linearity of fluorescence values for the reaction catalysed by varying LDH concentrations. Measurements started at time 0 seconds and finished at 180 seconds.

6.2.3 Determination of LDH levels in milk samples

Milk samples produced by 80 Holstein Friesian cows over a 7 months period were collected. The milk samples, representing different stages of lactation, are shown in Table 6.2. The teat end for each quarter was cleaned with 70% (v/v) ethanol prior to sampling. A total of 30 mL of each milk sample was collected in sterile tubes, after discarding the first 5 mL of milk taken during sampling. All samples were kept cool (at 4^{o}C) during transportation and were processed in the laboratory within 8 hours of collection. Milk was taken from each udder quarter of each individual cow. Samples were named according to the quarter position, i.e. front left, front right, back left, and back right.

Table 6.2. Summary of milk samples collected from 80 Holstein Friesian cows

Batch No.	Date of sampling	Total No. of milk samples *	No. of cows sampled	Lactation stage
1	17/10/07	25	7	Mid-late
2	26/10/07	25	7	Mid-late
3	30/10/07	25	7	Mid-late
4	09/11/07	25	7	Late
5	27/11/07	38	10	Late
6	06/12/07	25	7	Late
7	15/01/08	24	6	Early
8	11/02/08	24	6	Early
9	13/02/08	25	7	Early
10	14/02/08	10	3	Early
11	03/03/08	24	6	Early
12	17/04/08	25	7	Early
Total		**295**	**80**	

* Milk samples were not obtained from all four quarters of the cow in some cases.

LDH levels were determined for all milk samples as detailed in section 2.3.4.3. However, for samples from batch 1 the LDH activity of the positive control gave no results indicating that the LDH assay did not work. Analysis on samples from batch 1 was therefore excluded from this study. LDH levels detected from batch 2 to 12 ranged from a minimum 0 U/L to a maximum of over 10,000 U/L (Data not shown).

6.2.4 Correlation of LDH levels with Somatic Cell Count and NAGase concentrations

The LDH levels of all milk samples from batch 2 to 12 were measured, as detailed in section 2.3.4.3. The SCC of milk samples were determined by the Portacheck® milk test, as described in section 1.4.4. NAGase activity was determined using a fluorometric assay, as reported by Schuttel (Schuttel *et al.,* 1999). NAGase level determinations were only carried out on samples in batches 2-5, and batch 9. SCC levels were determined from batches 3-5, batch 7 and batch 9. The aim of this work was to investigate the correlation between LDH and SCC and LDH and NAGase in milk samples, in order to analyse the value of using LDH as a mastitis marker. Statistical analysis was carried out, as detailed in section 2.3.4.3. PASW statistics 18 software sets correlation values (r) greater than 0.80 as a good correlation. One-way ANOVA was used to determine the significance value (p). Data was considered statistically significant when the p value is less than 0.05. The p values and r values for comparison of LDH versus NAGase levels and LDH versus SCC levels are shown in Tables 6.3 (A) and (B), respectively.

The r value of batch 2 for LDH and NAGase (0.64) was lower than 0.80. However, it was still considered significant as the p value was 0.001 (less than 0.05). The r values of batch 3, 4 and 5 for LDH and NAGase were greater than 0.80 which indicated that the correlations between LDH and NAGase were good (Table 6.3 (A)). However, for the correlation between LDH and SCC levels, the r values of 3 out of the 5 batches (batch 3, 5 and 7) were less than 0.8, which, overall, indicated a poor correlation between LDH and SCC.

Tables 6.3 (A) and (B) show that LDH levels had a higher correlation with NAGase levels than SCC in milk samples. The reason could be that both LDH and NAGase are released from damaged cells in milk samples, while somatic cells (white blood cells) are produced as an inflammatory response to infection. Chagunda *et al.* (2006) reported a correlation of LDH to SCC of 0.48 and the correlation of LDH to NAGase of 0.43. These correlation values are much lower than the mean correlations (0.70 for LDH versus SCC and 0.86 for LDH versus NAGase) observed in this study. It was also reported that LDH showed a closer correlation to SCC than to NAGase contrary to what

was observed in this study (Chagunda *et al.,* 2006). The differences in findings may be due to the fact that Chagunda used the Fossomatic 5000™ for SCC determination whereas a Portacheck® device was used for this study. The SCC detection of Fossomatic 5000™ is based on the measurement of fluorescence levels which are produced from the interaction between ethidium bromide and the nuclear DNA of somatic cells. The Portacheck® test is based on the interaction between a dye on the test strips with enzymes present in the somatic cells. The difference in testing principles between the two devices may cause differences in correlation of results.

Table 6.3 (A). Correlation between LDH and NAGase

	r (correlation)	p (significance)
Batch 2	0.64	0.001
Batch 3	0.89	0.000 (< 0.001)
Batch 4	0.98	0.000 (< 0.001)
Batch 5	0.92	0.000 (< 0.001)
Mean	0.86	------

Table 6.3 (B). Correlation between LDH and SCC

	r (correlation)	p (significance)
Batch 3	0.59	0.002
Batch 4	0.86	0.000 (< 0.001)
Batch 5	0.42	0.008
Batch 7	0.67	0.001
Batch 9	0.96	0.000 (< 0.001)
Mean	0.70	------

* p-value refers to significance levels. The standard level for a p value, from PASW statistics 18 software, to be significant is 0.05. If PASW gives 0.000 in the output for a p-value, it can be reported as $p < 0.001$

A.

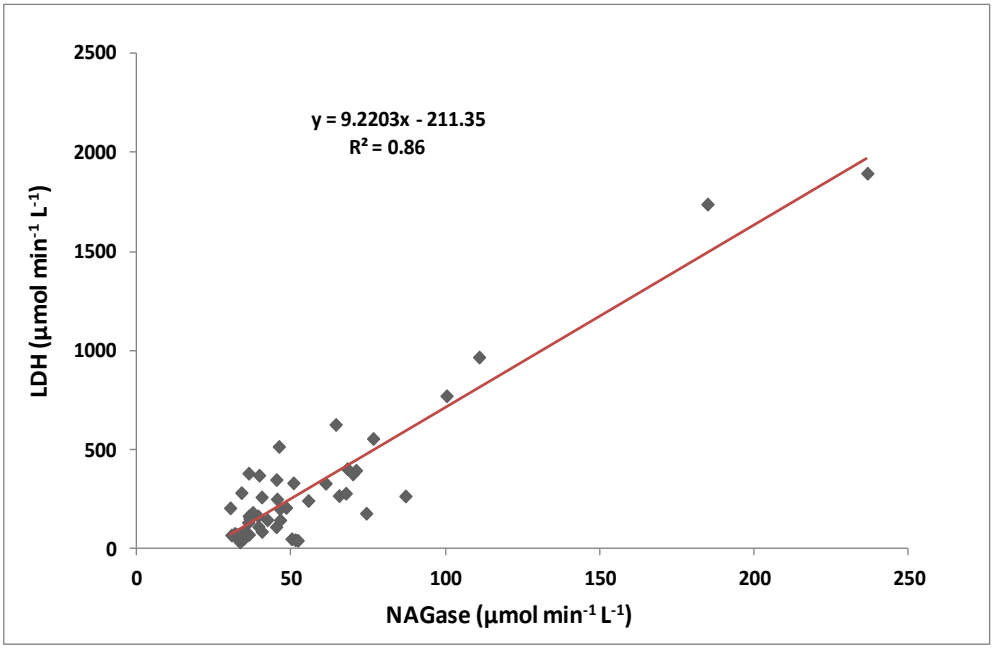

B.

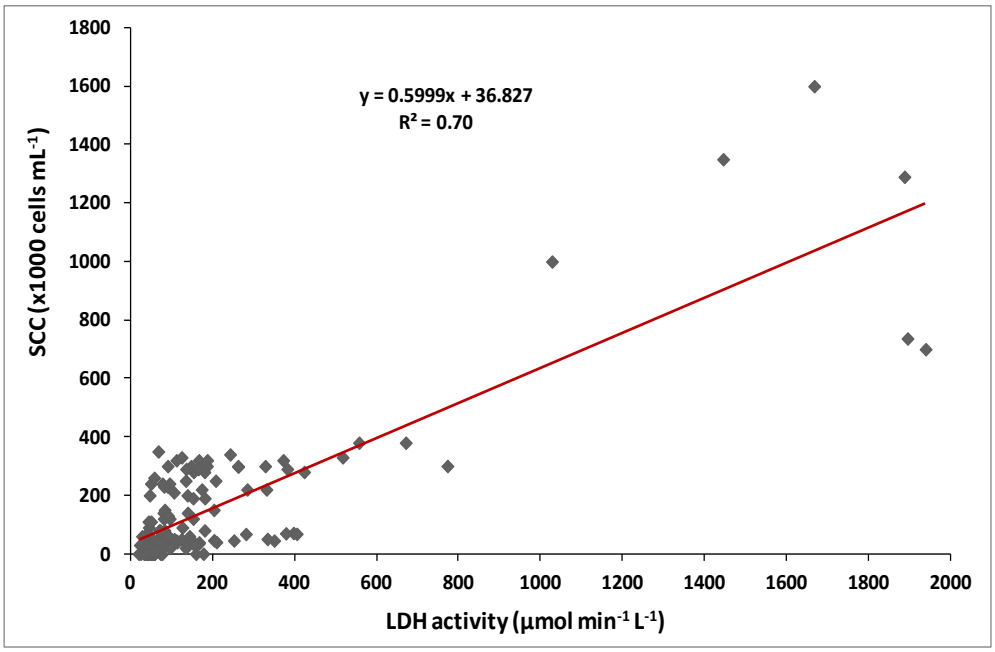

Figure 6.4. Scatter plot of the correction between LDH activity with NAGase activity and SCC. Graph A shows the correlation between NAGase and LDH activity in four batches of milk samples (batches 2, 3, 4, and 5), graph B shows the correlation between SCC and LDH activity in five batches of milk samples (batches 3, 4, 5, 7 and 9). The red straight lines indicate the best fitting line between two sets of data. The R^2 values indicate the correlation.

The scatter plots show good correlation between LDH and NAGase, LDH and SCC, which were 0.86 (Fig. 6.4(A)) and 0.70 (Fig. 6.4(B)). There values are corresponded to the values obtained by PASW statistics 18 in this study, 0.86 and 0.70 (Table 6.3).

6.2.5 LDH as a marker for the identification of mastitic milk samples

A LDH 'cut-off' level for mastitis in cows was reported to be 107.2 U/L (Dohoe and Leslie, 1991). Using batch 11 as an example, LDH levels in milk samples were measured and the mastitis status was identified using the 'cut-off' level of 107.2 U/L as determined by Dohoe and Leslie (1991) (Table 6.4).

As shown in Table 6.4, a total of 7 samples had LDH levels greater than the 'cut-off' level and, therefore, they were classified as 'mastitis-positive'. The remaining samples were below the 'cut-off' level and, therefore, they were classified as healthy.

Table 6.4. LDH levels as an indicator of mastitis

Sample No.	LDH (U/L)	Mastitis status*
254 FR	29	-
254 FL	35	-
254 BR	42	-
254 BL	37	-
260 FR	80	-
260 FL	42	-
260 BR	46	-
260 BL	115	+
319 FR	78	-
319 FL	88	-
319 BR	8436	+
319 BL	242	+
350 FR	28	-
350 FL	33	-
350 BR	92	-
350 BL	63	-
380 FR	164	+
380 FL	182	+
380 BR	493	+
380 BL	1475	+
704 FL	35	-
704 BR	22	-

* Mastitis status is represented by '- 'or '+' as mastitic-negative and positive, respectively.

6.2.6 Individual quarter vs composite milk samples for the identification of mastitis

To assess the value of using composite milk for the identification of mastitis status, SCC and LDH concentrations were analysed in a total of 100 milk samples including 80 milk samples from individual udder quarters and 20 composite milk samples. The variation of SCC concentrations and LDH concentrations between different quarters of 20 cows tested were shown in Figures 6.5 (A) and (B), respectively.

A variation in quarter health is observed across the animals tested (Fig. 6.5). In all 20 cows tested, increases and decreases observed in SCC concentrations corresponded to increases and decreases observed in LDH concentrations. Both SCC and LDH concentrations were above the 'cut-off' point for mastitis for all four quarters in 3 cows, 3 quarters in 1 cow, 2 quarters in 2 cows, 1 quarter in 5 cows and none of the quarters for 9 cows. Five cows (cow 2, 7, 14, 16, 18) in which one quarter showed SCC and LDH concentrations above the 'cut-off' point for mastitis gave a composite sample with levels below the 'cut-off' for mastitis for both LDH and SCC (Fig. 6.5). This shows that if milk from unhealthy quarters is diluted with milk from healthy quarters the identification of mastitis maybe problematic or even missed entirely.

A.

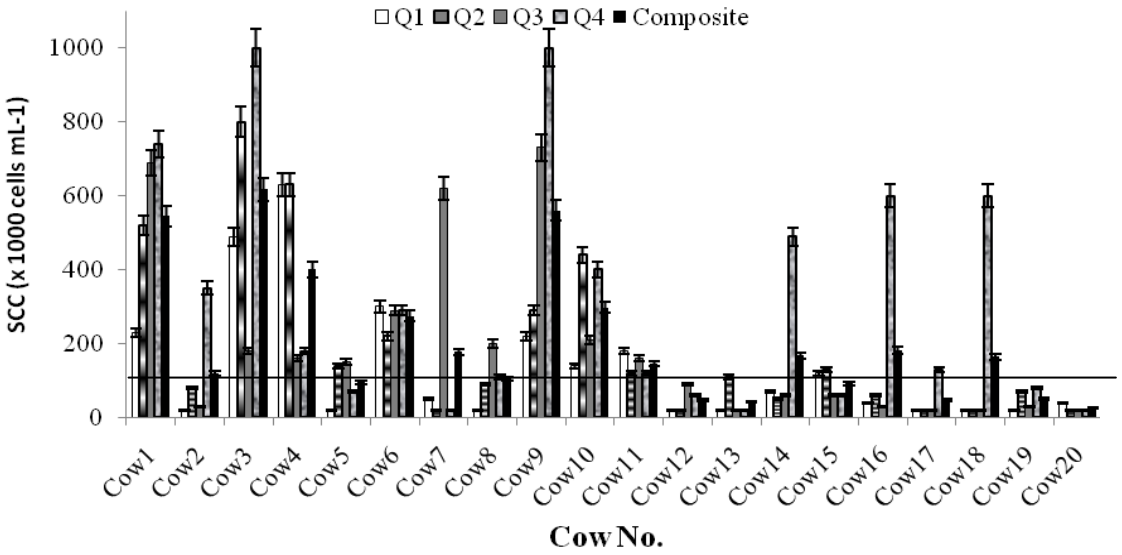

B.

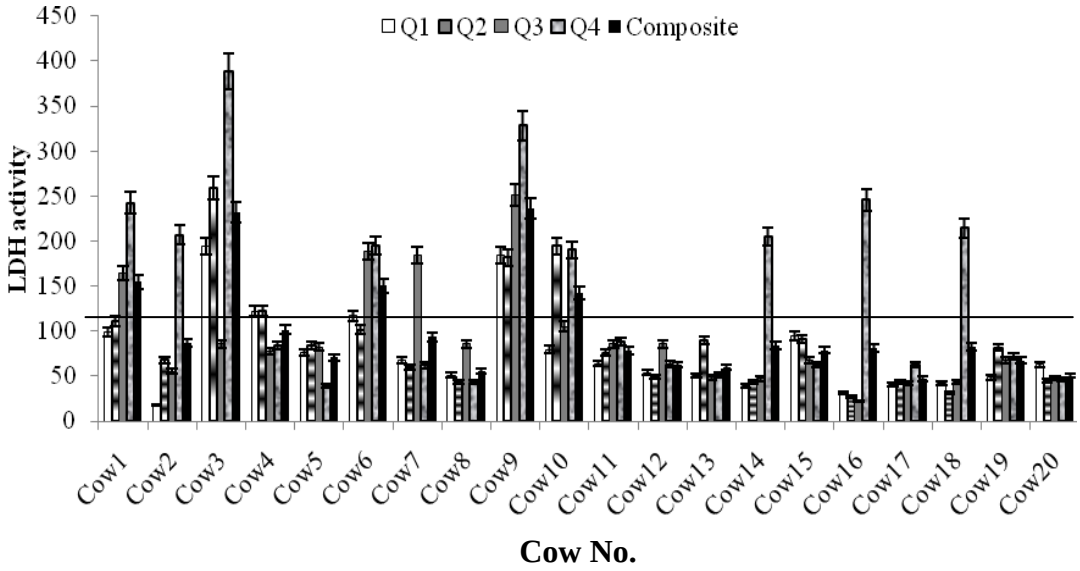

Figure 6.5. Variation of SCC concentrations and LDH concentrations between different quarters of 20 cows. Graph shows the SCC (A) and LDH activity (B) concentrations of milk samples in the four different quarters (quarter 1 (Q1) shown in white, Q2 shown in black and white stripes, Q3 shown in grey, Q4 shown in grey marble) and from a composite sample containing a mixture of all of these quarters (shown in black) from 20 different cows. Values shown represent the mean value ± standard deviation for assays measured in triplicate. The black line represents the 'cut-off' level for SCC (200,000 cells/mL) and for LDH (107.2 U/L) for the classification of mastitic or non-mastitic samples.

6.2.7 Effect of lactation stages on SCC and LDH

The SCC and concentrations of LDH and NAGase were analysed in milk samples at different stages of lactation. The variation of SCC concentrations and LDH concentrations over lactation stages are shown in Figures 6.6 (A) and (B), respectively.

The levels of indicators suggested as potential markers of mastitis were found to vary naturally depending on the stage of lactation (Fig. 6.6). The profiles of LDH and NAGase over the different lactation stages are different to that of the SCC profile. Samples from mid-late and late lactation stages showed a decrease in LDH and NAGase levels (results not shown) when compared to samples from an early stage of lactation, whereas samples from an early stage of lactation showed a decrease in SCC when compared to samples from the mid-late and late stages (Fig. 6.6 (A)). There was no significant difference observed in the levels of LDH between samples from the mid-late and the late stages of lactation (Fig. 6.6 (B)). Similarly, the SCC concentrations showed no significant changes in samples from the mid-late lactation stage when compared to samples from the late lactation stage. Lactation stage, therefore, had a significant influence on both SCC and LDH concentrations even in healthy cows.

A.

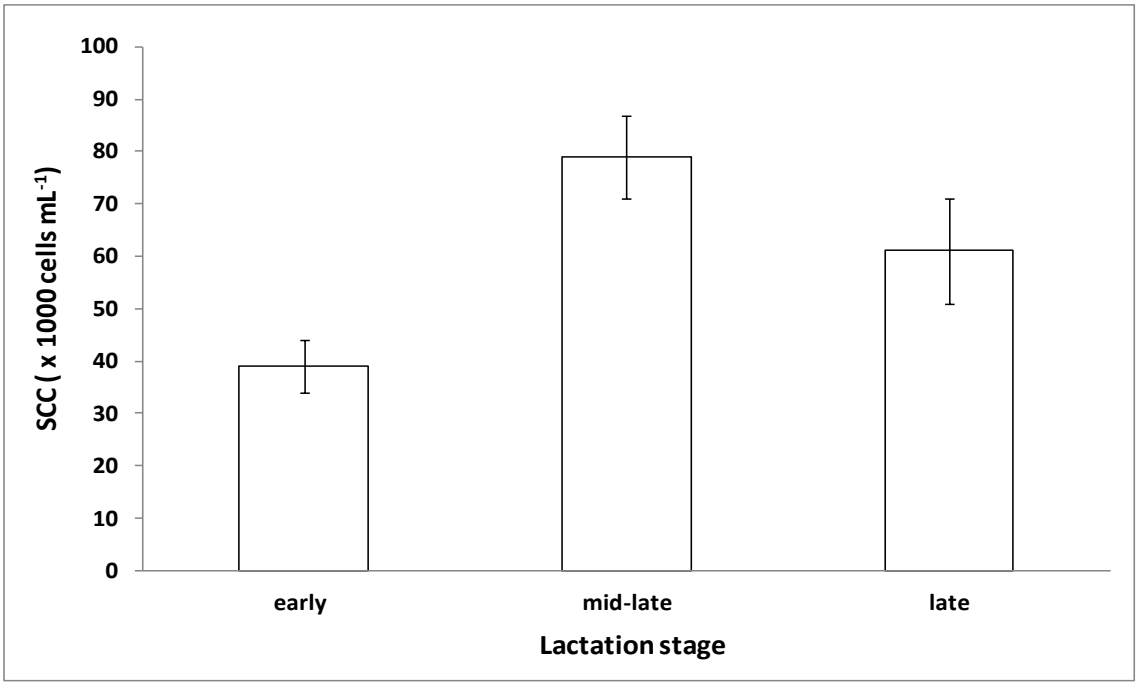

B.

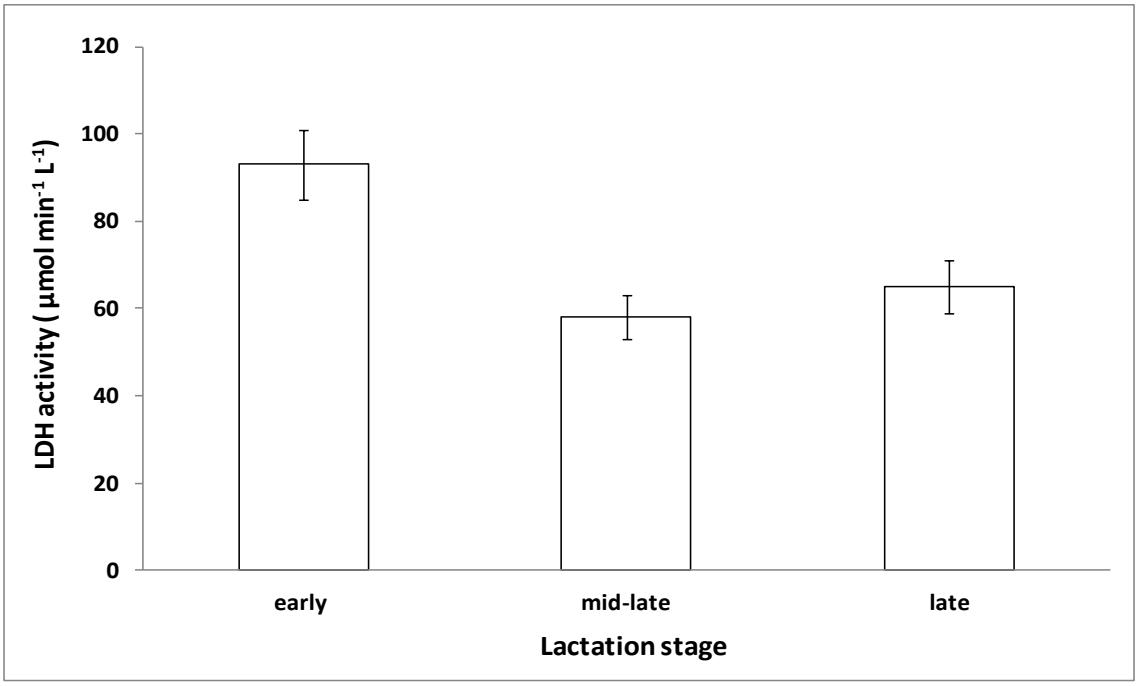

Figure 6.6. Variation of SCC concentrations and LDH concentrations over lactation stages. Graphs showing SCC (A) and LDH activity (B) of milk samples from healthy cows (SCC < 200,000 cells mL^{-1}) at different stages of lactation. Values represent mean values ± standard deviation for 76 milk samples from 19 different cows. All assays were performed in triplicate.

6.2.8 Detection of LDH levels in milk samples after storage

The aim of this element of the research was to examine the effect of different storage conditions on the LDH levels in milk samples.

6.2.8.1 Detection of LDH levels in milk samples stored for 56 hours at 4^{o}C

LDH activities in 24 milk samples from batch 12 were detected using the previously described fluorescence assay (section 2.3.4.3) before, during and after storage at 4^{o}C for 56 hours. The first LDH assay was performed on the milk samples 8 hours after sampling. LDH levels at 8 hours represent the time from sampling to arrival in the laboratory. Milk was stored at 4^{o}C after sampling and transported to the laboratory within 8 hours. These milk samples were then stored at 4^{o}C for an additional 24 and 48 hours and LDH levels were measured at 8, 24, and 48 hours. Using LDH levels at the 8 hour time point, samples were divided into healthy and mastitic sample groups using a LDH 'cut-off' level of 107.2 U/L (Dohoe and Leslie, 1991). A total of 22 samples were classified as healthy and one sample was classified as mastitic. Table 6.5 (A) presents LDH activities in the 22 healthy samples measured at 8 hours, 32 hours (8 hours plus 24 hours storage) and 56 hours (8 hours plus 48 hours storage) after sampling. The percentage differences from 8 hours to 32 hours, 8 hours to 56 hours and 32 hours to 56 hours were calculated. Table 6.5 (B) shows LDH levels in the one mastitic sample available for study.

Results shown in Tables 6.5 (A) and (B) indicate that LDH levels increased with storage. LDH levels increased 125% from 8 hours to 32 hours and a further 45% from 32 hours to 56 hours for healthy samples (Table 6.5 (A)). The increase could be caused by cell lysis resulting in the release of LDH during storage. Interestingly, all samples, except 273BR, showed an increase in LDH levels from 8 hours to 32 hours. However, four samples (350FL, 350BR, 704BL and 916FR) showed a decrease in LDH levels from 32 hours to 56 hours. This decrease may be due to proteolytic activity in the milk resulting in the breakdown of LDH.

Table 6.5 (A). Determination of LDH activities in healthy milk samples over a storage period of 56 hours

Sample No.	LDH (U/L) 8 h	LDH (U/L) 32h	LDH % difference from 8 to 56 h	LDH (U/L) 56 h	LDH % difference from 8 to 56 h	LDH % difference from 32 to 56 h
185 FR	20	43	115%	57	185%	33%
185 FL	48	69	44%	98	104%	42%
185 BR	34	92	171%	127	274%	38%
185 BL	20	55	175%	81	305%	47%
273 FR	18	35	94%	47	161%	34%
273 FL	16	21	31%	41	156%	95%
273 BR	53	50	-6%	69	30%	38%
273 BL	18	40	122%	41	128%	3%
350 FR	17	44	159%	57	235%	30%
350 FL	19	56	195%	44	132%	-21%
350 BR	28	79	182%	39	39%	-51%
350 BL	28	70	150%	81	189%	16%
426 FR	26	30	15%	55	112%	83%
426 FL	0	55	-----	59	-----	7%
426 BR	32	36	13%	82	156%	128%
426 BL	23	45	96%	64	178%	42%
704 FR	35	66	89%	78	123%	18%
704 FL	22	30	36%	35	59%	17%
704 BL	41	144	251%	96	134%	-33%
916 FR	29	87	200%	83	186%	-5%
916 FL	9	42	367%	60	567%	43%
916 BR	31	72	132%	73	135%	1%
Mean	**25**	**57**	**125%**	**66**	**170%**	**28%**
STDEV	**12**	**27**	**90%**	**23**	**113%**	**40%**

Table 6.5 (B). Determination of LDH activities in a mastitis milk sample over a storage period of 56 hours

Sample No.	LDH (U/L) 8 h	LDH (U/L) 32h	LDH % difference from 8 to 32 h	LDH (U/L) 6h	LDH % difference from 8 to 56 h	LDH % difference from 32 to 56 h
704 BR	741	2257	205%	2281	208%	1%

6.2.8.2 Detection of LDH levels in Freeze-thawed and 4°C-stored milk samples

To assess the effects of storage and handling conditions on LDH activities in milk samples, LDH level in 24 milk samples from batch 11 were investigated. The LDH assay was performed when the samples arrived in the laboratory (8 hours after sampling). The samples were then aliquoted into two sets. One set was stored at 4°C, and a second set was stored at -20°C. LDH activities at both 4 °C and -20 °C in the two sets were monitored after 32 hours (8 hours and additional 24 hours storage) storage since sampling. Healthy samples and mastitis samples were again classified using a LDH 'cut-off' level of 107.2 U/L (Dohoe and Leslie, 1991). Tables 6.6 (A) and (B) show the LDH levels in healthy (16) and mastitis (7) samples, respectively, at 8 hours and after 32 hours storage at both 4°C and -20°C. LDH percentage differences from 8 hours to 32 hours (stored at 4°C), and from 8 hours to 32 hours (stored at -20°C) were calculated.

Tables 6.6 (A) and (B) show that LDH activity increased after storage at both 4°C and -20°C for 32 hours. The LDH activity levels of both healthy and mastitic samples after storage at -20°C were higher than those stored at 4°C indicating that 4°C is a better storage temperature for LDH in milk samples. This may be as a result of the bursting of epithelial cells due to freeze-thawing. Overall, the percentage of LDH increase for healthy samples is lower than in mastitis-infected cows. The high standard deviation values in Table 6.11 (B) indicated high variations of LDH levels in mastitic samples. Storage of milk sample should therefore be at 4°C rather than -20°C but ideally LDH activity should be measured as soon as possible after sampling with minimum storage time.

Table 6.6 (A). LDH activities in healthy milk samples stored under different conditions

Sample No.	LDH(U/L) @ time 8 h	LDH (U/L) @ 32 h (stored at 4°C)	LDH % difference from 8 to 32 h (stored at 4°C)	LDH (U/L) @ 32 h (stored at -20°C)	LDH % difference from 8 to 32 h (stored at -20°C)
254 FR	29	91	214%	68	133%
254 FL	35	71	103%	88	154%
254 BR	42	66	56%	79	87%
254 BL	37	64	72%	79	113%
260 FR	80	107	34%	142	78%
260 FL	42	70	68%	84	100%
260 BR	46	75	63%	95	105%
319 FR	78	116	49%	128	64%
319 FL	88	143	62%	198	124%
350 FR	28	65	131%	61	115%
350 FL	33	67	106%	71	120%
350 BR	92	139	52%	155	69%
350 BL	63	99	56%	110	74%
704 FR	60	88	47%	84	40%
704 FL	35	68	95%	64	83%
704 BR	22	64	190%	73	229%
Mean	**50**	**87**	**87%**	**98**	**105%**
STDEV	**22**	**26**	**51%**	**38**	**43%**

Table 6.6 (B). LDH activities in mastitis milk samples stored under different conditions

Sample No.	LDH(U/L) @ time 8h	LDH (U/L) @ 32h (stored at 4°C)	LDH % difference from 8 h to 32 h (stored at 4°C)	LDH (U/L) @ 32 h (stored at -20°C)	LDH % difference from 8 h to 32 h (stored at -20°C)
260 BL	115	177	54%	252	119%
319 BR	8436	7961	-6%	9557	13%
319 BL	242	550	128%	1086	350%
380 FR	164	242	47%	296	81%
380 FL	182	366	101%	420	131%
380 BR	493	1465	197%	1748	255%
380 BL	1475	5160	250%	8828	499%
Mean	**1586**	**2274**	**110%**	**3169**	**206%**
STDEV	**3057**	**3067**	**89%**	**4153**	**170%**

6.3 Discussion

In this chapter, the determination of LDH levels in milk samples was described. In particular, the investigation of the correlation of LDH with other mastitis-associated biomarkers and the identification of healthy and mastitic samples using a previously reported LDH 'cut-off' level was discussed. In addition, studies on the effect of using composite milk samples for mastitis diagnosis and the effects of storage conditions on LDH levels are also described.

Using a reliable and reproducible fluorescence-based assay, LDH levels from a total of 295 milks samples were calculated, as detailed in section 2.3.4.3 (Table 6.2). Changes in SCC, LDH and NAGase were observed at different lactation stages. A rise of polymorphonuclear leukocytes in normal milk has been reported in late lactation resulting in a SCC increase in milk samples taken at this stage (Blackburn, 1966). An increase in SCC concentrations at the late lactation stage when compared to the early lactation stage was also observed in this study. There are conflicting reports in relation to NAGase concentrations at different stages of lactation. Chagunda *et al.* (2006) reported that in healthy cows, NAGase concentrations were higher in the early lactation stage and the concentrations decreased at the mid-lactation stage whereas, Lehtolainen *et al.* (2003) reported that NAGase concentrations were lower in the early rather than later stages of lactation. In this study milk samples in the early lactation stage showed higher concentrations of both LDH and NAGase activity than samples from the mid-late and late lactation stages (Fig. 6.6). However, the SCCs were lower at early lactation stage when compared to late lactation stages. It has been suggested by Erdem *et al.* (2010) that elevated SCC at the late stage of lactation can be explained by the increase in injured udder cells towards the end of the lactation.

Current assays for the detection of mastitis in milk usually involve the determination of SCC, however, NAGase is also used as an indicator for mastitis ((Malmqvist *et al.,* 1991; Lehtolainen *et al.,* 1998). The correlation of LDH with SCC and NAGase would indicate that LDH can be used as a marker for mastitis detection. Kitchen *et al.* (1980) and Zank and Schlatterer (1998) reported a correlation between LDH and SCC of 0.53 and 0.57, respectively (Lehtolainen *et al.,* 1998) (Malmqvist *et al.,* 1991). The

correlation of 0.70 observed in this study is higher than in these reports. Kitchen *et al.* (1980) and Zank and Schlatterer (1998) showed a correlation between LDH and NAGase of 0.76 and 0.74, respectively. This is lower to the correlation of 0.86 (Table 6.3) observed in this study. This result is not surprising as LDH and NAGase are released at the same time upon the destruction of the epithelial cells in the udder during mastitis infection (Dohoo and Leslie, 1991). The good correlation between LDH and NAGase indicates that LDH may also be a suitable marker for mastitis detection.

Babaei and co-workers (2007) reported that the activities of LDH and alkaline phosphatase (ALP) in milk significantly increase in cases of mastitis in cows (Place and Power, 1984). This was also recently studied by Katsolous and co-workers (2009), who reported that LDH was a more reliable indicator for mastitis in sheep and goats than ALP and aspartate aminotransferase (Pyorala, 2003). Time-series measurements of LDH levels in milk were made by Friggens and co-workers (Friggens *et al.,* 2007). LDH analysis was found to be able to demonstrate significant differences between healthy and mastitic cows. The time-series measurements of LDH levels in milk could also identify mastitic milk samples at early stage in the disease.

A LDH 'cut-off' level of 197 U/L for both sheep and goats was reported by Katsoulos *et al.* (2009), however, few 'cut-off' levels of LDH for the determination mastitic and non-mastitic samples for cows are reported. The LDH 'cut-off' level for mastitis of 107.2 U/L, selected for use in this report was originally determined by Dohoe and Leslie (Dohoe and Leslie, 1991). This 'cut-off' level was similar to that of 127±29.6 U/L reported by Babaei *et al*. (2007). They also reported LDH 'cut-off' levels for different grades of subclinical mastitis milk, i.e. 222.0±34.67 U/L for grade 1, 943.5±105.3 U/L for grade 2 and 1,098.5±107.1 U/L for grade 3. The determination of LDH levels has, therefore, the potential to discriminate between subclinical and clinical mastitis as well as different levels of sub-clinical mastitis infection.

Previous studies have shown that the ability of a mastitic marker to evaluate udder status is diminished when composite samples are used (Bansal *et al.*, 2005; Nielsen *et al.*, 2005; Forsbäck *et al.*, 2010). This is consistent with the observations in this study

where in five cases both LDH and NAGase concentrations were above the 'cut-off' point for mastitis in one quarter but the composite sample was below the 'cut-off' (Fig. 6.5).

The kinetic properties of LDH, like most proteins, are affected by environmental temperature. The environmental temperature may weaken the hydrogen bonds or hydrophobic bonds within the protein molecule, hence altering the protein's structure and subsequently affecting the activities of the protein. It was reported by Stillman and Somero (2001) that LDH activities from claw muscle tissue of porcelain crabs decreased by 50% in 10 minutes at a temperature range of 65^{o}C to 75^{o}C (Stillman and Somero, 2001). LDH activity in human plasma is stable for four to six weeks at -90^{o}C (Shain *et al.*, 1983). Few LDH stability studies in milk are reported. However, the activity of LDH purified from *Ralstonia eutropha* was stable for 3 months when stored at -20^{o}C and stable for six months when stored at 4^{o}C in 0.2-1M potassium chloride and 3.2 M ammonium sulfate (Steinbuechel and Schlegel, 1983). Similarly, the activity of LDH purified from *Fundulus heteroclitus* is stable at 4^{o}C for more than 8 months when stored in ammonium sulfate (Stillman and Somero, 2001). These reports show that when purified using affinity chromatography and stored in elution buffer without addition of protein stabilisers, LDH activity remains stable at both 4^{o}C and -20^{o}C which is contrary to what was observed in this study. In this study, however, the LDH was not purified and the LDH activity was measured in a complex milk matrix, where other factors such as cell lysis and proteolysis could affect LDH activity. Joyce and co-workers (1992) reported cell lysis in milk samples after freeze-thaw cycles. Cell lysis can release more LDH from the cells resulting in increased LDH activity (Viguier *et al.*, 2009). Freezing of the samples may be used as a storage method for milk but when the milk is thawed cell lysis can occur and, for this reason, freezing is not considered a good storage method. Proteolytic activity also naturally exists in raw milk which results in milk protein degradation and, thus, could also reduce LDH activity levels in milk. Larsen and co-workers (2004) showed that proteases digest protein in milk from cows infected with *Streptococcus uberis.* It was also reported by Larsen *et al*. (2004) that the level of degradation of milk proteins increased in milk with a high somatic cell count (Zank and Schlatterer, 1998). LDH activities in both healthy and mastitic samples were

significantly affected by storage at 4^{o}C following sampling. This observation has indicated that the measurement of LDH levels in milk samples should be performed immediately after sampling to avoid cell lysis and proteolysis.

The correlation between LDH and NAGase suggests LDH may be used as an indicator to detect bovine mastitis (Fig. 6.4). However, for efficient and effective use of LDH as a mastitis biomarker, LDH determinations should only be made on samples properly stored with due consideration given to lactation stage. Various samplings/storage conditions were shown to effect LDH levels and hence they must be considered when using LDH as an effective sub-clinical mastitis biomarker.

Chapter 7
Overall conclusions

7.1 Overall conclusions

Cardiovascular diseases (CVDs) are the number one cause of death globally. The World Health Organization estimated approximately 23.6 million people will die from CVDs by 2030. The impact of the use of classic CVD biomarkers such as creatine kinase (CK) and lactate dehydrogenase (LDH) has been limited due to lack of tissue specificity and sensitivity. Troponin, due to the presence of tissue-specific isoforms in cardiac muscle, was recommended as a biomarker for the diagnosis of the acute myocardial infarction (AMI) by the European Society of Cardiology and the American College of Cardiology in 2000. Troponin I, T and C make up a 3-unit troponin complex located on the actin filaments, which control muscle contraction by regulating calcium binding. Troponin T has two isoforms that are specific for cardiac and skeletal muscle, respectively (O'Brien, 2008). The cardiac isoform has a longer N-terminal and is 20% more helical than its skeletal isoform. Since cTnT has a distinctive structure compare to sTnT, it was selected as a 'gold-standard' biomarker for diagnosis of cardiovascular disease.

Bioanalytical tools that use antibodies in various immunoassay formats have a major impact on disease diagnosis. The current commercially available troponin T immunoassay involves using Fab fragments from two monoclonal antibodies. However, this cTnT assay was reported to have failed to meet recommended AMI analysis standards. Hence, one objective of this work was to produce anti-cTnT recombinant antibodies fragments (scFv and Fab) for the generation of an improved cTnT immunoassay.

The work in chapter three described the construction of avian anti-cTnT scFv antibodies. Using chicken as the host for immunisation can bring a number of advantages, as described in Chapter 3.1. One important advantage is that chickens are phylogenetically more distant to humans than other animal species, commonly used for immunisations.

Thus, the avian system can produce better immune responses to mammalian proteins. The chicken serum had a titre in excess of 1 in 10,000 after the 4th immunisation, which indicated a sufficient serum polyclonal response against cTnT.

A simple 'on-plate' screening method was used to select cTnT-specific scFv antibodies. It was shown that this method could analyse the specificity of the clones in antigen-coated ELISA plate wells, yielding high binding signals and also saving valuable selection time. In addition, this method eliminated the requirement for an antibody extraction process (Guo *et al.,* 2010). Further inhibition studies were performed using crude bacterial lysates extracted from a number of positive scFv clones. The F1 clone had the lowest IC_{50} value of 214 ng/mL. However, since non-specific proteins in crude bacterial lysates may interfere with performance studies, the F1 antibody was subsequently purified using immobilised metal affinity chromatography (IMAC).

An SPR kinetic study was performed to monitor the 'real-time' interaction between F1 antibodies and cTnT protein, thus determining its affinity for cTnT. Using an amine coupling approach, sufficient anti-HA antibodies (7,120 RU) was immobilised on the CM5 sensorchip surface. Kinetic analysis indicated that the F1 antibody had an affinity (K_D) of 2.40 nM. However, the experimental kinetic curves from F1 poorly overlaid the binding model curves, thus questioning the reliability of the kinetic results. An inhibition assay was subsequently developed to obtain reliable data for the determination of the antigen binding capacity of F1 antibody. It was revealed that the IMAC-purified F1 had an IC_{50} value of 85 ng/mL.

In chapter 4, the use of chain-shuffling to improve the antigen-binding capacity of anti-cTnT scFv antibodies was described. Both the heavy and light chain-shuffled

libraries were constructed and cTnT-specific clones were identified using biopanning and the 'on-plate' screening method. Interestingly, the chain-shuffled libraries had an increased number of positive cTnT-binding clones, being 66.7% for heavy chain-shuffled clones and 75% for the light chain-shuffled clones, in comparison to the wild-type clones (56.3%). This demonstrated that chain shuffling could enhance the generation of antibodies.

SPR-based Biacore^{TM} 4000 ranking of a total of 384 heavy and light chain-shuffled antibodies showed the clones had a wide stability range (7.2% to 76%). In further kinetic studies, four scFv antibodies (8C2, 7D6, 7D8 and 7H8) was found to have subnanomolar affinities. Importantly, cross reactivity studies demonstrated all four clones showed high specificity to cTnT with no significant cross reactivity to other troponin isoforms (sTnT, cTnI and sTnI). Furthermore, no significant variations were observed in the affinities of the four scFv clones over three different temperatures (20, 25 and 30^{o}C). Hence, temperature changes did not appear to affect the antigen-binding capacities of these anti-cTnT scFvs, indicating good stability.

Although all four clones (8C2, 7D6, 7D8 and 7H8) showed subnanomolar affinities, the 8C2 clone showed closer fitting with the theoretical binding curves (1:1 Langmuir binding model) than the other three clones on Biacore^{TM} kinetic analysis. The 8C2 clone was subsequently purified using immobilised metal affinity chromatography (IMAC). An ELISA inhibition assay demonstrated that the 8C2 scFv had an IC_{50} concentration of 38 ng/mL, which showed an improvement of approximately 2.2 fold compared to the wild-type F1 (85 ng/mL). In addition, the mutant scFv, 8C2 had a K_D value of 0.39 nM, which indicated an improvement of approximately 6 fold compared to the wild-type F1 (2.40 nM). These results indicated that chain shuffling was successfully applied to produce an affinity enhanced anti-cTnT scFv.

Chapter 5 described the production of avian anti-cTnT Fab antibodies. Fab fragments potentially have a number of distinctive advantages over scFv antibodies. An avian anti-cTnT Fab library was constructed and cTnT-specific Fab clones were selected using both biopanning and the 'on-plate' screening method. The number of positive Fab clones (25%) was significantly lower than the number of scFvs (56.3%) generated. The more complex expression process for Fab antibody fragments in *E.coli* cells, compared to scFvs, may lead to a lower displaying efficiency for display.

ELISA analysis of eight positive anti-cTnT Fab clones showed that the clones had low antibody expression levels. A number of parameters, including growth media, IPTG induction concentration and period of induction, were optimised in order to improve the expression levels. Using TB as the cell cultivation medium, Fab antibody A1 showed maximum expression level after 2 hours induction with 0.05 mM IPTG. Clone C5 had maximum expression after 6 hours induction with 0.5 mM IPTG. With clone D3, the highest expression occurred after a period of 6 hours induction with 0.5 mM IPTG. Future work on the anti-cTnT Fab antibodies involved the charactersiation of the successfully expressed Fab antibodies using SPR-based kinetic studies and, ELISA inhibition analysis. Ultimately the Fab antibodies will be paired with the scFv 8C2 antibody for the development of a sensitive cTnT immunoassay.

The work in chapter 6 involved an investigation of the use of LDH as an indicator for mastitis. To investigate the effectiveness of LDH as a biomarker for sub-clinical mastitis detection, the correlations between the concentrations of LDH, NAGase and SCC in milk samples were examined. The effect of lactation stage, storage conditions and choice of milk samples on LDH levels were also examined.

LDH activities were measured in 295 milk samples collected from each udder quarter of 80 cows using a standardised fluorescence assay. Milk samples were subsequently indentified as either healthy or mastitic using a LDH 'cut-off' level of 107.2 U/L (Dohoe and Leslie, 1991). Studies also demonstrated that the correlation between LDH and NAGase levels was better (0.86) than between LDH and somatic cell count (SCC; 0.7).

Lactation stages were found to affect SCC, LDH and NAGase levels. Milk samples in the early lactation stage showed higher concentrations of both LDH and NAGase than samples from the mid-late and late lactation stages. In contrast, the SCC levels were lower at early lactation stages when compared to late lactation stages. Studies of 100 milk samples from 20 cows showed that the SCC and LDH levels in a number of milk samples from individual udder quarters were above the 'cut-off' level for mastitis. However, their concentrations in the composite sample were below the 'cut-off' level. Therefore, the use of composite milk samples for the identification of mastitis could be problematic.

LDH activities in both healthy and mastitic samples were significantly affected by different storage conditions. The LDH activity levels of both healthy and mastitic samples after storage at -20^{o}C were higher than those stored at 4^{o}C, indicating that 4^{o}C is a better storage temperature for LDH in milk samples. Therefore, the lactation stage of cows and milk storage conditions must be considered when choosing to use LDH as a marker to ensure efficient diagnosis of mastitis.

Chapter 8
Bibliography

Abbas, A.K. and Lichtman, A.H. (2003). Cellular and Molecular Immunology, 5th edition. W.B. Saunders Co., Philadelphia, USA.

Abdel-Rady, A. and Sayed, M. (2009). Epidemiological Studies on Subclinical Mastitis in Dairy cows in Assiut Governorate. Vet. World., **2**(10):373-380.

Alberts, B., Johnson, A. and Lewis, J. (2002). Molecular Biology of the Cell. 4th edition. New York: Garland Science.

Allender, S., Scarborough, P., Peto, V., Raynor, M., Leal, J., Luengo-Fernández, R. and Gray, A. (2008). European Cardiovascular Disease Statistics, European Heart Network.

Anderson, P.A.W., Malouf, N.N., Oakeley, A.E., Pagani, E.D. and Allen, P.D. (1991). Troponin T isoform expression in humans: a comparison among normal and failing adult heart, fetal heart, and adult and fetal skeletal muscle. Circulation, **69**:1226-1233.

Andris-Widhopf, J., Rader, C., Steinberger, P., Fuller, R. and Barbas. 3rd, C. F., 2000. Methods for the generation of chicken monoclonal antibody fragments by phage display. J. Immunol. Methods., **242**:159-181.

Armbruster, D.A. and Pry, T. (2008). Limit of Blank, Limit of Detection and Limit of Quantitation. Clin. Biochem. Rev., Supplement (i): S49-S52.

Armbruster, D.A., Tillman, M.D. and Hubbs, L.M. (1994). Limit of detection (LOD)/limit of quantitation (LOQ): comparison of the empirical and the statistical methods exemplified with GC-MS assays of abused drugs. Clin Chem., **40**: 1233-1238.

Azaman, S.N.A., Ramanan, R.N., Tan, J.S., Rahim, R.A., Abdullah, M.P. and Ariff, A.B. (2010). Screening for the optimal induction parameters for periplasmic producing interferon-α2b in *Escherichia coli.* Afr. J. Biotechnol., **9**(38):6345-6354.

Babaei, H., Mansouri-Najand, L., Molaei, M.M., Kheradmand, A. and Sharifan, M. (2007). Assessment of lactate dehydrogenase, alkaline phosphatase and aspartate aminotransferase activities in cow's milk as an indicator of subclinical mastitis. Vet. Res. Commun., **31**:419-425.

Babuin, L. and Jaffe, A.S. (2005). Troponin: The biomarker of choice for the detection of cardiac injury, C. M. A. J., **173**:1191-1202.

Bacher, J.M., Reiss, B.d. and Ellington, A.D. (2002). Anticipatory evolution and DNA shuffling. Genome. Biol., **3**(8):1021.1-1021.4.

Bansal, B.K., Hamann, J., Grabowskit, N.T. and Singh, K. (2005). Variation in the composition of selected milk fraction samples from healthy and mastitic quarters, and its significance for mastitis diagnosis. J. Dairy. Res., **72**:144-152.

Bakuev, M.M., Ulumbekov, E.G. and Chelyshev, Yu. A. (1972). Interdependence of subunits in lactate dehydrogenase tetramers (results of a quantitative histochemical investigation). Bull. Exp. Biol. Med., **74** (2):896-898.

Barbas. 3rd, C. F., Burton, D. R., Scott, J. K. and Silverman, G. J. (2001). Analysis of antibody fragment-expressing clones in ELISA, In Phage Display (Protocol 11.3), A laboratory Manual, Cold Spring Harbor Laboratory Press, Cold Spring Harbor, New York.

Barbas. 3rd, C. F., Crowe. Jr, J. E., Cababa, D., Jones, T. M., Zebedeei, S. L., Murphy, B. R., Chanockt, R. M. and Burton, D. R. (1992). Human monoclonal Fab fragments derived from a combinatorial library bind to respiratory syncytial virus F glycoprotein and neutralize infectivity. Med. Sci., **89**:10164 -10168.

Berry, D. P. and Amer, P. (2005). Derivation of a health sub-index for the Economic Breeding Index in Ireland. Technical report to the Irish Cattle Breeding Federation.

Bhattacharya, S.K and Dubey, A.K. (1997). Effect of dissolved oxygen and oxygen mass transfer on overexpression of target gene in recombinant *E. coli*. Enzyme Microb. Technol., **20**:355-360.

BIAtechnology handbook. (1998). Pharmacia Biosensor AB, Uppsala, Sweden.

Bird, R.E. and Walker, B.W. (1991). Single chain variable regions. Trends. Biotech., **9**:132-137.

Bradbury, A.R. and Marks, J.D. (2004). Antibodies from phage antibody libraries. J. Immunol. Methods., **290**:29-49.

Bradley, A. J., and M. J. Green. (2001a). The aetiology of clinical mastitis in a cohort of Somerset dairy herds. Vet. Rec., **148**:683-686.

Bravo, D.T., Harris, D.O. and Parsons, S.M. (2004). Reliable, sensitive, rapid and quantitative enzyme-based assay for gamma-hydroxybutyric acid (GHB). J. Forensic. Sci., **49(2)**:379-87.

Bryan, P.N. (2000). Protein engineering of subtilisin. Biochim. Biophys. Acta., **1543**(2):203-222.

Bunk, D.M. and Welch, M.J. (2006). Characterization of a new certified reference material for human cardiac troponin I. Clin. Chem., **52**:212–219.

Burlina, A., Zaninotto, M., Secchiero, S., Rubin, D. and Accorsi, F. (1994). Troponin T as a marker of ischemic myocardial injury. Clin. Biochem., **27**:113-121.

Cadwell, R.C. and Joyce, G.F. (1994). Mutagenic PCR. Genome. Res.,**3**: S136-S140.

Cai, X., Garen, A. (1997) Comparison of fusion phage libraries displaying VH or single-chain Fv antibody fragments derived from the antibody repertoire of a vaccinated melanoma patient as a source of melanoma-specific targeting molecules. Proc. Natl. Acad. Sci., **94**:9261-9266.

Carmen, S. and Jermutus, L. (2002).Concepts in antibody phage display. Brief. Funct. Genomic. Proteomic., **1**(2): 189-120.

Carter, P. (1986). Site-directed mutagenesis. Biochem. J. **237**: 1-7.

Chagunda, M.G.G., Friggens, N.C., Rasmussen, M.D. and Larsen, T. (2006). A model for detection of individual cow mastitis based on an indicator measured in milk. J. Dairy. Sci., **89**:2980-2998.

Chagunda, M.G.G., Larsen, T., Bjerring, M. and Ingvartsen, K.L. (2006). L-lactate dehydrogenase and N-acetyl-b-D-glucosaminidase activities in bovine milk as indicators of non-specific mastitis. J. Dairy. Res., **73**:431-440.

Chang,C., Takayanagi, A., Yoshida, T. and Shimizu, N. (2011). Screening of scFv-displaying phages recognizing distinct extracellular domains of EGF receptor by target-guided proximity labeling method. J. Immunol. Methods., **372**:127-136.

Chen, K., Robinson, A., Van Dam, M., Martínez, P., Economou, C. and Arnold.H. (1991). Enzymatic engineering for nonaqueous solvents II. Additive effects of mutation on the stabilization and activity of subtilisin E in polar organic media. Biotechnology Progress, **7**:125-129.

Christ-Crain, M and Opal, S.M. (2010). Clinical review: The role of biomarkers in the diagnosis and management of community-acquired pneumonia. Crit. Care., **14**: 203-213.

Chu, W.W., Dieter, R.S. and Stone, C.K. (2002). A review of clinically relevant cardiac biochemical markers. Wisc. Med. J., **101**:40-48.

Cohn, W.E. and Moldave, K. (1993). Immunoglobulin gene diversification. Prog. Nucleic. Acid. Res. Mol. Biol., 27-44.

Conroy, P.J., Hearty, S., Leonard, P. and O'Kennedy, R.J. (2009). Antibody production, design and use for biosensor-based applications. Semin. Cell. Dev. Biol., **20**(1):10-26.

Cooper, M.A. (2006). Optical biosensors: where next and how soon?. Drug. Discov. Today.

Costanzo, M., Baryshnikova, A., Bellay, J., Kim, Y., Spear, E.D., Sevier, C.S., Ding, H., Koh, J.L., Toufighi, K., Mostafavi, S., Prinz, J., St. Onge, R.P., VanderSluis, B., Makhnevych, T., Vizeacoumar, F.J., Alizadeh, S., Bahr, S., Brost, R.L., Chen,

Y., Cokol, M., Deshpande, R., Li, Z., Lin, Z.Y., Liang, W., Marback, M., Paw, J., San Luis, B.J., Shuteriqi, E., Tong, A.H., van Dyk, N., Wallace, I.M., Whitney, J.A., Weirauch, M.T., Zhong, G., Zhu, H., Houry, W.A., Brudno, M., Ragibizadeh, S., Papp, B., Pál, C., Roth, F.P., Giaever, G., Nislow, C., Troyanskaya, O.G., Bussey, H., Bader, G.D., Gingras, A.C., Morris, Q.D., Kim, P.M., Kaiser, C.A., Myers, C.L., Andrews, B.J. and Boone, C. (2010). The genetic landscape of a cell. Science, **327**(5964):425-431.

Crescenzo, G.D., Woodward, L. and Srinivasan, B.(2008). Online optimization of surface plasmon resonance-based biosensor experiments for improved throughput and confidence. J. Mol. Recognit., **21**(4) :256-266.

Daniels, L. B. (2009). Multiple biomarker assessment in primary prevention of cardiovascular disease. Curr. Cardiov. Risk. Rep., **3**:131–136.

Davies, M.J. (2005). Post-prandial hyperglycaemia and prevention of cardiovascular disease. Diabetic. Med., **22**:6-9

Dhoot, G.K., Grearson, N. and Perry, S.V. (1979). Polymorphic forms of troponin T and troponin C and their localization in striated muscle cell types. Exp. Cell. Res., **122**:339-50.

Dohoo, I.R. and Leslie, K.E. (1991). Evaluation of changes in somatic cell counts as indicators of new intramammary infections. Prev. Vet. Med., **10**:225-237.

Donovan, R.S., Robinson, C.W. and Glick, B.R. (2000). Optimizing the expression of a monoclonal antibody fragment under the transcriptional control of the *Escherichia coli lac* promoter. Can. J. Microbiol., **46**(6):532-541.

Drent, M., Cobben, N.A.M., Henderson, R.F., Wouters, E.F.M. and Dieijen-Visser, M.V. (1996). Usefulness of lactate dehydrogenase and its isoenzymes as indicators of lung damage or inflammation. Eur. Respir. J., **9**:1736 -1742.

Drescher, D.G., Ramakrishana, N.A. and Drescher, M.J. (2009). Surface Plasmon resonance (SPR) analysis of binding interactions of proteins in inner-ear sensory epithelia. Methods. Mol. Biol., 493:323-343.

Ebashi, S. and Endo, M. (1968). Calcium ion and muscle contraction. Prog. Biophys. Molec. Biol., **18**:123-183.

Eijsink, V.J.H, Gaseidnes, S., Borchert, T.V. and Burg, B. (2005). Directed evolution of enzyme stability. Biomol. Eng., **22**:21-30.

Erskine, R. J., R. J. Eberhart, L. J. Hutchinson, S. B. Spencer, and M. A. Campbell. (1988). Incidence and types of clinical mastitis in dairy herds with high and low somatic cell counts. J. Am. Vet. Med. Assoc. **192**:761-769.

Esslemont, R. J. and Kossaibati, M. A. (1997) Culling in 50 dairy herds in England. Veterinary Record, 140: 36-39.

Filatov, V.L., Katrukha, A.G., Bulargina, T.V., and Gusev, N.B. (1999). Troponin: Structure, properties, and mechanism of functioning. Biochem., **64**:969-985.

Finlay, W.J.J., Shaw, I., Reilly, J.P. and Kane, M. (2006). Generation of high-affinity chicken single-chain Fv antibody fragments for measurement of the Pseudonitzschia pungens toxin domoic acid. Appl. Environ. Microbiol., **72**:3343-3349.

Fitzgerald J, Leonard P, Darcy E, Danaher M, O'Kennedy R. (2011). Light-chain shuffling from an antigen-biased phage pool allows 185-fold improvement of an anti-halofuginone single-chain variable fragment. Anal. Biochem., **410**(1):27-33.

Flicker, P.F., Phillips, G.N.Jr. and Cohen, C. (1982). Troponin and its interactions with tropomyosin: an electron microscope study. J. Mol. Biol., **162**:495-501.

Forsback, L., Lindmark-Månsson, H., Svennersten-Sjaunja, K., Bach Larsen. L. and Andrén, A. (2011). Effect of storage and separation of milk at udder quarter level on milk composition, proteolysis, and coagulation properties in relation to somatic cell count. J. Diary. Sci. **94**(11):5341-5349.

Fosmire, G.J. and Timasheff, S.N. (1972). Molecular weight of beef heart lactate dehydrogenase. Biochem., **11**:2455-2460.

Fox, P.F. and Kelly, A.L. (2006). Indigenous enzymes in milk: Overview and historical aspects—Part 2. Int. Dairy. J., **16**(6):517-532.

Frank, R. and Hargreaves, R. (2003). Clinical biomarkers in drug discovery and development**.** Nat. Rev. Drug. Discov., **2**(7): 566- 580.

Freund, C., Rossa, A., Guthb, B., Pliickthunb, A and Tad A. (1993). Characterization of the linker peptide of the single-chain F, fragment of an antibody by NMR spectroscopy. Eur. J. Biochem., **320**(2), 97-100.

Freyre, F.M., Vazquez, J.E., Ayala, M., Canaan-Haden, L., Bell, H. and Rodriguez, I. (2000). Very high expression of an anti-carcinoembryonic antigen single chain Fv antibody fragment in the yeast Pichia pastoris. J. Biotechnol., **6**:157-163.

Friggens, N.C., Chagunda, M.G., Bjerring, M., Ridder. C., Hojsgaard, S. and Larsen, T. (2007). Estimating Degree of Mastitis from Time-Series Measurements in Milk: A Test of a Model Based on Lactate Dehydrogenase Measurements. J. Dairy. Sci., **90** (12):5415-5427.

Full, L.E., Ruisanchez, C. and Monaco, C. (2009). The inextricable link between atherosclerosis and prototypical inflammatory diseases rheumatoid arthritis and systemic lupus erythematosus. Arthritis. Res. Ther., **11**:217-223.

Gabrielli, E., Pericolini, E., Cenci, E., Ortelli, F., Magliani. W., Ciociola, T., Bistoni, F., Conti, S., Vecchiarelli, A. and Polonelli, L. (2009) Antibody complementarity-determing regions (CDRs): a bridge between adaptive and innate immunity. PLoS One **4**(12):e8187.

Gaskin, D.J.H., Starck, K., Turner, N.A. and Vulfson, E.N. (2001). Phage display combinatorial libraries of short peptides: ligand selection for protein purification, Enzyme. Microb. Tech., **28**(9-10):766-772.

Galvani, M., Ferrini, D., Ghezzi, F. and Ottani, F. (2001). Cardiac markers and risk stratification: an integrated approach. Clinica. Chimica. Acta., **311**(1):9-17.

Gaziano, T.A. (2005). Cardiovascular Disease in the Developing World and Its Cost-Effective Management, Circulation, **112**:3547-3553.

Giannitsis, E. and Katus, H. A. (2010). Current Recommendations for Interpretation of the Highly Sensitive Troponin T Assay for Diagnostic, Therapeutic and Prognostic Purposes in Patients with a Non-ST-segment-elevation Acute Coronary Syndrome. Eur. Heart. J., **5**(2):44-47.

Goldstein, B., Coombs, D., He, X., Pineda, A.R. and Wofsy, C. (1999). The influence of transport on the kinetics of binding to surface receptors: application to cells and BIAcore. J. Mol. Recognit., **12**:293-299.

Gonzalo, C., Martínez, J.R., Carriedo, J.A., San Primitivo, F. (2003). Fossomatic Cell-Counting on Ewe Milk: Comparison with Direct Microscopy and Study of Variation Factors. J. Dairy Sci., **86**(1):138-145.

Goodenough, P.W. (1995). A review of protein engineering for the food industry. Int. J. Food. Sci. Tech., **30**(2):119-139.

Gopinath, S.C.B. (2010). Biosensing applications of surface plasmon resonance-based Biacore technology. Sensor. Actuat. B-Chem., **150**: 722-733.

Graumann, K. and Premstaller, A, (2006). Manufacturing of recombinant therapeutic proteins in microbial systems. Biotechnol. J., **1**:164-186.

Greaser, M.L., Yamaguchi, M., Brekke, C., Potter, J., and Gergely, J. (1972). Cold Spring Harbor Symp. Quant. Biol., **37**:235-244.

Gomes, P. and Andreu, D. (2002). Direct kinetic assay of interactions between small peptides and immobilized antibodies using a surface plasmon resonance biosensor. J. Immunol. Methods., **259**: 217-230.

Gronwall, C. and Stahl, S. (2009). Engineered affinity proteins--generation and applications. J. Biotechnol., **140**: 254-269.

Grossman, T., L. Frost, and P. Silverman. (1990). Structure and function of conjugative pili: monoclonal antibodies as probes for structural variants of F pili. J. Bacteriol., **172:**1174-1179.

Gruber, K., Klintschar, G., Hayn, M., Schlacher, A., Steiner, W. and Kratky, C. (1998). Thermophilic xylanase from Thermomyces lanuginosus: High resolution X-ray structure and modeling studies. Biochem., **37**: 13475-13485.

Grundy, S.M. (2004). Obesity, Metabolic Syndrome, and Cardiovascular Disease. J. Clin. Endocrinol. Metab, **89**(6): 2595-2600.

Guilbault, G.G. (1975). Fluorometric determination of dehydrogenase activity using resorufin. Methods Enzymol., **41**:53-56.

Guo, W.L., Leonard, P., and O'Kennedy, R. (2010). Simple method of 'on-plate' growth for improved antibody screening. J. Immunol. Methods., **359**:61-64.

Gusev, N. B., Barskaya, N. V., Verin, A. D., Duzhenkova, I. V., Khuchua, Z. A. and Zheltova, A.O . (1983). Some properties of cardiac troponin T structure. Biochem. J., **213**:123-129.

Hallermayer. K., Klenner, D. and Vogel. R. (1999). Use of recombinant cardiac troponin T for standardization of third generation troponin T methods. Scand. J. Clin. Invest., **59**:128-131.

Harrison, D, G and Gongora, M.C. (2009) Oxidative stress and hypertension. Med. Clin. North. Am., **93** (3):621-35.

Hicks, G.P., Ziesemer, R.A. and Tietz, N.W. (1973). The use of laboratory computers in monitoring kinetic enzyme assays. Clin. Chem., **19**(1):27-30.

Hillerton, J.E. and Berry, E.A. (2005). Treating mastitis in the cow - a tradition or an archaism. J. Appl. Microbiol., **98**:1250-1255.

Hiss, S., Mueller, U., Neu-Zahren, A. and Sauerwein, H. (2007). Haptoglobin and lactate dehydrogenase measurements in milk for the identification of subclinically diseased udder quarters. Vet. Med., **52** (6):245-252.

Hochholzer, W., Morrow. D.A. and Giugliano, R.P. (2010) Novel biomarkers in cardiovascular disease: update 2010. Am. Heart. J., **160**:583-594.

Hof, D., Hoeke, M.O. and Raats, J.M. (2008). Multiple-antigen immunization of chickens facilitates the generation of recombinant antibodies to autoantigens. Clin. Exp. Immunol., **151**:367-377.

Hogeveen, H. (2005). Mastitis is an economic problem. Proceedings of the British Mastitis Conference, Stoneleigh, 1-13.

Hong, H.J. and Kim, S.T. (2002). Antibody Engineering. Biotechnol. Bioprocess Eng., **7**: 150-154.

HoraK. J. (1999). Cardiac Troponins in Acute Coronary Syndromes. The Blessing from Heave? Heart views. **1**:116-122.

Hudson, P. and Winter, G. (1991). Multi-subunit proteins on the surface of filamentous phage: methodologies for displaying antibody (Fab) heavy and light chains. Nucleic. Acid. Res., **19**:4133-4137.

Hudson, P.J. (1998). Recombinant antibody fragments. Curr. Opin. Biothchnol., **9**:395-402.

Hust, M. and Dubel, S. (2004). Mating antibody phage display with Proteomics. Trends. Biotech., **22**(1):8-14.

Huston, J.S., Fish, W.W., Mann, K.G. and Tanford, C. (1972). Studies on the subunit molecular weight of beef heart lactate dehydrogenase. Biochem., **11**:1609-1612.

Ignarro, L.J., Balestrieri, M.L. and Napoli, C. (2006). Nutrition, physical activity, and cardiovascular disease: An update. Cardiovasc. Res., **73:**326-334.

Inbar, R. and Shoenfeld, Y. (2009). Elevated cardiac troponins: the ultimate marker for myocardial necrosis, but not without a differential diagnosis. Isr. Med. Assoc. J., **11**(1):50-53.

Jacobs, E., Hissin, P.J., Propper, W., Mayer, L. and Sarkoz, L. (1986). Stability of lactate dehydrogenase at different storage temperatures. Clin. Biochem., **19**(3):3183-3188.

Jaffe, A.S., (2005). Use of biomarkers in the emergency department and chest pain unit. Cardiol. Clin., **23**:453-465.

Jaffe, A.S., Babuin, L. and Apple, F.S. (2006). Biomarkers in acute cardiac disease: the present and the future. J. Am. Coll. Cardiol., **48**:1-11.

Jamison, D.T., Breman, J.G., Measham, A.R., Alleyne, G., Claeson, M., Evans, D.B., Jha, P., Mills, A. and Musgrove. P. (2006). Disease Control Priorities in Developing Countries, 2nd edition. Washington (DC), World Bank.

Janeway, C.A., Travers, P. and Walport., M. (2001). Immunobiology: The Immune System in Health and Disease, 5th edition. New York: Garland Science.

Jin, J.P., Huang, Q.Q., Yeh, H.I., and Lin, J.J.C. (1992). Complete nucleotide sequence and structural organization of rat cardiac troponin T gene. J. Mol. Biol., **227**:1269-1276.

Joern, J.M. (2003). DNA shuffling, in Directed Evolution Library Creation. Totawa, NJ: Humana Press, 85-89.

Jordan, E., Hust, M., Roth, A., Biedendieck, R., Schirrmann, T., Jahn, D. and Dübel, S. (2007). Production of recombinant antibody fragments in Bacillus megaterium. Microb. Cell. Fact., **6:**2.

Joyce, P.J., O'Sullivan, C.A., Shattock, A.G. and Sloan, T.M. (1992). Immunodiagnostic assays for use in the detection and determination of mastitis. US Patent 5,168,044.

Karlsson, R., and Larsson, A. (2004). Affinity measurement using surface plasmon resonance. Methods. Mol. Biol., **248**:389–415.

Katona, E. E., Ajzner, E., Tóth, K., Kárpáti, L. and Muszbek, L. (2001). Enzyme-linked immunosorbent assay for the determination of blood coagulation factor XIII A-subunit in plasma and in cell lysates. J. Immunol. Methods., **258**(1-2):127-135.

Katsoulos, P.D., Christodoulopoulos, G., Minas, A., Karatzia, M.A., Pourliotis, K. and Kritas, S.K. (2009). The role of lactate dehydrogenase, alkaline phosphatase and aspartate aminotransferase in the diagnosis of subclinical intramammary infections in dairy sheep and goats. J. Dairy. Res., **18**:1-5.

Katus, H.A. (2008). Development of the Cardiac Troponin T Immunoassay. Clin. Chem., **54**(9):1576-1577.

Katus, H.A., Remppis, A., Neumann, F.J., Scheffold, T., Diederich, K.W., Vinar, G., Noe, A., Matern, G. and Kuebler, W. (1991). Diagnostic efficiency of troponin T measurements in acute myocardial infarction. Circulation, **83**:902-912.

Kay, B.K., Adey, N.B., He, Y.S., Manfredi, J.P., Mataragon, A.H., and Fowlkes, D.M. (1993). An M13 phage library displaying 38-amino-acid peptides as a source of novel sequences with affinity to selected targets. Gene, **128**:59-65.

Kay, B.K., and Hoess, R.H. (1996). Principles and Applications of Phage Display. Academic Press Inc., San Diego, CA.

Kemp, M., Donovan, J., Higham, H. and Hooper, J. (2004). Biochemical markers of myocardial injury. Br. J. Anaesth. **93**(1):63-67.

Kitchen, B.J., Middleton, G., Durward, I.G., Andrews, R.J. and Salmon, M.C., (1980). Mastitis diagnostic tests to estimate mammary gland epithelial cell damage. J. Dairy. Sci., **63**:978-983.

Koerbin, G., Tate, J.R. and Hickman. P.E. (2010). Analytical characteristics of the Roche highly sensitive troponin T assay and its application to a cardio-healthy population. Ann. Clin. Biochem., **47**:524-528.

Kramer, K., Fiedler, M., Skerra, A. and Hock, B. (2002). A generic strategy for subcloning antibody variable regions from the scFv phage display vector pCANTAB 5 E into pASK85 permits the economical production of Fab fragments and leads to improved recombinant immunoglobulin stability. Biosens. & Bioelectron.,**17**:305-313.

Kuang, Y., Tani, K., Synnott, A.J., Ohshima, K., Higuchi, H., Nagahata, H. and Tanji, Y. (2009). Characterization of bacterial population of raw milk from bovine mastitis by culture-independent PCR-DGGE method. Biochem. Eng. J., **45**:76-81.

Kumar, C.G. and Takagi, H. (1999). Microbial alkaline proteases: from a bioindustrial viewpoint. Biotechnol. Adv., **17:**561-594.

Larsen, L.B., Rassmussen, M.D., Bjerring, M. and Nielsen, J.H. (2004). Proteases and protein degradation in milk from cows infected with Streptococcus uberis. Int. Dairy. J., **14**:899-907.

Larsen, T. (2005). Determination of lactate dehydrogenase (LDH) activity in milk by a fluorometric assay. J. Dairy. Sci., **72**:209-216.

Lee, N., Holtzapple, C.K. and Stanker, L.H. (1998). Cloning, expression, and characterization of recombinant Fab antibodies against dioxin. J. Agric. Food. Chem., **46**:3381-3388.

Lehtolainen, L., Pohjanvirta, T., Pyörälä, S. and Pelkonen, S. (1998). Association between virulence factors and clinical course of *Escherichia coli* mastitis. Acta. Vet. Scand., **44**:203-205.

Leonard, P, Hearty, S. and O'Kennedy, R. (2011). Measuring Protein–Protein Interactions Using Biacore. Methods. Mol. Biol., **681**(2):403-418.

Leonard, P., Säfsten, P., Hearty, S., McDonnell, B., Finlay, W., O'Kennedy, R. (2007). High throughput ranking of recombinant avian scFv antibody fragments from crude lysates using the Biacore A100. J. Immunol. Methods., **323**:172-179.

Li, N., Qu, L-J., Liu, Y., Li. Q., Gu, H. and Chen, Z. (1999). The refolding, purification, and activity analysis of a rice Bowman-Birk inhibitor expressed in *Escherichia coli.* Protein Express. Pur., **15**:99-104.

Libby, P. (2006). Inflammation and cardiovascular disease mechanisms. Am. J. Clin. Nutr., **83**:456S-460S.

Liddell, J.M., (2009). Production strategies for antibody fragment therapeutics. BioPharm. International., 36-42.

Lim, W., Qushmaq, I., Cook, D. J., Crowther, M. A., Heels-Ansdell, D. and Devereaux, P. J. (2005). Elevated troponin and myocardial infarction in the intensive care unit: a prospective study. Crit. Care., **9**:636-644.

Liu, M., Wu, B., Wang, W.Z., Lee, L.M., Zhang, S.H., Kong, L.Z. (2007) Stroke in China: epidemiology, prevention, and management strategies. Lancet Neurol., **6**(5):456-464.

Lou, J., Geren, I., Garcia-Rodriguez, C., Forsyth, C. M., Wen, W., Knopp, K., Brown, J., Smith, T., Smith, L. A. and Marks, J. D. (2010). Affinity maturation of human botulinum neurotoxin antibodies by light chain shuffling via yeast mating. Protein. Eng. Des. Sel., **23**(4):311-319.

Lowe, G. D. (2001). The relationship between infection, inflammation, and cardiovascular disease: an overview. Ann. Periodontol., **6**(1):1-8.

Ma, J.K.C., Drake, P.M.W. and Christou, P. (2003). The production of recombinant pharmaceutical proteins in plants. Nat. Rev., **4**:704-805.

Madurawe, R.D., Chase, T.E., Tsao, E.I. and Bentley, W.E. (2000). A recombinant lipoprotein antigen against Lyme disease expressed in *E. coli*: fermentor operating strategies for improved yield. Biotechnol. Progress., **16**:571-576.

Magari, M., Sawatari, T., Kawano, Y., Cascalho, M., Wabl., M. and Kanayama, N. (2002). Contribution of light chain rearrangement in peripheral B cells to the generation of high-affinity antibodies. Eur. J. Immunol., **32**:957-966.

Mair, J. (1997). Progres in myocardial damage detection: new biochemical markers for clinicians. Crit. Rev. Clin. Lab. Sci., **34**:1-66.

Mair, J., Dienstl, F. and Puschendorf, B. (1992). Cardiac troponin T in the diagnosis of myocardial injury. Crit. Rev. Clin. Lab. Sci., **29**:31-35.

Manderson. D., Dempster. R. and Chisti, Y. (2006). A recombinant vaccine against hydatidosis: production of the antigen in *Escherichia coli*. J. Ind. Microbiol. Biotechnol., **33**: 173-182.

Makin, H.L.J. (2010). Immunoassay of Steroids. Steroid Analysis. 2nd edition, 283-372.

Malmqvist, U., Arner, A. and Uvelius, B. (1991). Lactate dehydrogenase activity and isoform distribution in normal and hypertrophic smooth muscle tissue from the rat. Pflug. Arch. Eur. J. Phy., **419**(3-4):230-234.

Markert, Y., Köditz, J., Mansfeld, J., Arnold, U. and Ulbrich-Hofmann, R. (2001) Increased proteolytic resistance of ribonuclease A by protein engineering. Protein. Eng., **14**(10): 791–796.

Marks, J.D., Hoogenboom, H.R., Griffiths, A.D. and Winter, G. (1992). Molecular evolution of proteins on filamentous phage. J. Biol. Chem., **267**:16007-16010.

Marques, S., Silva, E., Kraft, C., Carvalheira, J., Videira, A., Huss, V.A., Thompson, G. (2008). Bovine mastitis associated with Prototheca blaschkeae. J. Clin. Microbiol., **46**(6):1941-1945.

Mathieu, V., Fastrez, J. and Soumillion, P. (2010). Engineering allosteric regulation into the hinge region of a circularly permuted TEM-1 b-lactamase. Protein. Eng. Des. Sel., **23**(9):699-709.

McDonnell, B., Hearty, S., Leonard, P. and O'Kennedy, R. (2009). Cardiac biomarkers and the case for point-of-care testing. Clin. Biochem., **42**(7-8):549-561.

Miltenburg, J.D., deLange, D., Crauwels, A.P.P., Bongers, J.H., Tielen, M.J.M., Schukken, Y.H. and Elbers, A.R.W. (1996). Incidence of clinical mastitis in a random sample of dairy herds in the southern Netherlands. Vet. Rec. **139**: 204-207.

Mohkam, M., Zarkesh-Esfahani, S.H. and Fazeli, M. (2011). Construction of a Recombinant Fab Fragment of a Monoclonal Antibody against Leptin Receptor. Asian. J. Biotechnol., (5):493-506.

Morrow, D.A. (2006). Cardiovascular biomarkers: pathophysiology and disease management. Humana Press. Inc., Totowa, New Jersey.

Muller-Bardorff, M., Hallermayer, K., Schroder, A., Ebert, C., Borgya, A., Gerhardt, W., Remppis, A., Zehelein, J. and Katus, h. A. (1997). Improved troponin T ELISA specific for cardiac troponin T isoform: assay development and analytical and clinical validation. Clin. Chem., **43**:3 458-466.

Murray, C. J. and Lopez. A.D. (1996). Global Burden of Disease and Injury Series, Vols. I and II, Global Health Statistics. Boston: Harvard School of Public Health.

Murphy, S. C., Cranker, K., Senyk, G.F., Barbano, D.M., Saeman, A.I. and Galton, D.M. (1988). Influence of bovine mastitis on lipolysis and proteolysis in milk. J. Dairy Sci., **71**: 65-69.

Myszka, D.G. (2004). Analysis of small-molecule interactions using Biacore S51 technology. Anal. Biochem., **329**: 316-323.

Narat, M. (2003). Production of antibodies in chickens. Food. Tech. Biotech., **41**: 259-267.

Neal, B., Chapman, N. and Pate, A. (2002). Managing the global burden of cardiovascular disease. Eur. Heart. J. Suppl., **4**:F2-F6.

Nielsen, N. I., Larsen, T., Bjerring, M. and Ingvartsen, K. L. (2005). Quarter health, milking interval and sampling time during milking affect the concentration of milk constituents. J. Dairy Sci., **88**:3186-3200.

Nyyssönen, E., Penttila, M., Harkki, A., Saloheimo, A., Knowles, J.K., Keranen, S. (1993). Efficient production of antibody fragments by the filamentous fungus Trichoderma reesei. Biotechnol., **11**:591-595.

O'Brien, P.J. (2008) Cardiac troponin is the most effective translational safety biomarker for myocardial injury in cardiotoxicity. Toxicology, **245**:206-218.

Ohtsuki, I. (1979). Molecular arrangement of troponin T in thin filament. J. Biochem., **86**:491-497.

Ohtsuki, I. and Morimoto, S. (2008). Troponin: regulatory function and disorders. Biochem Biophys. Res. Commun., **369**:62-73.

Okamoto, T., Mukai, Y., Yoshioka, Y., Shibata, H., Kawamura, M., Yamamoto, Y., Nakagawa, S., Kamada, H., Hayakawa, T., Mayumi, T. and Tsutsumi, Y. (2004). Optimal construction of non-immune scFv phage display libraries from mouse bone marrow and spleen established to select specific scFvs efficiently binding to antigen, Biochem. Biophys. Res. Commun., **323**(2), 583-591.

Pan, B.S., and Potter, J.D. (1992). Two genetically expressed troponin T fragments representing alpha and beta isoforms exhibit functional differences. J. Biol. Chem., **267**:23052-23056.

Panteghini, M., Pagani, F. and Yeo., K.T.J. (2004). Evaluation of imprecision for cardiac troponin assays at low-range concentrations. Clin. Chem., **50**:327-332.

Park, S.G., Lee, J.S., Je, E.Y., Kim, I.J., Chung, J.H. and Choi, I.H. (2000). Affinity maturation of natural antibody using a chain shuffling technique and the expression of recombinant antibodies in *Escherichia coli*. Biochem. Biophys. Res. Commun., **275**:553-557.

Parmacek, M.S. and Solaro, R.J. (2004). Biology of the troponin complex in cardiac myocytes. Prog. Cardiovasc. Dis., **47**:159-176.

Paschke, M. (2006) Phage display systems and their applications. Appl. Microbiol. Biotechnol., **70**:2-11.

Pasupathi, P., Saravanan, G and Faroo, J. (2009). Oxidative Stress Bio Markers and Antioxidant Status in Cigarette Smokers Compared to Nonsmoker. J. Pharm. Sci. Res., **1**(2):55-62.

Pauly, D., Chacana, P.A., Calzado, E.G., Brembs, B. and Schade, R. (2011). IgY Technology: Extraction of Chicken Antibodies from Egg Yolk by Polyethylene Glycol (PEG) Precipitation. J. Vis. Exp., **51**:e3084.

Peeters, K. Wilde, C.D., Jaeger, G.D., Angenon, G. and Depicker, A. (2001). Production of antibodies and antibody fragments in plants. Vaccine, **19:**2756–2761.

Perry, S.V. (1998). Troponin T: genetics, properties and function. J. Muscle. Res. Cell. Motil., **19**:575-602.

Phillips, K.A., Bebber. S.V. and Issa. A.M. (2006). Diagnostics and biomarker development: priming the pipeline. Nat. Rev. Drug. Discov., **5**:463-469.

Place, A.R. and Powers, D.A. (1984). Purification and characterization of the lactate dehydrogenase (LDH-B4) allozymes of Fundulus heteroclitus. J. Biol. Chem., **259**:1299-1308.

Pluckthun, A. (1990). Antibodies from *Escherichia coli*. Nature, **347**:497-498.

Pluckthun, A. (1991). Antibody engineering: advances from the use of *Escherichia coli* expression systems. Biotechnol., **9**:545-551.

Poduslo, J.F., Gilles, E.J., Ramakrishnan, M., Howell, K.G. and Wengenack, T.M. (2010). HH Domain of Alzheimer's Disease Ab Provides Structural Basis for Neuronal Binding in PC12 and Mouse Cortical/Hippocampal Neurons. PLoS ONE, **5**(1):e8813.

Porrozzi, R., Teva, A., Amaral, V.F., Santos da Costa, M.V., Grimaldi, G. Jr. (2004). Cross-immunity experiments between different species or strains of *Leishmania* in rhesus macaques (*Macaca Mulatta*). Am. J. Trop. Med. Hyg., **71**: 297-305.

Porter, R. R. (1958). Separation and isolation of fractions of rabbit gamma-globulin containing the antibody and antigenic combining sites.Nature, **182**:670-671.

Preventing Chronic Diseases: A Vital Investment. (2005). World Health Organization Global Report.

Pyorala, S. (2003). Indicators of inflammation in the diagnosis of mastitis. Vet. Res., **34**: 565-578.

Quintero-Hernandez, V., Juarez-Gonzalez, V.R., Ortiz-Leon, M., Sanchez, R., Possani, L.D. and Becerril, B. (2007). The change of the scFv into the Fab format improves the stability and in vivo toxin neutralization capacity of recombinant antibodies. Mol. Immunol., **44**:1307-1315.

Radostits, O. M., Blood, D.C. and Gay, C.C. (1994). Veterinary Medicine. A textbook of disease of cattle, sheep, pig, goat and horses. W.B. Saunders Co., London.

Rahbarizadeh, F., Rasaee, M.J., Forouzandeh, M. and Allameh, A.A. (2006). Over expression of anti-MUC1 single-domain antibody fragments in the yeast Pichia pastoris. Mol. Immunol., **43**:426–435.

Reed, G.F., Lynn, F. and Meade, B.D. (2002). Use of coefficient of variation in assessing variability of quantitative assays. Clin. Diagn. Lab. Immunol., **9**:1235-1239.

Reddy, K.S. (2002). Cardiovascular diseases in the developing countries: dimensions, determinants, dynamics and directions for public health action. J. Public. Health. Nutr., **5**(1A): 231-237.

Reiter, Y., Brinkmann, U., Lee, B. and Pastan, I. (1996). Engineering antibody Fv fragments for cancer detection and therapy: disulfide-stabilized Fv fragments. Nat. Biotechnol., **14**:1239-1245.

Rich, R.L. and Myszka, D.G. (2000). Advances in surface plasmon resonance biosensor analysis. Curr. Opin. Biotechnol., **11**(1):54-61.

Rich, R.L. and Myszka, D.G. (2005). Survey of the year 2003 commercial optical biosensor literature. J. Mol. Recognit., **18**:1-39.

Rizzo, M., Kotur-Stevuljevic, J., Berneis, K., Spinas, G., Rini, G, B., Jelic-Ivanovic, Z., Spasojevic-Kalimanovska, V and Vekic, J. (2009). Atherogenic dyslipidemia and oxidative stress: a new look. Transl. Res., **153**(5):217-223.

Robbens, J., Raeymaekers, A., Steidler, L., Fiers, W. and Remaut, E. (1995). Production of soluble and active recombinant murine interleukin-2 in *Escherichia coli*: high level expression, kil-induced release, and purification. Protein. Express. Pur., **6**:481-486.

Rose, I.A., and Warms, J.V. (1987). A specific endpoint assay for ubiquitin. Proc. Natl. Acad. Sci., **84**, 1477-1481.

Rothlisberger, D., Honegger, A. and Pluckthun, A. (2005). Domain interactions in the Fab fragment: a comparative evaluation of the single-chain Fv and Fab format engineered with variable domains of different stability. J. Mol. Biol., **347**:773-789.

Rubingh, D.N., (1997). Protein engineering from a bioindustrial point of view. Curr. Opin. Biotechnol., **8**(4):417-422.

Sacks, F.M. and Katan, M. (2002). Randomized clinical trials on the effects of dietary fat and carbohydrate on plasma lipoproteins and cardiovascular disease. Am. J. Med., **113**(9):13-24.

Safsten, P., Klakamp, S.L., Drake, A.W., Karlsson, R. and Myszka, D.G. (2006). Screening antibody–antigen interactions in parallel using Biacore A100. Anal. Biochem., **353**:181-190.

Schalm, O.M. and Noorlander, B.S. (1957). Experiments and observations leading to the development of the California mastitis test. J. Amer. Vet. Med. Assoc., **130**:199-204.

Schüttel, M. (1999). Activities of N-acetyl-β-D-glycosamidase in milk, blood and urine of lactating cattle. Dissertation, Dr. Med. Vet. Tierärtslicher Hochschule, Hannover, Germany.

Schwappach, D.L.B., Boluarte, T.A. and Suhrcke, M. (2007). The economics of primary prevention of cardiovascular disease: a systematic review of economic evaluations. Cost. Eff. Resour. Alloc., **5**:5.

Scott, J.K. and Smith, G.P. (1990). Searching for peptide ligands with an epitope library. Science, **249**:386-390.

Shain, S.A., Boesel, R.W., Klipper, R.W. and Lancaster, C.M. (1983). Creatine kinase and lactate dehydrogenase: stability of isoenzymes and their activity in stored human plasma and prostatic tissue extracts and effect of sample dilution. Clin. Chem., **29**(5):832-835.

Shan. G. (2011) Principles of immunoassays. Immunoassays in Agricultural Biotechnology. John Wiley & Sons, Inc., Hoboken, New Jersey. 6-22.

Shaw, W.V. (1987). Protein engineering. The design, synthesis and characterization of factitious proteins. Biochem.J., **246**:1-17.

Shusta, E. V., Raines, R. T., Pluckthun, A. and Wittrup, K. D. (1998). Increasing the secretory capacity of Saccharomyces cerevisiae for production of single-chain antibody fragments. Nat. Biotechnol., **16**:773-777.

Skerra, A, Pfitzinger, I., Pluckthun, A. (1993). The functional expression of antibody Fv fragments in *Escherichia coli*: improved vectors and a generally applicable purification technique. Biotechnol., **9**:273-278.

Smith, G.P. (1985). Filamentous fusion phage: novel expression vectors that display cloned antigens on the virion surface. Science, **228**(4705):1315-1317.

Smith, K.A., Nelson, P.N., Warren, P., Astley, S.J., Murray, P.G. and Greenman, J. (2004). Demystified… recombinant antibodies. J. Clin. Pathol., **57**:912-917.

Snyder, M.R., Potter, J.D. and Prendergast, F. (1996). Secondary and tertiary structural analysis of troponin T. Biophys. J., **70**:A381.

Srisawasdi, P., Kroll, M.H. and Lolekha, P.H. (2007). Advantages and disadvantages of serum cholesterol determination by the kinetic vs the end point method. Am. J. Clin. Pathol., **127**(6):906-918.

Stahl, S. J., Watts, N.R., Rader, C., Dimattia, M.A., Mage, R.G., Palmer, I., Kaufman, J.D., Grimes, J.M., Stuart, D.I., Steven, A.C. and Wingfield, P.T. (2010). Generation and characterization of a chimeric rabbit/human Fab for co-crystallization of HIV-1. Rev. J. Mol. Biol., **397**(3):697-708.

Stemmer, W.P.C. (1994a). DNA shuffling by random mutagenesis and reassembly: *in vitro* recombination for molecular evolution. Proc. Natl. Acad. Sci., **91**:10747-10751.

Stemmer, W.P.C. (1994b) Rapid evolution of a protein *in vitro by* DNA shuffling. Nature, **340:**389-391.

Stills, H.F. (1994). Polyclonal antibody production. 2nd edition, P.J. Manning, D.H. Ringler, and C.E. Newcomer, eds. San Diego: Academic Press.

Strausberg, S.L., Alexander, P.A., Gallagher, D.T., Gilliland, G.L., Barnett, B.L. and Bryan, P.N. (1995). Directed Evolution of a Subtilisin with Calcium-Independent Stability. Nat. Biotechnol., **13**:669-673.

Steinbuechel, A. and Schlegel, H. G. (1983). NAD-linked L (+)-lactate dehydrogenase from the strict aerobe Alcaligenes eutrophus. 1. Purification and properties. Eur. J. Biochem., **130**:321-328.

Stillman, J.H. and Somero, G.N. (2001). A comparative analysis of the evolutionary patterning and mechanistic bases of lactate dehydrogenase thermal stability in porcelain crabs, genus Petrolisthes. J. Exp. Biol., **204**:767-776.

Sumandea, M. P., Vahebi, S., Sumandea, C.A., Garcia-Cazarin, M.L., Staidle, J. and Homsher, E. (2009). Impact of cardiac troponin T N-terminal deletion and phosphorylation on myofilament function. Biochem., **48** (32):7722-7731.

Sun, Y., Hwang, Y and Nahm. M.H. (2001). Avidity, potency, and cross-reactivity of monoclonal antibodies to pneumococcal capsular polysaccharide serotype 6B. Infect. Immun. **69**:336-344.

Tachibana., H, Matsumoto, N., Cheng, X.J., Tsukamoto, H. and Yoshihara, E. (2004b). Improved affinity of a human anti-Entamoeba histolytica Gal/GalNAc lectin Fab

fragment by a single amino acid modification of the light chain. Clin. Diagn. Lab. Immunol., **11**:1085-1088.

Tate, J.R. (2008). Troponin revisited 2008: assay performance. Clin. Chem. Lab. Med., **46**:1489-1500.

Thompson, C.B. (1992). Creation of immunoglobulin diversity by intrachromosomal gene conversion. Trends. Genet., **8**:416-422.

Townsend, P.J., Farza, H. and MacGeoch, C. (1994). Human cardiac troponin T: identification of fetal isoforms and assignment of the TNNT2 locus to chromosome 1q. Genom., **21**:311-316.

Updegraff, G.E. and Anderson, V.C. (1991). Bubble noise and wavelet spills recorded 1m below the ocean surface. J. Acoust. Soc. Am., **89**:2264-2279.

Vasan, R.S. (2006). Biomarkers of cardiovascular disease: molecular basis and practical considerations. Circulation, **113**:2335-2362.

Viguier, C., Arora, S., Gilmartin, N., Welbeck, K. and O'Kennedy, R. (2009). Mastitis detection: current trends and future perspectives. Trends. Biotechnol., **8**:486-493.

Vimalraj, T. R., Kavitha, N. and Dhanalakshmi, B. (2006). Incidence of bovine mycotic mastitis. Indian. Vet. J., **83**(10):1120-1121.

Waggoner, A. (2006). Fluorescent labels for proteomics and genomics, Curr. Opin. Chem. Biol, **10**(1): 62-66.

Wakarchuk, W.W., Sung, W.L., Campbell, R.L., Cunningham, A., Watson, D.C. and Yaguchi, M. (1994). Thermostabilization of the Bacillus circulans xylanase by the introduction of disulfide bonds. Protein. Eng., **7**:1379-1386.

Watts, J. L. (1988). Etiological agents of bovine mastitis. Vet. Microbiol., **16**:41-66.

Wellenberg, G.J., Poel, W,H. and Oirschot, J.T. (2002). Viral infections and bovine mastitis. Vet. Microbiol., **88**:27-45.

Wiebe, M. (2003). Stable production of recombinant proteins in filamentous fungi – problems and improvements. Mycol., **17**(3):140-144.

Wilson, C. and Agard, D.A. (1991). Engineering substrate specificity. Curr. Opinion Struct. Biol., **1**:617-623.

Winter, G., Griffiths, A.D., Hawkins, R.E. and Hoogenboom, H.R. (1994). Making antibodies by phage display technology. Annu. Rev. Immunol., **12**:433-455.

Wu, A.H.B., Valdes, R.Jr. and Apple, F.S. (1994). Cardiac troponin T immunoassay for diagnosis of acute myocardial infarction. Clin. Chem., **40**:900-907.

Yuan, B., Schulz, P., Liu, R. and Sierks, M.R. (2006). Improved affinity selection using phage display technology and off-rate based selection. Electron. J. Biotechn, **9**(2):171-175.

Yee, L. and Blanch, H.W. (1993). Recombinant trypsin production in high cell density fed-batch cultures of *Escherichia coli.* Biotechnol. Bioeng., **41**:781-790.

Yin. J., Tomycz, L., Bonner, G. and Wang, D.I. (2002). A simple and rapid assay of collagen-like polymer in crude lysate from *Escherichia coli*. J. Microbiol. Methods., **49**(3):321-323.

Yoshinaga, K., Matsumoto, M., Torikai, M., Sugyo, K., Kuroki, S., Nogami, K., Matsumoto, R., Hashiguchi, S., Ito, Y., Nakashima, T. and Sugimura, K. (2008). Ig L-chain shuffling for affinity maturation of phage library-derived human anti-human MCP-1 antibody blocking its chemotactic activity. J. Biochem., **143**(5):593-601.

Yuan, L, Kurek, I., English, J. and Keenan, R. (2005). Laboratory-Directed Protein Evolution. Microbiol. Mol. Biol, R., 373-392.

Zacher, A.N.I., Stock, C.A., Golden, J.W.I. and Smith, G.P. (1980). A new filamentous phage cloning vector: fd-tet. Gene, **9**:127-140.

Zank, W. and Schlatterer, B. (1998). Assessment of subacute mammary inflammation by soluble biomarkers in comparison to somatic cell counts in quarter milk samples from dairy cows. J. Vet. Med. Sci., **A**(45):45-51.

Zhang, W.W. (2003). The use of gene-specific IgY antibodies for drug target discovery Drug Discov. Today., **8**:364-371.

Zoller, M.J. (1991). New molecular biology methods for protein engineering. Curr. Opin. Biotechnol., **2**:526-531.

Zoller, M.J. (1992). New recombinant DNA methodology for protein engineering. Curr. Opin. Biotechnol., **3**:348-354.

Journal of Immunological Methods 359 (2010) 61–64

Contents lists available at ScienceDirect

Journal of Immunological Methods

journal homepage: www.elsevier.com/locate/jim

Technical Note

Simple method of 'on-plate' growth for improved antibody screening

Wei Li Guo [1], Paul Leonard [1], Richard O'Kennedy *

Biomedical Diagnostics Institute and School of Biotechnology, National Centre for Sensor Research, Dublin City University, Dublin 9, Ireland

ARTICLE INFO

Article history:
Received 31 January 2010
Received in revised form 12 May 2010
Accepted 13 May 2010
Available online 21 May 2010

Keywords:
ELISA
Phage display
Antibodies
Screening

ABSTRACT

Antibody phage display is a powerful biomolecular selection technology now routinely used for refining antibody diversity towards analytes of both therapeutic and diagnostic interest. Post selection, automated robotic systems can be utilised to pick, express and analyse large numbers of putative analyte-specific clones allowing the parallel screening of thousands of antibodies in less time. Most screening techniques involve a spatial addressing process whereby the selected antibodies are extracted from the cells and analysed to verify specificity. Using a simple 'on-plate' growth and screening approach, we show that antibody-expressing clones can be simultaneously cultured and analysed rapidly in antigen-coated ELISA plate wells yielding high binding signals and saving valuable selection time, while also eliminating the necessity for antibody extraction. The utilisation of the 'on-plate' technique for the screening of Fab and scFv antibodies, and a comparative analysis with commonly used antibody extraction processes, are described.

0022-1759/$ – see front matter © 2010 Elsevier B.V. All rights reserved.
doi:10.1016/j.jim.2010.05.004

This text redacted due to 3rd party copyright
This text redacted due to 3rd party copyright
This text redacted due to 3rd party copyright
This text redacted due to 3rd party copyright
This text redacted due to 3rd party copyright
This text redacted due to 3rd party copyright
This text redacted due to 3rd party copyright
This text redacted due to 3rd party copyright
This text redacted due to 3rd party copyright
This text redacted due to 3rd party copyright
This text redacted due to 3rd party copyright
This text redacted due to 3rd party copyright
This text redacted due to 3rd party copyright
This text redacted due to 3rd party copyright
This text redacted due to 3rd party copyright
This text redacted due to 3rd party copyright
This text redacted due to 3rd party copyright
This text redacted due to 3rd party copyright
This text redacted due to 3rd party copyright
This text redacted due to 3rd party copyright
This text redacted due to 3rd party copyright
This text redacted due to 3rd party copyright
This text redacted due to 3rd party copyright
This text redacted due to 3rd party copyright
This text redacted due to 3rd party copyright
This text redacted due to 3rd party copyright
This text redacted due to 3rd party copyright
This text redacted due to 3rd party copyright

New 'on-plate' growth for improved ELISA-based antibody screening

Authors:

Wei Li Guo*, Paul Leonard* and Richard O'Kennedy

*These authors contributed equally

Authors: institution(s)/affiliation(s) for each author:

Wei Li Guo

School of Biotechnology and
Biomedical Diagnostics Institute,
National Centre for Sensor Research,
Dublin City University, Dublin 9, Ireland.
wei.guo2@mail.dcu.ie

Paul Leonard

School of Biotechnology and
Biomedical Diagnostics Institute,
National Centre for Sensor Research,
Dublin City University, Dublin 9, Ireland.
paul.leonard@dcu.ie

Richard O'Kennedy

School of Biotechnology and
Biomedical Diagnostics Institute,
National Centre for Sensor Research,
Dublin City University, Dublin 9, Ireland.
richard.okennedy@dcu.ie

Corresponding author:

Prof. Richard O'Kennedy
School of Biotechnology and
Biomedical Diagnostics Institute,
National Centre for Sensor Research,
Dublin City University, Dublin 9, Ireland.
richard.okennedy@dcu.ie
Tel.: +353-1-7005319, Fax: +353-1-7005412

Keywords:

ELISA, phage display, antibodies, screening

Short Abstract:

A new 'on-plate' technique for the screening of recombinant antibodies is described and a comparative analysis with common antibody extraction processes is made. Using this approach, antibody-expressing clones can be analysed rapidly in antigen-coated ELISA plate wells yielding high binding signals and also saving valuable selection time.

Long Abstract:

Phage display technology is routinely used for selecting antibodies to antigens of interest for both therapeutic and diagnostic purposes. The selection of antibodies against the desired antigen is achieved by iterative cycles of biopanning. The conventional ELISA-based antibody screening method is wildly used for the selection and ranking antigen-specific clones post biopanning. In addition, automated robotic systems facilitate the selection and ranking process from a large number of putative antigen-specific antibodies [1]. The antibody screening process involves the inoculation of colonies from clone output titre plates from the final rounds of biopanning process into microtitre plates allowing antibody expression [2]. In conventional ELISA-based antibody screening methods, an antibody extraction step by cell lysis is involved. Typically, repeated freeze-thaw cycles at -70^{o}C/37^{o}C [3, 4], periplasmic extraction with Tris-EDTA Sucrose buffer [5] or sonication [6] are utilized to extract antibody-containing cell lysate. Post extraction step, cell lysates are incubated in antigen-coated microtitre wells and antibody-antigen binding signals are measured with a labeled secondary antibody. Antibody binding data can be obtained within

36 hours after colony inoculation. Based on the conventional ELISA screening approach, herein we describe a simple 'on-plate' screening method for antibody analysis. In comparison with common ELISA-based analysis, this simple 'on-plate' method eliminates bacterial cell removal step, therefore, requires less screening time. It also generates high binding signals and facilitates automation [7]. During the 'on-plate' screening process, interaction time between antibody and antigen is significantly increased due to the overnight growth of antibody-expressing clones on antigen-coated ELISA plates, allowing binding reaction reach equilibrium (Fig. 1). Low expression clones can also be detected due to the long interaction time. The analysis on both scFv and Fab antibody fragments revealed that the simple 'on-plate' technique produces higher binding signals than other screening methods that require an antibody exaction step.

Protocol Text:

1 'on-plate' antibody screening process

This experiment is designed to aid the screening of antibodies and antibody fragments after phage-based selection. Phage infected *E. coli* cells are cultured on agar plates and colonies harbouring antibody genes of interest selected for 'on-plate' ELISA analysis [8].

1.1) Rescue output phage from selected rounds of biopanning and infect the phage into *E. coli* cells by mixing phage particles with exponentially growing *E. coli* cells. Dilute the infected culture in sterile media and spread on Luria broth agar plates (10 g/L Tryptone, 5 g/L yeast extract, 10 g/L NaCl) supplemented with antibiotics of choice (see Note 1 below). Incubate the plates at 37^{o}C for 18 to 24 hours.

Note 1: The antibiotics needed depend on the phagemid and *E. coli* strain used in the experiment.

1.2) Pick a total of ninety-six single clones from selected output agar plates with sterile micropipette tips or inoculation loop. Inoculate into microtitre plate wells containing 200 µL of SB broth (10 g/L MOPS, 30 g/L Tryptone and 20 g/L yeast extract) supplemented with antibiotics (see Note 1 above). Grow shaking at 37^{o}C for 6-8 hours at 200 rpm.

1.3) Coat a Nunc maxisorb plate (ELISA plate) with 100 µL /well of a 1-5 µg/mL antigen solution in phosphate buffered saline, pH 7.4 (PBS containing 0.15 M NaCl, 10 mM Na_2HPO_4, 18 mM KH_2PO_4, 2.5 mM KCl) for 1 hour at 37^oC. Remove the antigen solution by inversion and block with 200 µL /well of 3% (w/v) BSA in PBS for 1 hour at 37^oC.

1.4) Remove 20 µL of culture from step 1.1 and transfer to a sterile tube/microtitre plate well. This is a master stock and can be used to re-culture the clone at a later stage. Add 20 µL of 10 mM IPTG to the remaining 180 µL of culture (the final concentration of IPTG should be 1mM). Remove the blocking solution from the ELISA plate by inversion (as in step 1.3) and immediately transfer the induced culture to the ELISA plate using a multichannel micropipette and sterile tips.

Note 2: IPTG is used for expression of genes cloned under the control of a *lac* promoter system and should be used at a concentration of 0.5 to 1 mM [9].

1.5) Incubate the culture-induced ELISA plate overnight (12-18 hours) at 30^oC with agitation at 220 rpm.

1.6) Remove the cells and culture media after overnight 'on-plate' expression by inversion and wash four times with 200µL /well PBST pH 7.4 (0.05% (v/v) Tween 20, 0.15 M NaCl, 10 mM Na_2HPO_4, 18 mM KH_2PO_4 and 2.5 mM KCl).

Note 3: At this step cells could be removed and stored as a back-up culture before washing if required.

1.7) Add 100 µL/well of a 25 ng/mL enzyme-labelled secondary antibody diluted in PBST pH 7.4 containing 0.5% (w/v) BSA to each well and incubate stationary for 1 hour at 37^oC.

Note 4: The specificity of the secondary antibody used will depend on the affinity tag incorporated into the plasmid or antibody gene. Horse radish peroxidase (HRP) and alkaline phosphatase (AP)-labeled antibodies are commonly used as secondary antibodies for detection of bound antibody.

1.8) Wash the wells five times with 200 µL/well PBST, pH 7.4, and add 100 µL/well of enzyme substrate (see Note 5 below) to each well for detection of bound antibody. Incubate for 30 minutes at 37 ^{o}C and stop the reaction with the addition of 50 µL/well of 1M HCl.

Note 5: Tetramethylbenzidine (TMB) and p-nitrophenyl phosphate, disodium salt (PNPP) substrates are commonly used for HRP and AP-labeled antibodies, respectively.

1.9) Read the absorbance of the solutions in the wells of the ELISA plate using a microtitre plate reader and record the results. Identify well positions with signals 3 or more times background (the stringency of selection 'cutoff' will depend on one's individual requirements). Inoculate 5 µL of the master clone stock (step 1.4), corresponding to each positive well, into a fresh microtitre plate or tube and grow as required for further testing or cell banking.

2 Optional: Protocol for the comparison with 'off-plate' analysis

The same antibody cultures used for 'on-plate' analysis, described above, can also be cultured 'off-plate' in tubes overnight for a direct comparison between the methods, if required.

2.1) Inoculate 5 µL of antibody-containing cultures (the number of clones will depend on the number of positive clones from 1.9 above) from the stock plate into a 20 mL tube containing 2 mL of SB broth supplemented with antibiotics. Grow overnight at 37^{o}C with agitation at 200 rpm.

2.2) Transfer 200 µL of the overnight culture into a 250 mL flask containing 40 mL of SB broth supplemented with antibiotics and grow shaking at 200 rpm until an O.D.$_{600}$ of 0.8 is reached. At this point add IPTG to a final concentration of 1 mM and grow at 30^{o}C shaking overnight at 200 rpm.

2.3) Aliquot 10 mL of the overnight cultures into separate tubes prior to the extraction of antibody by either Tris-EDTA sucrose (TES) buffer addition, sonication or freeze-thaw cycles.

2.4) For TES samples, centrifuge the 10 mL of overnight culture at 3,300 g for 10 minutes and resuspend the pellet in 2 mL of TES buffer (0.2 M Tris-HCl, pH 8.0, 0.5 mM EDTA, 0.5 M sucrose) for 30 minutes. Centrifuge the solution at 6,000 g for 5 minutes to remove the cell

debris. Add 200 µL of the supernatant to the desired number of wells of the antigen-coated ELISA plate (as described in step 1.3 above).

2.5) For extraction by sonication, centrifuge the 10 mL overnight culture at 3,300 g for 10 minutes and resuspend the pellet in 2 mL PBST. Sonicate for 50 seconds (40 amps for three 10 second pulses with a 10 second interval between pulses) and centrifuge at 6,000 g for 5 minutes to remove cell debris. Finally, add 200 µL of supernatant to wells of the antigen-coated ELISA plate.

2.6) For the freeze-thaw samples, freeze 2 mL of culture at -70^{o}C and thaw at 37^{o}C. Repeat this process three times. Remove cell debris by centrifugation at 6,000 g and add 200 µL of supernatant to wells of the antigen-coated ELISA plate.

2.7) Incubate all samples at 37^{o}C for 1 hour and detect, as described in steps 1.6 -1.9 above, for the 'on-plate' analysis.

Results:

The simple 'on-plate' screening method was applied to scFv and Fab clones selected by phage display against cardiac troponin T (cTnT). The 'on-plate' approach was performed on forty-eight anti-cTnT scFv clones from selected rounds of biopanning. It was shown that a wide range of binding signals (signals > 3.0 to < 0. 1) were detected (Fig. 2). As expected, binding signals and number of positive clones increased from rounds four to five of biopanning This was due to the increased stringency during biopanning process and subsequent enrichment of target specific clones. Although cell growth was observed in every well, no binding signals were detected in a number of wells, which indicates that no non-specific binding phenomena were caused by overnight cell growth on ELISA plate. High binding signals were generated (signal > 3.0) due to long interaction time between antibodies and antigen. In addition, low binding signals (signal < 0.4) were also detected, which were not detected using freeze-thaw methods (data not shown). During the screening process, antibodies were produced by bacterial cells and released from the periplasm of aging and dying cells by natural leakage into culture media [10]. The natural leakage eliminated the requirement for cloning specific antibody secretion signal sequences and, therefore, the 'on-plate' method could be used for any cell and plasmid combination.

Comparison of the ‘on-plate’ screening method described here with commonly used ELISA-based screening approaches requiring an antibody extraction step showed that the ‘on-plate’ method yielded the highest responses. This indicated that the increased antibody/antigen incubation time of the ‘on-plate’ method allowed the interaction to reach equilibrium which was not the case for the 1 hour incubation with the same clones (Fig. 3). For the smaller and more easily expressed scFv clones, high binding signals were observed irrespective of the method used. Lower signals were observed with the Fab clones. The TES and freeze-thaw methods generated the lowest signals for both Fab antibody fragments and the ‘off-plate’ method for one of the Fab antibody fragments.

Discussion:

The screening of two scFv and two Fab antibodies using the ‘on-plate’ approach reveals a number of advantages in comparison with conventional ELISA-based methods (that require cell lysis). Firstly, the ‘on-plate’ approach yielded higher signals due to longer interaction time antibody and antigen (Fig. 3). Secondly, this ‘on-plate’ approach reduced experimental time with less manipulative steps due to the elimination of cell lysis process. In addition, the preparation of backup stocks is also simplified by plating the overnight expressed culture on appropriate agar plates. Finally, by eliminating the need for centrifugation and the need for pipetting highly viscous cell extract solutions (which can interfere with accuracy of automated robotic pipetting), the ‘on-plate’ approach can improve the efficiency of automated robotic antibody screening systems.

Even though incubating cells with antigen could possibly lead to antigen degradation, the consistent high binding signals obtained indicates that the purified cardiac troponin T remains stable (no signs of degradation) throughout the screening process. Similarly, we have observed no loss of antibody binding signals when screening antibody fragments against a number of analytes such as hapten-protein conjugates, peptides and biomarkers of cancer.

This protocol describes the analysis of cardiac troponin T antibodies using a simple ‘on-plate’ screening method. As an alternative to conventional ELISA-based screening, the ‘on-plate’ screening approach saves valuable experimental time and cost during sample analysis; in

addition, this approach may be incorporated in to automated robotic system, therefore, facilitating high throughput analysis with reduced overall complexity.

Acknowledgments:

The authors would like to thank Prof. Carlos F. Barbas III (Scripps Research Institute) for generously making the pComb vector system available to us. This material is based upon works supported by the Science Foundation Ireland under Grant No. 05/CE3/B754.

Disclosures: We have nothing to disclose

References:

1 Leonard, P., Säfsten, P., Hearty, S., McDonnell, B., Finlay, W., O'Kennedy, R., High throughput ranking of recombinant avian scFv antibody fragments from crude lysates using the Biacore A100, Journal of Immunological Methods, 323. 172-179 (2007).

2 Barbas. 3rd, C. F., Burton, D. R., Scott, J. K., Silverman, G. J., Analysis of antibody fragment-expressing clones in ELISA, In Phage Display (Protocol 11.3), A laboratory Manual, Cold Spring Harbor Laboratory Press, Cold Spring Harbor, New York (2001).

3 Barbas. 3rd, C. F., Crowe. Jr, J. E., Cababa, D., Jones, T. M., Zebedeei, S. L., Murphy, B. R., Chanockt, R. M., Burton, D. R., Human monoclonal Fab fragments derived from a combinatorial library bind to respiratory syncytial virus F glycoprotein and neutralize infectivity, Medical Sciences 89, 10164 -10168 (1992).

4 Shamlou, P. A., Breen, L. H., Bell, W. V., Pollo, M., Thomas, B. A., A new scaleable freeze-thaw technology for bulk protein solutions, Biotechnology and Applied Biochemistry 46, 13-26 (2007).

5 Deng, X. K., Nesbit, L. A., John Morrow Jr, K., Recombinant single-chain variable fragment antibodies direct against *Clostridium difficile* toxin B produced by use of an optimized phage display system, Clinical and Diagnostic Laboratory Immunology 10, 587-595 (2003).

6 Wang, H., Tong, Y., Fang, M., Ru, B., High-level expression of human TFF3 in *Escherichia coli.* Peptides. 26, 1213–1218 (2005).

7 Guo, W.L., Leonard, P., and O'Kennedy, R., Simple method of ‘on-plate’ growth for improved antibody screening . Journal of Immunological Methods. 359:61-64 (2010).

8 Andris-Widhopf, J., Rader, C., Steinberger, P., Fuller, R., Barbas. 3rd, C. F., Methods for the generation of chicken monoclonal antibody fragments by phage display. Journal of Immunological Methods. 242, 159-181 (2000).

9 Hansen, L. H., Knudsen, S., Sørensen, S. J., The Effect of the *lacY* gene on the induction of IPTG inducible promoters, studied in *Escherichia coli* and *Pseudomonas fluorescens,* Current Microbiology. 36, 341-347 (1998).

10 Yoon, S.H., Kim, S.K., Kim, J.F., Secretory production of recombinant proteins in *Escherichia coli*, Biotechnology. 4, 23-29 (2010).

Tables and Figures:

Figure 1: Schematic of the 'on-plate' screening method with diagrammatic insert showing secreted scFv antibodies binding to immobilised analyte during overnight cell culture. Colonies from the output panning plates are inoculated into 96 well culture plates containing sterile media and grown for 3-4 hours at 37^{o}C. Meanwhile, a microtitre plate is coated with the analyte of interest and blocked with an appropriate blocking solution. After addition of the induction agent the cultures are transferred to the analyte-coated plate and grown overnight with shaking. The following day the cells are simply removed by centrifuging (kept if required) and bound antibody fragments detected with an enzyme-labelled tag-specific secondary antibody.

Figure 2: Representative monoclonal ELISA plate result after 4 and 5 rounds of biopanning of an anti-cTnT scFv library using the 'on-plate' method. Even though cell growth (as characterised by turbid culture media) was observed in each well of the ELISA plate, the antibody binding signals ranged from less than 0.1 to greater than 3.0 absorbance units indicating that the growth of cells in the ELISA plates caused no increase in non-specific binding.

Figure 3: Comparison of 'on-plate' expression with commonly used antibody extraction methods performed prior to monoclonal ELISA. Two scFv (left panel) and two Fab (right panel) fragments specific to cTnT were prepared using different methodologies and analysed by ELISA (values are the average of 4 replicates for each antibody). The 'on-plate' data are derived from growing cultures in antigen-coated microtitre plate wells. The 'off-plate' data are derived from growing the cells in tubes overnight and adding the cultures to the ELISA plate wells for 1 hour without any cell removal. The TES data are derived from the supernatant of cell lysis in Tris-EDTA sucrose (TES) buffer for 30 minutes prior to addition to the ELISA plate wells for 1 hour. The sonication data are derived from the supernatant of sonicated cell pellets incubated for 1

hour on the ELISA plate and the freeze-thaw data are derived from incubating media supernatants on the ELISA plate for 1 hour after three freeze-thaw cycles. The ‘on-plate’ negative control data are derived from growing cultures in blocked microtitre plate wells lacking antigen so that the difference in signal from the ‘on-plate’ data is due to specific antigen binding.